ENLARGED LOCAL STABILIZATIONS OF

A CLASS OF UNCERTAIN NONLINEAR

SYSTEMS USING LYAPUNOV

ATTRACTIVE REGION CONTROL

By

PINIT NGAMSOM

Bachelor of Engineering
King Mongkut's Institute of Technology - Ladkrabang
Ladkrabang, Bangkok, Thailand
1992

Master of Science
Texas A&M University - Kingsville
Kingsville, Texas
1996

Submitted to the Faculty of the
Graduate College of the
Oklahoma State University
in partial fulfillment of
the requirements for
the Degree of
DOCTOR OF PHILOSOPHY
May, 2001

ENLARGED LOCAL STABILIZATIONS OF
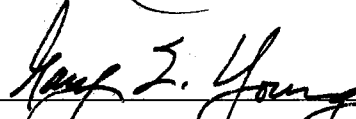
A CLASS OF UNCERTAIN NONLINEAR

SYSTEMS USING LYAPUNOV

ATTRACTIVE REGION CONTROL

Thesis Approved:
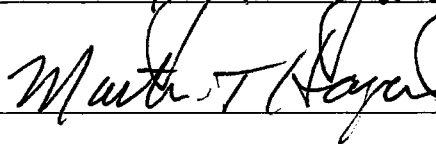
_____
Thesis Adviser

_____

_____

_____
Dean of the Graduate College

ii

ACKNOWLEDGEMENTS

TABLE OF CONTENTS

LIST OF TABLES

LIST OF FIGURES

NOMENCLATURE

$\mathbf{A}$ Free-response matrix in the linearized model $\dot{\mathbf{x}} = \mathbf{A}\mathbf{x} + \mathbf{B}\mathbf{u}(\mathbf{x})$

$\overline{\mathbf{A}}$ $[\mathbf{A} - \mathbf{BK}]$

$\overline{\mathbf{A}}_l$ $\overline{\mathbf{A}}_n + \sum_{j=1}^{r} h_{lj} \mathbf{E}_j$

$|\mathbf{x}|$ Absolute vector of vector $\mathbf{x}$, defined as $|\mathbf{x}| \equiv [\,|x_1| \quad |x_2| \quad \ldots \quad |x_n|\,]^T$

$|c|$ Absolute value of a real number c

$\mathbf{B}$ Input matrix in the linearized model $\dot{\mathbf{x}} = \mathbf{A}\mathbf{x} + \mathbf{B}\mathbf{u}(\mathbf{x})$

B_L $\{\mathbf{x} \mid \dot{V}(\mathbf{x}) < 0\} \cup \{\mathbf{0}\}$ when the control is linear

β_C (Beta) $\{\mathbf{x} \mid 0 \le V(\mathbf{x}) < C,\ C \in \mathfrak{R}^+\}$

β_{C_L} $\{\beta_C \mid \beta_{C,C=C_L} \subseteq B_L,\ \beta_{C,C>C_L} \not\subset B_L,\ C_L \in \mathfrak{R}^+\}$

β_{C_S} $\{\mathbf{x} \mid 0 \le V(\mathbf{x}) < C_S, C_S \in \mathfrak{R}^+,\ [G(\mathbf{x}) = 0] \Rightarrow [F(\mathbf{x}) < 0]\}$

$\mathbf{C}$ Output matrix in the output equation $\mathbf{y} = \mathbf{C}\mathbf{x}$

c A real number

$\Delta\mathbf{f}$ $\mathbf{f}(\mathbf{x}) - \mathbf{A}_n\mathbf{x}$

$\Delta\mathbf{g}$ $\mathbf{g}(\mathbf{x}) - \mathbf{B}_n$

$\mathbf{E}_j$	Known uncertainty specification matrices associated with uncertain function $h_j(\mathbf{x})$
ε	(Epsilon) A variable bounded by $0 < \varepsilon < \dfrac{2}{\sigma_{max}^2(\mathbf{Q}^{-1/2}\mathbf{P})}$
$\mathbf{f}(\mathbf{x})$	Free-response vector in the nonlinear model $\dot{\mathbf{x}} = \mathbf{f}(\mathbf{x}) + \mathbf{g}(\mathbf{x})\mathbf{u}(\mathbf{x})$
$\mathbf{f}_\Omega(\mathbf{x},t)$	$\mathbf{f}_\Sigma(\mathbf{x},t,u)\big|_{u=-\mathbf{Kx}}$
$\mathbf{f}_\Sigma(\mathbf{x},t,u)$	Uncertain vector of dimension n
$F(\mathbf{x})$	$\mathbf{x}^T\mathbf{P}\mathbf{f}(\mathbf{x})$
$F_L(\mathbf{x})$	$\mathbf{x}^T\mathbf{PAx}$
$\mathbf{g}(\mathbf{x})$	Input connection matrix in the nonlinear model $\dot{\mathbf{x}} = \mathbf{f}(\mathbf{x}) + \mathbf{g}(\mathbf{x})\mathbf{u}(\mathbf{x})$
$G(\mathbf{x})$	$\mathbf{x}^T\mathbf{P}\mathbf{g}(\mathbf{x})$ where $\mathbf{g}(\mathbf{x}) \in \mathfrak{R}^n$
$G_L(\mathbf{x})$	$\mathbf{x}^T\mathbf{PB}$ where $\mathbf{B} \in \mathfrak{R}^n$
$\mathbf{G}(\mathbf{x})$	$\mathbf{x}^T\mathbf{P}\mathbf{g}(\mathbf{x})$ where $\mathbf{g}(\mathbf{x}) \in \mathfrak{R}^{n\times m}$
$\mathbf{G}_L(\mathbf{x})$	$\mathbf{x}^T\mathbf{PB}$ where $\mathbf{B} \in \mathfrak{R}^{n\times m}$
$\nabla\Omega(\mathbf{x})$	Gradient of $\Omega(\mathbf{x})$, defined as $\left[\dfrac{\partial\Omega(\mathbf{x})}{\partial x_1} \quad \dfrac{\partial\Omega(\mathbf{x})}{\partial x_2} \quad \cdots \quad \dfrac{\partial\Omega(\mathbf{x})}{\partial x_n}\right]^T$
$h_j(\mathbf{x})$	Uncertain function $h_j(\mathbf{x})$ associated with $\mathbf{E}_j$
h_{uj}	Known upper bound of $h_j(\mathbf{x})$
h_{lj}	Known lower bound of $h_j(\mathbf{x})$
$\mathbf{K}$	Linear state feedback gain matrix

$l_j(\mathbf{x})$	$h_j(\mathbf{x}) - h_{lj}$
λ_{Ξ}	(Lambda) Eigenvalue of matrix Ξ
$\lambda_{\Xi i}^{+}$	Positive eigenvalues of matrix Ξ
$\lambda_{\Xi i}^{-}$	Negative eigenvalues of matrix Ξ
$\lambda_{\max}(\Xi)$	Maximum eigenvalue of matrix Ξ
$\lambda_{\min}(\Xi)$	Minimum eigenvalue of matrix Ξ
Λ_{Ξ}	(Lambda) Diagonal matrix whose diagonal elements are eigenvalues of matrix Ξ
m	Number of inputs or the dimension of the control vector $\mathbf{u}(\mathbf{x})$
$\mathbf{M}$	$\frac{1}{2}[\mathbf{PA} + [\mathbf{PA}]^{T}]$
μ	(Mu) $\lambda_{\min}^{1/2}(2\varepsilon\mathbf{Q} - \varepsilon^{2}\mathbf{PP})$
n	Order of the system of interest
n	Designates that an object Ξ_n is nominal
$\mathbf{N}$	$\frac{1}{2}[[\mathbf{PB}]\mathbf{K} + \mathbf{K}^{T}[\mathbf{PB}]^{T}]$
$\overline{\mathbf{N}}$	$\mathbf{N}\big|_{\mathbf{K}^{T} = \rho[\mathbf{PB}]}$
η	(Eta) Second parameter for generating LARC ($\eta \geq 1$)
η_u	Upper bound of η
$\|\Xi\|$	Spectral norm of matrix Ξ
$\|\mathbf{x}\|$	2-norm of vector $\mathbf{x}$

O_ζ	Boundary of the region ζ
Ω	(Omega) Dummy function
Φ	(Phi) $[\mathbf{P}\overline{\mathbf{A}}_l + \overline{\mathbf{A}}_l^T \mathbf{P}]$
Ψ_j	(Psi) $[\mathbf{P}\mathbf{E}_j + \mathbf{E}_j^T \mathbf{P}]$
Ψ_j^D	$\mathbf{T}_{\Psi_j}^T \Psi_j \mathbf{T}_{\Psi_j}$
$\Psi_j^{D,0+}$	$\Psi_j^D \big|_{[\Psi_j^D(i,i)<0] \to [\Psi_j^D(i,i)=0]}$
Ψ_j^{0+}	$[\mathbf{T}_{\Psi_j}^{-1}]^T [\Psi_j^{D,0+}] \mathbf{T}_{\Psi_j}^T$
$\mathbf{P}$	Symmetric positive definite matrix for constructing a quadratic Lyapunov function
$\mathbf{p}_i$	Common boundary points between β_{C_L} and B_L
q	The number of outputs or degrees of freedom
$\mathbf{Q}$	Symmetric positive definite matrix satisfying the Lyapunov equation $-\mathbf{Q} = \dfrac{1}{2}[\mathbf{P}\overline{\mathbf{A}} + \overline{\mathbf{A}}^T \mathbf{P}]$ in which $\overline{\mathbf{A}}$ is strictly stable
r	The number of uncertain terms $h_j(\mathbf{x})\mathbf{E}_j$ in the structured uncertainty specifications
$r_{\lambda_\mathbf{M}}$	Eigenvalue ratio of $\mathbf{M}$ defined as $r_{\lambda_\mathbf{M}} \equiv \left\| \dfrac{\max(\lambda_{\mathbf{M}i}^+)}{\max(\lambda_{\mathbf{M}j}^-)} \right\|$
$R_{[\Omega<0] \cup \{\mathbf{0}\}}$	$\{\mathbf{x} \mid \Omega(\mathbf{x}) < 0\} \cup \{\mathbf{0}\}$
$\mathrm{Re}(s)$	Real part of a complex number s

$\Re$	Space of real numbers
$\Re^n$	Vector space of dimension n
$\Re^{n \times n}$	Matrix space of dimension $n \times n$
$\Re^+$	Set of real positive numbers
ρ	(Rho) The first parameter for generating LARC ($\rho \in \Re^+$)
ρ_u	The upper bound of ρ
ρ_l	The lower bound of ρ
$\sigma(\Xi)$	(Sigma) A singular value of the matrix Ξ
$\sigma_{\max}(\Xi)$	The maximum singular value or the spectral norm of the matrix Ξ
$S_{\Omega=0}$	$\{\mathbf{x} \mid \Omega(\mathbf{x}) = 0\}$
t	Time
$\mathbf{T}_\Xi$	Linear transformation operating on matrix Ξ for changing basis
$\mathbf{u}(\mathbf{x})$	Control vector of dimension m
$\mathbf{u}_{LARC}(\mathbf{x})$	Linear control vector of dimension m resulting from Lyapunov Attractive Region Control (LARC)
$\mathbf{u}_{LQR}(\mathbf{x})$	Linear control vector of dimension m resulting from Linear Quadratic Regulator (LQR)
$\mathbf{u}_{PP}(\mathbf{x})$	Linear control vector of dimension m resulting from Pole Placement (PP)
$\mathbf{v}_\Xi$	Eigenvector of the matrix Ξ
$V(\mathbf{x})$	Quadratic Lyapunov function $\dfrac{1}{2}\mathbf{x}^T\mathbf{P}\mathbf{x}$

$\dot{V}(\mathbf{x})$	Time derivative of the quadratic Lyapunov function $V(\mathbf{x})$ along trajectories of the nonlinear model of interest
$\dot{V}_L(\mathbf{x})$	Time derivative of a quadratic Lyapunov function along trajectories of the linearized model
$\mathbf{x}$	State vector, defined as $\mathbf{x} = [x_1 \quad x_2 \quad \dots \quad x_n]^T$
$\overline{\mathbf{x}}$	Normalized vector of $\mathbf{x}$, defined as $\overline{\mathbf{x}} = \dfrac{\mathbf{x}}{\|\mathbf{x}\|}$
$\mathbf{x}_{C_{Si}}$	Intersection points between $S_{G=0}$ and $S_{F=0}$
$\dot{\mathbf{x}}$	Time derivative of $\mathbf{x}$
Ξ	(Xi) A dummy matrix
$\Xi(i,j)$	The (i,j) element of matrix Ξ
Ξ^T	Transposition of the matrix Ξ
Ξ_T	Matrix Ξ in a transformed basis
$\mathbf{y}$	Output vector of dimension q
$\mathbf{z}_{\{\mathbf{v}_{\Xi 1},\dots,\mathbf{v}_{\Xi n}\}}^{\Omega=0}$	$\{\mathbf{z} \mid \Omega(\mathbf{z}) = 0, \mathbf{z} = c_1\mathbf{v}_{\Xi 1} + \dots + c_n\mathbf{v}_{\Xi n}, c_i \in \Re, i = 1,\dots,n\}$
$\mathbf{Z}$	$\Phi + \sum_{j=1}^{r}[(h_{uj} - h_{lj})\Psi_j^{0+}]$
ζ	(Zega) Dummy set or region

Chapter I

The Fundamental Idea of LARC

1.1   Introduction

We are interested in systems whose mathematical description can be written as:

$$\dot{\mathbf{x}} = \mathbf{f}(\mathbf{x},t) + \mathbf{g}(\mathbf{x},t)\mathbf{u}$$
$$\mathbf{y} = \mathbf{C}\mathbf{x}$$

where the vector $\mathbf{f}(\mathbf{x},t) \in \Re^n$, matrix $\mathbf{g}(\mathbf{x},t) \in \Re^{n \times m}$. Both $\mathbf{f}(\mathbf{x},t)$ and $\mathbf{g}(\mathbf{x},t)$ are possibly time-varying, nonlinear, and uncertain. We describe $\mathbf{f}(\mathbf{x},t)$ and $\mathbf{g}(\mathbf{x},t)$ as "uncertain" rather than "unknown" because we assume that some knowledge of these objects is available. In most of our discussions, the control $\mathbf{u}$ is restricted to be linear in $\mathbf{x}$ for simplicity, although nonlinear controllers may give better results as shown in Chapter V. The vector $\mathbf{x} \equiv [x_1 \ x_2 \ \dots x_n]^T \in \Re^n$ is the state vector, $\mathbf{C} \in \Re^{q \times n}$ is the output matrix, $\mathbf{y} \in \Re^q$ is the output vector, and $\mathbf{u}(\mathbf{x}) \in \Re^m$ is the control vector. The state $\mathbf{x}$ is assumed to be available for feedback. We restrict that $\mathbf{f}(\mathbf{x},t)$, $\mathbf{g}(\mathbf{x},t)$, and $\mathbf{u}(\mathbf{x})$ are such that $\dot{\mathbf{x}}$ is piecewise continuous in t, and is locally Lipschitz in the operating region of interest in $\Re^n$ $\forall t \geq 0$. In general, it is most desirable that the system of interest be globally uniformly asymptotically stable. However, control problems for some physically simple systems such as underactuated systems (systems in which $m < q$) are surprisingly difficult to solve in a systematic fashion (Slotine, and Li, 1991). It has been our experience that this statement is true. In particular, we find that it can be very difficult to guarantee global

stability for underactuated systems using standard Lyapunov-based nonlinear control techniques such as sliding-mode control (Utkin, 1992), (Itkis, 1976), (Slotine, and Li, 1991), (Khalil, 1996), or adaptive control (Narendra, and Annaswamy, 1989), (Sastry, and Bodson, 1989), (Slotine, and Li, 1991), (Khalil, 1996). This is because it is not clear how to obtain an attractive sliding surface (for sliding-mode control), or to find an adaptive law guaranteeing the negative definiteness a Lyapunov function (for adaptive control). The backstepping technique is a systematic Lyapunov-based controller design technique that can be employed to guarantee global stability. However, its applications are limited to strict-feedback nonlinear systems (Khalil, 1996), and it appears that a very limited number of physical systems falls into this category. In addition to these Lyapunov-based techniques, feedback linearization is a well-known differential-geometry-based technique (Isidori, 1989), (Nijmeijer, and Schaft, 1990), (Vidyasagar, 1993). When applying this technique, we find that there are numerous physically simple systems that are not feedback linearizable. In addition, it can be very difficult obtain a set of appropriate transformations for practical physical systems, and it is not clear if such transformations remain valid in the presence of uncertainties. Faced with these difficulties, many researchers explore intelligent control techniques such as fuzzy logic, and incorporate human reasoning and decision making with analytical tools such as Lyapunov stability to construct stabilizing controllers (Wang, 1997), (Wang, 1994), (Yin, and Lee, 1995). In these references, we observe that global stability can be guaranteed only for simple systems. By embedding human reasoning and decision making into a fuzzy logic controller, it is possible to stabilize locally a fairly complex underactuated nonlinear system, such as the double-inverted-pendulum system (Misawa,

Arrington, and Ledgerwood, 1995). Using linearization, local stability of the closed-loop system can be examined. However, it has been our experience that the process of embedding human knowledge into a fuzzy rule base can be very tedious. In addition, it usually is very time-consuming to re-embed the knowledge when physical parameters of the system are changed. We find that it can be very difficult to handle robustness issues because of complex nonlinearities in the controller.

Assuming that global stability using existing nonlinear control techniques cannot be guaranteed in a reasonable amount of time, it may be sufficient that the system be locally uniformly asymptotically stable about the equilibrium point at the origin. When local stabilization is acceptable, a typical approach is to approximate the nonlinear system about the origin using a linearized model. A linear controller is then designed to stabilize the linearized model, since this implies local stability for the corresponding nonlinear system. Based on this approach, considerable works in control theory have been directed toward performance and robustness of linear systems under linear controllers. It has been our experience that considerably less attention is directed toward the associated problem of attractive regions of nonlinear systems under linear controllers. In our opinion, a large attractive region is an important property associated with local stability. Indeed, our objective is to design $\mathbf{u}(\mathbf{x})$ such that the nonlinear system is locally uniformly asymptotically stable about the origin with a reasonably large attractive region. In our discussions, we define an attractive region as a set of initial conditions from which trajectories converge to the origin. We assume the equilibrium point at the origin because

we can move a nonzero equilibrium point to the origin by changing variables. The equilibrium point at the origin is our "operating point", unless otherwise stated.

While linear controllers have been widely accepted for local stabilization, some researchers employ nonlinear controllers for the same purpose. For time-invariant problems with a set of constant operating points containing the origin, a possibility for local stabilization is to employ pseudolinearization (Reboulet, and Champetier, 1984) to linearize the nonlinear model using nonlinear transformations, such that the resulting linearized model in the transformed coordinate is the same about all operating points. This is desirable because it allows one to design a single linear control law in the transformed coordinate that is applicable for all operating points. However, it is not clear from the formulation how this can produce a reasonably large attractive region about a particular operating, or equilibrium, point. In addition, this reference does not discuss how to handle uncertainties when performing the transformation. For time-invariant problems with a continuum of constant operating points, such as stabilizing an inverted pendulum on a cart without controlling the cart position, extended linearization (Baumann, and Rugh, 1986) can be employed for local stabilization. Using this technique, one can employ a special choice of nonlinear control such that the linearized model of the nonlinear closed-loop system is stable and is the same for all operating points. In this reference, extended linearization is applied to the afore-mentioned cart-and-pole problem, and it is shown by means of simulations that the resulting attractive region is fairly large, but without showing how appropriate design parameters could be chosen to produce such results and how to handle modeling uncertainties. In addition, it

is not clear from the formulation how such linearization can produce a reasonably large attractive region for the nonlinear system. We note that when the cart position is not a controlled variable and no uncertainty is present in the model, it is not difficult to implement global stabilization of the pole angle (Slotine and Li, 1991). We do not consider techniques for moving from one operating point to another, such as gain scheduling, because we want to focus on obtaining a reasonably large attractive region about the equilibrium at the origin. We now discuss applications of linear controllers in the following situations:

Situation 1

In this situation, the linearized model about the origin of the system of interest is available and is time-invariant, but reliable uncertainty specifications are unavailable. In our discussion, a linear time-invariant model is called a "linearized model" if and only if it accurately represents the system of interest in sufficiently small regions about the origin, and stability of such linearized model implies local stability of the nonlinear system of interest. Assuming that the linearized model is locally state controllable or stabilizable, it is well known that a linear state-feedback controller can stabilize the corresponding nonlinear system in a sufficiently small neighborhood about an equilibrium point. Note that an uncertain nonlinear model can have a "certain" linearized model about an equilibrium point. To see this, consider the uncertain nonlinear model $\dot{x}_1 = \sin(x_1) + ax_1^2 + u$, where $a \in \Re^+$ is uncertain and the origin is the equilibrium point of interest. The linearized model about the origin is given by $\dot{x}_1 = x_1 + u$. We see that there is no uncertainty in the linearized model.

Given a linearized model without uncertainty specifications, it seems reasonable that we admit standard linear system theory or optimal control theory (Kwakernaak, and Sivan, 1972), (Kailath, 1980), (Zhou, 1996), (Skogestad, and Postlenthwaite, 1996), (Ogata, 1997), (Burl, 1999) for local stabilization. Using these approaches, some linear uncertainty specifications or linear stability margins are <u>assumed</u> for the linearized model, and a linear controller is designed to meet such specifications or margins. This may be achieved by relocating the eigenvalues of the linearized model, by optimizing a performance index subjected to the linearized model, or by shaping frequency-domain plots of the linearized model. A primary objective of such a linear controller is to provide good response characteristics while maintaining reasonable relative stability for the linearized model. However, the relationships between these properties and the size of the attractive region of the corresponding nonlinear system are not obvious. Indeed, such a linear controller guarantees only the existence, but not the size, of an attractive region about the equilibrium point of the nonlinear system. Indeed, it appears from numerous examples that a linear controller can perform effectively and robustly for a linearized model while yielding a small attractive region for the corresponding nonlinear system. Although it may happen that a linear state-feedback controller yields a reasonably large attractive region for the nonlinear system, the above techniques do not suggest in general how design parameters should be chosen to produce such a desirable result. It has been our experience that this usually comes at the expense of considerable trial-and-error.

Situation 2

In this situation, the linearized model may or may not be available. However, a

"nominal" linear time-invariant model and the associated uncertainty specifications are available. In our discussions, a "nominal model" is different from a linearized model in the sense that it may not represent the nonlinear model accurately in sufficiently small regions about the origin, and stability of a nominal model may not imply local stability of the nonlinear system. In most cases, we employ the linearized model as a nominal model. This is because the linearized model provides accurate information about behaviors of the nonlinear system in sufficiently small regions about the origin, while behaviors in larger regions about the origin may be drawn from the uncertainty specifications. However, the linearized model is not necessarily an appropriate nominal model, because the nonlinear model may be poorly cast and the corresponding linearized model may be associated with some undesirable characteristics of uncertainties. To see what we mean by a "nominal model", consider the following representation of the system of interest:

$$\dot{\mathbf{x}} = \mathbf{A}_n \mathbf{x} + \mathbf{B}_n \mathbf{u}(\mathbf{x}) + [\mathbf{f}(\mathbf{x},t) - \mathbf{A}_n \mathbf{x} + \mathbf{g}(\mathbf{x},t)\mathbf{u}(\mathbf{x}) - \mathbf{B}_n \mathbf{u}(\mathbf{x})]$$
$$\equiv \mathbf{A}_n \mathbf{x} + \mathbf{B}_n \mathbf{u}(\mathbf{x}) + \mathbf{f}_\Sigma(\mathbf{x},t,\mathbf{u}(\mathbf{x}))$$
$$\equiv \overline{\mathbf{A}}_n \mathbf{x} + \mathbf{f}_\Omega(\mathbf{x},t)$$

where $\mathbf{A}_n \in \mathfrak{R}^{n \times n}$, $\mathbf{B}_n \in \mathfrak{R}^{n \times m}$, $\mathbf{u}(\mathbf{x}) = -\mathbf{K}\mathbf{x}$, $\mathbf{K} \in \mathfrak{R}^{m \times n}$, $\overline{\mathbf{A}}_n \equiv [\mathbf{A}_n - \mathbf{B}_n \mathbf{K}] \in \mathfrak{R}^{n \times n}$,

$\mathbf{f}_\Sigma(\mathbf{x},t,\mathbf{u}(\mathbf{x})) \equiv [\mathbf{f}(\mathbf{x},t) - \mathbf{A}_n \mathbf{x} + \mathbf{g}(\mathbf{x},t)\mathbf{u}(\mathbf{x}) - \mathbf{B}_n \mathbf{u}(\mathbf{x})]$, and $\mathbf{f}_\Omega(\mathbf{x},t) \equiv \mathbf{f}_\Sigma(\mathbf{x},t,\mathbf{u}(\mathbf{x}))\big|_{\mathbf{u}=-\mathbf{K}\mathbf{x}}$.

The uncertain vector $\mathbf{f}_\Omega(\mathbf{x},t)$ lumps together all the nonlinearities, uncertainties, and modeling errors perturbing the nominal linear model $\dot{\mathbf{x}} = \mathbf{A}_n \mathbf{x} + \mathbf{B}_n \mathbf{u}(\mathbf{x})$, and we may now consider the system as a nominal linear model subjected to time-varying nonlinear uncertain perturbations. The subscript "n" denotes the available "nominal" model. This notation is the same as that for the order or dimension "n" of the system, but the intended meaning of "n" will be clear from the context.

Several researchers have examined stability of nonlinear systems $\dot{\mathbf{x}} = \overline{\mathbf{A}}_n \mathbf{x} + \mathbf{f}_\Omega(\mathbf{x},t)$

when $\overline{\mathbf{A}}_n$ and uncertainty specifications for $\dfrac{\left\| \mathbf{f}_\Omega(\mathbf{x},t) \right\|}{\left\| \mathbf{x} \right\|}$ are given. The objective is to find

a bound on $\dfrac{\left\| \mathbf{f}_\Omega(\mathbf{x},t) \right\|}{\left\| \mathbf{x} \right\|}$ for which the nonlinear system remains stable for all possible

$\mathbf{f}_\Omega(\mathbf{x},t)$ obeying this bound. One of the first papers addressing this problem was by Patal

et al (Patel, Toda, and Sridhar, 1977). This paper proposes that an LQR

$\mathbf{u}(\mathbf{x}) = \mathbf{u}_{LQR}(\mathbf{x}) \equiv -\mathbf{K}_{LQR}\mathbf{x}$ be designed first to stabilize the linear "nominal" model

$\dot{\mathbf{x}} = \mathbf{A}_n \mathbf{x} + \mathbf{B}_n \mathbf{u}(\mathbf{x})$, and to obtain $\overline{\mathbf{A}}_n$ without examining $\mathbf{f}_\Omega(\mathbf{x},t)$ in the design process.

Once such LQR is obtained, an allowable bound on $\dfrac{\left\| \mathbf{f}_\Omega(\mathbf{x},t) \right\|}{\left\| \mathbf{x} \right\|}$ for stability of the

nonlinear system is computed from a theorem developed therein. Using this theorem,

Patel et al showed robustness of an LQR in the presence of time-varying nonlinear

uncertainties. However, they neither demonstrated why an LQR should be chosen for this

purpose, nor proposed a guideline for how design parameters for the LQR should be

chosen to produce a reasonably large uncertainty bound. The formulation of uncertainty

bound in this paper does not exploit whatever structure of $\mathbf{f}_\Omega(\mathbf{x},t)$ may be available.

However, $\mathbf{f}_\Omega(\mathbf{x},t)$ is assumed to be both structured, and time-invariant (i.e.,

$\mathbf{f}_\Omega(\mathbf{x},t) = \mathbf{f}_\Omega(\mathbf{x}) = \mathbf{E}\mathbf{x}$, $\mathbf{E} \in \Re^{n \times n}$) in an example therein. In 1985, Vedavalli (Vedavalli,

1985) showed that a known structure of uncertainties could be employed to reduce

conservatism of the uncertainty bound in (Patel, Toda, and Sridhar, 1977). Indeed, he

proposed a less conservative bound for structured uncertainties $\mathbf{f}_\Omega(\mathbf{x}) = \mathbf{E}\mathbf{x}$. Since then,

less conservative bounds for structured, unstructured, linear, nonlinear, time-invariant,

and time-varying uncertainties have been proposed in several research works when $\overline{\mathbf{A}}_n$ is

given (Zhou, and Khargonekar, 1987), (Gao, and Antsaklis, 1993), (Chen, and Han, 1994), (Olas, 1994), (Olas, and Ahmadkhanlou, 1994), (Kim, 1995), (Lee et al, 1996). These research works focus on system analysis rather than on controller design. They do not suggest if a particular linear controller may have certain advantages over others.

It has been pointed out by Chen and Chen (Chen, and Chen, 1990), (Chen, and Chen, 1991) that applications of several existing robust control design techniques ((Chen, 1987), (Chen, and Leitmann, 1987), and references quoted therein) for linear systems with time-varying nonlinear uncertain perturbations are restrictive because they rely on assumptions such as the matching condition, which can be difficult to satisfy in practice. In addition, they pointed out that techniques that employ a necessary and sufficient condition for quadratic stabilization (Barmish, 1985) can be difficult to apply (Barmish, 1985) or to be conservative (Khargonekar, 1990). Our investigations agree with theirs. Using a two-level optimization scheme, Chen and Chen propose a linear controller design technique when the structure of the uncertain vector $\mathbf{f}_\Omega(\mathbf{x},t)$ is available. By means of examples, they showed that the resulting technique is applicable to several practical systems. When this optimization-based technique is applied to common examples employed in the existing research works, the results are considerably less conservative. Indeed, these are the least conservative we have found in the literature for those examples.

Our discussions progress from time-invariant Single-Input Multiple-Output (SIMO) systems to time-varying Multiple-Input Multiple-Output (MIMO) systems. The reader is

cautioned that properties, structures, and restrictions of the systems of interest are different from chapter to chapter. However, we impose that $\dot{\mathbf{x}}$ is piecewise continuous in t, and is locally Lipschitz in the operating region of interest in $\Re^n$ $\forall t \geq 0$ throughout our discussions. This is to guarantee existence and uniqueness of the solution of the differential equation of motion when applying Lyapunov stability (Khalil, 1996). We begin our discussions by considering SIMO time-invariant systems:

$$\begin{aligned} \dot{\mathbf{x}} &= \mathbf{f}(\mathbf{x}) + \mathbf{g}(\mathbf{x})u(\mathbf{x}) \\ \mathbf{y} &= \mathbf{Cx} \end{aligned} \tag{1.1}$$

where $\mathbf{f}(\mathbf{x}) \in \Re^n$, $\mathbf{g}(\mathbf{x}) \in \Re^n$, and $u(\mathbf{x}) \in \Re$.

1.2 Fundamental Idea of LARC

The fundamental idea of LARC is to employ a quadratic Lyapunov function to obtain a reasonably large attractive region for local stabilization of the nonlinear systems. We consider the available exact linearized model of (1.1) about the origin:

$$\dot{\mathbf{x}} = \mathbf{Ax} + \mathbf{B}u(\mathbf{x}) \tag{1.2}$$

Suppose that (1.2) is state controllable, and that we apply a linear state feedback control:

$$u(\mathbf{x}) = -\mathbf{Kx} \tag{1.3}$$

where $\mathbf{K} \equiv [k_1 \quad k_2 \quad \ldots \quad k_n]$ is a matrix of constants that locates all the eigenvalues of $\overline{\mathbf{A}} \equiv [\mathbf{A} - \mathbf{BK}] \in \Re^{n \times n}$ in the LHP. We employ (1.3) throughout our discussions unless otherwise stated. The linearized model under (1.3) is given by:

$$\dot{\mathbf{x}} = [\mathbf{A} - \mathbf{BK}]\mathbf{x} \equiv \overline{\mathbf{A}}\mathbf{x} \tag{1.4}$$

For $\overline{\mathbf{A}}$, we assign a positive-definite strictly-increasing quadratic Lyapunov function:

$$V(\mathbf{x}) = \frac{1}{2}\mathbf{x}^T\mathbf{P}\mathbf{x} \tag{1.5}$$

where $\mathbf{P}$ is a symmetric positive definite matrix satisfying the Lyapunov equation:

$$-\mathbf{Q} = \frac{1}{2}[\mathbf{P}\overline{\mathbf{A}} + \overline{\mathbf{A}}^T\mathbf{P}] \tag{1.6}$$

where $\mathbf{Q}$ is a symmetric positive definite matrix to be specified. For convenience, we select $\mathbf{Q} = \mathbf{I}$. Then $\mathbf{P}$, which we sometimes call "the original $\mathbf{P}$", may be obtained by solution of (1.6). Substituting this solution for $\mathbf{P}$ in (1.5) and differentiating the result with respect to time along the trajectories of the <u>nonlinear system</u> in (1.1) yield:

$$\begin{aligned}\dot{V}(\mathbf{x}) &= \mathbf{x}^T\mathbf{P}\mathbf{f}(\mathbf{x}) + \mathbf{x}^T\mathbf{P}\mathbf{g}(\mathbf{x})u(\mathbf{x}) \\ &\equiv F(\mathbf{x}) + G(\mathbf{x})u(\mathbf{x})\end{aligned} \tag{1.7}$$

where $F(\mathbf{x}) \equiv \mathbf{x}^T\mathbf{P}\mathbf{f}(\mathbf{x})$ and $G(\mathbf{x}) \equiv \mathbf{x}^T\mathbf{P}\mathbf{g}(\mathbf{x})$ are nonlinear scalar functions of state $\mathbf{x}$, and $F(\mathbf{0}) = G(\mathbf{0}) = 0$.

In what follows, we denote the 2-norm of $\mathbf{x}$ by $\|\mathbf{x}\|$, the transpose of $\mathbf{x}$ by $\mathbf{x}^T$, the boundary of a region ζ by O_ζ, abbreviate "region about the origin" with "region", "hyperplane" with "plane" unless otherwise stated, and define the following regions:

$$\beta_C \equiv \{\mathbf{x} \mid 0 \leq V(\mathbf{x}) < C, \ C \in \mathfrak{R}^+\} \tag{1.8}$$

$$B_L \equiv \{\mathbf{x} \mid \dot{V}(\mathbf{x}) < 0\} \cup \{\mathbf{0}\} \tag{1.9}$$

Since $V(\mathbf{x})$ is a quadratic positive definite function, β_C shrinks in <u>all</u> its dimensions as C decreases. This implies that we can force $\max(\|\mathbf{x}\|)$, $\forall \mathbf{x} \in \beta_C$ to be as small as we like by choosing a sufficiently small C. In fact, we propose to select $C = C_L$ such that β_C is

contained in B_L, whose existence is guaranteed by Lyapunov stability if $u(\mathbf{x})$ stabilizes

(1.2). We now define:

$$\beta_{C_L} \equiv \{\beta_C \mid \beta_{C,C=C_L} \subseteq B_L, \ \beta_{C,C>C_L} \not\subset B_L, \ C_L \in \Re^+\} \tag{1.10}$$

By definition (1.10), we see that β_{C_L} and B_L have at least one point in common at their

boundaries. Such a point is called a "common boundary point", and is denoted by $\mathbf{p}_i$

$\in \Re^n$, $i = 1, 2, \dots$. By definition (1.10), we see that β_{C_L} is radially large if and only if B_L

is radially large. We note that trajectories originating in $\beta_{C,C=C_B}$ for sufficiently large C_B

may or may not converge to the origin if $B_L \subset \beta_{C,C=C_B}$, $C_B \in \Re^+$. Indeed, the two

situations in which $\mathbf{x}_0 \in \beta_{C,C=C_L} \subset B_L$ and $\mathbf{x}_1 \in B_L \subset \beta_{C,C=C_B}$ can be illustrated in Fig.

1.1. Given that $\dot{V}(\mathbf{x})|_{\mathbf{x} \neq 0} < 0$ in B_L with $\dot{V}(\mathbf{0}) = 0$, we are guaranteed only the

convergence of the trajectory originating in $\beta_{C,C=C_L} \subset B_L$. Fig 1.1 illustrates possible

convergence and divergence from $\mathbf{x}_0$ and $\mathbf{x}_1$ respectively. Note that the trajectory from

$\mathbf{x}_1$ can escape from B_L although the trajectory travels such that Lyapunov function $V(\mathbf{x})$

decreases in B_L. This is because there are some portions of $\beta_{C,C=C_B}$ that do not belong

to B_L.

We call β_{C_L} a "Lyapunov Attractive Region" (LAR). By the Lyapunov stability, the

existence, uniqueness, and convergence of trajectories originating in β_{C_L} is guaranteed.

Our fundamental idea is to find a quadratic Lyapunov function and a controller that yield

a reasonably large β_{C_L}. By the sufficiency of Lyapunov stability, we know that the

attractive region must contain β_{C_L}. Because of this fundamental idea, we call our

technique Lyapunov Attractive Region Control (LARC). When such β_{C_L} is radially

unbounded and global stabilization is possible with $\mathbf{Q} = \mathbf{I}$, this stabilization is known as

"quadratic stabilization" (Barmish, 1985).
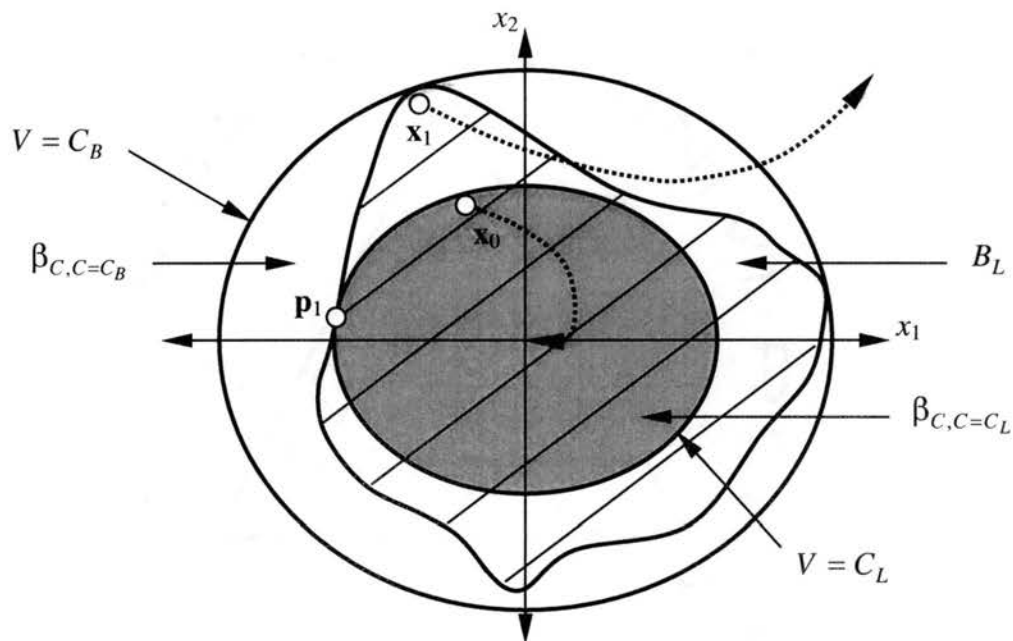
Fig. 1.1   Convergence and Divergence of Trajectories
Originating from $\mathbf{x}_0 \in \beta_{C,C=C_L} \subset B_L$ and from $\mathbf{x}_1 \in B_L \subset \beta_{C,C=C_B}$
Remark: $0 < C_L < C_B$

1.3   Theorems

In this section, we investigate how the quadratic Lyapunov function (1.5) can be chosen

to satisfy a necessary condition for obtaining a large β_{C_L} with system nonlinearities. In

our discussions, we assume that the following "basic conditions" are satisfied:

*C*1) **A** in (1.2) is strictly unstable.

Remark: From our experience, it is possible to develop LARC without

imposing *C*1. However, we find that imposing this can simplify

greatly several key analyses without loss of generality. Indeed, if

$\lambda_i(\mathbf{A}) \le 0 \ \ \forall i$, we write $[\mathbf{A} - \mathbf{BK}_U] = \mathbf{A}_U$ such that $\mathbf{A}_U$ is unstable

by using pole placement. This is always possible if *C*2 is satisfied.

Then substitute $\mathbf{A}_U + \mathbf{BK}_U$ for **A** in (1.2). Now, let $u(\mathbf{x}) = -\mathbf{K}_S\mathbf{x}$ to

obtain:

$$\dot{\mathbf{x}} = [\mathbf{A}_U + \mathbf{BK}_U]\mathbf{x} - \mathbf{BK}_S\mathbf{x}$$
$$= \mathbf{A}_U\mathbf{x} - \mathbf{B}[\mathbf{K}_S - \mathbf{K}_U]\mathbf{x}$$
$$\equiv \mathbf{A}_U\mathbf{x} - \mathbf{BKx}$$

where $\mathbf{K} \equiv \mathbf{K}_S - \mathbf{K}_U$, $\{\mathbf{A}, \mathbf{A}_U\} \in \Re^{n \times n}$, $\{\mathbf{K}^T, \mathbf{K}_U^T, \mathbf{K}_S^T\} \in \Re^n$. In

further analysis, we regard $\mathbf{A}_U$ as **A**. The matrix **K** is to be generated

using our procedure.

*C*2) [**A**, **B**] in (1.2) is controllable or stabilizable where controllability and

stabilizability are defined according to (Zhou et al, 1996) with $\mathbf{B} \ne \mathbf{0}$.

*C*3) $u(\mathbf{x}) = -\mathbf{Kx}$ where **K** is determined such that $\overline{\mathbf{A}} \equiv [\mathbf{A} - \mathbf{BK}]$ is stable. If **A** is

stable, the true linear gain matrix is given by $\mathbf{K}_S = \mathbf{K} - \mathbf{K}_U$.

*C*4) The symmetric positive definite matrix **P** is determined from the Lyapunov

equation $-\mathbf{Q} = \dfrac{1}{2}[\mathbf{P}\overline{\mathbf{A}} + \overline{\mathbf{A}}^T\mathbf{P}]$, where $\mathbf{Q} \in \Re^{n \times n}$ is a symmetric positive definite

matrix.

Lemma 1.1   (Relationship between $S_{G_L=0}$ and $R_{[F_L<0]\cup\{0\}}$)

If the basic conditions $C1$–$C4$ are satisfied then:

$$S_{G_L=0} \subset R_{[F_L<0]\cup\{0\}}$$

where $R_{[F_L<0]\cup\{0\}} \equiv \{\mathbf{x} \mid F_L(\mathbf{x}) < 0\} \cup \{\mathbf{0}\}$, $S_{G_L=0} \equiv \{\mathbf{x} \mid G_L(\mathbf{x}) = 0\}$, $G_L(\mathbf{x}) \equiv \mathbf{x}^T\mathbf{PB}$,

$F_L(\mathbf{x}) \equiv \mathbf{x}^T\mathbf{PAx}$, and $\mathbf{P}$ and $\mathbf{Q}$ are symmetric positive definite matrices.

Proof

Consider the time derivative of the quadratic Lyapunov function (1.5) along the

trajectories of the linearized model (1.2) under a linear control $u(\mathbf{x})$ in (1.3):

$$\begin{aligned}
\dot{V}_L(\mathbf{x}) &= \mathbf{x}^T\mathbf{PAx} + \mathbf{x}^T\mathbf{PB}u(\mathbf{x}) \\
&\equiv F_L(\mathbf{x}) + G_L(\mathbf{x})u(\mathbf{x})
\end{aligned}$$

(1.11)

where $G_L(\mathbf{x}) \equiv \mathbf{x}^T\mathbf{PB} \in \Re$, $F_L(\mathbf{x}) \equiv \mathbf{x}^T\mathbf{PAx} \in \Re$. The subscript "$L$" in $\dot{V}_L(\mathbf{x})$, $G_L(\mathbf{x})$ and

$F_L(\mathbf{x})$ denotes that they are defined with respect to the linearized model. Notice that

$G_L(\mathbf{x})$ is a linear function of $\mathbf{x}$ implying that $S_{G_L=0}$ exists and is a plane in n-space. By

Lyapunov stability, the existence of the stabilizing linear gain matrix $\mathbf{K}$ guarantees the

existence of a symmetric positive definite matrix $\mathbf{P}$ such that $\dot{V}_L(\mathbf{x})$ is globally negative

definite. The coexistence of the plane $S_{G_L=0}$ and the globally negative definite function

$\dot{V}_L(\mathbf{x})$ implies that:

1)   The region $R_{[F_L<0]\cup\{0\}}$ exists.

2) $S_{G_L=0} \subset R_{[F_L<0]\cup\{0\}}$

This completes the proof.

Since (1.2) approximates (1.1) about the origin, it can be drawn directly from Lemma 1.1 that for the nonlinear systems (for which we drop subscripts "L"), $S_{G=0} \subset R_{[F<0] \cup \{0\}}$ in sufficiently small regions about the origin when $C1 - C4$ are satisfied. We claim that the "largest possible LAR" corresponding to a solution $\mathbf{P}$ of the Lyapunov equation is the region:

$$\beta_{C_S} \equiv \{\mathbf{x} \mid 0 \leq V(\mathbf{x}) < C_S, \ [G(\mathbf{x}) = 0] \Rightarrow [F(\mathbf{x}) < 0]\} \tag{1.12}$$

where $C_S \in \mathfrak{R}^+$ is the largest possible number such that both of the conditions in (1.12) are satisfied. For a given $\mathbf{P}$, β_{C_S} can be obtained by increasing C in (1.8) from C_L in (1.10) until the boundary of β_C <u>first</u> touches a point where $G = 0$ and $F = 0$ at $C = C_S$, where $C_S \geq C_L > 0$. We denote the region $\beta_{C,C=C_S}$ by β_{C_S} and such a point by $\mathbf{x}_{C_{Si}}$, $i = 1, 2, \ldots$. By the definition of $\mathbf{x}_{C_{Si}}$, it is necessary that $\dot{V}(\mathbf{x}_{C_{Si}}) = 0 \ \forall i$. In addition, $\mathbf{x}_{C_{Si}} \neq \mathbf{0}$ because the boundary of β_{C_L} does not contain $\mathbf{0}$. The latter follows directly from (1.10) by noting the existence of B_L is guaranteed if $\overline{\mathbf{A}}$ is stable, $\mathbf{x}_{C_{Si}} \in O_{B_L}$, and $\mathbf{0} \notin O_{B_L}$. To show the existence of β_{C_S} such that $\beta_{C_L} \subseteq \beta_{C_S}$, it is sufficient to show that the interior of β_{C_L} does not contain $\mathbf{x}_{C_{Si}} \ \forall i$. Indeed, we know from (1.10) that $\beta_{C_L} \subseteq B_L$. Accordingly, it is necessary that $\dot{V}(\mathbf{x})\big|_{\mathbf{x} \neq \mathbf{0}} < 0$ if $\mathbf{x}$ is contained in the interior of β_{C_L}. Because $\dot{V}(\mathbf{x}_{C_{Si}}) = 0 \ \forall i$, it follows that $\mathbf{x}_{C_{Si}}$ are not contained in the interior of $\beta_{C_L} \ \forall i$. We see from (1.7) and (1.12) that:

1)   The existence of $\mathbf{x}_{C_{Si}}$, $i = 1, 2, \ldots$ limits the dimensions of β_{C_S}.

2)   We can force $\dot{V}(\mathbf{x})$ to be negative definite in β_{C_S} by manipulating $u(\mathbf{x})$.

Because our fundamental idea is to obtain a large β_{C_L}, it is desirable that β_{C_S} be as large as possible because β_{C_S} is the largest possible β_{C_L} that can be obtained by manipulating $u(\mathbf{x})$. This implies that the matrix $\mathbf{P}$ in the quadratic Lyapunov function (1.5) should chosen such that $\mathbf{x}_{C_{Si}}$ is as far from the origin as possible. A possible approach to do this is to exploit specific structures and nonlinearities in the functions $F(\mathbf{x})$ and $G(\mathbf{x})$.

However, we do not follow this approach because:

1)   We realize that the characteristics of $S_{F=0}$ and $S_{G=0}$ in many physical systems are extremely difficult to analyze to find such $\mathbf{P}$. Accordingly, reasonable simplifications are needed to make the problem tractable.

2)   We desire that the applicability of the resulting scheme is not limited by specific structures of the systems other than (1.1).

To explore how to construct such $\mathbf{P}$ for the quadratic Lyapunov function, we now consider some important characteristics of $G_L(\mathbf{x})$ and of $F_L(\mathbf{x})$ in the following theorems:

Theorem 1.1   (Characteristics of Eigenvalues of $\mathbf{M}$)

If the basic conditions $C1$-$C4$ are satisfied then the symmetric matrix:

$$\mathbf{M} \equiv \frac{1}{2}[\mathbf{PA} + [\mathbf{PA}]^T]$$
(1.13)

has only real eigenvalues, with exactly one positive eigenvalue and $n-1$ negative eigenvalues.

Proof

We begin by referring to the Lyapunov stability theorem and state without proof that the existence of such $\mathbf{P}$ in Theorem 1.1 is guaranteed when $C1 - C4$ are satisfied. Now we differentiate the quadratic Lyapunov function (1.5) along the trajectories of the linearized model (1.2):

$$
\begin{aligned}
\dot{V}_L(\mathbf{x}) &= \frac{1}{2}[\mathbf{x}^T\mathbf{A}^T\mathbf{Px} + \mathbf{x}^T\mathbf{PAx} + \mathbf{B}^T\mathbf{Px}u(\mathbf{x}) + \mathbf{x}^T\mathbf{PB}u(\mathbf{x})] \\
&= \frac{1}{2}\mathbf{x}^T\big[\mathbf{PA} + [\mathbf{PA}]^T\big]\mathbf{x} + \mathbf{x}^T\mathbf{PB}u(\mathbf{x}) \qquad\qquad (1.14) \\
&\equiv \mathbf{x}^T\mathbf{Mx} + \mathbf{x}^T\mathbf{PB}u(\mathbf{x}) \\
&\equiv F_L(\mathbf{x}) + G_L(\mathbf{x})u(\mathbf{x})
\end{aligned}
$$

where $\mathbf{M} \equiv \frac{1}{2}[\mathbf{PA} + [\mathbf{PA}]^T]$, $F_L(\mathbf{x}) \equiv \mathbf{x}^T\mathbf{Mx}$, and $G_L(\mathbf{x}) \equiv \mathbf{x}^T\mathbf{PB}$. Note for (1.14) that $\mathbf{M}$ is symmetric because $\mathbf{\Xi} + \mathbf{\Xi}^T$ is symmetric for all $\mathbf{\Xi} \in \Re^{n\times n}$, and $\mathbf{x}^T\mathbf{PB} = \mathbf{B}^T\mathbf{Px}$ because $\mathbf{P}$ is symmetric and $\mathbf{x}^T\mathbf{PB} \in \Re$. Since $\mathbf{M}$ is a real symmetric matrix, it has a set of n real eigenvalues $\lambda_\mathbf{M}$ and a set of the corresponding n real orthogonal eigenvectors $V_\mathbf{M}$, where $\lambda_\mathbf{M} = \{\lambda_{\mathbf{M}1},...,\lambda_{\mathbf{M}n}\}$ and $V_\mathbf{M} = \{\mathbf{v}_{\mathbf{M}1},...,\mathbf{v}_{\mathbf{M}n}\}$ respectively (Hagan et al, 1996). Without loss of generality, we assume that $\mathbf{v}_{\mathbf{M}i}$ are normalized such that $\mathbf{v}_{\mathbf{M}i}^T\mathbf{v}_{\mathbf{M}i} = 1$, $i = 1,2,...,n$. It is clear that we can employ this set of orthonormal eigenvectors as a basis set for generating $\Re^n$.

Notice that $C2$ and $C3$ imply the existence of $u(\mathbf{x})$ such that $\dot{V}_L(\mathbf{x})$ is globally negative definite. By Lemma 1.1, this guarantees that $F_L(\mathbf{x}) < 0$ on $S_{G_L=0} \equiv \{\mathbf{x} \mid G_L(\mathbf{x}) = 0\}$ and on $S_{u=0} \equiv \{\mathbf{x} \mid u(\mathbf{x}) = 0\}$ except at the origin where $F_L(\mathbf{0}) = G_L(\mathbf{0}) = u(\mathbf{0}) = 0$. By $C1$,

(Proof of Theorem 1.1 (Cont.))

$F_L(\mathbf{x}) \equiv \mathbf{x}^T \mathbf{M} \mathbf{x}$ must be positive at some $\mathbf{x}$ that does not belong to $S_{G_L=0}$ and $S_{u=0}$ except at the origin. Next, we consider $S_{G_L=0}$. Since $\mathbf{P}$ and $\mathbf{B}$ are constant matrices, we see that the surface $S_{G_L} = 0$ exists and is a plane. Expanding the equation $G_L(\mathbf{x}) = 0$, we obtain a homogeneous linear equation:

$$
\begin{aligned}
G_L(\mathbf{x}) &= 0 \\
&= \hat{c}_1 x_1 + \hat{c}_2 x_2 + ... + \hat{c}_n x_n \\
&\equiv \hat{\mathbf{C}} \mathbf{x}
\end{aligned}
\tag{1.15}
$$

where $\hat{c}_i$, $i = 1, 2, ..., n$ are real constants and $\hat{\mathbf{C}} \equiv [\hat{c}_1 \quad \hat{c}_2 \quad ... \quad \hat{c}_n]$. We see that the surface $S_{G_L=0} \equiv \{\mathbf{x} \mid G_L(\mathbf{x}) = 0\}$ is the set of all solutions of the linear equation (1.15) in n unknowns and thus a subspace of $\Re^n$. From basic linear algebra (Curtis, 1984), (Roman, 1992), we have:

Theorem 1.1.1

The dimension of the solution space of a system of homogeneous linear equations in n unknowns is n-r where r is the rank of the coefficient matrix.

Accordingly, the dimension of the solution space of (1.15) is $n - 1$, because the dimension of $\hat{\mathbf{C}}$ is $1 \times n$, such that $\text{rank}(\hat{\mathbf{C}}) = 1$. Since the dimension of a subspace of solution vectors is defined as the number of linearly independent vectors in a basis set generating the subspace, we have that the number of linearly independent vectors that generates the subspace defined by:

$$
S_{G_L=0} \equiv \{\mathbf{x} \mid G_L(\mathbf{x}) = 0\} = S_{G_L=0}
\tag{1.16}
$$

(Proof of Theorem 1.1 (Cont.))

is n-1. Depending on the point we want to discuss, we alternatively denote the set

$\{\mathbf{x} \mid G_L(\mathbf{x}) = 0\}$ by $S_{G_L=0}$ or by $\mathcal{S}_{G_L=0}$ when we want to consider it as a subspace or as a

surface, respectively.

Since $\dot{V}_L(\mathbf{x})$ is globally negative definite, it must be true that $F_L(\mathbf{x}) \equiv \mathbf{x}^T \mathbf{M} \mathbf{x} < 0$ on

$S_{u=0}$ where $\mathbf{x} \neq 0$. In addition, it is immediate from (1.14) that $F_L(\mathbf{x}) > 0$ for some

$\mathbf{x} \notin S_{u=0}$ because $\mathbf{A}$ is unstable. Since $F_L(\mathbf{x})$ is quadratic, the fact that $F_L(\mathbf{x})$ changes

signs implies that the real symmetric matrix $\mathbf{M}$ has at least one positive eigenvalue, and at

least one negative eigenvalue. Now, assume for the moment that $\mathbf{M}$ has more than one

positive eigenvalue, and arrange the set of eigenvalues and eigenvectors of $\mathbf{M}$ as

$\lambda_{\mathbf{M}} = \{\lambda_{\mathbf{M}1}, \lambda_{\mathbf{M}2}, \dots, \lambda_{\mathbf{M}j}, \dots, \lambda_{\mathbf{M}n}\}$ and $V_{\mathbf{M}} = \{\mathbf{v}_{\mathbf{M}1}, \mathbf{v}_{\mathbf{M}2}, \dots, \mathbf{v}_{\mathbf{M}j}, \dots, \mathbf{v}_{\mathbf{M}n}\}$ such that $\lambda_{\mathbf{M}1}$,

$\lambda_{\mathbf{M}2}, \dots, \lambda_{\mathbf{M}j}$ are positive. Arranging in this fashion, we have that $j < n$ because we have

shown that $\mathbf{M}$ has at least one negative eigenvalue. Now, we apply the linear

transformation:

$$\mathbf{x} = \mathbf{T}_{\mathbf{M}} \mathbf{z} \tag{1.17}$$

where $\mathbf{z} \in \mathfrak{R}^n$, and

$$\mathbf{T}_{\mathbf{M}} = [\mathbf{v}_{\mathbf{M}1} \mid \mathbf{v}_{\mathbf{M}2} \mid \dots \mid \mathbf{v}_{\mathbf{M}n}] \tag{1.18}$$

Accordingly,

$$F_L(\mathbf{x})\big|_{\mathbf{x}=\mathbf{T}_{\mathbf{M}}\mathbf{z}} = F_{L_T}(\mathbf{z}) = \mathbf{z}^T \mathbf{T}_{\mathbf{M}}^T \mathbf{M} \mathbf{T}_{\mathbf{M}} \mathbf{z} \equiv \mathbf{z}^T \mathbf{M}_T \mathbf{z} \tag{1.19}$$

where $\mathbf{M}_T \equiv \mathbf{T}_{\mathbf{M}}^T \mathbf{M} \mathbf{T}_{\mathbf{M}}$. Using this reduction to principal axes (Ortega, 1990), we have

that $\mathbf{M}_T$ is a diagonal matrix whose diagonal entries are the eigenvalues $\lambda_{\mathbf{M}i}$, $i = 1, \dots, n$

(Proof of Theorem 1.1 (Cont.))

of **M**. Expanding the right-hand side of (1.19) yields:

$$F_L(\mathbf{x})\big|_{\mathbf{x}=\mathbf{T_M z}} = F_{L_T}(\mathbf{z}) = \lambda_{M1}z_1^2 + \lambda_{M2}z_2^2 + \ldots + \lambda_{Mn}z_n^2 = 0 \qquad (1.20)$$

Since z_i is along $\mathbf{v}_{Mi}$ $i = 1, \ldots, n$, and λ_{M1}, λ_{M2}, ..., λ_{Mj} are positive, it follows that:

$$
\begin{aligned}
\mathbf{\Theta} &\equiv \{\mathbf{x} \mid \mathbf{x} = z_1\mathbf{v}_{M1} + z_2\mathbf{v}_{M2}\ldots + z_j\mathbf{v}_{Mj}, \text{where } z_1, z_2, \ldots, z_j \in \mathfrak{R}\} \\
&\in \{\mathbf{x} \mid F_L(\mathbf{x}) = \mathbf{x}^T\mathbf{M}\mathbf{x} > 0\} \cup \{\mathbf{0}\} \equiv R_{[F_L>0]\cup\{\mathbf{0}\}}
\end{aligned}
\qquad (1.21)
$$

where $\mathbf{\Theta}$ is a <u>subspace</u> generated by the basis set $\{\mathbf{v}_{M1}, \mathbf{v}_{M2}, \ldots, \mathbf{v}_{Mj}\}$. The subspace

$\mathbf{\Theta}$ has dimension j, and $F_L(\mathbf{x}) > 0$ for all $\mathbf{x}$ belonging to this subspace except at the

origin where $F_L(\mathbf{0}) = 0$. From basic linear algebra (Curtis, 1984), (Roman, 1992), we

have:

Theorem 1.1.2

Let W and Z be finitely generated subspaces of a vector space $\overline{V}$. Then $W \cap Z$ and

$W + Z$ are finitely generated subspaces, and we have:

$$\dim(W + Z) + \dim(W \cap Z) = \dim(W) + \dim(Z) \qquad (1.22)$$

where $W + Z = \{\mathbf{w} + \mathbf{z} \mid \mathbf{w} \in W, \mathbf{z} \in Z\}$.

Applying this theorem to our problem, we let $W \equiv S_{G_L=0}$ and $Z \equiv \mathbf{\Theta}$. We have that:

*F*1) $\dim(W+Z)$ is at most n because $\mathbf{x} \in \mathfrak{R}^n$ $\forall \mathbf{x}$.

*F*2) $\dim(W) = n-1$ because the rank of $\hat{\mathbf{C}}$ in (1.15) is one.

*F*3) $\dim(Z) = j > 1$ because we assume that **M** has more than one positive eigenvalue.

(Proof of Theorem 1.1 (Cont.))

F4) $\dim(W \cap Z) = \dim(\{\mathbf{0}\}) = 0$ because $F_L(\mathbf{x}) < 0$ on $S_{G_L=0}$ except at the origin

where $F_L(\mathbf{0}) = G_L(\mathbf{0}) = 0$.

It follows from F2 and F3 that $\dim(W) + \dim(Z) > n$. Since $\dim(W+Z)$ is at most n, it

follows from (1.22) that $\dim(W \cap Z) \geq 1$. But this cannot be true by F4. This

contradiction implies that $\mathbf{M}$ has exactly one positive eigenvalue. By our arrangement,

this positive eigenvalue is $\lambda_{\mathbf{M}1}$. This completes the first part of the proof.

From the fact that $\mathbf{M}$ has exactly one positive eigenvalue, it may not be obvious that the

remaining n-1 eigenvalues of $\mathbf{M}$ are all negative. However, the following analysis shows

that this is true. We recall now that and there are $n-1$ linearly independent vectors

spanning $S_{G_L=0}$. Since $\dot{V}_L(\mathbf{x})$ is negative definite, $S_{G_L=0}$ must be contained in

$\{\mathbf{x} \mid F_L(\mathbf{x}) = \mathbf{x}^T \mathbf{M}\mathbf{x} < 0\} \cup \{\mathbf{0}\} \equiv R_{[F_L<0]\cup\{\mathbf{0}\}}$. This is true if and only if $R_{[F_L<0]\cup\{\mathbf{0}\}}$

contains at least n-1 linearly independent vectors because these are needed to span $S_{G_L=0}$.

Since we know now that $\lambda_{\mathbf{M}1} > 0$, it follows that $R_{[F_L<0]\cup\{\mathbf{0}\}}$ does not contain $\mathbf{v}_{\mathbf{M}1}$. If $\mathbf{M}$

has at least one zero eigenvalue $\lambda_{\mathbf{M}k}$ in $\{\lambda_{\mathbf{M}2},...,\lambda_{\mathbf{M}k},..., \lambda_{\mathbf{M}n}\}$ then $R_{[F_L<0]\cup\{\mathbf{0}\}}$ does not

contain two linearly independent vectors $\mathbf{v}_{\mathbf{M}1}$ and $\mathbf{v}_{\mathbf{M}k}$. This implies that $R_{[F_L<0]\cup\{\mathbf{0}\}}$ can

contain at most n-2 linearly independent vectors because $R_{[F_L<0]\cup\{\mathbf{0}\}} \subset \mathfrak{R}^n$. We see that

this contradicts the known fact that $R_{[F_L<0]\cup\{\mathbf{0}\}}$ contains at least n-1 linearly independent

vectors spanning $S_{G_L=0}$. Accordingly, no eigenvalue of $\mathbf{M}$ can be zero and we then

conclude that the remaining eigenvalues $\lambda_{\mathbf{M}2},..., \lambda_{\mathbf{M}n}$ are all negative. This completes

the proof of Theorem 1.1.

We consider next the concept of symmetry of a surface about an axis. Our following

discussion can be found in (Curtis, 1984), (Roman, 1992) respectively. Let us begin by

using a two dimensional example to recall the concept. Assuming that we have a parabola

$f(x, y) = y - x^2 = 0$. A simple means to describe the symmetry of the parabola about the

y axis is to assert that the right half of the parabola exactly coincides with the left half

when the x-y plane is folded along the y axis. However, it is clear that this simple means

works well only in two-dimensional cases. To be more precise, we observe that such

plane folding can be algebraically described as a linear transformation which sends the

point (x, y) to $(-x, y)$ such that both (x, y) and $(-x, y)$ are on the parabola. In n-

dimensional space, this implies that the symmetry of a surface $f(x_1, ..., x_{i-1}, x_i, x_{i+1},$

$..., x_n) = 0$ about the x_i-axis can be asserted if and only if $f(-x_1, ..., -x_{i-1}, x_i, - x_{i+1},$

$..., -x_n) = 0$. This leads us to:

Theorem 1.2 (Symmetry of $S_{F_L=0}$ about Eigenvectors of **M**)

The surface $S_{F_L=0}$ is symmetric about the axes along the eigenvectors $\mathbf{v}_{M1}, ..., \mathbf{v}_{Mn}$ of **M**.

In addition, $S_{F_L=0}$ is symmetric about the plane spanned by $\mathbf{v}_{M2}, ..., \mathbf{v}_{Mn}$.

Proof

We first diagonalize **M** using the linear transformation $\mathbf{x} = \mathbf{T_M z}$, where $\mathbf{T_M}$ is given by

(1.18). From the proof of Theorem 1.1, the surface $S_{F_L=0}$ can be described in the

transformed basis by:

$$F_L(\mathbf{x})\big|_{\mathbf{x}=\mathbf{T}_\mathbf{M}\mathbf{z}} = F_{L_T}(\mathbf{z}) = \lambda_{M1}z_1^2 + \lambda_{M2}z_2^2 + \ldots + \lambda_{Mn}z_n^2 = 0 \qquad (1.20)$$

It is clear that if the vector $\mathbf{z}_1 = [z_1 \; \ldots \; z_{i-1} \; z_i \; z_{i+1} \; \ldots \; z_n]^T$ satisfies (1.20) then so does

the vector $\mathbf{z}_2 = [-z_1 \; \ldots \; -z_{i-1} \; z_i \; -z_{i+1} \; \ldots \; -z_n]^T$ for $i = 1, \ldots, n$, and it follows that the

surface $F_{L_T}(\mathbf{z}) = 0$ is symmetric about the z_i axis. By construction of

the transformation matrix $\mathbf{T}$, the z_i axis in the basis $\{\mathbf{v}_{M1},\ldots,\mathbf{v}_{Mn}\}$ points in the direction

of $\mathbf{v}_{Mi}$ in the original basis for $i = 1, \ldots, n$ because $\{\mathbf{v}_{M1},\ldots,\mathbf{v}_{Mn}\}$ is used as the basis for

the reduction to principal axes. Accordingly, we conclude that the surface $S_{F_L=0}$ is

symmetric about the axes along the eigenvectors $\mathbf{v}_{M1},\ldots,\mathbf{v}_{Mn}$ in the original basis. This

completes the first part of the proof.

We now consider a vector in the plane spanned by the set $\{\mathbf{v}_{M2},\ldots,\mathbf{v}_{Mn}\}$ for which

$\lambda_{Mi} < 0 \;\; 1 = 2,3,\ldots,n$. A vector in $\mathfrak{R}^n$ belongs to this plane if and only if the first

component of this vector is zero in the principal basis of $\mathbf{M}$. For convenience, we denote

a vector in this plane by $\mathbf{z}_{\{\mathbf{v}_{M2},\ldots,\mathbf{v}_{Mn}\}} = [0 \; z_2 \; \ldots \; z_n]^T$. Now consider a vector

$\mathbf{z} \in S_{F_L=0}$ denoted by $\mathbf{z} \equiv \mathbf{z}_{F_L=0,1} = [z_1 \; z_2 \; \ldots \; z_n]^T$. We see that the symmetry of $S_{F_L=0}$

about the plane spanned by $\{\mathbf{v}_{M2},\ldots,\mathbf{v}_{Mn}\}$ can be asserted if $\mathbf{z} = [-z_1 \; z_2 \; \ldots \; z_n]^T$ also

belongs to $S_{F_L=0}$. Indeed, examining (1.20) shows that if $\mathbf{z}_{F_L=0,1}$ belong $S_{F_L=0}$ then so is

$\mathbf{z} = [-z_1 \; z_2 \; \ldots \; z_n]^T$ denoted by $\mathbf{z}_{F_L=0,2}$. This completes the proof of Theorem 1.2.

We now state the symmetry property of $S_{F_L=0}$ about the plane spanned by $\{\mathbf{v}_{M2},\ldots,\mathbf{v}_{Mn}\}$

using geometry. From (1.20), we see that $F_L(\mathbf{x})\big|_{\mathbf{x}=\mathbf{T}_\mathbf{M}\mathbf{z}} < 0$ at every point $\mathbf{z} = \mathbf{z}_{\{\mathbf{v}_{M2},\ldots,\mathbf{v}_{Mn}\}}$

$= \begin{bmatrix} 0 & z_2 & \dots & z_n \end{bmatrix}^T$ on this plane because $\lambda_{Mi} < 0$, $i = 2, 3, \dots, n$ except at the origin

where $F_L(\mathbf{0}) = 0$. Starting at a point $\mathbf{z} = \mathbf{z}_{\{v_{M2}, \dots, v_{Mn}\}}$, it follows from (1.20) that

$F_L(\mathbf{x})\big|_{\mathbf{x} = \mathbf{T}_M \mathbf{z}}$ increases from a negative value as the first component of $\mathbf{z}_{\{v_{M2}, \dots, v_{Mn}\}}$

increases from zero because $\lambda_{M1} > 0$. In addition, we know by inspecting (1.20) that

there exists a sufficiently large value of z_1 for this first component such that

$F_L(\mathbf{x})\big|_{\mathbf{x} = \mathbf{T}_M \mathbf{z}} = 0$ at a new point $\mathbf{z} = \begin{bmatrix} z_1 & z_2 & \dots & z_n \end{bmatrix}^T$ denoted by $\mathbf{z}_{F_L = 0,1}$. It follows that the

vector $\mathbf{z}_{F_L = 0,1} - \mathbf{z}_{\{v_{M2}, \dots, v_{Mn}\}} = \begin{bmatrix} z_1 & 0 & \dots & 0 \end{bmatrix}^T$ denoted by $\mathbf{z}_{\Delta 1}$ is <u>orthogonal</u> to the plane

spanned by $\{\mathbf{v}_{M2}, \dots, \mathbf{v}_{Mn}\}$ because $[\mathbf{z}_{\Delta 1}^T][\mathbf{z}_{\{v_{M2}, \dots, v_{Mn}\}}] = 0$. Geometrically, the vector

$\mathbf{z}_{\Delta 1}$ emanates orthogonally from the plane spanned by $\{\mathbf{v}_{M2}, \dots, \mathbf{v}_{Mn}\}$, and terminates at

$\mathbf{z} = \mathbf{z}_{F_L = 0,1} \in S_{F_L = 0}$.

Now, consider the situation when we start from $\mathbf{z} = \mathbf{z}_{\{v_{M2}, \dots, v_{Mn}\}}$, but the first component

of $\mathbf{z}_{\{v_{M2}, \dots, v_{Mn}\}}$ decreases from zero. By examining (1.20), we see that $F_L(\mathbf{x})\big|_{\mathbf{x} = \mathbf{T}_M \mathbf{z}} = 0$

exactly at the point $\mathbf{z} = \begin{bmatrix} -z_1 & z_2 & \dots & z_n \end{bmatrix}^T$ denoted by $\mathbf{z}_{F_L = 0,2}$. In the same fashion, we

have that $\mathbf{z}_{F_L = 0,2} - \mathbf{z}_{\{v_{M2}, \dots, v_{Mn}\}} = \begin{bmatrix} -z_1 & 0 & \dots & 0 \end{bmatrix}^T$ denoted by $\mathbf{z}_{\Delta 2}$ is orthogonal to the

plane spanned by $\{\mathbf{v}_{M2}, \dots, \mathbf{v}_{Mn}\}$ because $\mathbf{z}_{\Delta 2}^T \mathbf{z}_{\{v_{M2}, \dots, v_{Mn}\}} = 0$. Geometrically, the vector

$\mathbf{z}_{\Delta 2}$ emanates orthogonally from the plane spanned by $\{\mathbf{v}_{M2}, \dots, \mathbf{v}_{Mn}\}$ in the direction

opposite to that of $\mathbf{z}_{\Delta 1}$, and terminates at $\mathbf{z} = \mathbf{z}_{F_L = 0,2} \in S_{F_L = 0}$. <u>Notice that the lengths of</u>

<u>the orthogonal vectors</u> $\mathbf{z}_{\Delta 1}$ <u>and</u> $\mathbf{z}_{\Delta 2}$ <u>are the same</u>. It is because of this property that we

assert the symmetry of $S_{F_L = 0}$ about the plane spanned by $\{\mathbf{v}_{M2}, \dots, \mathbf{v}_{Mn}\}$.

1.4   Effects of Nonlinearities on LAR

Because of the nonlinearities in the original equation of motion (1.1), the deviations of

$S_{G=0}$ from $S_{G_L=0}$, and of $S_{F=0}$ from $S_{F_L=0}$ is to be expected <u>except</u> at the origin. In this

section, we consider the situation when $S_{F=0}$ approaches $S_{G=0}$ and intersects $S_{G=0}$ at

$\mathbf{x}_{C_{Si}}$ $i = 1,2,...$ where $G(\mathbf{x}_{C_{Si}}) = F(\mathbf{x}_{C_{Si}}) = 0$, although $S_{F_L=0}$ does not intersect $S_{G_L=0}$.

The existence of $\mathbf{x}_{C_{Si}}$ implies that β_{C_S} (defined in (1.12)) is not radially unbounded and

makes it impossible to guarantee global stability using the current quadratic Lyapunov

function, which depends only on the matrix $\mathbf{P}$. For the nonlinear systems (1.1), we desire

that β_{C_L} be large. But since $\beta_{C_L} \subseteq \beta_{C_S}$, it is necessary that β_{C_S} be large. Because of

this, it is necessary that such intersection $\mathbf{x}_{C_{Si}}$ are far from the origin $\forall i$ to obtain a large

β_{C_S}.

Proposition 1.1   (Eigenvector Condition)

Intuitively, we know that if $\mathbf{P}$ is chosen such that $S_{G_L=0}$ runs close to a particular portion

of $S_{F_L=0}$, then small deviations of $S_{G=0}$ from $S_{G_L=0}$ and of $S_{F=0}$ from $S_{F_L=0}$ can result

in an intersection $\mathbf{x}_{C_{Si}}$ between $S_{G=0}$ and $S_{F=0}$. For this proposition 1.1, we restrict

ourselves to two dimensional systems. For a two-dimensional system, this situation can

be illustrated in Fig. 1.2, which is drawn according to Lemma 1.1, Theorem 1.1, and

Theorem 1.2. We note for Fig. 1.2 (a) and (b) the following representations:

1) $F(\mathbf{x}) = 0$ on the two bold solid curves denoted by $S_{F=0,1}$ and $S_{F=0,2}$.

2) $F_L(\mathbf{x}) = 0$ on the two thin solid lines denoted by $S_{F_L=0,1}$ and $S_{F_L=0,2}$.

3) $G(\mathbf{x}) = 0$ on the bold dashed curve denoted by $S_{G=0}$.

4) $G_L(\mathbf{x}) = 0$ on the thin dashed line denoted by $S_{G_L=0}$.
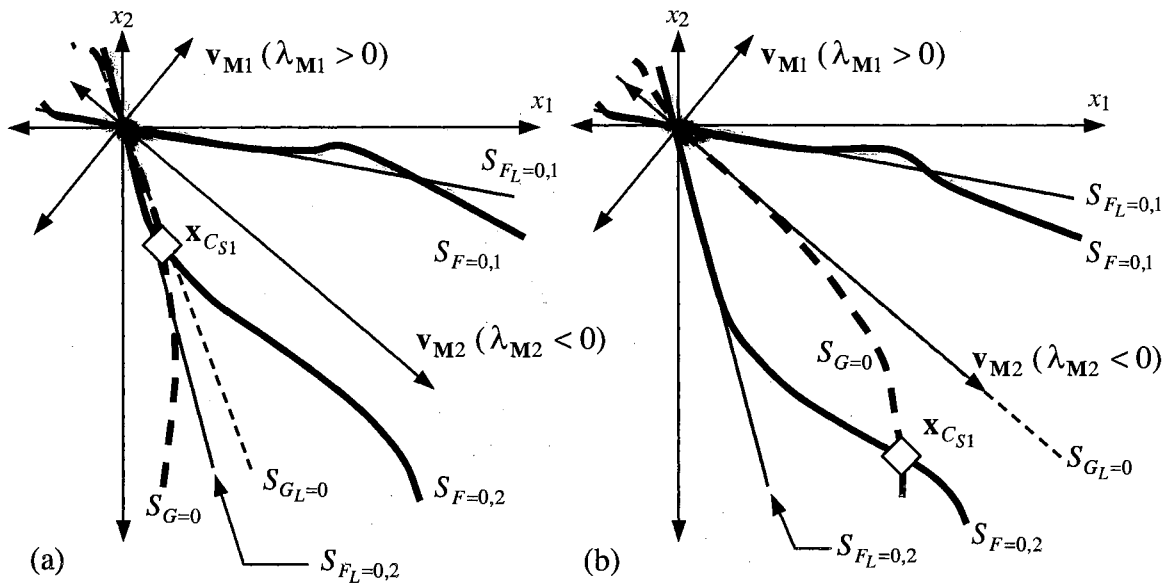
Fig. 1.2   Effects of $\mathbf{P}$ on the Location of $\mathbf{x}_{C_{Si}}$

Symbol: $\Diamond$ $\equiv$ intersection point between $S_{G=0}$ and $S_{F=0,2}$

(a) $S_{G_L=0}$ runs close to $S_{F_L=0,2}$ and far from $S_{F_L=0,1}$, locating the intersection between $S_{F=0}$ and $S_{G=0}$ undesirably close to the origin.

(b) $S_{G_L=0}$ runs midway between the lines $S_{F_L=0,1}$ and $S_{F_L=0,2}$, locating the intersection point between $S_{F=0}$ and $S_{G=0}$ reasonably far from the origin.

We denote the matrix $\mathbf{P}$ corresponding to Fig. 1.2 (a) and (b) by $\mathbf{P}_a$ and $\mathbf{P}_b$ respectively.

In Fig. 1.2 (a), $\mathbf{P}_a$ is a poor choice because it locates $S_{G_L=0}$ close to $S_{F_L=0,2}$ but far from $S_{F_L=0,1}$. In Fig. 1.2 (b), $\mathbf{P}_b$ locates $S_{G_L=0}$ on the symmetry axis of $S_{F_L=0,2}$ and $S_{F_L=0,1}$.

By Theorem 1.1 and 1.2, this symmetry axis is exactly along the eigenvector $\mathbf{v}_{M2}$ corresponding to a negative eigenvalue λ_{M2}. Assuming that the respective surfaces in

Fig. 1.2 (a) and (b) have the same degrees of deviations resulting from nonlinearities, the orientation of surfaces in Fig. 1.2 (b) should locate $\mathbf{x}_{C_{S1}}$ farther from the origin than that resulting from the orientation of surfaces in Fig. 1.2 (a). Noticing this, we propose:

Proposition 1.1   (Eigenvector Condition)

We propose to choose $\mathbf{P}$ such that $S_{F_L=0}$ is symmetric about $S_{G_L=0}$ and

$S_{G_L=0} \subset R_{[F_L<0]\cup\{0\}}$. This is equivalent to choosing $\mathbf{P}$ such that $\{\mathbf{v_{M2}}, \mathbf{v_{M3}}, \ldots, \mathbf{v_{Mn}}\}$ spans $S_{G_L=0}$, where $\lambda_{M1} > 0 > \lambda_{M2} \geq \ldots \geq \lambda_{Mn}$. When $n = 2$, this amounts to choosing $\mathbf{P}$ such that $\mathbf{v_{M2}}$ spans $S_{G_L=0}$.

In short, our particular choice of $\mathbf{P}$ is heuristic. However, the heuristic choice of $\mathbf{P}$ that centers $S_{G_L=0}$ between $S_{F_L=0,1}$ and $S_{F_L=0,2}$ seems to be reasonable. Under this particular orientation, we know by continuity that small deviations due to nonlinearities will not place the intersection point $\mathbf{x}_{C_{Si}}$ arbitrarily close to the origin, and $\mathbf{x}_{C_{Si}}$ are increasingly far from the origin as the degree of deviation decreases. Because of this, it seems reasonable to say that this particular choice of $\mathbf{P} = \mathbf{P_b}$ locates $\mathbf{x}_{C_{Si}}$ "reasonably far" from the origin and force β_{C_S} to be "reasonably large". By locating $\mathbf{x}_{C_{Si}}$ "reasonably far" from the origin, we refer to the illustration in Fig. 1.2 from which it is conceivable that $\left\| \mathbf{x}_{C_{Si}} \right\| \to \infty$ as the degree of nonlinearities becomes smaller but need not be zero.

Proposition 1.2   (Eigenvalue Ratio)

In addition to choosing $\mathbf{P}$ such that $S_{F_L=0}$ is symmetry about $S_{G_L=0}$ as in Proposition 1.1,

we want to choose $\mathbf{P}$ such that $S_{F_L=0}$ is as far from the plane spanned by $\{\mathbf{v_{M2}}, \ldots, \mathbf{v_{Mn}}\}$

as possible. This is because if the objective in Proposition 1.1 can be satisfied, then this

plane is the same as $S_{G_L=0}$ and thus we desire that $S_{F_L=0}$ be as far from this plane as

possible. In this section, we show that this new requirement can be accomplished by

forcing the eigenvalue ratio to be small. The eigenvalue ratio is defined as:

$$r_{\lambda_{\mathbf{M}}} \equiv \left| \frac{\max(\lambda_{\mathbf{M}i}^{+})}{\max(\lambda_{\mathbf{M}j}^{-})} \right| \tag{1.23}$$

where $\lambda_{\mathbf{M}i}^{+}$ are positive eigenvalues of $\mathbf{M}$, $\lambda_{\mathbf{M}j}^{-}$ are the negative eigenvalues of $\mathbf{M}$ such

that $\mathbf{v_{M}}_j$ spans $S_{G_L=0}$ when the eigenvector condition is satisfied. Recall from Theorem

1.1 that no eigenvalue of $\mathbf{M}$ can be zero, and all the corresponding n eigenvectors are

orthonormal. Suppose the eigenvalues of $\mathbf{M}$ are arranged as $\lambda_{\mathbf{M}1} > 0 > \lambda_{\mathbf{M}2} \geq \ldots \geq \lambda_{\mathbf{M}n}$,

we have $i = 1$ because $\lambda_{\mathbf{M}1}$ is the only positive eigenvalue of $\mathbf{M}$, and $j = 2, \ldots, n$

because $\lambda_{\mathbf{M}j} < 0$ such that $\mathbf{v_{M}}_j$ spans $S_{G_L=0}$ when the eigenvector condition is satisfied.

Accordingly, $r_{\lambda_{\mathbf{M}}} = -\lambda_{\mathbf{M}1} / \lambda_{\mathbf{M}2}$. Given a linearized model, we notice that $\mathbf{M}$ depends

only on $\mathbf{P}$.

We now investigate how the eigenvalue ratio $r_{\lambda_{\mathbf{M}}}$ affects the relative orientation between

$S_{F_L=0}$ and $S_{G_L=0}$ when the eigenvector condition is satisfied. Consider the expression for

$F_L(\mathbf{x}) = 0$ in the principal-axes coordinate:

$$F_L(\mathbf{x})\big|_{\mathbf{x}=\mathbf{T_M z}} = F_{L_T}(\mathbf{z}) = \lambda_{M1}z_1^2 + \lambda_{M2}z_2^2 + \ldots + \lambda_{Mn}z_n^2 = 0 \qquad (1.20)$$

where the z_i − axis is along $\mathbf{v}_{Mi}$, $i=1,2,\ldots,n$. For convenience, we arrange the

eigenvalues of $\mathbf{M}$ for SIMO systems as:

$$\lambda_{M1} > 0 > \lambda_{M2} \geq \ldots \geq \lambda_{Mn} \qquad (1.24)$$

where $\lambda_{M1} = \max(\lambda_{Mi}^+)$, $\lambda_{M2} = \max(\lambda_{Mj}^-)$, and $r_{\lambda_M} = |\lambda_{M1}/\lambda_{M2}| = -\lambda_{M1}/\lambda_{M2}$. Now,

consider a point in the $z_1 - z_2$ plane spanned by $\{\mathbf{v}_{M1}, \mathbf{v}_{M2}\}$. We denote this point by

$\mathbf{z}_{\{\mathbf{v}_{M1}, \mathbf{v}_{M2}\}} = [z_1 \; z_2 \; 0 \; \ldots \; 0]^T \in \Re^n$. Given a value of z_2 for $\mathbf{z}_{\{\mathbf{v}_{M1}, \mathbf{v}_{M2}\}}$, we know by

inspection that there exists a value of z_1 such that (1.20) is satisfied and

$\mathbf{z}_{\{\mathbf{v}_{M1}, \mathbf{v}_{M2}\}} \in S_{F_L=0}$. Such $\mathbf{z}_{\{\mathbf{v}_{M1}, \mathbf{v}_{M2}\}}$ then belongs to the intersection of the $z_1 - z_2$ plane

and $S_{F_L=0}$, and we denote this point by $\mathbf{z}_{\{\mathbf{v}_{M1}, \mathbf{v}_{M2}\}}^{F_L=0} = [z_1 \; z_2 \; 0 \; \ldots \; 0]^T$.

At a given point $\mathbf{z}_{\{\mathbf{v}_{M1}, \mathbf{v}_{M2}\}}^{F_L=0}$, we see from (1.20) that if λ_{M1} is small relative to λ_{M2} then

z_1 must be large relative to z_2 and vice versa. In a two-dimensional system ($n = 2$), the

effects of large and small r_{λ_M} can be illustrated in Fig. 1.3. In Fig. 1.3, the z_1 − axis is

spanned by $\mathbf{v}_{M1}$, the z_2 − axis by $\mathbf{v}_{M2}$, and the symbols ∘ represents the point

$\mathbf{z}_{\{\mathbf{v}_{M1}, \mathbf{v}_{M2}\}}^{F_L=0}$ located at the distance $|z_2|$ along the z_2 − axis. The ratio r_{λ_M} corresponding

to Fig. 1.3 (a) is larger than that corresponding to Fig. 1.3 (b). Indeed, we must have that

$F_L(\mathbf{x})\big|_{\mathbf{x}=\mathbf{T_M z}} = 0$ at the point $\mathbf{z}_{\{\mathbf{v}_{M1}, \mathbf{v}_{M2}\}}^{F_L=0}$, and thus (1.20) implies that the distance $|z_1|_b$ in

Fig. 1.3 (b) must be greater than the distance $|z_1|_a$ in Fig. 1.3 (a). Because of this, the

surface $S_{F_L=0}$ in Fig. 1.3 (b) runs farther from the z_2 − axis than it does in Fig. 1.3 (a).

In Fig. 1.3 (a), $S_{F_L=0}$ runs close to $S_{G_L=0}$ and thus we see that $\mathbf{x}_{C_{Si}}$ can be close to the

origin in the presence of small deviations of $S_{F=0}$ from $S_{F_L=0}$ and of $S_{G=0}$ from $S_{G_L=0}$.

It can be shown by examples that the undesirable situations in Fig. 1.2 (a) and Fig. 1.3 (a)

can occur at the same time when an inappropriate $\mathbf{P}$ is chosen to construct the quadratic

Lyapunov function. Proposition 1.2 is now given:

(a) (b)
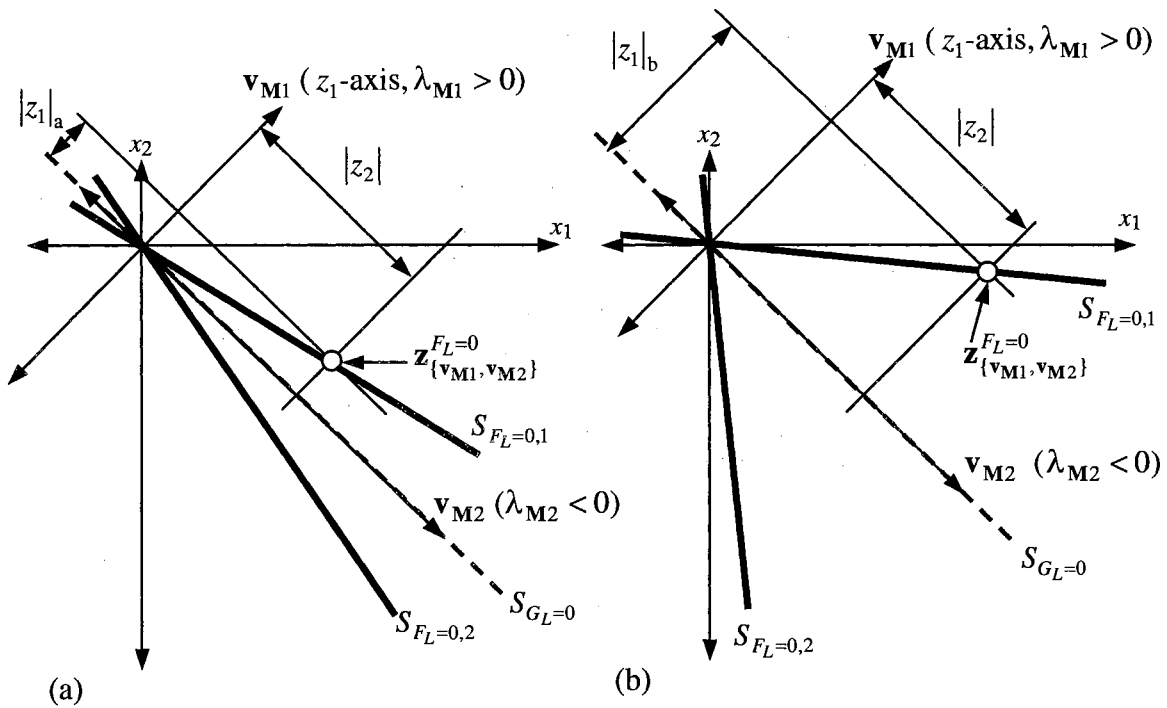
Fig. 1.3 Effects of Eigenvalue Ratio to the Relative Orientation
between $S_{F_L=0}$ and $S_{G_L=0}$ when the Eigenvector Condition is Satisfied

Symbol: $\circ$ $\equiv$ points on $S_{F_L=0}$ locating at the same distance $|z_2|$ along $\mathbf{v_{M2}}$

Remarks: 1) $|z_1|_b > |z_1|_a$

2) $\mathbf{P_a}$ is such that r_{λ_M} is large, forcing $S_{G_L=0}$ to run close to $S_{F_L=0}$.

3) $\mathbf{P_b}$ is such that r_{λ_M} is small, forcing $S_{G_L=0}$ to run far from $S_{F_L=0}$.

Proposition 1.2 (Eigenvalue ratio)

From a set of $\mathbf{P}$ matrices satisfying the eigenvector condition in Proposition 1.1, we

propose to choose a particular $\mathbf{P}$ matrix such that the eigenvalue ratio r_{λ_M} defined in

(1.23) is small to force $S_{F_L=0}$ away from $S_{G_L=0}$ while maintaining the symmetry of

$S_{F_L=0}$ about $S_{G_L=0}$.

In addition to the previous graphical approach, the role of eigenvalue ratio can be seen

using a geometrical approach. To see this when $n = 2$, we note that a given $\mathbf{z}_{\{\mathbf{v}_{M1},\mathbf{v}_{M2}\}}^{F_L=0}$ is

far from the space spanned by $\mathbf{v}_{M2}$ if the "angle" θ between $\mathbf{z}_{\{\mathbf{v}_{M1},\mathbf{v}_{M2}\}}^{F_L=0}$ and the

projection of $\mathbf{z}_{\{\mathbf{v}_{M1},\mathbf{v}_{M2}\}}^{F_L=0}$ onto the space spanned by $\mathbf{v}_{M2}$ is large. A vector in the space

spanned by $\mathbf{v}_{M2}$ is along the z_2 − axis and is denoted by $\mathbf{z}_{\{\mathbf{v}_{M2}\}}$. Geometrically, the

cosine of this angle is given by:

$$\cos(\theta) = \frac{\left[\mathbf{z}_{\{\mathbf{v}_{M1},\mathbf{v}_{M2}\}}^{F_L=0}\right]^T \mathbf{z}_{\{\mathbf{v}_{M2}\}}}{\left\|\mathbf{z}_{\{\mathbf{v}_{M1},\mathbf{v}_{M2}\}}^{F_L=0}\right\|\left\|\mathbf{z}_{\{\mathbf{v}_{M2}\}}\right\|} = \frac{[z_1 \quad z_2][0 \quad z_2]^T}{\sqrt{z_1^2+z_2^2}\sqrt{z_2^2}} = \frac{\sqrt{z_2^2}}{\sqrt{z_1^2+z_2^2}} \qquad (1.25)$$

where $\mathbf{z}_{\{\mathbf{v}_{M2}\}} = [0 \quad z_2]^T$ because $\mathbf{z}_{\{\mathbf{v}_{M2}\}}$ is along $\mathbf{v}_{M2}$, and $\{\mathbf{v}_{M1},\mathbf{v}_{M2}\}$ is an

orthonormal basis.

Since we desire that θ be large, we want $\cos(\theta)$ to be small. Given a value of z_2, we see

from (1.25) that this can be accomplished by forcing z_1 to be large. From (1.20) this is

possible if and only if r_{λ_M} is small and we see that the conclusions from the

previous graphical approach and this geometrical approach are the same. In an n-

dimensional system, applying the same argument for points on the plane formed by $\mathbf{v}_{M1}$

and a vector $\mathbf{v}_{\mathbf{M}j}$, $j = 2,3,4,\ldots,n$ shows that the angle between $\mathbf{z}^{F_L=0}_{\{\mathbf{v}_{\mathbf{M}1},\mathbf{v}_{\mathbf{M}j}\}}$ and $\mathbf{z}_{\{\mathbf{v}_{\mathbf{M}j}\}}$ is

minimum when $j = 2$ because of the arrangement of the eigenvalues of $\mathbf{M}$ in (1.24).

For the following discussions, we note that because of the orthogonality of the

eigenvectors of $\mathbf{M}$ and because the z_i – axis is along $\mathbf{v}_{\mathbf{M}i}$, $i = 1,2,\ldots,n$:

1)   The projection of a vector $\mathbf{z}^{F_L=0}_{\{\mathbf{v}_{\mathbf{M}1},\mathbf{v}_{\mathbf{M}2},\ldots,\mathbf{v}_{\mathbf{M}n}\}} = [z_1 \quad z_2 \quad \ldots \quad z_n]^T \in S_{F_L=0} \in \mathfrak{R}^n$

onto the plane spanned by $\{\mathbf{v}_{\mathbf{M}2},\ldots,\mathbf{v}_{\mathbf{M}n}\}$ is denoted by:

$$\mathbf{z}^{F_L=0}_{\{\mathbf{v}_{\mathbf{M}1},\mathbf{v}_{\mathbf{M}2},\ldots,\mathbf{v}_{\mathbf{M}n}\}}\Big|_{z1=0} \equiv \mathbf{z}_{\{\mathbf{v}_{\mathbf{M}2},\ldots,\mathbf{v}_{\mathbf{M}n}\}} = [0 \quad z_2 \quad \ldots \quad z_n]^T$$

2)   A vector belonging to the intersection of $S_{F_L=0}$ and the plane spanned by

$\{\mathbf{v}_{\mathbf{M}1},\mathbf{v}_{\mathbf{M}2}\}$ is denoted by:

$$\mathbf{z}^{F_L=0}_{\{\mathbf{v}_{\mathbf{M}1},\mathbf{v}_{\mathbf{M}2},\ldots,\mathbf{v}_{\mathbf{M}n}\}}\Big|_{z3=z4=\ldots=z_n=0} \equiv \mathbf{z}^{F_L=0}_{\{\mathbf{v}_{\mathbf{M}1},\mathbf{v}_{\mathbf{M}2}\}} = [z_1 \quad z_2 \quad 0 \quad \ldots \quad 0]^T$$

where $\mathbf{z}^{F_L=0}_{\{\mathbf{v}_{\mathbf{M}1},\mathbf{v}_{\mathbf{M}2}\}}$ is such that (1.20) is satisfied.

3)   The projection of $\mathbf{z}^{F_L=0}_{\{\mathbf{v}_{\mathbf{M}1},\mathbf{v}_{\mathbf{M}2}\}} = [z_1 \quad z_2 \quad 0 \quad \ldots \quad 0]^T$ onto the plane spanned by

$\{\mathbf{v}_{\mathbf{M}2},\ldots,\mathbf{v}_{\mathbf{M}n}\}$ is the vector:

$$\mathbf{z}_{\{\mathbf{v}_{\mathbf{M}2}\}} \equiv \mathbf{z}^{F_L=0}_{\{\mathbf{v}_{\mathbf{M}1},\mathbf{v}_{\mathbf{M}2}\}}\Big|_{z1=0} = [0 \quad z_2 \quad 0 \quad \ldots \quad 0]^T$$

For all points $\mathbf{z}^{F_L=0}_{\{\mathbf{v}_{\mathbf{M}1},\mathbf{v}_{\mathbf{M}2},\ldots,\mathbf{v}_{\mathbf{M}n}\}}$ belonging to $S_{F_L=0}$, we claim that the angle between

$\mathbf{z}^{F_L=0}_{\{\mathbf{v}_{\mathbf{M}1},\mathbf{v}_{\mathbf{M}2},\ldots,\mathbf{v}_{\mathbf{M}n}\}}$ and the plane spanned by $\{\mathbf{v}_{\mathbf{M}2},\ldots,\mathbf{v}_{\mathbf{M}n}\}$ is minimum when

$\mathbf{z}^{F_L=0}_{\{\mathbf{v}_{\mathbf{M}1},\mathbf{v}_{\mathbf{M}2},\ldots,\mathbf{v}_{\mathbf{M}n}\}} = \mathbf{z}^{F_L=0}_{\{\mathbf{v}_{\mathbf{M}1},\mathbf{v}_{\mathbf{M}2}\}}$. To show this, it is sufficient to show that the angle

between a vector $\mathbf{z}^{F_L=0}_{\{v_{M1},v_{M2},\ldots,v_{Mn}\}} = [z_1 \quad z_2 \quad \ldots \quad z_n]^T$ and its projection

$\mathbf{z}_{\{v_{M2},\ldots,v_{Mn}\}} = [0 \quad z_2 \quad \ldots \quad z_n]^T$ onto this plane is minimum when $z_3 = z_4 = \ldots =$

$z_n = 0$ or when $\mathbf{z}^{F_L=0}_{\{v_{M1},v_{M2},\ldots,v_{Mn}\}} = \mathbf{z}^{F_L=0}_{\{v_{M1},v_{M2}\}} = [z_1 \quad z_2 \quad 0 \quad \ldots \quad 0]^T$. This is shown in

the proof of Theorem 1.3 and it follows from this result that we can get the idea of how

close $S_{F_L=0}$ is to the plane spanned by $\{v_{M2}, \ldots, v_{Mn}\}$ by examining the angle θ

between $\mathbf{z}^{F_L=0}_{\{v_{M1},v_{M2}\}} = [z_1 \quad z_2 \quad 0 \quad \ldots \quad 0]^T$ and its projection onto the plane spanned by

$\{v_{M2},\ldots,v_{Mn}\}$. We denote such projection by $\mathbf{z}_{\{v_{M2}\}} = [0 \quad z_2 \quad 0 \quad \ldots \quad 0]^T$. This is

because such result indicates that θ is the infimum (greatest lower bound) of the angles

between all vectors belonging to $S_{F_L=0}$ and the corresponding projections onto the plane

spanned by $\{v_{M2}, \ldots, v_{Mn}\}$. Note that the angle between $\mathbf{z}^{F_L=0}_{\{v_{M1},v_{M2}\}}$ and the plane

spanned by $\{v_{M2},\ldots,v_{Mn}\}$ is the angle between $\mathbf{z}^{F_L=0}_{\{v_{M1},v_{M2}\}}$ and its projection onto this

plane denoted by $\mathbf{z}_{\{v_{M2}\}}$. We have shown previously using (1.20), Fig. 1.3 and (1.25) that

the size of this angle is governed by the eigenvalue ratio $r_{\lambda_M} = -\lambda_{M1}/\lambda_{M2}$, where the

eigenvalues of $\mathbf{M}$ are arranged as in (1.24). It is then desirable to choose $\mathbf{P}$ such that r_{λ_M}

is small because a small r_{λ_M} corresponds to a large θ, which implies that $S_{F_L=0}$ is "far"

from the plane spanned by $\{v_{M2}, \ldots, v_{Mn}\}$.

Theorem 1.3 (Implication of Eigenvalue Ratio)

Let the set of n orthonormal eigenvectors $\{v_{M1}, v_{M2}, \ldots, v_{Mn}\}$ be employed for

generating $\Re^n$. If the basic conditions $C1 - C4$ be satisfied, then the angle θ between a

vector $\mathbf{z}_{\{\mathbf{v}_{M1},\mathbf{v}_{M2},...,\mathbf{v}_{Mn}\}}^{F_L=0} = [z_1 \quad z_2 \quad ... \quad z_n]^T \in S_{F_L=0}$ and its projection $\mathbf{z}_{\{\mathbf{v}_{M2},...,\mathbf{v}_{Mn}\}}$

$= [0 \quad z_2 \quad z_3 \quad ... \quad z_n]^T$ onto the plane spanned by $\{\mathbf{v}_{M2}, ..., \mathbf{v}_{Mn}\}$ is the smallest when

$z_3 = z_4 = ... = z_n = 0$ or when:

$$\mathbf{z}_{\{\mathbf{v}_{M1},\mathbf{v}_{M2},...,\mathbf{v}_{Mn}\}}^{F_L=0} = \mathbf{z}_{\{\mathbf{v}_{M1},\mathbf{v}_{Mn}\}}^{F_L=0} = [z_1 \quad z_2 \quad 0 \quad ... \quad 0]^T$$

where the eigenvalues of $\mathbf{M}$ are arranged such that $\lambda_{M1} > 0 > \lambda_{M2} \geq ... \geq \lambda_{Mn}$ and

$\mathbf{z}_{\{\mathbf{v}_{M1},\mathbf{v}_{M2},...,\mathbf{v}_{Mn}\}}^{F_L=0} \neq \mathbf{0}$.

Proof

The projection of $\mathbf{z}_{\{\mathbf{v}_{M1},\mathbf{v}_{M2},...,\mathbf{v}_{Mn}\}}^{F_L=0} = [z_1 \quad z_2 \quad ... \quad z_n]^T \in S_{F_L=0}$ onto the plane spanned

by $\{\mathbf{v}_{M2}, ..., \mathbf{v}_{Mn}\}$ is the vector:

$$\mathbf{z}_{\{\mathbf{v}_{M2},...,\mathbf{v}_{Mn}\}} = [0 \quad z_2 \quad z_3 \quad ... \quad z_n]^T$$

Note that we do not consider the case in which $z_1 = 0$. Indeed, we see from the equation

for $S_{F_L=0}$ given in (1.20) that if $z_1 = 0$, then (1.20) is satisfied only at the origin because

$\lambda_{M1} > 0 > \lambda_{M2} \geq ... \geq \lambda_{Mn}$. Since Theorem 1.3 does not apply at the origin, this special

case is irrelevant. Our original problem is to find $\mathbf{z}_{\{\mathbf{v}_{M1},\mathbf{v}_{M2},...,\mathbf{v}_{Mn}\}}^{F_L=0}$ such that the angle

between $\mathbf{z}_{\{\mathbf{v}_{M1},\mathbf{v}_{M2},...,\mathbf{v}_{Mn}\}}^{F_L=0}$ and $\mathbf{z}_{\{\mathbf{v}_{M2},...,\mathbf{v}_{Mn}\}}$ is <u>minimized</u> over all possible

$\mathbf{z}_{\{\mathbf{v}_{M1},\mathbf{v}_{M2},...,\mathbf{v}_{Mn}\}}^{F_L=0} \neq \mathbf{0}$. From basic geometry, the cosine of the angle θ between

$\mathbf{z}_{\{\mathbf{v}_{M1},\mathbf{v}_{M2},...,\mathbf{v}_{Mn}\}}^{F_L=0}$ and the corresponding projection $\mathbf{z}_{\{\mathbf{v}_{M2}, ..., \mathbf{v}_{Mn}\}}$ is given by:

(Proof of Theorem 1.3 (Cont.))

$$\cos(\theta) = \frac{[\mathbf{z}_{\{v_{M1}, v_{M2}, \ldots, v_{Mn}\}}^{F_L=0}]^T \, \mathbf{z}_{\{v_{M2}, \ldots, v_{Mn}\}}}{\left\| [\mathbf{z}_{\{v_{M1}, v_{M2}, \ldots, v_{Mn}\}}^{F_L=0}]^T \right\| \left\| \mathbf{z}_{\{v_{M2}, \ldots, v_{Mn}\}} \right\|}$$

$$= \frac{z_2^2 + z_3^2 + \ldots + z_n^2}{\sqrt{z_1^2 + z_2^2 + \ldots + z_n^2}\,\sqrt{z_2^2 + z_3^2 + \ldots + z_n^2}} \qquad (1.26)$$

$$= \frac{\sqrt{z_2^2 + z_3^2 + \ldots + z_n^2}}{\sqrt{z_1^2 + z_2^2 + \ldots + z_n^2}}$$

Notice that $1 > \cos(\theta) > 0$, and $\mathbf{z}_{\{v_{M1}, v_{M2}, \ldots, v_{Mn}\}}^{F_L=0} \neq \mathbf{0}$ must obey (1.23) and (1.24). Since

the numerator <u>and</u> denominator in (1.26) are greater than zero, we know from basic

trigonometry that $0 < \theta < (\pi/2)$. In this range, we have that $\cos(\theta)$ monotonically

increases as θ decreases. Accordingly, the original problem can be cast as an

optimization problem for which the objective is to find $\mathbf{z}_{\{v_{M1}, v_{M2}, \ldots, v_{Mn}\}}^{F_L=0} \neq \mathbf{0}$ that

<u>maximizes</u> the right-hand side of (1.26), with constraints given by (1.20) and by Theorem

1.1:

$$\text{Maximize}: \ J_1 = \frac{\sqrt{z_2^2 + z_3^2 + \ldots + z_n^2}}{\sqrt{z_1^2 + z_2^2 + \ldots + z_n^2}}$$

$$\text{Subjected to}: \ 1) \ \ \lambda_{M1} z_1^2 + \lambda_{M2} z_2^2 + \ldots + \lambda_{Mn} z_n^2 = 0 \qquad (1.27)$$

$$: 2) \ \ \lambda_{M1} > 0 > \lambda_{M2} \geq \lambda_{M3} \geq \ldots \geq \lambda_{Mn}$$

Since the numerator and the denominator of the objective function are positive, squaring

the objective function does not change the solution. For simplicity, we now convert

(1.27) to:

$$\text{Maximize}: \ J_2 = J_1^2 = \frac{z_2^2 + z_3^2 + \ldots + z_n^2}{z_1^2 + z_2^2 + \ldots + z_n^2}$$

$$\text{Subjected to}: \ 1) \ \ \lambda_{M1} z_1^2 + \lambda_{M2} z_2^2 + \ldots + \lambda_{Mn} z_n^2 = 0 \qquad (1.28)$$

$$: 2) \ \ \lambda_{M1} > 0 > \lambda_{M2} \geq \lambda_{M3} \geq \ldots \geq \lambda_{Mn}$$

(*Proof of Theorem 1.3 (Cont.)*)

where the range of the objective function J_2 is $0 < J_2 < 1$ because $0 < J_1 < 1$. This is

equivalent to:

$$\text{Minimize}: J_3 = J_2^{-1} = \frac{z_1^2}{z_2^2 + z_3^2 + \ldots + z_n^2} + 1$$

$$\text{Subjected to}: 1) \quad \lambda_{M1} z_1^2 + \lambda_{M2} z_2^2 + \ldots + \lambda_{Mn} z_n^2 = 0 \quad\quad (1.29)$$

$$: 2) \quad \lambda_{M1} > 0 > \lambda_{M2} \geq \lambda_{M3} \geq \ldots \geq \lambda_{Mn}$$

where the range of the objective function J_3 is $1 < J_3 < \infty$. To find the solution

$\mathbf{z}^{F_L = 0}_{\{ \mathbf{v_{M1}}, \mathbf{v_{M2}}, \ldots, \mathbf{v_{Mn}} \}} = [z_1 \quad z_2 \quad \ldots \quad z_n]^T \neq \mathbf{0}$ for (1.29), we consider the following

arguments:

1) The component z_1 corresponding to the solution vector is nonzero. Otherwise,

$z_1 = 0$ and all the constraints in (1.29) are satisfied simultaneously only at the

origin. This leads to a contradiction since we omit the origin and we require that

all constraints be satisfied.

2) The set $\{z_2, z_3, \ldots, z_n\}$ corresponding to the solution vector contains at least one

nonzero element. Otherwise, all the constraints in (1.29) are satisfied

simultaneously only at the origin. Since we omit the origin, $\{z_2, z_3, \ldots, z_n\}$ must

contain at least one nonzero element.

3) The constraints in (1.29) implies that:

$$0 > \lambda_{M2}(z_2^2 + z_3^2 + \ldots + z_n^2) \geq \lambda_{M2} z_2^2 + \lambda_{M3} z_3^2 + \ldots + \lambda_{Mn} z_n^2 = -\lambda_{M1} z_1^2$$

$$0 < z_2^2 + z_3^2 + \ldots + z_n^2 \leq \frac{\lambda_{M2} z_2^2 + \lambda_{M3} z_3^2 + \ldots + \lambda_{Mn} z_n^2}{\lambda_{M2}} = \frac{-\lambda_{M1} z_1^2}{\lambda_{M2}}$$

where $z_2^2 + z_3^2 + \ldots + z_n^2 = \frac{\lambda_{M2} z_2^2 + \lambda_{M3} z_3^2 + \ldots + \lambda_{Mn} z_n^2}{\lambda_{M2}}$ when $z_i = 0$,

(Proof of Theorem 1.3 (Cont.))

$i = 3, 4, \ldots, n$. Accordingly, $z_2^2 + z_3^2 + \ldots + z_n^2$ is maximum for a given z_1 when

$z_i = 0$, $i = 3, 4, \ldots, n$.

It follows from the arguments in $1 - 3$ that J_3 in (1.29) is minimum when:

$$\mathbf{z}_{\{\mathbf{v_{M1}}, \mathbf{v_{M2}}, \ldots, \mathbf{v_{M}}n\}}^{F_L=0} = [z_1 \quad z_2 \quad 0 \quad \ldots \quad 0]^T = \mathbf{z}_{\{\mathbf{v_{M1}}, \mathbf{v_{M2}}\}}^{F_L=0}$$

At the solution $\mathbf{z}_{\{\mathbf{v_{M1}}, \mathbf{v_{M2}}\}}^{F_L=0}$, the minimum of the objective function J_3 in (1.29) is given

by:

$$J_3^* = \frac{z_1^2}{z_2^2} + 1 \tag{1.30}$$

To find the minimum of J_3, we substitute $\mathbf{z}_{\{\mathbf{v_{M1}}, \mathbf{v_{M2}}\}}^{F_L=0} = [z_1 \quad z_1 \quad 0 \quad \ldots \quad 0]^T$ into the

first constraint in (1.29) to produce:

$$\lambda_{\mathbf{M1}} z_1^2 + \lambda_{\mathbf{M2}} z_2^2 = 0$$

This is the same as:

$$z_1^2 = -\frac{\lambda_{\mathbf{M2}} z_2^2}{\lambda_{\mathbf{M1}}} > 0 \tag{1.31}$$

where we recall that $\lambda_{\mathbf{M1}} > 0$ and $\lambda_{\mathbf{M2}} < 0$. Notice that we can always find a value of z_1

for every set of $\{\lambda_{\mathbf{M1}}, \lambda_{\mathbf{M2}}, z_2\}$ where $\lambda_{\mathbf{M1}} > 0$ and $\lambda_{\mathbf{M2}} < 0$ such that (1.31) is

satisfied. Now, we substitute $-\dfrac{\lambda_{\mathbf{M2}} z_2^2}{\lambda_{\mathbf{M1}}}$ for z_1^2 in (1.30). This produces the minimum

values for J_3:

$$J_3^* = -\frac{\lambda_{\mathbf{M2}}}{\lambda_{\mathbf{M1}}} + 1 = \frac{\lambda_{\mathbf{M1}} - \lambda_{\mathbf{M2}}}{\lambda_{\mathbf{M1}}} > 1 \tag{1.32 a}$$

This solution corresponds to the <u>maximum</u> value of J_2 and J_1:

(Proof of Theorem 1.3 (Cont.))

$$0 < J_2^* = (J_3^*)^{-1} = \frac{\lambda_{M1}}{\lambda_{M1} - \lambda_{M2}} < 1 \qquad (1.32\ b)$$

$$0 < J_1^* = \sqrt{J_2^*} = \sqrt{\frac{\lambda_{M1}}{\lambda_{M1} - \lambda_{M2}}} < 1 \qquad (1.32\ c)$$

This completes the proof of Theorem 1.3.

Recall that we want to choose $\mathbf{P}$ such that the eigenvalue ratio $r_{\lambda_M} = -\lambda_{M1}/\lambda_{M2}$ is small. By inspecting (1.32), a small r_{λ_M} corresponds to a large J_3, to a small J_2, and to a small J_1. Since $J_1 = \cos(\theta)$, a small J_1 implies that the angle between a vector belonging to $S_{F_L=0}$ and its projection onto $S_{G_L=0}$ is large by Theorem 1.3. In views of Proposition 1.1 and 1.2, we want to find $\mathbf{P}$ such that $S_{F_L=0}$ is symmetric about $S_{G_L=0}$ and r_{λ_M} is small because this forces a possible intersection point $\mathbf{x}_{CSi}$ between $S_{F=0}$ and $S_{G=0}$ "reasonably far" from the origin.

For all mathematical descriptions (1.1) having the same linearized model, choosing $\mathbf{P} = \mathbf{P}_b$ to orient $S_{G_L=0}$ and $S_{F_L=0}$ as in Fig. 1.2 (b) and Fig. 1.3 (b) does <u>not</u> necessarily yield the largest β_{C_S} over all possible choices of $\mathbf{P}$ because:

1)   Specific nonlinearities have not been taken into account.

2)   Mathematical optimization has not been employed to search for the optimal $\mathbf{P}$ that yields the largest β_{C_S}.

In Proposition 1.1 and 1.2, we have obtained two desired relative orientations between

$S_{G_L=0}$ and $S_{F_L=0}$. Because of continuity, we see that these orientations locate $\mathbf{x}_{C_{Si}}$

reasonably far from the origin and thus yield a reasonably large β_{C_S}. This is necessary

for obtaining a large β_{C_L} because $\beta_{C_L} \subseteq \beta_{C_S}$. In Proposition 1.1 (eigenvector condition),

we restrict ourselves to systems with $n = 2$, while we consider the general case when n is

an arbitrary positive integer in Proposition 1.2 (eigenvalue ratio). This is because the

general case of the former requires deeper analysis in Chapter II. In further

developments:

1) We need to find a mathematical condition corresponding to the desired relative

orientation between $S_{G_L=0}$ and $S_{F_L=0}$ in Proposition 1.1 for n-dimensional

systems.

2) We need a condition that guarantees the existence or nonexistence of **P** that yields

such relative orientation.

3) If such **P** exists, a method for obtaining **P** is required.

4) A controller construction aiming to obtain a large LAR is required.

Items 1, 2 and 3 are addressed in Chapter II while item 4 is discussed in Chapter II

without robustness issues, and in Chapter III with robustness issues. Next, we give a

simple example to illustrate various mathematical objects we have discussed. At this

point, we do not employ an underactuated system such as a double-inverted-pendulum

system or a cart-and-pole system as an example because handling such a system using a

LARC requires later results in our developments.

Example 1.1 (An Artificial System)

Consider the following second-order artificial system by:

$$\begin{bmatrix} \dot{x}_1 \\ \dot{x}_2 \end{bmatrix} = \begin{bmatrix} 10x_2 + 10x_1 + 10\sin(x_1)^2\sin(x_2) - x_1^2 \\ 5x_1^2 + \sin(x_2) \end{bmatrix} + \begin{bmatrix} 0 \\ \cos(x_2) + 1.5 \end{bmatrix} u \qquad \text{(E 1.1.1)}$$

$$\dot{\mathbf{x}} \equiv \mathbf{f}(\mathbf{x}) + \mathbf{g}(\mathbf{x})u$$

The outputs of the system (E 1.1.1 a) are the state variables x_1 and x_2, and the input is the

control $u(\mathbf{x})$. When $u(\mathbf{x}) = 0$, the system has two unstable equilibrium points

$\mathbf{x}_{01} = [0 \quad 0]^T$, and $\mathbf{x}_{02} = [0.1886 \quad -0.1788]^T$. We constrain our interest to $\mathbf{x}_{01}$, the

origin. The linearized model about the origin is given by:

$$\begin{bmatrix} \dot{x}_1 \\ \dot{x}_2 \end{bmatrix} = \begin{bmatrix} 10 & 10 \\ 0 & 1 \end{bmatrix} \begin{bmatrix} x_1 \\ x_2 \end{bmatrix} + \begin{bmatrix} 0 \\ 2.5 \end{bmatrix} u \qquad \text{(E 1.1.2)}$$

$$\dot{\mathbf{x}} = \mathbf{A}\mathbf{x} + \mathbf{B}u$$

To stabilize the system (E 1.1.1) locally about the origin, the following linear control is

applied:

$$u(\mathbf{x}) = -[60 \quad 20]\mathbf{x} \equiv -\mathbf{K}\mathbf{x} \qquad \text{(E 1.1.3)}$$

This places the two eigenvalues of the matrix $\overline{\mathbf{A}} \equiv [\mathbf{A} - \mathbf{B}\mathbf{K}]$ at $\lambda_{1,2} = -19.5 \pm j25.095$

in the LHP. This linear control is chosen primarily to stabilize the nonlinear system

locally; there are infinitely many other possibilities. We now employ $\overline{\mathbf{A}}$ to find $\mathbf{P}$ using

(1.6) in which we set $\mathbf{Q} = \mathbf{I}$ for convenience. This produces:

$$\mathbf{P} \equiv \mathbf{P}_{(E1.1.4)} = \begin{bmatrix} 0.3289 & 0.0253 \\ 0.0253 & 0.0154 \end{bmatrix} \qquad \text{(E 1.1.4)}$$

From (1.6), this yields the quadratic Lyapunov function:

$$V(\mathbf{x}) = \frac{1}{2}\mathbf{x}^T \mathbf{P}_{(E1.1.4)}\mathbf{x} \qquad \text{(E 1.1.5)}$$

The function $F(\mathbf{x})$ and $G(\mathbf{x})$ corresponding to $\mathbf{P}_{(E1.1.4)}$ are given by:

$$F(\mathbf{x}) = \mathbf{x}^T \mathbf{P}_{(E1.1.4)} \mathbf{f}(\mathbf{x})$$

$$= (0.3289x_1 + 0.0253x_2)(10x_2 + 10x_1 + 10\sin^2(x_1)\sin(x_2) - x_1^2) \quad \text{(E 1.1.6)}$$

$$+ (0.0253x_1 + 0.0154x_2)(5x_1^2 + \sin(x_2))$$

$$G(\mathbf{x}) = \mathbf{x}^T \mathbf{P}_{(E1.1.4)} \mathbf{g}(\mathbf{x})$$
$$= (0.0253x_1 + 0.0154x_2)(\cos(x_2) + 1.5) \quad \text{(E 1.1.7)}$$

The linear approximations of $F(\mathbf{x})$ and $G(\mathbf{x})$ corresponding to the linearized model (E-1.1.2) are given by:

$$F_L(\mathbf{x}) = \frac{1}{2}\mathbf{x}^T[\mathbf{P}_{(E1.1.4)}\mathbf{A} + [\mathbf{P}_{(E1.1.4)}\mathbf{A}]^T]\mathbf{x} = \mathbf{x}^T\mathbf{M}\mathbf{x} = \mathbf{x}^T\begin{bmatrix} 3.2890 & 1.7835 \\ 1.7835 & 0.2680 \end{bmatrix}\mathbf{x} \quad \text{(E 1.1.8)}$$

$$G_L(\mathbf{x}) = \mathbf{x}^T\mathbf{P}_{(E1.1.4)}\mathbf{B} = 0.0632x_1 + 0.0384x_2 \quad \text{(E 1.1.9)}$$

where $\mathbf{M} = \begin{bmatrix} 3.2890 & 1.7835 \\ 1.7835 & 0.2680 \end{bmatrix}$. The relevant surfaces, the regions β_{C_L}, B_L, and their two common boundary points corresponding to the linear control $u(\mathbf{x})$ in (E 1.1.3) are shown in Fig. E1.1.1. Note for Fig. E1.1.1 that:

1) $S_{F=0}$ is represented by two thin solid curves, namely $S_{F=0,1}$, and $S_{F=0,2}$.

2) $S_{G=0}$ is represented by a thick solid straight line.

3) B_L is the region with diagonal solid lines, and O_{B_L} is represented by two thick dashed curves, namely $O_{B_L,1}$, and $O_{B_L,2}$.

4) β_{C_L} is the elliptical region with diagonal dotted lines, whose boundary is $O_{\beta_{C_L}}$.

5) The symbol $\circ$ denotes an intersection between $O_{\beta_{C_L}}$ and O_{B_L}, which is a common boundary point.

In Fig. E1.1.1, we see that the surfaces $S_{G=0}$ and $S_{F=0}$ do not intersect in the $x_1 - x_2$

plane except at the origin. Thus the boundary of β_{C_L} does not contain an intersection

point between $S_{G=0}$ and $S_{F=0}$. We now proceed to find β_{C_S} (defined in (1.12))

corresponding to $\mathbf{P}_{(E1.1.4)}$. This can be determined by finding first the intersection $\mathbf{x}_{C_{Si}}$

$i = 1, 2, ...$ then expand β_C from $C = C_L$ until the boundary of β_C first reaches $\mathbf{x}_{C_{Si}}$ at

$C = C_S$. We do this in Fig. E1.1.2 for which we note that:
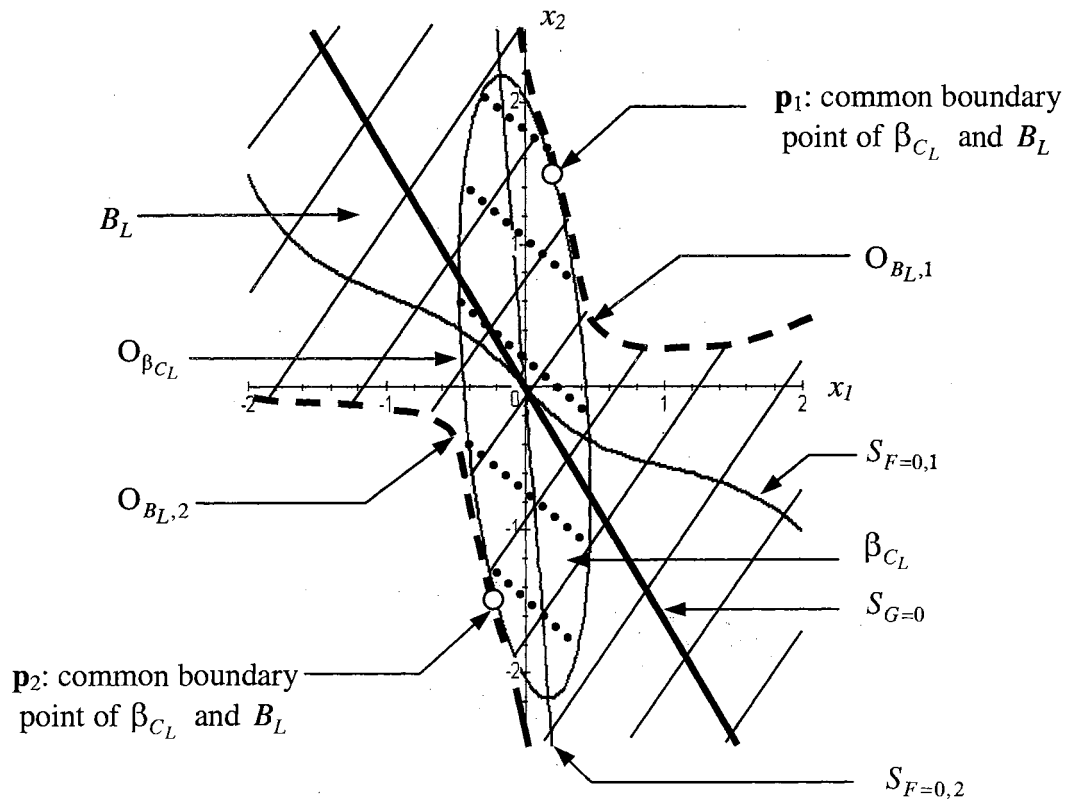
Fig. E1.1.1   Region β_{C_L} and B_L for (E 1.1.1) under Linear Control in (E 1.1.3)

1) $S_{F=0}$ is represented by two thin solid curves namely $S_{F=0,1}$, and $S_{F=0,2}$.

2) $S_{F_L=0}$ is represented by two thin dash curves namely $S_{F_L=0,1}$ and $S_{F_L=0,2}$. The surface $S_{F=0,2}$ overlaps $S_{F_L=0,2}$ and we see only $S_{F=0,2}$ in the figure.

1) $S_{G=0}$ is represented by a thick solid curve.

2) $S_{G_L=0}$ is represented by a thick dash curve. The line $S_{G=0}$ overlaps $S_{G_L=0}$ and we see only $S_{G=0}$ in the figure.

3) The symbol $\diamond$ represents the point $\mathbf{x}_{C_{S1}}$ at which $S_{F=0,1}$ intersects $S_{G=0}$ (i.e., $F(\mathbf{x}_{C_{S1}}) = G(\mathbf{x}_{C_{S1}}) = 0$). In the figure, this point is on $O_{\beta_{CS}} = S_{V=5.5}$.

Graphically, we see from Fig. E1.1.2 which is a zoom-out version of Fig. E1.1.1 that the ellipse β_{C_S} is the largest possible LAR corresponding to $\mathbf{P}_{(E1.1.4)}$ because $S_{G=0}$ intersects $S_{F=0,1}$ at $\mathbf{x}_{C_{S1}}$ on the boundary of this ellipse. Notice that β_{C_L} in Fig. E1.1.1 resulting from the linear control (E 1.1.3) is significantly smaller than the corresponding β_{C_S} in Fig. E1.1.2. Under $\mathbf{P}_{(E1.1.4)}$, the eigenvalues and eigenvector of $\mathbf{M}$ are given by:

$$\lambda_{M1} = 4.1156, \quad \mathbf{v}_{M1} = [-0.9073 \quad -0.4205]^T \qquad \text{(E 1.1.10 a)}$$

$$\lambda_{M2} = -0.5587, \quad \mathbf{v}_{M2} = [0.4205 \quad -0.9073]^T \qquad \text{(E 1.1.10 b)}$$

The surface $S_{G_L=0}$ is the line $c\,\mathbf{x}_{G_L=0}$, where $c \in \Re$ and $\mathbf{x}_{G_L=0} = [0.5195 \quad -0.8544]^T$.

According to Theorem 1.2, $\mathbf{v}_{M2}$ is the symmetry axis of $S_{F_L=0}$ such that $F_L(\mathbf{x})|_{\mathbf{x} \neq 0} < 0$ along $\mathbf{v}_{M2}$. We see from (E 1.1.10) that $S_{G_L=0}$ is not spanned by $\mathbf{v}_{M2}$. Indeed, $S_{G_L=0}$ is spanned by the unit vector $\mathbf{x}_{G_L=0}$ and it can be shown that the angle between $\mathbf{x}_{G_L=0}$ and $\mathbf{v}_{M2}$ is 0.1123 radian. The eigenvalue ratio is $r_{\lambda_M} = 7.3668$.
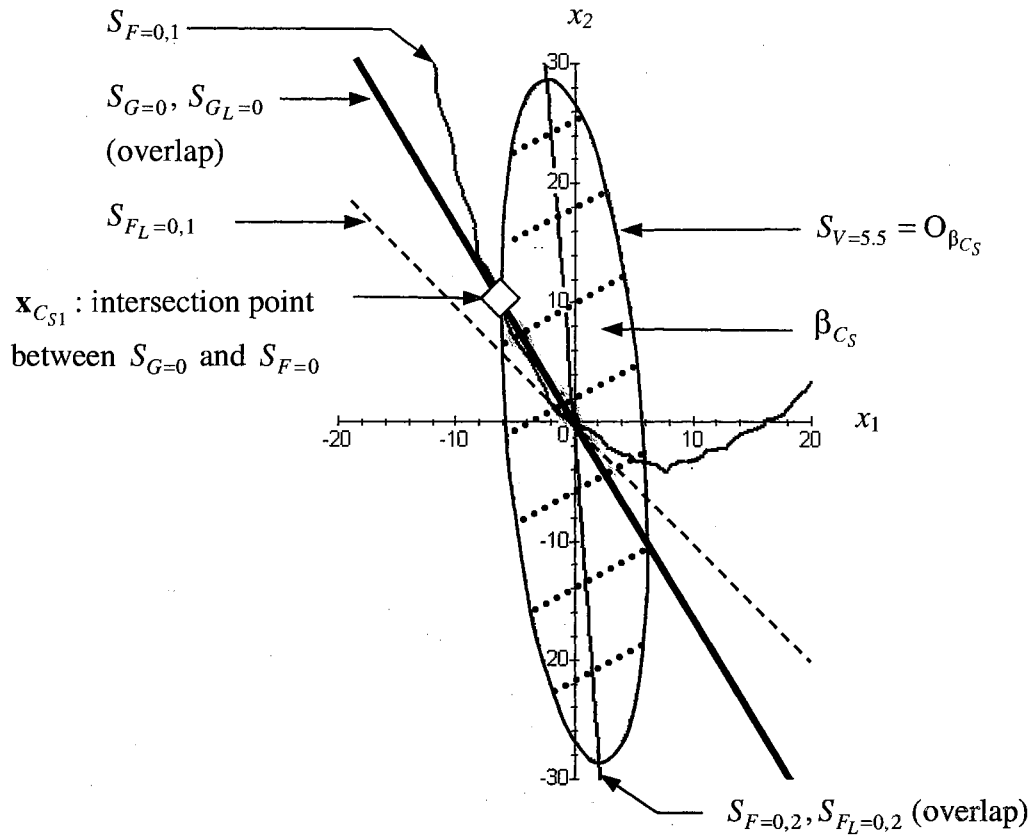
Fig. E1.1.2 β_{C_S} or the Largest LAR Corresponding to $P_{(E1.1.4)}$

when $S_{G_L=0}$ is not on the Symmetry Axis of $S_{F_L=0}$

Remarks: 1) Some portions of $S_{F=0}$ and of $S_{G=0}$ overlap $S_{F_L=0}$ and $S_{G_L=0}$

2) $F_L(x)|_{x \neq 0} < 0$ on $S_{G_L=0}$

Now, let us find β_{C_S} corresponding to:

$$P \equiv P_{(E1.1.10)} = \begin{bmatrix} 0.6446 & 0.0728 \\ 0.0728 & 0.0354 \end{bmatrix} \qquad (E\ 1.1.10)$$

Note that $P_{(E1.1.10)}$ is obtained from (2.12) with $\rho = 225$ using later results in our

development for which details will be presented in Chapter II. We substitute $P_{(E1.1.10)}$ for

$\mathbf{P}_{(E1.1.4)}$ in (E 1.1.6), (E 1.1.7), (E 1.1.8), and (E 1.1.9) to obtain a new set of functions

$F(\mathbf{x})$, $F_L(\mathbf{x})$, $G(\mathbf{x})$, and $G_L(\mathbf{x})$:

$$F(\mathbf{x}) = \mathbf{x}^T \mathbf{P}_{(E1.1.10)} \mathbf{f}(\mathbf{x})$$

$$= (0.6446x_1 + 0.0728x_2)(10x_2 + 10x_1 + 10\sin^2(x_1)\sin(x_2) - x_1^2) \qquad \text{(E 1.1.12)}$$

$$+ (0.0728x_1 + 0.0354x_2)(5x_1^2 + \sin(x_2))$$

$$F_L(\mathbf{x}) = \frac{1}{2}\mathbf{x}^T[\mathbf{P}_{(E1.1.10)}\mathbf{A} + [\mathbf{P}_{(E1.1.10)}\mathbf{A}]^T]\mathbf{x} = \mathbf{x}^T\mathbf{M}\mathbf{x} = \mathbf{x}^T \begin{bmatrix} 6.4461 & 3.6233 \\ 3.6233 & 0.7631 \end{bmatrix} \mathbf{x} \quad \text{(E 1.1.13)}$$

$$G(\mathbf{x}) = \mathbf{x}^T \mathbf{P}_{(E1.1.10)} \mathbf{g}(\mathbf{x})$$

$$= (0.0728x_1 + 0.0354x_2)(\cos(x_2) + 1.5) \qquad \text{(E 1.1.14)}$$

$$G_L(\mathbf{x}) = \mathbf{x}^T \mathbf{P}_{(E1.1.10)} \mathbf{B} = 0.1819x_1 + 0.0885x_2 \qquad \text{(E 1.1.15)}$$

where $\mathbf{M} = \begin{bmatrix} 6.4461 & 3.6233 \\ 3.6233 & 0.7631 \end{bmatrix}$. To find graphically the largest possible LAR β_{C_S}

corresponding to $\mathbf{P}_{(E1.1.10)}$, we plot the new surfaces $S_{F=0}$, $S_{F_L=0}$, $S_{G=0}$, and $S_{G_L=0}$

corresponding to $\mathbf{P}_{(E1.1.10)}$ in Fig. E1.1.3 using the same notations and symbols as for

figures E1.1.1, and E1.1.2. Note from figures E1.1.2, and E1.1.3 that β_{C_S} corresponding

to $\mathbf{P}_{(E1.1.4)}$ is significantly smaller than that corresponding to $\mathbf{P}_{(E1.1.10)}$. The boundary of

β_{C_S} corresponding to $\mathbf{P}_{(E1.1.10)}$ is approximately $S_{V=27}$ where $V = \frac{1}{2}\mathbf{x}^T \mathbf{P}_{(E1.1.10)} \mathbf{x}$. Under

$\mathbf{P}_{(E1.1.10)}$, the eigenvalues and eigenvectors of $\mathbf{M}$ are given by:

$$\lambda_{M1} = 8.2092, \ \mathbf{v}_{M1} = [0.8992 \quad 0.4376]^T \qquad \text{(E 1.1.16 a)}$$

$$\lambda_{M2} = -1, \ \mathbf{v}_{M2} = [-0.4376 \quad 0.8992]^T \qquad \text{(E 1.1.16 b)}$$

Using (E 1.1.15), it can be shown that the surface $S_{G_L=0}$ is the line $c\,\mathbf{x}_{G_L=0}$ and

$F_L(\mathbf{x}) < 0$ along this line, where $c \in \Re$ and $\mathbf{x}_{G_L=0} = [0.43755 \quad -0.89920]^T$.
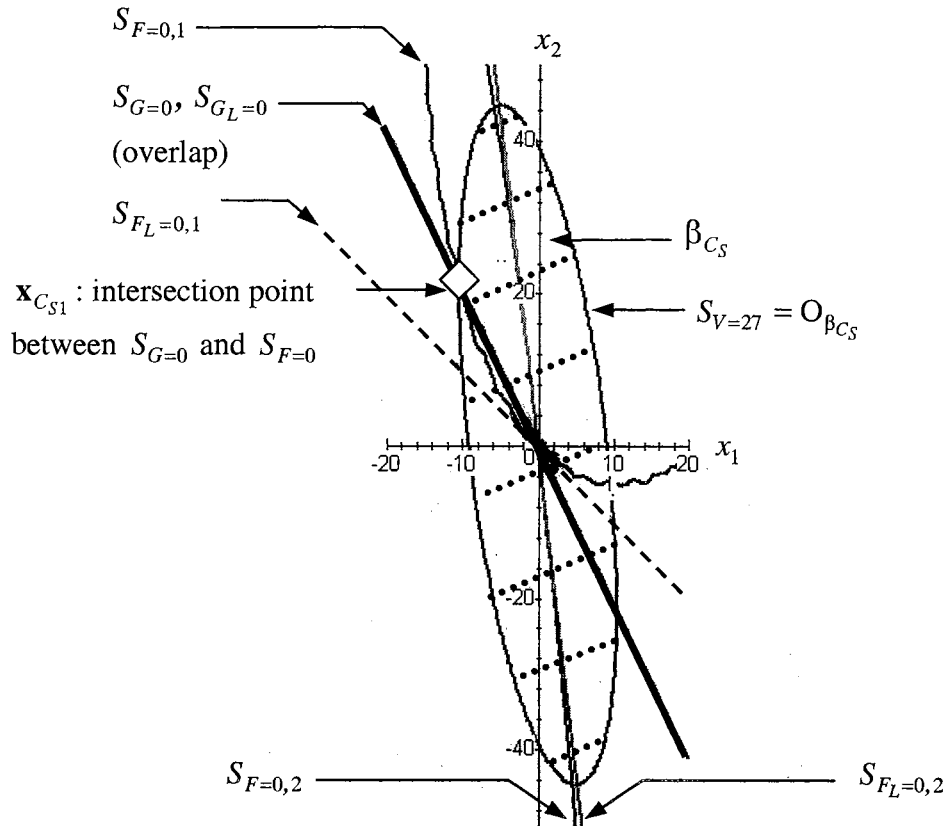
Fig. E1.1.3 β_{C_S} or the Largest LAR Corresponding to $\mathbf{P}_{(E1.1.10)}$ when $S_{G_L=0}$ is on the Symmetry Axis of $S_{F_L=0}$ with $r_{\lambda_M} = 8.2092$

Remarks: 1) Some portions of $S_{F=0}$ and of $S_{G=0}$ overlap $S_{F_L=0}$ and $S_{G_L=0}$ respectively.

2) $F_L(\mathbf{x})|_{\mathbf{x}\neq 0} < 0$ on $S_{G_L=0}$

Now, we see that $S_{G_L=0}$ is spanned by the eigenvector $\mathbf{v}_{M2}$ in (E 1.1.16 b), and $\mathbf{v}_{M2}$ is

the same as $\mathbf{x}_{G_L=0}$. Since we know from Theorem 1.2 that $S_{F_L=0}$ is symmetric about

$\mathbf{v}_{M2}$, it follows that $S_{F_L=0}$ is symmetric about $S_{G_L=0}$. The eigenvalue ratio is

$r_{\lambda_M} = 8.2092$. For this particular problem, the eigenvalue ratio corresponding to $\mathbf{P}_{(E1.1.10)}$

is approximately 11.4% larger than that corresponding to $\mathbf{P}_{(E1.1.4)}$ but because $S_{G_L=0}$ is

exactly on the plane spanned by $\mathbf{v}_{M2}$, we see that $\mathbf{x}_{C_{S1}}$ corresponding to $\mathbf{P}_{(E1.1.10)}$ is

farther from the origin than that corresponding to $\mathbf{P}_{(E1.1.4)}$. This forces β_{C_S} corresponding

to $\mathbf{P}_{(E1.1.10)}$ to be larger than that corresponding to $\mathbf{P}_{(E1.1.4)}$.

To see how a large eigenvalue ratio can affect β_{C_S} when the eigenvector condition is

satisfied, we examine β_{C_S} corresponding to:

$$\mathbf{P} \equiv \mathbf{P}_{(E1.1.17)} = \begin{bmatrix} 4.3990 & 2.6830 \\ 2.6830 & 2.1917 \end{bmatrix} \qquad \text{(E 1.1.17)}$$

Note that $\mathbf{P}_{(E1.1.17)}$ is obtained from (2.12) with $\rho = 1$ using later results in our

development for which details will be presented in Chapter II. We substitute $\mathbf{P}_{(E1.1.17)}$ for

$\mathbf{P}_{(E1.1.4)}$ in (E 1.1.6), (E 1.1.7), (E 1.1.8), and (E 1.1.9) to obtain a new set of functions

$F(\mathbf{x})$, $F_L(\mathbf{x})$, $G(\mathbf{x})$, and $G_L(\mathbf{x})$:

$$
\begin{aligned}
F(\mathbf{x}) &= \mathbf{x}^T \mathbf{P}_{(E1.1.17)} \mathbf{f}(\mathbf{x}) \\
&= (4.3990x_1 + 2.6830x_2)(10x_2 + 10x_1 + 10\sin^2(x_1)\sin(x_2) - x_1^2) \qquad \text{(E 1.1.18)} \\
&\quad + (2.6830x_1 + 2.1917x_2)(5x_1^2 + \sin(x_2))
\end{aligned}
$$

$$F_L(\mathbf{x}) = \frac{1}{2}\mathbf{x}^T [\mathbf{P}_{(E1.1.17)}\mathbf{A} + [\mathbf{P}_{(E1.1.17)}\mathbf{A}]^T]\mathbf{x} = \mathbf{x}^T \mathbf{M}\mathbf{x} = \mathbf{x}^T \begin{bmatrix} 43.9900 & 36.7515 \\ 36.7515 & 29.0217 \end{bmatrix} \mathbf{x} \quad \text{(E 1.1.19)}$$

$$
\begin{aligned}
G(\mathbf{x}) &= \mathbf{x}^T \mathbf{P}_{(E1.1.17)} \mathbf{g}(\mathbf{x}) \\
&= (2.6830x_1 + 2.1917x_2)(\cos(x_2) + 1.5)
\end{aligned}
\qquad \text{(E 1.1.20)}
$$

$$G_L(\mathbf{x}) = \mathbf{x}^T \mathbf{P}_{(E1.1.17)} \mathbf{B} = 6.7075x_1 + 5.4793x_2 \qquad \text{(E 1.1.21)}$$

where $\mathbf{M} = \begin{bmatrix} 43.9900 & 36.7515 \\ 36.7515 & 29.0217 \end{bmatrix}$. To find graphically the largest possible LAR β_{C_S}

corresponding to $\mathbf{P}_{(E1.1.17)}$, we plot the new surfaces $S_{F=0}$, $S_{F_L=0}$, $S_{G=0}$, and $S_{G_L=0}$

corresponding to $\mathbf{P}_{(E1.1.17)}$ in Fig. E1.1.4 using the same notations and symbols as for

the previous figures. Note from figures E1.1.3, and E1.1.4 that β_{C_S} corresponding

to $\mathbf{P}_{(E1.1.10)}$ is significantly larger than that corresponding to $\mathbf{P}_{(E1.1.17)}$. The boundary of

β_{C_S} corresponding to $\mathbf{P}_{(E1.1.17)}$ is approximately $S_{V=6.5}$ where $V = \frac{1}{2}\mathbf{x}^T \mathbf{P}_{(E1.1.17)} \mathbf{x}$.
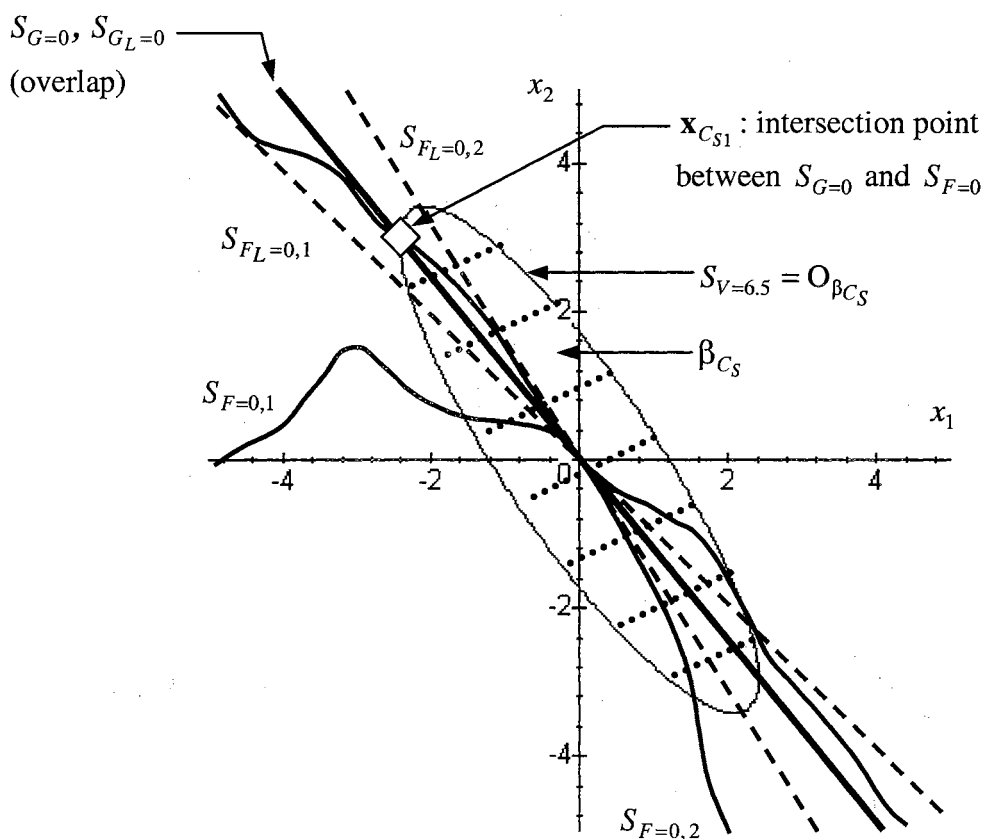
Fig. E1.1.4 β_{C_S} or the Largest LAR Corresponding to $\mathbf{P}_{(E1.1.17)}$ when $S_{G_L=0}$ is on the
Symmetry Axis of $S_{F_L=0}$ with $r_{\lambda_M} = 74.0117$

Remarks: 1) Some portions of $S_{F=0}$ and of $S_{G=0}$ overlap $S_{F_L=0}$ and $S_{G_L=0}$
respectively. 2) $F_L(\mathbf{x})|_{\mathbf{x}\neq 0} < 0$ on $S_{G_L=0}$

Under $\mathbf{P}_{(E1.1.17)}$, the eigenvalues and eigenvectors of $\mathbf{M}$ are given by:

$$\lambda_{M1} = 74.0117, \quad \mathbf{v}_{M1} = [0.7745 \ 0.6326]^T \qquad \text{(E 1.1.22 a)}$$

$$\lambda_{M2} = -1, \quad \mathbf{v}_{M2} = [-0.6326 \ 0.7745]^T \qquad \text{(E 1.1.22 b)}$$

Using (E 1.1.21), it can be shown that the surface $S_{G_L=0}$ is the line $c\,\mathbf{x}_{G_L=0}$ and

$F_L(\mathbf{x}) < 0$ along this line, where $c \in \Re$ and $\mathbf{x}_{G_L=0} = [-0.6326 \ 0.7745]^T$. Now, we see

that $S_{G_L=0}$ is spanned by the eigenvector $\mathbf{v}_{M2}$ in (E 1.1.22 b), and $\mathbf{v}_{M2}$ is the same as

$\mathbf{x}_{G_L=0}$. Since we know from Theorem 1.2 that $S_{F_L=0}$ is symmetric about $\mathbf{v}_{M2}$, it follows

that $S_{F_L=0}$ is symmetric about $S_{G_L=0}$. The eigenvalue ratio is $r_{\lambda_M} = 74.0117$. For this

particular problem, the eigenvalue ratio corresponding to $\mathbf{P}_{(E1.1.10)}$ is approximately

900% larger than that corresponding to $\mathbf{P}_{(E1.1.17)}$, although both $\mathbf{P}_{(E1.1.10)}$ and $\mathbf{P}_{(E1.1.17)}$

satisfy the eigenvector condition. Notice that $S_{F=0}$ intersects $S_{G=0}$ much closer to the

origin under $\mathbf{P}_{(E1.1.17)}$ than it does under $\mathbf{P}_{(E1.1.10)}$. Accordingly, β_{C_S} corresponding to

$\mathbf{P}_{(E1.1.17)}$ is significantly smaller than that corresponding to $\mathbf{P}_{(E1.1.10)}$.

1.5   Summary

1)   There are numerous physical nonlinear systems whose mathematical descriptions

present structural and algebraic difficulties when designing a globally stabilizing

controller for. Examples are underactuated systems such as double-inverted-

pendulum systems (Misawa, Arrington, and Ledgerwood 1995), (Walker et al,

1991), and cart-and-pole systems (Wang, 1994), (Ogata, 1997), (Slotine, and Li,

1991). For such systems, we often admit locally stabilizing controllers designed by applying linear system theory to suitable linearized models. Theoretically, we expect the linear controller to stabilize the nonlinear system in a region where the linear approximation is valid. However, we generally do not examine the size of this region when designing a linear controller. After such design, simulations are employ to numerically estimate the resultant attractive region.

2)   A major drawback of a linear controller designed by applying linear system theory to a linearized model is that the attractive region of the corresponding nonlinear system can be unsatisfactorily small. It is known that a linear controller can be designed either by relocating the eigenvalues of the linearized model or by optimizing a performance index, although their relationships to the attractive region of the corresponding nonlinear system are not obvious. The fundamental idea of LARC is to employ a quadratic Lyapunov function and a linear controller to guarantee local stability with a reasonably large LAR. Since Lyapunov stability guarantees that an attractive region must contain a LAR, LARC indirectly produces a reasonably large attractive region.

3)   By definition, a LAR does not contain the intersection between the surfaces $S_{G=0}$ and $S_{F=0}$ denoted by $\mathbf{x}_{C_{Si}}$, $i = 1, 2, ...$ Accordingly, a necessary condition for a large LAR is that either $\mathbf{x}_{C_{Si}}$ does not exist or that $\left\| \mathbf{x}_{C_{Si}} \right\|$ is large $\forall i$. Since the surfaces $S_{G=0}$ and $S_{F=0}$ depend on the equation of motion and $\mathbf{P}$, we can only

search for a special choice of $\mathbf{P}$ that removes or expels $\mathbf{x}_{C_{Si}}$ from the origin. A possible approach for obtaining such $\mathbf{P}$ is to exploit specific nonlinearities and structures of $F(\mathbf{x})$ and $G(\mathbf{x})$. However,

3.1)   We realize that the characteristics of $F(\mathbf{x})$ and $G(\mathbf{x})$ in many physical systems are extremely difficult to analyze for such purpose, and thus reasonable simplifications are needed to make the problem tractable.

3.2)   Depending solely on specific nonlinearities and structures of $F(\mathbf{x})$ and $G(\mathbf{x})$ can limit the applicability of the resulting scheme.

Accordingly, we primarily formulate LARC based on the characteristics of $S_{G_L=0}$ and $S_{F_L=0}$. This is because there are infinitely many $F(\mathbf{x})$ and $G(\mathbf{x})$ that can be approximated by $F_L(\mathbf{x})$ and $G_L(\mathbf{x})$ in operating regions about the origin. In addition, this simplifies the problem because $F_L(\mathbf{x})$ and $G_L(\mathbf{x})$ are obtained from a linearized model. We will orient $S_{G_L=0}$ and $S_{F_L=0}$ such that the location of a possible $\mathbf{x}_{C_{Si}}$ is reasonably far from the origin in the presence of nonlinearities.

4)   In the presence of possibly complex nonlinearities in (1.1), we orient $S_{G_L=0}$ on the symmetry plane of $S_{F_L=0}$ such that $F_L(\mathbf{x})|_{\mathbf{x}\neq\mathbf{0}}<0$ on $S_{G_L=0}$, and r_{λ_M} is small. Geometrically, it is conceivable from Fig. 1.2 that this relative orientation locates $\mathbf{x}_{C_{Si}}$ "reasonably far" from the origin in the sense that $\left\|\mathbf{x}_{C_{Si}}\right\| \to \infty$ as the degree of nonlinearities becomes smaller but need not be zero. Notice that the effects of

nonlinearities have been handled implicitly by such choice of relative orientation. However, this may not remove $\mathbf{x}_{C_{Si}}$ or maximize $\left\| \mathbf{x}_{C_{Si}} \right\|$ when possible, because specific nonlinearities and structures of $F(\mathbf{x})$ and of $G(\mathbf{x})$ have not been included in the formulation, and optimization has not been employed.

Chapter II

Eigenvector Condition and Controller Generation

2.1   Introduction

We have pointed out in Chapter I that a linear controller designed primarily for stabilizing

a linearized model may yield a small attractive region for the corresponding nonlinear

model. We apply Lyapunov stability in Chapter I to show that a large attractive region

could be obtained by forcing the corresponding LAR to be large. By our definition, we see

that a LAR (denoted by β_{C_L}) depends on $\mathbf{P}$ and $u(\mathbf{x})$. To obtain a large LAR, it is

necessary to locate every intersection point between $S_{F=0}$ and $S_{G=0}$ (denoted by $\mathbf{x}_{C_{Si}}$) far

from the origin to obtain a large β_{C_S}. We know by inspection that $\mathbf{x}_{C_{Si}}$ and β_{C_S} depend

on $\mathbf{P}$ and the equation of motion (1.1). Since the equation of motion is given, we can alter

only $\mathbf{P}$ to produce the desired results. We introduced in Proposition 1.1 the "eigenvector

condition" for systems with $n = 2$, which is a particular relative orientation of $S_{F_L=0}$ and

$S_{G_L=0}$ that locates $\mathbf{x}_{C_{Si}}$ reasonably far from the origin and produces a reasonably large

β_{C_S}. However, the existence and choice of $\mathbf{P}$ yielding such relative orientation in

arbitrary n-space was not clear.

In this chapter:

1)   We formulate the generalized version of the eigenvector condition for representing

such particular relative orientation of $S_{F_L=0}$ and $S_{G_L=0}$ in n-space.

2)   We establish conditions for the existence or nonexistence of $\mathbf{P}$ that satisfies the eigenvector condition.

3)   We address computational methods for obtaining $\mathbf{P}$ to satisfy the eigenvector condition, provided that such $\mathbf{P}$ exists.

4)   We generate a linear control $u_{LARC}(\mathbf{x})$ for obtaining a reasonably large LAR when the eigenvector condition can be satisfied.

For these purposes, the basic conditions $C1 - C4$ given in Section 1.3 will be recalled frequently.

2.2   Mathematical Description of Eigenvector Condition

According to the two dimensional case discussed in Proposition 1.1, we want to locate $S_{G_L=0}$ on the symmetry plane of $S_{F_L=0}$ so that small deviations of $S_{F=0}$ from $S_{F_L=0}$ and of $S_{G=0}$ from $S_{G_L=0}$ do not put possible intersections $\mathbf{x}_{C_{Si}}$ between $S_{F=0}$ and $S_{G=0}$ close to the origin. At the same time, we require that $S_{G_L=0} \subset R_{[F_L<0]\cup\{0\}}$ for stability of the linearized model as pointed out in Lemma 1.1. Notice that $S_{G_L=0}$ in a two-dimensional system is a line. Accordingly, we can satisfy these requirements in a two-dimensional system by locating $S_{G_L=0}$ on the line along the eigenvector $\mathbf{v}_{M2}$ corresponding to the negative eigenvalue λ_{M2} of $\mathbf{M}$ because $z_2\mathbf{v}_{M2} \subset R_{[F_L<0]\cup\{0\}} \quad \forall z_2 \in \Re$. We now want to find a precise mathematical condition that is equivalent to such relative orientation in n-space. To do this, we draw from the proofs of Theorem 1.1 and 1.2 that:

1) $F_L(\mathbf{x})$ is a quadratic function and the surface $S_{F_L=0}$ is symmetric about the n real

orthonormal eigenvectors $\mathbf{v}_{M1}, \ldots, \mathbf{v}_{Mn}$ of the symmetric matrix $\mathbf{M}$.

2) The matrix $\mathbf{M}$ has exactly one positive eigenvalue λ_{M1} and n-1 negative

eigenvalues $\lambda_{M2}, \ldots, \lambda_{Mn}$.

3) $S_{G_L=0}$ is a plane of dimension n-1 and we must have that $S_{G_L=0} \subset R_{[F_L<0]\cup\{\mathbf{0}\}}$ for

stability of the linearized model.

According to these results, we can orient $S_{G_L=0}$ such that $S_{F_L=0}$ is symmetric about

$S_{G_L=0}$ and $S_{G_L=0} \subset R_{[F_L<0]\cup\{\mathbf{0}\}}$ by locating the eigenvectors $\mathbf{v}_{M2}, \ldots, \mathbf{v}_{Mn}$ corresponding to

the negative eigenvalues $\lambda_{M2}, \ldots, \lambda_{Mn}$ on $S_{G_L=0}$. In other words, we want to find $\mathbf{P}$ such

that $\{\mathbf{v}_{M2}, \ldots, \mathbf{v}_{Mn}\}$ is a basis set for generating $S_{G_L=0}$. Since $S_{G_L=0}$ is a plane of

dimension n-1 and all the eigenvectors of $\mathbf{M}$ are orthogonal, this condition can be satisfied

by choosing $\mathbf{P}$ such that the normal vector of $S_{G_L=0}$ or $\nabla(G_L(\mathbf{x})) = [\mathbf{PB}]$ points in the

direction of the eigenvector $\mathbf{v}_{M1}$ corresponding to the only positive eigenvalue λ_{M1} of $\mathbf{M}$.

This latter condition is more convenient to apply to SIMO systems than the former

because it involves only two vectors, namely $\nabla(G_L(\mathbf{x}))$ and $\mathbf{v}_{M1}$. Accordingly, the term

"eigenvector condition" is associated with the latter condition in this chapter unless

otherwise stated.

2.2   Theorems

To find **P** that satisfies the eigenvector condition, we examine properties of the functions

$F_L(\mathbf{x})$ and $G_L(\mathbf{x})$ further in the following theorems:

Theorem 2.1   (Relationship between Eigenvectors of **M** and **N**)

If the basic conditions $C1 - C4$ in Chapter I are satisfied with $\mathbf{Q} = c\mathbf{I}$ where $c \in \mathfrak{R}^+$, then

the sets of eigenvectors of $\mathbf{N} \equiv \dfrac{1}{2}[[\mathbf{PB}]\mathbf{K} + \mathbf{K}^T[\mathbf{PB}]^T]$ and of $\mathbf{M} \equiv \dfrac{1}{2}[\mathbf{PA} + \mathbf{A}^T\mathbf{P}]$ are the

same.

Proof

It is clear that the existence of the symmetric positive definite matrix **P** satisfying the

Lyapunov equation is guaranteed by Lyapunov stability if $C1 - C4$ are satisfied. Now, let

Q in $C4$ be $c\mathbf{I}$ where $c \in \mathfrak{R}^+$ and consider the Lyapunov matrix equation:

$$
\begin{aligned}
-\mathbf{Q} = -c\mathbf{I} &= \frac{1}{2}[\mathbf{P\overline{A}} + [\mathbf{P\overline{A}}]^T] \\
&= \frac{1}{2}\Big[\mathbf{P}[\mathbf{A} - \mathbf{BK}] + [\mathbf{A} - \mathbf{BK}]^T\mathbf{P}\Big] \\
&= \frac{1}{2}[\mathbf{PA} + \mathbf{A}^T\mathbf{P}] - \frac{1}{2}[[\mathbf{PB}]\mathbf{K} + \mathbf{K}^T[\mathbf{PB}]^T] \\
&\equiv \mathbf{M} - \mathbf{N}
\end{aligned}
\tag{2.1}
$$

where $\mathbf{N} \equiv \dfrac{1}{2}[[\mathbf{PB}]\mathbf{K} + \mathbf{K}^T[\mathbf{PB}]^T] = \dfrac{1}{2}[\mathbf{PBK} + [\mathbf{PBK}]^T]$ and $\mathbf{M} \equiv \dfrac{1}{2}[\mathbf{PA} + \mathbf{A}^T\mathbf{P}]$

$= [\mathbf{PA} + [\mathbf{PA}]^T]$ are symmetric because $\Xi + \Xi^T$ is symmetric for all $\Xi \in \mathfrak{R}^{n \times n}$.

Since **M** is real symmetric, it has n real eigenvalues λ_{Mi} and n real orthonormal

eigenvectors $\mathbf{v}_{Mi}$, $i = 1,...,n$ (Hagan et al, 1996). Now recall the linear transformation

matrix $\mathbf{T_M}$ from (1.18):

$$\mathbf{T_M} = [\mathbf{v}_{M1} \mid \mathbf{v}_{M2} \mid \cdots \mid \mathbf{v}_{Mn}] \tag{1.18}$$

We premultiply and postmultiply every term in (2.1) by $\mathbf{T_M^{-1}}$ and $\mathbf{T_M}$ respectively to

produce:

$$-c\mathbf{T_M^{-1}IT_M} = \mathbf{T_M^{-1}MT_M} - \mathbf{T_M^{-1}NT_M} \tag{2.2}$$

Since $\mathbf{Mv}_{Mi} = \lambda_{Mi}\mathbf{v}_{Mi}$, $i = 1,...,n$, we obtain:

$$\mathbf{T_M^{-1}MT_M} = \mathbf{\Lambda_M} \tag{2.3}$$

where $\mathbf{\Lambda_M} \in \mathfrak{R}^{n \times n}$ is a diagonal matrix whose diagonal elements are λ_{Mi}, $i = 1,...,n$.

Since $-c\mathbf{T_M^{-1}IT_M} = -c\mathbf{I}$, (2.2) can be rewritten as:

$$\begin{aligned} -c\mathbf{I} &= \mathbf{\Lambda_M} - \mathbf{T_M^{-1}NT_M} \\ \mathbf{T_M^{-1}NT_M} &= c\mathbf{I} + \mathbf{\Lambda_M} \end{aligned} \tag{2.4}$$

From the right-hand side of (2.4), we see that $\mathbf{T_M^{-1}NT_M} \equiv \mathbf{\Lambda_N}$ is diagonal. This shows that

N can be diagonalized by using the eigenvectors $\mathbf{v}_{Mi}$, $i = 1, ..., n$ of **M**. Accordingly, we

see that **N** and **M** have the same set of eigenvectors and the diagonal elements of $\mathbf{\Lambda_N}$ are

the eigenvalues of **N**. This completes the proof.

Theorem 2.2 (Properties of Eigensystem of **N**)

If the basic conditions $C1 - C4$ are satisfied then the matrix $\mathbf{N} \equiv \dfrac{1}{2}[[\mathbf{PB}]\mathbf{K} + \mathbf{K}^T[\mathbf{PB}]^T]$

has the following properties:

*P*1)   **N** has exactly one positive eigenvalue.

*P*2)   **N** has at most one negative eigenvalue.

Remark: The remaining eigenvalues of **N** other than those in *P*1 and *P*2 are

all zeros.

*P*3)   The eigenvector corresponding to the positive eigenvalue in 1) bisects the angle

between the vector [**PB**] and the vector $\mathbf{K}^T$.

Remark: We say that a vector **v** "bisects" the vectors [**PB**] and $\mathbf{K}^T$ if

$$c\mathbf{v} = [\mathbf{PB}]/\|\mathbf{PB}\| + \mathbf{K}^T / \| \mathbf{K}^T \|, \ c \in \Re^+ .$$

*P*4)   If the negative eigenvalue in *P*2 exists, then the corresponding eigenvector bisects

the angle between the vector [**PB**] and the vector $-\mathbf{K}^T$.

Proof

The existence of the symmetric positive definite matrix **P** satisfying the Lyapunov

equation is guaranteed by Lyapunov stability if *C*1 – *C*4 are satisfied. We now substitute

$-\mathbf{Kx}$ for $u(\mathbf{x})$ in (1.14) to produce:

$$\dot{V}_L(\mathbf{x}) = \frac{1}{2}\mathbf{x}^T \left[\mathbf{P}[\mathbf{A} - \mathbf{BK}] + [\mathbf{A} - \mathbf{BK}]^T \mathbf{P} \right] \mathbf{x}$$

$$= \frac{1}{2}\mathbf{x}^T [\mathbf{PA} + \mathbf{A}^T\mathbf{P}]\mathbf{x} - \frac{1}{2}\mathbf{x}^T [\mathbf{P}[\mathbf{BK}] + [\mathbf{BK}]^T\mathbf{P}]\mathbf{x} \qquad (2.5)$$

$$= \mathbf{x}^T\mathbf{Mx} - \mathbf{x}^T\mathbf{Nx}$$

where $\mathbf{N} \equiv \frac{1}{2}[\mathbf{P}[\mathbf{BK}] + [\mathbf{BK}]^T \mathbf{P}] = \frac{1}{2}[[\mathbf{PB}]\mathbf{K} + \mathbf{K}^T[\mathbf{PB}]^T]$ and $\mathbf{M} \equiv \frac{1}{2}[\mathbf{PA} + \mathbf{A}^T\mathbf{P}]$

$= [\mathbf{PA} + [\mathbf{PA}]^T]$ are symmetric because $\Xi + \Xi^T$ is symmetric for all $\Xi \in \Re^{n \times n}$. Now

rewrite:

$$\mathbf{x}^T \mathbf{N} \mathbf{x} = \frac{1}{2} \mathbf{x}^T [\mathbf{P}[\mathbf{BK}] + [\mathbf{BK}]^T \mathbf{P}] \mathbf{x}$$
$$= \mathbf{x}^T [\mathbf{PB}] \mathbf{Kx} \tag{2.6}$$
$$= g_{\mathrm{N1}}(\mathbf{x}) g_{\mathrm{N2}}(\mathbf{x})$$

where $g_{\mathrm{N1}}(\mathbf{x}) \equiv \mathbf{x}^T \mathbf{PB} \in \Re$, $g_{\mathrm{N2}}(\mathbf{x}) \equiv \mathbf{Kx} \in \Re$, and $[\mathbf{PB}]$ and $\mathbf{K}^T \in \Re^n$. Now, we consider the following possibilities:

a) $\mathbf{PB} = c\mathbf{K}^T$, $c \in \Re^+$

In this case, it is clear that $\mathbf{x}^T \mathbf{N} \mathbf{x}$ is zero in the plane $\mathbf{x}^T \mathbf{PB} = \mathbf{Kx} = 0$ and is

positive along the vector $\nabla g_{\mathrm{N1}}(\mathbf{x}) = \mathbf{PB} = c\nabla g_{\mathrm{N2}}(\mathbf{x}) = c\mathbf{K}^T$. This implies that our

theorem is satisfied with $\mathbf{N} = \mathbf{N}^T$ has only one positive eigenvalue λ_{N1}

corresponding to the eigenvector $\mathbf{v}_{\mathrm{N1}} = \mathbf{PB} = \mathbf{K}^T$, and has *n*-1 zero eigenvalues

corresponding to *n*-1 eigenvectors of $\mathbf{N}$ spanning the solution space of the linear

equation $\mathbf{x}^T \mathbf{PB} = \mathbf{Kx} = 0$.

b) $\mathbf{PB} = -c\mathbf{K}^T$, $c \in \Re^+$

If $\mathbf{K}$ is chosen such that $\overline{\mathbf{A}} = [\mathbf{A} - \mathbf{BK}]$ is stable, then it is impossible that $\mathbf{PB} =$

$-c\mathbf{K}^T$, $c \in \Re^+$. Otherwise, we have that $\mathbf{x}^T \mathbf{N} \mathbf{x} = -c\mathbf{x}^T [\mathbf{PB}][\mathbf{PB}]^T \mathbf{x} \leq 0$ and

$\dot{V}_L(\mathbf{x}) = \mathbf{x}^T \mathbf{M} \mathbf{x} - \mathbf{x}^T \mathbf{N} \mathbf{x}$ cannot be negative definite. This is because we know from

Theorem 1.1 that $\mathbf{M}$ has exactly one positive eigenvalue implying that

$\exists \mathbf{x} : \mathbf{x}^T \mathbf{M} \mathbf{x} > 0$. If $\mathbf{x}^T \mathbf{N} \mathbf{x} \leq 0$, then it is clear that $\dot{V}_L(\mathbf{x}) > 0$ when $\mathbf{x}^T \mathbf{M} \mathbf{x} > 0$

contradicting the known fact that there exists a quadratic Lyapunov function for

every stable linear system.

c) $\mathbf{PB} \neq a\mathbf{K}^T$, $a \in \mathfrak{R}$

In this case, $\mathbf{PB}$ and $\mathbf{K}^T$ are linearly independent. When $n = 2$, we change the

basis by using the linear transformation $\mathbf{z} = [z_1 \ z_2]^T = \overline{\mathbf{T}}_{\mathbf{N}}\mathbf{x}$ defined by

$z_1 = g_{\mathrm{N}1}(\mathbf{x})/\|\nabla g_{\mathrm{N}1}(\mathbf{x})\| = \mathbf{x}^T\mathbf{PB}/\|\mathbf{PB}\|$, and $z_2 = g_{\mathrm{N}2}(\mathbf{x})/\|\nabla g_{\mathrm{N}2}(\mathbf{x})\| = \mathbf{Kx}/\|\mathbf{K}^T\|$.

For higher-order systems, we find additional $n\text{-}2$ linear equations $z_i = g_{\mathrm{N}i}(\mathbf{x})$, $i =$

$3, ..., n$ such that $\{\nabla g_{\mathrm{N}1}(\mathbf{x}), \nabla g_{\mathrm{N}2}(\mathbf{x}), ..., \nabla g_{\mathrm{N}n}(\mathbf{x})\}$ are linearly independent to

complete the linear transformation. The existence of this set of n linearly

independent vectors is guaranteed because this is the definition of $\mathfrak{R}^n$. This

produces:

$$\overline{\mathbf{T}}_{\mathbf{N}} = [\nabla g_{\mathrm{N}1}(\mathbf{x})/\|\nabla g_{\mathrm{N}1}(\mathbf{x})\| \big| \nabla g_{\mathrm{N}2}(\mathbf{x})/\|\nabla g_{\mathrm{N}2}(\mathbf{x})\| \big| ... \big| \nabla g_{\mathrm{N}n}(\mathbf{x})/\|\nabla g_{\mathrm{N}n}(\mathbf{x})\|]^T \quad (2.7)$$

Under the transformation $\mathbf{z} = \overline{\mathbf{T}}_{\mathbf{N}}\mathbf{x}$, we have:

$$
\begin{aligned}
\mathbf{x}^T\mathbf{Nx} &= \mathbf{x}^T[\mathbf{PB}]\mathbf{Kx} \\
&= \|\mathbf{PB}\|\,\|\mathbf{K}^T\|\,z_1 z_2 \\
&= \|\mathbf{PB}\|\,\|\mathbf{K}^T\|
\begin{bmatrix} z_1 \\ z_2 \\ z_3 \\ \vdots \\ z_n \end{bmatrix}^T
\begin{bmatrix}
0 & 0.5 & 0 & \cdots & 0 \\
0.5 & 0 & 0 & \cdots & 0 \\
0 & 0 & 0 & \cdots & 0 \\
\vdots & \vdots & \vdots & \ddots & 0 \\
0 & 0 & 0 & \cdots & 0
\end{bmatrix}
\begin{bmatrix} z_1 \\ z_2 \\ z_3 \\ \vdots \\ z_n \end{bmatrix}
\qquad (2.8) \\
&\equiv \|\mathbf{PB}\|\,\|\mathbf{K}^T\|\,\mathbf{z}^T\mathbf{N}_{\overline{T}}\mathbf{z}
\end{aligned}
$$

where $\mathbf{N}_{\overline{T}} \equiv \begin{bmatrix}
0 & 0.5 & 0 & \cdots & 0 \\
0.5 & 0 & 0 & \cdots & 0 \\
0 & 0 & 0 & \cdots & 0 \\
\vdots & \vdots & \vdots & \ddots & 0 \\
0 & 0 & 0 & \cdots & 0
\end{bmatrix}$. Because of the special structure of $\mathbf{N}_{\overline{T}}$, direct

computations show that:

$$\lambda_{N_{\bar{T}}1} = 0.5, \mathbf{v}_{N_{\bar{T}}1} = [1 \quad 1 \ 0 \ 0 \ \cdots \ 0]^T$$

$$\lambda_{N_{\bar{T}}2} = -0.5, \mathbf{v}_{N_{\bar{T}}2} = [1 \ -1 \ 0 \ 0 \ \cdots \ 0]^T$$

$$\lambda_{N_{\bar{T}}3} = 0.0, \mathbf{v}_{N_{\bar{T}}3} = [0 \quad 0 \ 1 \ 0 \ \cdots \ 0]^T \qquad (2.9)$$

$$\vdots \qquad \qquad \vdots$$

$$\lambda_{N_{\bar{T}}n} = 0.0, \mathbf{v}_{N_{\bar{T}}n} = [0 \quad 0 \ 0 \ 0 \ \cdots \ 1]^T$$

where $\lambda_{N_{\bar{T}}i}$ and $\mathbf{v}_{N_{\bar{T}}i}$, $i = 1, \ldots, n$ are the eigenvalues and eigenvectors of $N_{\bar{T}}$

respectively. Unlike similarity transformations, the linear transformation $\mathbf{z} = \overline{\mathbf{T}}_{\mathbf{N}}\mathbf{x}$

does not preserve the eigenvalues of $\mathbf{N}$ in general because the eigenvalues of $N_{\bar{T}}$

are as given in (2.9) for all $\mathbf{N}$. However, this linear transformation shows that the

quadratic function $\mathbf{x}^T\mathbf{N}\mathbf{x}$ increases along $\mathbf{v}_{N_{\bar{T}}1}$ and decreases along $\mathbf{v}_{N_{\bar{T}}2}$. This

implies that the real symmetric matrix $\mathbf{N}$ has one positive eigenvalue associated

with an eigenvector pointing in the direction of $\mathbf{v}_{N_{\bar{T}}1}$, and has one negative

eigenvalue associated with an eigenvector pointing in the direction of $\mathbf{v}_{N_{\bar{T}}2}$. In the

transformed basis, $\mathbf{v}_{N_{\bar{T}}1} = [1 \ 1 \ 0 \ 0 \ \cdots \ 0]^T$ implies that $\mathbf{v}_{N_{\bar{T}}1}$ bisects the angle

between the $z_1 - \text{axis}$ and the $z_2 - \text{axis}$. Accordingly, we have that the

eigenvector of $\mathbf{N}$ corresponding to the only positive eigenvalue of $\mathbf{N}$ bisects the

angle between the vectors $[\mathbf{PB}]$ and $\mathbf{K}^T$ in the original basis because the $z_1 - \text{axis}$

is along the vector $[\mathbf{PB}]$, and the $z_2 - \text{axis}$ is along the vector $\mathbf{K}^T$ in the original

basis. In the same fashion, we have that the eigenvector of $\mathbf{N}$ corresponding to the

only negative eigenvalue of $\mathbf{N}$ bisects the angle between the vectors $\mathbf{PB}$ and $-\mathbf{K}^T$

in the original basis.

Combining the results in cases a), b), and c), we conclude that $P1$, $P2$, $P3$, and $P4$ in

Theorem 2.2 hold. This completes the proof.

Lemma 2.1   (Relationship between v_{M1} and v_{N1})

If the basic conditions $C1 - C4$ are satisfied with $\mathbf{Q} = c\mathbf{I}$ where $c \in \mathfrak{R}^+$, then the direction

of the eigenvector v_{M1} corresponding to the only positive eigenvalue λ_{M1} of $\mathbf{M}$

(Theorem 1.1) and the direction of the eigenvector v_{N1} corresponding to the only positive

eigenvector λ_{N1} of $\mathbf{N}$ (Theorem 2.2) are the same.

Proof

For convenience, we now expand (2.4):

$$c\begin{bmatrix} -1 & 0 & \cdots & 0 \\ 0 & -1 & \cdots & 0 \\ \vdots & \vdots & \ddots & 0 \\ 0 & 0 & 0 & -1 \end{bmatrix} = \begin{bmatrix} \lambda_{M1} - \lambda_{N1} & 0 & \cdots & 0 \\ 0 & \lambda_{M2} - \lambda_{N2} & \cdots & 0 \\ \vdots & \vdots & \ddots & 0 \\ 0 & 0 & 0 & \lambda_{Mn} - \lambda_{Nn} \end{bmatrix} \tag{2.10}$$

where $c \in \mathfrak{R}^+$. We recall from Theorem 1.1 that $\mathbf{M}$ has exactly one positive eigenvalue

and n-1 negative eigenvalues, and from Theorem 2.2 that $\mathbf{N}$ has exactly one positive

eigenvalue and at most one negative eigenvalue. Since $c \in \mathfrak{R}^+$, we see from (2.10) that:

$$\lambda_{Mi} - \lambda_{Ni} = -c < 0 \tag{2.11}$$

where $i = 1, \ldots, n$. Accordingly, this inequality is satisfied at an index $j \in \{1, \ldots, n\}$ where

λ_{Mj} is the only positive eigenvalue of $\mathbf{M}$ if and only if $\lambda_{Nj} > 0$. This shows the position

matching between the only positive eigenvalue of M and the only positive eigenvalue of N in the principal basis of M. To summarize, we list the known facts:

1) M has only one positive eigenvalue λ_{Mj}.

        Remark: In Theorem 1.1, j is assumed to be 1 for convenience.

2) M and N share the same set of eigenvectors (Theorem 2.1).

3) N has only one positive eigenvalue λ_{Nj} (Theorem 2.2).

4)   (2.10) is in diagonal form.

Accordingly, the position matching of λ_{Mj} and λ_{Nj} in (2.10) implies that both v_{Mj} and

v_{Nj} are the eigenvectors corresponding to λ_{Mj} and to λ_{Nj}. Without loss of generality, we

let $j = 1$ to be consistent with the notation employed in Theorem 1.1. Because

eigenvectors can be different by scalar multiples, Lemma 2.1 follows and the proof is

completed.

Lemma 2.2   (Symmetry of [**PB**] and $\mathbf{K}^T$ about v_{M1})

If the basic conditions $C1 - C4$ are satisfied with $\mathbf{Q} = c\mathbf{I}$ where $c \in \Re^+$, then the

eigenvector v_{M1} corresponding to the only positive eigenvalue λ_{M1} of M bisects the

angle between the vector [**PB**] and the vector $\mathbf{K}^T$.

Proof

By Lemma 2.1, we know that the directions of the eigenvectors v_{M1} and v_{N1} are the

same. Applying $P3$ in Theorem 2.2, we see that v_{M1} bisects the angle between the vector

[PB] and the vector $\mathbf{K}^T$. This completes the proof.

2.3 Generating P to Satisfying the Eigenvector Condition

In this section, we apply Lemma 2.2 to construct a theorem that provides an equation for

generating $\mathbf{P}$ to satisfy the eigenvector condition. It turns out fortunately that such $\mathbf{P}$ is the

solution of a steady-state Riccati equation for which several solving methods are

available. This finding implies a necessary and sufficient condition for the existence of

such $\mathbf{P}$.

Theorem 2.3   (Generating $\mathbf{P}$ to Satisfy the Eigenvector Condition)

The symmetric positive definite matrix $\mathbf{P}$ satisfying the eigenvector condition is the

unique symmetric positive definite solution of the steady state Riccati equation:

$$\begin{aligned} \mathbf{0} &= -2\mathbf{Q} - [\mathbf{PA} + \mathbf{A}^T\mathbf{P}] + 2\rho\mathbf{PBB}^T\mathbf{P} \\ &= -c\mathbf{I} - \mathbf{M} + \overline{\mathbf{N}} \end{aligned} \qquad (2.12)$$

where $\mathbf{Q} = c\mathbf{I}$, $\mathbf{M} \equiv \dfrac{1}{2}[\mathbf{PA} + \mathbf{A}^T\mathbf{P}]$, $\overline{\mathbf{N}} \equiv \dfrac{1}{2}[[\mathbf{PB}]\mathbf{K} + \mathbf{K}^T[\mathbf{PB}]^T]\big|_{\mathbf{K}^T = \rho[\mathbf{PB}]}$, and

ρ and $c \in \Re^+$. The existence of such $\mathbf{P}$ is guaranteed provided that [A, B] is controllable

or stabilizable.

Proof

We rearrange (2.5):

$$\begin{aligned} \dot{V}_L(\mathbf{x}) &= \mathbf{x}^T\mathbf{M}\mathbf{x} - \mathbf{x}^T\mathbf{N}\mathbf{x} \\ &= \mathbf{x}^T\mathbf{M}\mathbf{x} - \mathbf{x}^T[\mathbf{PB}]\mathbf{K}\mathbf{x} \\ &= F_L(\mathbf{x}) + G_L(\mathbf{x})u(\mathbf{x}) \end{aligned} \qquad (2.13)$$

where $F_L(\mathbf{x}) = \mathbf{x}^T \mathbf{M} \mathbf{x}$, $G_L(\mathbf{x}) = \mathbf{x}^T \mathbf{PB}$, and $u(\mathbf{x}) = -\mathbf{Kx}$. From the sufficiency in Lemma 2.2, we know that $\mathbf{v}_{M1}$ bisects the angle between $\mathbf{K}^T$ and $\nabla(G_L(\mathbf{x})) = [\mathbf{PB}]$ provided that we choose $\mathbf{Q} = c\mathbf{I}$. Accordingly, setting

$$\mathbf{K}^T = \rho\,[\mathbf{PB}] \tag{2.14}$$

where $\rho \in \mathfrak{R}^+$ forces $\mathbf{v}_{M1}$ to point in the direction of $[\mathbf{PB}]$ and the eigenvector condition is satisfied automatically with the directions of $\mathbf{K}^T$, $[\mathbf{PB}]$, and $\mathbf{v}_{M1}$ being the same. To see the consequence of this setting, we reproduce (2.1):

$$
\begin{aligned}
-\mathbf{Q} = -c\mathbf{I} &= \frac{1}{2}[\overline{\mathbf{PA}} + [\overline{\mathbf{PA}}]^T] \\
&= \frac{1}{2}[\mathbf{PA} + \mathbf{A}^T\mathbf{P} - [\mathbf{PB}]\mathbf{K} - \mathbf{K}^T[\mathbf{PB}]^T] \\
&\equiv \mathbf{M} - \mathbf{N}
\end{aligned}
\tag{2.1}
$$

where $\mathbf{N} \equiv \frac{1}{2}[[\mathbf{PB}]\mathbf{K} + \mathbf{K}^T[\mathbf{PB}]^T]$, and $\mathbf{M} \equiv \frac{1}{2}[\mathbf{PA} + \mathbf{A}^T\mathbf{P}]$. Substituting $\rho\,[\mathbf{PB}]$ for $\mathbf{K}^T$ in (2.1) produces:

$$-2\mathbf{Q} = -2c\mathbf{I} = \mathbf{PA} + \mathbf{A}^T\mathbf{P} - \rho\,[\mathbf{PB}][\mathbf{PB}]^T - \rho\,[\mathbf{PB}][\mathbf{PB}]^T$$

Rearranging the last equation yields:

$$
\begin{aligned}
0 &= -2c\mathbf{I} - [\mathbf{PA} + \mathbf{A}^T\mathbf{P}] + 2\rho\,\mathbf{PB}\,\mathbf{B}^T\mathbf{P} \\
&= -c\mathbf{I} - \mathbf{M} + \overline{\mathbf{N}}
\end{aligned}
\tag{2.12}
$$

It is clear that (2.12) is a steady-state Riccati equation, whose general form is usually discussed extensively in optimal control literature. A standard topic in this subject is the condition for which the solution matrix $\mathbf{P}$ of the Riccati equation is symmetric positive definite and is unique. To find such condition for our particular setup, we refer to Theorem 13.7 and Corollary 13.8 in (Zhou et al, 1996), while we note that other

references such as (Kwakernaak, and Sivan, 1972) can be employed for the same purpose

but with a different approach. Our setup has the following special properties:

1)   The matrix $\mathbf{Q}$ can be written as $\mathbf{Q} = \overline{\mathbf{C}}^T \overline{\mathbf{C}}$ where $\overline{\mathbf{C}} = \sqrt{c}\mathbf{I}$ and rank$(\overline{\mathbf{C}}) = n$

2) $\text{rank}\left(\begin{bmatrix} \overline{\mathbf{C}} \\ \overline{\mathbf{C}}\mathbf{A} \\ \vdots \\ \overline{\mathbf{C}}\mathbf{A}^{n-1} \end{bmatrix}\right) = n$ because rank$(\overline{\mathbf{C}}) = n$.

3)   The matrix $[\mathbf{PBB}^T\mathbf{P} + \mathbf{Q}]$ is positive definite. Indeed,

$$\mathbf{x}^T[\mathbf{PBB}^T\mathbf{P} + \mathbf{Q}]\mathbf{x} = \mathbf{x}^T[\mathbf{PBB}^T\mathbf{P}]\mathbf{x} + \mathbf{x}^T\mathbf{Q}\mathbf{x}$$

$$= \left\|\mathbf{B}^T\mathbf{Px}\right\|^2 + \left\|\sqrt{c}\mathbf{Ix}\right\|^2$$

Since rank$(\sqrt{c}\mathbf{I}) = n$, it follows that $\left\|\sqrt{c}\mathbf{Ix}\right\|^2 = 0$ only at the origin. Combining

this with the fact that $\left\|\mathbf{B}^T\mathbf{Px}\right\|^2 \geq 0$, we see that $\mathbf{x}^T[\mathbf{PBB}^T\mathbf{P} + \mathbf{Q}]\mathbf{x}$ is a positive

definite function and thus $[\mathbf{PBB}^T\mathbf{P} + \mathbf{Q}]$ is positive definite.

Using the above properties, it can be drawn from (Zhou et al, 1996) that the existence of

the unique symmetric positive definite solution $\mathbf{P}$ of the Riccati equation (2.12) is

guaranteed provided that $[\mathbf{A}, \mathbf{B}]$ is controllable or stabilizable. This completes the proof.

A Remark on the Formulation of LARC

We observe that another investigator might have begun a study of this problem by starting

with the general LQR formulation and the Riccati equation asking "Can $\mathbf{Q}$ be selected

such that $S_{G_L=0}$ bisects $S_{F_L=0}$ and $S_{G_L=0} \subset R_{[F_L<0]\cup\{0\}}$? ", because the investigator might

have seen intuitively that this would provide a basis for a large LAR. In such case, the

investigator would have eventually found that $\mathbf{Q} = c\mathbf{I}$, $c \in \Re^+$ was a proper choice, and

might then claim that this was simply another special case of the LQR problem. However, in addition to such intuition being highly unlikely and the corresponding proof being not obvious, in order to obtain a large LAR, one should also achieve a large angle between the bisecting $S_{G_L=0}$ and $S_{F_L=0}$. We have shown in Chapter I that this requires a small eigenvalue ratio, which is not addressed by simply solving an LQR problem.

2.4   Controller Generation

In this section, we are interested in generating a LARC when uncertainties are not considered explicitly. The fundamental idea of LARC is to force $\dot{V}(\mathbf{x})$ to be negative definite in radially large regions about the origin. We see that this cannot be accomplished at intersection points between $S_{F=0}$ and $S_{G=0}$, and between $S_{F=0}$ and $S_{u=0}$. When the relative orientations of these surfaces are poor, these intersection points can occur arbitrarily close to the origin, and result in an arbitrarily small LAR in the presence of small nonlinearities. Accordingly, we employ the concepts of eigenvector condition (Proposition 1.1) and eigenvalue ratio (Proposition 1.2) to locate these points "reasonably far" from the origin. By locating $\mathbf{x}_{C_{Si}}$ "reasonably far" from the origin, we refer to the illustration in Fig. 1.2 (b) from which we see that $\left\| \mathbf{x}_{C_{Si}} \right\| \to \infty$ as the degree of nonlinearities becomes smaller but need not be zero.

Theorem 2.3 shows that a choice of $\mathbf{P}$ that satisfies the eigenvector condition is the unique symmetric positive definite solution of the Riccati equation (2.12). This Riccati equation is obtained from Lemma 2.2 by substituting a special choice of linear gain

$\rho[\mathbf{PB}]^T = \rho \mathbf{B}^T \mathbf{P}$ for $\mathbf{K}$ in the Lyapunov equation. However, there are infinitely many possible values for $\rho \in \mathfrak{R}^+$ and thus we have infinitely many corresponding $\mathbf{P}$ matrices satisfying the eigenvector condition. To choose an appropriate choice of $\mathbf{P}$, we consider the eigenvalue ratios corresponding to these $\mathbf{P}$ matrices. According to Proposition 1.2, we want to choose $\mathbf{P}$ that yields a small eigenvalue ratio. Such a choice of $\mathbf{P}$ is our "appropriate" choice for the quadratic Lyapunov function in the sense of eigenvector condition (Proposition 1.1) and eigenvalue ratio (Proposition 1.2).

After we find an appropriate quadratic Lyapunov function, it remains to choose $u(\mathbf{x})$ such that the resulting LAR is reasonably large. To obtain a choice of $u(\mathbf{x}) = \mathbf{Kx}$ for this purpose, we reexamine a local approximation of $\dot{V}(\mathbf{x})$ about the origin:

$$\begin{aligned} \dot{V}_L(\mathbf{x}) &= \mathbf{x}^T \mathbf{Mx} - \mathbf{x}^T \mathbf{Nx} \\ &= \mathbf{x}^T \mathbf{Mx} - \mathbf{x}^T [\mathbf{PB}]\mathbf{Kx} \\ &= F_L(\mathbf{x}) + G_L(\mathbf{x})u(\mathbf{x}) \end{aligned} \qquad (2.13)$$

where $\mathbf{P}$ is obtained from Theorem 2.3 to satisfy the eigenvector condition. Now, we recall from the definition of eigenvector condition that $S_{F_L=0}$ is symmetric about $S_{G_L=0}$ such that $S_{G_L=0} \subset R_{[F_L<0]\cup\{0\}}$. By examining (2.13), it is reasonable that we orient $S_{u=0}$ and $S_{G_L=0}$ in the same fashion such that $S_{F_L=0}$ is symmetric about $S_{u=0}$, and $S_{u=0} \subset R_{[F_L<0]\cup\{0\}}$. This particular relative orientation follows from the same reasoning we employ to establish the eigenvector condition. Indeed, if $S_{u=0}$ is close to a particular portion of $S_{F_L=0}$ then the deviations of $S_{F=0}$ from $S_{F_L=0}$ may locate an intersection between $S_{u=0}$ and $S_{F=0}$ arbitrarily close to the origin. At such an intersection, it is clear

that we cannot force $\dot{V}$ to be negative because $u = F = 0$ and the resulting LAR is then small. We see that such linear control corresponds to the linear gain matrix

$\mathbf{K} = \rho[\mathbf{PB}]^T = \rho\mathbf{B}^T\mathbf{P}$ employed in the Riccati equation to solve for $\mathbf{P}$. Corresponding to such linear gain matrix is the linear control:

$$u(\mathbf{x}) = -\mathbf{Kx} = -\rho\mathbf{B}^T\mathbf{Px} \tag{2.15}$$

where $\rho \in \mathfrak{R}^+$, and $\mathbf{K} \equiv \rho\mathbf{B}^T\mathbf{P}$. Since we set $\mathbf{Q} = c\mathbf{I}$ in Theorem 2.3, the existence of

such $\mathbf{P}$ guarantees that $\overline{\mathbf{A}} \equiv [\mathbf{A} - \mathbf{BK}]$ is stable, and $\dot{V}(\mathbf{x})$ is locally negative definite by

Lyapunov stability. It turns out that theorem 2.3 not only gives $\mathbf{P}$ that satisfies the

eigenvector condition when $\mathbf{Q} = c\mathbf{I}$, $c \in \mathfrak{R}^+$ but it also implies that such $\mathbf{P}$ can be

generated from other particular choices of $\mathbf{Q} \neq c\mathbf{I}$. This leads to our generalized version

of $u(\mathbf{x})$ denoted by $u_{LARC}(\mathbf{x})$. The formulation is given in Lemma 2.3.

Lemma 2.3   (The General Form of LARC)

If the linear gain matrix $\mathbf{K} = \rho\mathbf{B}^T\mathbf{P}$ is constructed from the solution $\mathbf{P}$ of the Riccati

equation in Theorem 2.3 with $\mathbf{Q} = c\mathbf{I}$, and ρ and $c \in \mathfrak{R}^+$ then the linear gain matrix:

$$\mathbf{K}_{LARC} = \eta\rho\mathbf{B}^T\mathbf{P} \tag{2.16 a}$$

where $\eta \geq 1$, satisfies the Riccati equation in Theorem 2.3 with $\mathbf{P}$ obtained previously and

$\mathbf{Q} \neq c\mathbf{I}$ being a symmetric positive definite matrix. Furthermore, the linearized model is

guaranteed to be stable under the linear control:

$$u_{LARC}(\mathbf{x}) = -\mathbf{K}_{LARC}\mathbf{x} \tag{2.16 b}$$

Proof

Recall that the Lyapunov equation is given by:

$$-Q = \frac{1}{2}[PA + A^T P] - \frac{1}{2}[[PB]K + K^T [PB]^T]]$$
$$\equiv M - N$$

where $M \equiv \frac{1}{2}[PA + A^T P]$ and $N \equiv \frac{1}{2}[[PB]K + K^T [PB]^T]$. We substitute $\eta \rho [PB]$ for

K^T in the above Lyapunov equation to produce:

$$Q = -M + \eta \overline{N}$$
$$= -M + \overline{N} + (\eta - 1)\overline{N} \qquad (2.17)$$
$$= cI + (\eta - 1)\overline{N}$$

where we note from (2.12) that $\overline{N} = N \big|_{K^T = \rho[PB]} = \rho PBB^T P$ and $cI = -M + \overline{N}$. Since

$\eta \geq 1$, $\overline{N} = \overline{N}^T$ and $\overline{N}$ is positive semidefinite, it appears from (2.17) that Q is symmetric

positive definite and $Q \neq cI$. By Lyapunov stability, the existence of such Q guarantees

stability of the linearized model. This completes the proof.

By inspecting the proof of Lemma 2.3, we see that LARC guarantees stability of the

linearized model for any arbitrarily large $\eta \in \Re^+$. This implies that we can increase η

and energize the linear system as strongly as we like while maintaining stability. Of

course, this statement assumes that every component in the linear control system is

sufficiently strong for such inputs. When the model is assumed to be exact or when

uncertainty specifications are unavailable, we employ the eigenvalue-ratio plot

(Proposition 1.2) to determine an appropriate value for ρ while fixing $\eta = 1$ for

simplicity. Generally, we want to find a value of ρ that generates a LARC with the

smallest eigenvalue ratio for the reasons given in Proposition 1.2. In Chapter III, the role

of η will be developed and a mathematical procedure for selecting numerical values for

ρ and η to produce a certain LAR will be given.

We now introduce Procedure 1 for generating a LARC:

Step 1   Generate an array containing increasingly large values of $\rho \in \Re^{+}$. For each

value of ρ, solve the Riccati equation (2.12) using $\mathbf{Q} = c\mathbf{I}\mid_{c=1}$ to obtain the

corresponding $\mathbf{P}$. Compute and record the eigenvalue ratios $r_{\lambda_{\mathbf{M}}}$

corresponding to every $\mathbf{P}$ and plot $r_{\lambda_{\mathbf{M}}}$ versus ρ. Typically, our array of ρ

is 0.0001, 0.001, 0.01, ..., 100, 1000, 10000. However, an appropriate

range and step size depend of the system at hands. The key is to capture a

portion of the plot where the slope changes significantly. In all of our

examples, we find that 1-3 trial-and-error are sufficient to find such

portion. When such portion is captured, replot it using a linear scale for ρ.

Step 2   Select a value of ρ that corresponds to a <u>small</u> $r_{\lambda_{\mathbf{M}}}$ from a "flat" portion of

the plot. At such points, $r_{\lambda_{\mathbf{M}}}$ does not change significantly when ρ

changes.

Step 3   For a value of ρ selected in Step 2, we find the corresponding LARC using

(2.16). Then verify that sufficient control energy is available to implement

the controller by considering the resulting linear gain matrix and the

required operating region. If not, reconsider the eigenvalue-ratio plot and

choose a new value for ρ. Normally, a larger value of ρ results in a larger $\mathbf{K}_{LARC}$ and a greater demand of control energy. Assuming that we have sufficient control energy, having a very large $\mathbf{K}_{LARC}$ does not always produce satisfactory results. To see this, consider an ideal situation in which $\mathbf{B}$ can approximate $\mathbf{g(x)}$ with small errors in operating regions about the origin. In this ideal situation, a very large $\mathbf{K}_{LARC}$ can forces $G(\mathbf{x})u_{LARC}(\mathbf{x})$ to be positively large in such regions, and we see from (2.13) that this can result in a small LAR.

In all of our examples, Step 1 – Step 3 are sufficient to generate a LAR with a reasonably large attractive region. Note that numerical simulations are not required for these steps. However, we find that incorporating numerical simulations to tune the parameter ρ can lead to larger attractive regions. In the next section, we give a simple tuning procedure using numerical simulations.

2.5   Controller Tuning

The fundamental idea of LARC is to force $\dot{V}(\mathbf{x})$ to be negative definite in radially large regions about the origin and obtain a large LAR. Using the concepts of eigenvector condition and eigenvalue ratio, it is reasonable to expect that LARC yields reasonably large attractive regions. However, we do not expect a LARC to yield an optimally large attractive region because explicit nonlinearities and optimization has not been included into the formulation of LARC.

The objective of this section is to give a guideline for tuning LARC to obtain a larger attractive region. This guideline is straightforward, but may not be the most efficient in general. In addition, we note that the required amount of computations increases rapidly with the order of the system, such that the availability of computing resources must be considered. However, we find in all of our examples that this tuning guideline leads to satisfactory results in a timely fashion, provided that the initial choice of LARC is generated by using Procedure 1 given in the previous section. Each problem takes less than 30 minutes using a PC with a 450 MHz AMD K6-III CPU and 64 MB PC-100 SDRAM running MATLAB IV under Windows 98 SE. This $600 computer is called "our computer" for convenience.

From linear optimal control theory, we know by inspection that the Riccati equation (2.12) corresponds to the quadratic performance index:

$$J = \int_0^\infty (\mathbf{x}^T \overline{\mathbf{Q}} \mathbf{x} + u(\mathbf{x}) \overline{\mathbf{R}} u(\mathbf{x}))\, dt$$
$$= \int_0^\infty (2c\mathbf{x}^T \mathbf{I} \mathbf{x} + \frac{1}{2\rho} u^2(\mathbf{x}))\, dt \tag{2.18}$$

where $\rho,\ c \in \Re^+$, $\overline{\mathbf{Q}} = 2c\mathbf{I}$ and $\overline{\mathbf{R}} = \dfrac{1}{2\rho}[1]$. In addition, we recognize that the linear optimal control that minimize J is given by:

$$u(\mathbf{x}) = u_{LQR}(\mathbf{x}) = -\overline{\mathbf{R}}^{-1} \mathbf{B}^T \mathbf{P} \mathbf{x} = -2\rho \mathbf{B}^T \mathbf{P} \mathbf{x} \tag{2.19}$$

This shows that the surfaces $S_{u_{LQR}=0}$ and $S_{u_{LARC}=0}$ are the same and are given by $\{\mathbf{x} \mid \mathbf{B}^T \mathbf{P} \mathbf{x} = 0\}$. When the performance index (2.18) is employed to generate $u_{LQR}(\mathbf{x})$, the following striking relationship is observed from (2.16) and (2.19):

$$u_{LQR}(\mathbf{x}) = \frac{2}{\eta} u_{LARC}(\mathbf{x}) = u_{LARC}(\mathbf{x})\big|_{\eta=2} \qquad (2.20)$$

Because of the relationship between LQR and LARC in (2.20), we note that for SIMO

linear systems:

1)   It can be inferred that if the response characteristics resulting from LQR are

acceptable then so are those resulting from LARC with $\eta = 2$.

2)   Robustness properties of LARC can be drawn directly from those of LQR.

However, we emphasize that LARC is primarily formulated for nonlinear systems.

Although it is possible to apply a LARC to a linear system, this may not offer advantages

over existing techniques because the available solutions of linear differential equations

have not been incorporated into the formulation of LARC.

We know from optimization theory that minimizing the performance index J in (2.18)

and $c_1 J$ should produce the same solution $\forall c_1 \in \mathfrak{R}^+$. This implies that $u_{LQR}(\mathbf{x})$ in

(2.19) depends on the ratio of c and $1/\rho$. Since $u_{LQR}(\mathbf{x}) = \frac{2}{\eta} u_{LARC}(\mathbf{x})$, it follows that

$u_{LARC}(\mathbf{x})$ depends on the ratio of c and $1/\rho$ when η is fixed. In this case, it is sufficient

to fix $c = 1$ and alter ρ to produce different $u_{LARC}(\mathbf{x})$. We now give the following

heuristic guideline for tuning the value of ρ aiming for large attractive regions.

Step 1   For the initial selection of ρ determined from the procedure in the previous

section, we employ numerical simulations to estimate the corresponding

attractive region for the nonlinear system, and record boundary points of

such attractive region. We understand that the attractive region in this

section is estimated numerically but we simply call it an attractive region

for convenience. Initial conditions for simulations may be distributed evenly in the required operating region about the origin for simplicity.

Step 2   For a new value of ρ determined from the procedure given in the previous section, start numerical simulations at initial conditions just outside the numerically estimated attractive region recorded in Step 1. If the new $u_{LARC}(\mathbf{x})$ yields convergence from these initial conditions, verify convergence from initial conditions near the origin. Otherwise, change ρ in the opposite direction and restart Step 2. This is terminated when we are satisfied with the resulting attractive region, or when the computation time reaches a limit, or when we find from the record that the attractive region is not getting larger by tuning ρ.

Continuing with Step 3, we may tune the direction of the gain matrix if a larger attractive region is required. It turns out that direction tuning can be conducted conveniently if we write the controller found from Step 1 – 2 in the normalized form:

$$
\begin{aligned}
u_{LARC}(\mathbf{x}) &= -\rho\|\mathbf{PB}\|\frac{\mathbf{B}^T\mathbf{P}}{\|\mathbf{PB}\|}\mathbf{x} \\
&= -\rho\|\mathbf{PB}\|\overline{\mathbf{K}}_{LARC}\mathbf{x} \\
&= -\rho\|\mathbf{PB}\|[\overline{k}_1 \quad \dots \quad \overline{k}_n]\mathbf{x}
\end{aligned}
\tag{2.23}
$$

where $\dfrac{\mathbf{B}^T\mathbf{P}}{\|\mathbf{PB}\|} = [\overline{k}_1 \quad \dots \quad \overline{k}_n] \equiv \overline{\mathbf{K}}_{LARC}^T$.

Step 3   (optional) Perturb the direction of $\overline{\mathbf{K}}_{LARC}^{T}$ by increasing a component $\overline{k}_{j}$,

$j \in \{1,...,n\}$ by a small value, normalize the perturbed $\overline{\mathbf{K}}_{LARC}^{T}$ using the 2-

norm, and run simulations at initial conditions just outside the previous

attractive region. If the simulations show convergence, restart Step 3. If the

trajectories diverge, restore $\overline{k}_{j}$, change the index j, and restart Step 3. All

components of $\overline{\mathbf{K}}_{LARC}^{T}$ are perturbed in the same fashion, and all

perturbation must be "feasible" or $\lambda_{i}(\mathbf{A} - \rho \|\mathbf{PB}\| \overline{\mathbf{K}}_{LARC}) < 0 \;\; \forall i$ for local

stability.

We now present examples where the generation of $u_{LARC}(\mathbf{x})$ and the selection of ρ are

discussed. For simplicity, we fix the direction of $\mathbf{K}_{LARC}$ and fix $\eta = 1$ although tuning

the direction of $\mathbf{K}_{LARC}$ and the value for η can produce better results. Under these

restrictions, the only one design parameter is ρ for every n-dimensional system. Clearly,

this facilitates controller design for high-order systems. It is not our intention to convince

the readers that an attractive region resulting from LARC is the largest when compared to

those resulting from other techniques. We want to show that a LARC can be generated

systematically using the concepts of eigenvector condition and of eigenvalue ratio, and

can produce reasonably large attractive regions in a timely fashion. Notice that LARC

ultimately generates a set of constant linear gain matrices, which is obviously a subset of

all possible linear gain matrices generatable by using pole placement.

The strength of LARC comes from the formulation of eigenvector condition (Proposition 1.1) and the eigenvalue ratio (Proposition 1.2) in which effects of nonlinearities have been incorporated implicitly to choose a quadratic Lyapunov function that allows us to obtain a reasonably large LAR. Note that it is not obvious how the formulations of existing linear control techniques such as optimal controls and pole placement are related to attractive regions of the nonlinear systems (1.1). In addition, it is not clear how several parameters for such controls should be selected to produce a reasonably large attractive region. Accordingly, we present several possibilities for those schemes. The reader is cautioned that the results presented in these examples are generally not the best possible from their respective schemes.

Example 2.1 (An Artificial System)

The nonlinear system is reproduced from (E 1.1.1):

$$\begin{bmatrix} \dot{x}_1 \\ \dot{x}_2 \end{bmatrix} = \begin{bmatrix} 10x_2 + 10x_1 + 10\sin(x_1)^2\sin(x_2) - x_1^2 \\ 5x_1^2 + \sin(x_2) \end{bmatrix} + \begin{bmatrix} 0 \\ \cos(x_2) + 1.5 \end{bmatrix} u \qquad \text{(E 2.1.1)}$$

$$\dot{\mathbf{x}} \equiv \mathbf{f}(\mathbf{x}) + \mathbf{g}u$$

The corresponding linearized model about the origin is reproduced from (E 1.1.2):

$$\begin{bmatrix} \dot{x}_1 \\ \dot{x}_2 \end{bmatrix} = \begin{bmatrix} 10 & 10 \\ 0 & 1 \end{bmatrix} \begin{bmatrix} x_1 \\ x_2 \end{bmatrix} + \begin{bmatrix} 0 \\ 2.5 \end{bmatrix} u \qquad \text{(E 2.1.2)}$$

$$\dot{\mathbf{x}} = \mathbf{A}\mathbf{x} + \mathbf{B}u$$

In the followings, we apply pole placement, LQR, and LARC to generate linear controls for local stabilization of (E 2.1.1) and compare the dimensions of the resulting attractive regions. For each technique, we employ several sets of parameters to generate the corresponding controllers. The results are summarized below:

a) *Linear Controls Resulting from Pole Placement*

We apply pole placement to locate the eigenvalues of $\overline{\mathbf{A}} \equiv [\mathbf{A} - \mathbf{B}\mathbf{K}_{PP}]$ at several

locations in the LHP for local stabilization. The subscript *PP* stands for pole placement.

Some specific possibilities are presented below:

*a*1)   The linear control:

$$u(\mathbf{x}) = u_{PP}(\mathbf{x}) = -\begin{bmatrix} 60 & 20 \end{bmatrix}\mathbf{x} \equiv -\mathbf{K}_{PP}\mathbf{x} \qquad \text{(E 2.1.3)}$$

is applied to the nonlinear system (E 2.1.1) to places the two eigenvalues of the matrix

$\overline{\mathbf{A}} \equiv [\mathbf{A} - \mathbf{B}\mathbf{K}_{PP}]$ at $\lambda_{1,2} = -19.5 \pm j25.095$ in the LHP.

*a*2)   The linear control:

$$u(\mathbf{x}) = u_{PP}(\mathbf{x}) = -\begin{bmatrix} 51.9986 & 12.4023 \end{bmatrix}\mathbf{x} \equiv -\mathbf{K}_{PP}\mathbf{x} \qquad \text{(E 2.1.4)}$$

is applied to the nonlinear system (E 2.1.1) to places the two eigenvalues of the matrix

$\overline{\mathbf{A}} \equiv [\mathbf{A} - \mathbf{B}\mathbf{K}_{PP}]$ at $\lambda_{1,2} = -10 \pm j30$ in the LHP.

*a*3)   The linear control:

$$u(\mathbf{x}) = u_{PP}(\mathbf{x}) = -\begin{bmatrix} 100 & 24.8 \end{bmatrix}\mathbf{x} \equiv -\mathbf{K}_{PP}\mathbf{x} \qquad \text{(E 2.1.5)}$$

is applied to the nonlinear system (E 2.1.1) to places the two eigenvalues of the matrix

$\overline{\mathbf{A}} \equiv [\mathbf{A} - \mathbf{B}\mathbf{K}_{PP}]$ at $\lambda_{1,2} = -30 \pm j30$ in the LHP.

b) *Linear Controls Resulting from LQR*

We apply LQR to minimize several performance indexes <u>with respect to the linearized</u>

<u>model</u> (E 2.1.2). Some specific possibilities are presented below:

*b*1)   The LQR:

$$u(\mathbf{x}) = u_{LQR}(\mathbf{x}) = -\begin{bmatrix} 71.4724 & 33.1405 \end{bmatrix}\mathbf{x} \equiv -\mathbf{K}_{LQR}\mathbf{x} \qquad \text{(E 2.1.6)}$$

is applied to the nonlinear system (E 2.1.1) to minimize the performance index:

$$J = \int_0^\infty [\mathbf{x}^T \begin{bmatrix} 1 & 0 \\ 0 & 0.5 \end{bmatrix} \mathbf{x} + 0.001 u_{LQR}^2(\mathbf{x})] dt \qquad \text{(E 2.1.7)}$$

This LQR locates the eigenvalues of $\overline{\mathbf{A}} \equiv [\mathbf{A} - \mathbf{BK}_{LQR}]$ at $\lambda_1 = -17.9715$ and

$\lambda_2 = -53.8797$ in the LHP.

*b*2)   The LQR:

$$u(\mathbf{x}) = u_{LQR}(\mathbf{x}) = -[79.1464 \quad 40.8145]\mathbf{x} \equiv -\mathbf{K}_{LQR}\mathbf{x} \qquad \text{(E 2.1.8)}$$

is applied to the nonlinear system (E 2.1.1) to minimize the performance index:

$$J = \int_0^\infty [\mathbf{x}^T \begin{bmatrix} 0.5 & 0 \\ 0 & 1 \end{bmatrix} \mathbf{x} + 0.001 u_{LQR}^2(\mathbf{x})] dt \qquad \text{(E 2.1.9)}$$

This LQR locates the eigenvalues of $\overline{\mathbf{A}} \equiv [\mathbf{A} - \mathbf{BK}_{LQR}]$ at $\lambda_1 = -12.2976$, and

$\lambda_2 = -78.7386$ in the LHP.

*b*3)   The LQR:

$$u(\mathbf{x}) = u_{LQR}(\mathbf{x}) = -[85.7899 \quad 41.4668]\mathbf{x} \equiv -\mathbf{K}_{LQR}\mathbf{x} \qquad \text{(E 2.1.10)}$$

is applied to the nonlinear system (E 2.1.1) to minimize the performance index:

$$J = \int_0^\infty [\mathbf{x}^T \mathbf{Ix} + 0.001 u_{LQR}^2(\mathbf{x})] dt \qquad \text{(E 2.1.11)}$$

This LQR locates the eigenvalues of $\overline{\mathbf{A}} \equiv [\mathbf{A} - \mathbf{BK}_{LQR}]$ at $\lambda_1 = -14.2599$, and

$\lambda_2 = -78.4071$ in the LHP.

c)   *Linear Controls Resulting from LARC*

To generate our LARC, we follow the guidelines given in Section 2.4. The plot of

eigenvalue ratio r_{λ_M} versus ρ in Fig. E2.1.1 is generated from our PC in approximately 2

seconds. Note that because we employ $\mathbf{Q} = \mathbf{I}$, the negative eigenvalue of $\mathbf{M}$ is at -1 and it follows that $r_{\lambda_M} = \lambda_{M1}$. From Fig. E2.1.1, we see that the eigenvalue ratio decreases when ρ increases but the decreasing of the eigenvalue ratio becomes small for large values of ρ. We construct and examine our LARC at $\rho = 2000, 3000,$ and 4000 because the eigenvalue ratios corresponding to these values of ρ are small and because the eigenvalue ratio does not decrease significantly for larger values of ρ.

Using the tuning guideline in Section 2.4, we start from $\rho = 2000$ and increase ρ to 3000 and 4000:
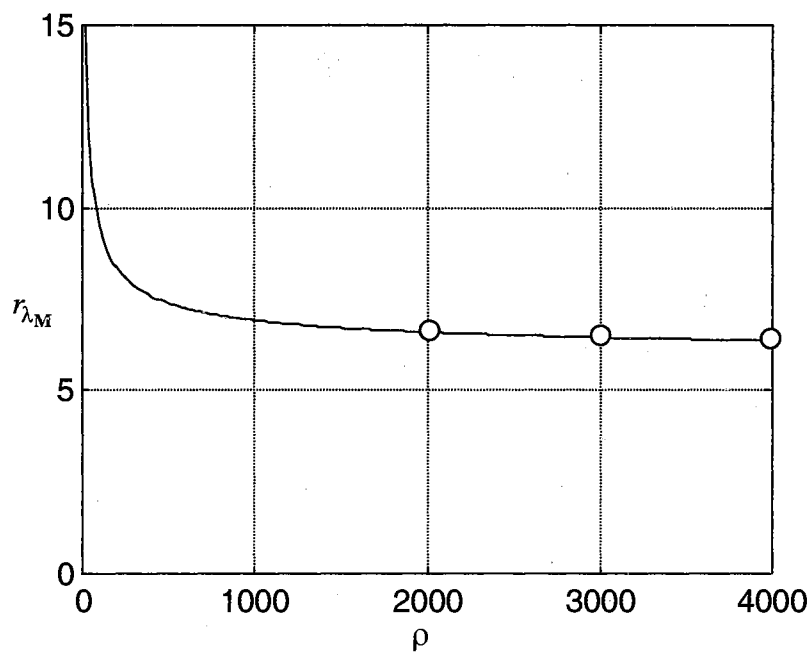
Fig. E2.1.1   A Plot of Eigenvalue Ratio Versus ρ

Symbol: $\circ \equiv$ points where we construct and examine the corresponding LARC

$c1)$ The LARC:

$$u(\mathbf{x}) = u_{LARC}(\mathbf{x}) = -[112.7540 \quad 49.7081]\mathbf{x} \equiv -\mathbf{K}_{LARC}\mathbf{x} \qquad (E\ 2.1.12)$$

is applied to the nonlinear system (E 2.1.1) to satisfy the eigenvector condition with

$\rho = 2000$. This LARC locates the eigenvalues of $\overline{\mathbf{A}} \equiv [\mathbf{A} - \mathbf{B}\mathbf{K}_{LARC}]$ at $\lambda_1 = -16.3686$,

and $\lambda_2 = -96.9017$ in the LHP.

$c2$)   The LARC:

$$u(\mathbf{x}) = u_{LARC}(\mathbf{x}) = -[137.0262 \quad 59.7663]\mathbf{x} \equiv -\mathbf{K}_{LARC}\mathbf{x} \qquad \text{(E 2.1.13)}$$

is applied to the nonlinear system (E 2.1.1) to satisfy the eigenvector condition with

$\rho = 3000$. This LARC locates the eigenvalues of $\overline{\mathbf{A}} \equiv [\mathbf{A} - \mathbf{B}\mathbf{K}_{LARC}]$ at $\lambda_1 = -15.8390$,

and $\lambda_2 = -122.5767$ in the LHP.

$c3$)   The LARC:

$$u(\mathbf{x}) = u_{LARC}(\mathbf{x}) = -[157.4870 \quad 68.2440]\mathbf{x} \equiv -\mathbf{K}_{LARC}\mathbf{x} \qquad \text{(E 2.1.14)}$$

is applied to the nonlinear system (E 2.1.1) to satisfy the eigenvector condition with

$\rho = 4000$. This LARC locates the eigenvalues of $\overline{\mathbf{A}} \equiv [\mathbf{A} - \mathbf{B}\mathbf{K}_{LARC}]$ at $\lambda_1 = -15.5573$,

and $\lambda_2 = -144.0527$ in the LHP.

By means of numerical simulations, we found that the linear controls $u_{PP}(\mathbf{x})$ in $a3$),

$u_{LQR}(\mathbf{x})$ in $b3$), and $u_{LARC}(\mathbf{x})$ in $c3$) produce the largest attractive regions for their

respective schemes. The resulting attractive regions are shown in Table E2.1.1. By

inspection, the largest numerically estimated attractive region corresponds to $u_{LARC}(\mathbf{x})$ in

$c3$). We now investigate the validity of theorems in Chapter 1 and 2 while showing in

details the construction of $u_{LARC}(\mathbf{x})$ in $c3$). To generate a LAR controller with $\rho = 4000$

and $c = 1$, we solve the Riccati equation:

$$0 = -2c\mathbf{I} - \mathbf{P}\mathbf{A} - \mathbf{A}^T\mathbf{P} + 2\rho\,\mathbf{P}\mathbf{B}\,\mathbf{B}^T\mathbf{P} \qquad \text{(E 2.1.14)}$$

		x_1										
		-25	-20	-15	-10	-5	0	5	10	15	20	25
	100											
	90											
	80											
	70											
	60											
	50											
	40											
	30											
	20											
	10											
x_2	0											
	-10											
	-20											
	-30											
	-40											
	-50											
	-60											
	-70											
	-80											
	-90											
	-100											
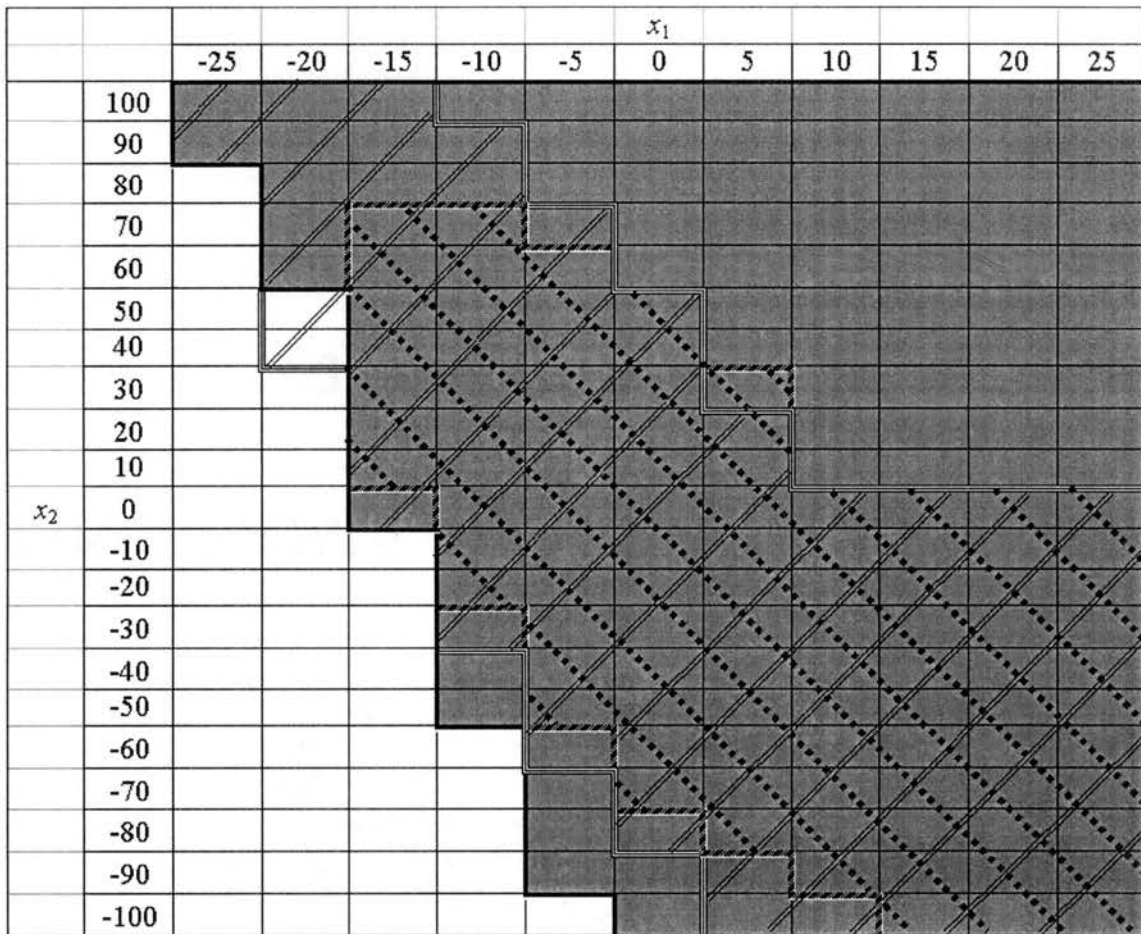
Table E2.1.1   Attractive Regions of the Artificial System under Different Controls

Legends: ■ ≡ convergence under LARC $c3$), ▨ ≡ convergence under LQR $b3$)

▨ ≡ convergence under pole placement $a3$), □ ≡ divergence

This yields:

$$\mathbf{P} = \begin{bmatrix} 0.5201 & 0.0157 \\ 0.0157 & 0.0068 \end{bmatrix} \tag{E 2.1.15}$$

The corresponding LARC is:

$$
\begin{aligned}
u_{LARC}(\mathbf{x}) &= -\rho\mathbf{B}^T\mathbf{P}\mathbf{x} \\
&= -[157.4870 \quad 68.2440]\mathbf{x} \\
&\equiv -\mathbf{K}_{LARC}\mathbf{x}
\end{aligned}
\tag{E 2.1.12}
$$

where $\mathbf{K}_{LARC} = [157.4870 \quad 68.2440]$. We compute further:

$$\mathbf{M} \equiv \frac{1}{2}[\mathbf{PA} + \mathbf{A}^T\mathbf{P}] = \begin{bmatrix} 5.2005 & 2.6869 \\ 2.6869 & 0.1643 \end{bmatrix} \qquad \text{(E 2.1.16 a)}$$

$$\lambda_{\mathbf{M}} \equiv [\lambda_{M1} \quad \lambda_{M2}] = [6.3648 \quad -1.0000] \qquad \text{(E 2.1.16 b)}$$

$$\mathbf{v}_{\mathbf{M}} \equiv [\mathbf{v}_{M1} \quad | \quad \mathbf{v}_{M2}] = \begin{bmatrix} 0.9176 & -0.3976 \\ 0.3976 & 0.9176 \end{bmatrix} \qquad \text{(E 2.1.16 c)}$$

where $\mathbf{v}_{Mi} \in \Re^n$, $\|\mathbf{v}_{Mi}\| = 1$, $i = 1, 2$.

$$\mathbf{N} = \frac{1}{2}[[\mathbf{PB}]\mathbf{K}_{LARC} + \mathbf{K}_{LARC}^T[\mathbf{PB}]^T] = \begin{bmatrix} 6.2005 & 2.6869 \\ 2.6869 & 1.1643 \end{bmatrix} \qquad \text{(E 2.1.17 a)}$$

$$\lambda_{\mathbf{N}} \equiv [\lambda_{N1} \quad \lambda_{N2}] = [7.3648 \quad 0.0000] \qquad \text{(E 2.1.17 b)}$$

$$\mathbf{v}_{\mathbf{N}} \equiv [\mathbf{v}_{N1} \quad | \quad \mathbf{v}_{N2}] = \begin{bmatrix} 0.9176 & -0.3976 \\ 0.3976 & 0.9176 \end{bmatrix} = \mathbf{v}_{\mathbf{M}} \qquad \text{(E 2.1.17 c)}$$

$$[\mathbf{PB}] = [0.0394 \quad 0.0171]^T \qquad \text{(E 2.1.18 a)}$$

$$[\overline{\mathbf{PB}}] = \frac{[\mathbf{PB}]}{\|\mathbf{PB}\|} = [0.9176 \quad 0.3976]^T \qquad \text{(E 2.1.18 b)}$$

$$\overline{\mathbf{K}}_{LARC}^T = \frac{\mathbf{K}_{LARC}^T}{\|\mathbf{K}_{LARC}^T\|} = [0.9176 \quad 0.3976]^T \qquad \text{(E 2.1.19)}$$

We notice the following properties of $\mathbf{M}$ and $\mathbf{N}$ predicted by our theorems:

1) $\mathbf{M}$ has exactly one positive eigenvalue λ_{M1}.

2) $\mathbf{N}$ has exactly one positive eigenvalue λ_{N1} and has no negative eigenvalue.

3) $\mathbf{M}$ and $\mathbf{N}$ share the same set of eigenvectors.

4) $\mathbf{v}_{M1} = \mathbf{v}_{N1}$.

5) The eigenvector $\mathbf{v_{N1}}$ corresponding to the only positive eigenvalue λ_{N1} bisects the angle between the vector $[\mathbf{PB}]$ and $\mathbf{K}_{LARC}^{T}$. Indeed:

$$\mathbf{v_{N1}}.[\overline{\mathbf{PB}}] = \mathbf{v_{N1}}.\mathbf{K}_{LARC}^{T} = [\overline{\mathbf{PB}}].\mathbf{K}_{LARC}^{T} = 1$$

6) The directions of the vectors $[\mathbf{PB}]$ and $\mathbf{K}_{LARC}^{T}$ are the same. Indeed:

$$[\overline{\mathbf{PB}}] = \overline{\mathbf{K}}_{LARC}^{T}$$

These imply that the directions of $\nabla G_L(\mathbf{x}) = [\mathbf{PB}]$ and of $\mathbf{v_{M1}}$ are the same and the eigenvector condition is satisfied.

Example 2.2 (A Double-Inverted-Pendulum System with Lower-Joint Control)

We consider in this example the problem of stabilizing about their upright positions both

links of a double-inverted-pendulum system using torque control at the lower joint only.

This forth-order system is a nonlinear underactuated system, whose the number of inputs

(one) is less than the number of outputs (two). No global stabilizing controller for this

system has been reported in the literature. Difficulty in designing a controller for this

system arises not only because of the nonlinearities, but also because the system has only

one input available to stabilize two outputs. This system appears in (Walker et al 1991)

using feedback linearization and in (Misawa, Arrington, and Ledgerwood, 1995) using a

LQR controller. In this example, we examine the numerically estimated attractive regions

resulting from our LARC and from the LQR in (Misawa, Arrington, and Ledgerwood,

1995).

Figure E2.2.1 illustrates the elements of this example, and numerical values for

parameters are given in Table E2.2.1.
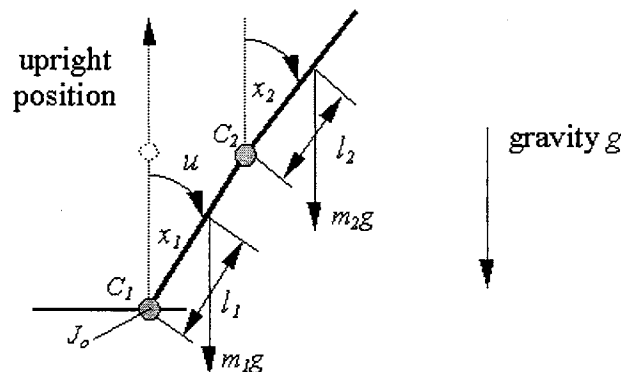
Fig. E2.2.1 A Double Inverted Pendulum System (Misawa et al, 1995)
Remark: Control torque u is applied to joint 1 only.

The equations of motion are:

$$\mathbf{H}_m \begin{bmatrix} \ddot{x}_1 \\ \ddot{x}_2 \end{bmatrix} + \mathbf{H}_c \begin{bmatrix} \dot{x}_1 \\ \dot{x}_2 \end{bmatrix} + \mathbf{H}_g = \begin{bmatrix} u \\ 0 \end{bmatrix} \qquad \text{(E 2.2.1 a)}$$

where the matrices in (E 2.2.1 a) are:

$$\mathbf{H}_m = \begin{bmatrix} J_0 + I_1 + m_1 l_1^2 + m_2 L_1^2 & m_2 L_1 l_2 \cos(x_1 - x_2) \\ m_2 L_1 l_2 \cos(x_1 - x_2) & m_2 l_2^2 + I_2 \end{bmatrix} \qquad \text{(E 2.2.1 b)}$$

$$\mathbf{H}_g = \begin{bmatrix} -g(m_1 l_1 + m_2 L_1)\sin(x_1) \\ -m_2 g l_2 \sin(x_2) \end{bmatrix} \qquad \text{(E 2.2.1 c)}$$

$$\mathbf{H}_c = \begin{bmatrix} C_1 + C_2 & m_2 \dot{x}_2 L_1 l_2 \sin(x_1 - x_2) - C_2 \\ -m_2 \dot{x}_1 L_1 l_2 \sin(x_1 - x_2) - C_2 & C_2 \end{bmatrix} \qquad \text{(E 2.2.1 d)}$$

Physical Parameters	Nomenclatures	Estimated Values	Units
mass	m_1	0.132	kg
	m_2	0.088	
total length	L_1	0.2032	m
	L_2	0.2540	
distance to center of gravity form pivot	l_1	0.1574	m
	l_2	0.1109	
damping coefficient	C_1	0.00118	N.m.s
	C_2	0.00056	
inertia	I_1	0.00362	$kg.m^2$
	I_2	0.00114	
	J_0	0.00006	

Table E2.2.1   Nomenclatures of Physical Parameters and the
Corresponding Numerical Values of the Double Inverted Pendulum (Misawa et al, 1995)

The equation of motion for this system can be written in the form:

$$\dot{\mathbf{x}} = \mathbf{f}(\mathbf{x}) + \mathbf{g}(\mathbf{x})u \qquad \text{(E 2.2.2 a)}$$

where:

$$\mathbf{x} = [x_1 \quad x_2 \quad x_3 \quad x_4]^T = [x_1 \quad x_2 \quad \dot{x}_1 \quad \dot{x}_2]^T \qquad \text{(E 2.2.2 b)}$$

$$\mathbf{f(x)} = \begin{bmatrix} x_3 \\ x_4 \\ \dfrac{\left\{\begin{array}{l}(\sin(x_1 - x_2)x_3^2 + 0.2824x_3 - 0.2824x_4 + 48.2776\sin(x_2))\cos(x_1 - x_2) \\ + 0.9833x_3 + 1.1206\sin(x_1 - x_2)x_4^2 - 0.3165x_4 - 214.3082\sin(x_1)\end{array}\right\}}{-5.9809 + \cos^2(x_1 - x_2)} \\ \dfrac{\left\{\begin{array}{l}(-0.8774x_3 - \sin(x_1 - x_2)x_4^2 + 0.2824x_4 + 191.2383\sin(x_1))\cos(x_1 - x_2) \\ -5.3371\sin(x_1 - x_2)x_3^2 - 1.5071x_3 + 1.5071x_4 - 257.6614\sin(x_2)\end{array}\right\}}{-5.9809 + \cos^2(x_1 - x_2)} \end{bmatrix}$$

(E 2.2.2 c)

$$\mathbf{g(x)} = \begin{bmatrix} 0 \\ 0 \\ \dfrac{-565.1008}{-5.9809 + \cos^2(x_1 - x_2)} \\ \dfrac{504.2688\cos(x_1 - x_2)}{-5.9809 + \cos^2(x_1 - x_2)} \end{bmatrix}$$

(E 2.2.2 d)

For the singular point at the origin, the linearized model of (E 2.2.2) is given by:

$$\dot{\mathbf{x}} = \begin{bmatrix} 0 & 0 & 1 & 0 \\ 0 & 0 & 0 & 1 \\ 43.0258 & -9.6925 & -0.2541 & 0.1202 \\ -38.3942 & 51.7297 & 0.4787 & -0.3593 \end{bmatrix}\mathbf{x} + \begin{bmatrix} 0 \\ 0 \\ 113.4531 \\ -101.2401 \end{bmatrix}u$$

$$\equiv \mathbf{Ax + B}u$$

(E 2.2.3)

It can be shown that (E 2.2.3) is unstable and is controllable. In the followings, we employ LARC and LQR from (Misawa et al, 1995) for local stabilization of (E 2.2.1) and compare the dimensions of the resulting attractive regions. Information regarding these linear controls is summarized below:

a)   *Linear Control Resulting from LQR*   (Misawa et al, 1995)

The LQR from (Misawa et al, 1995) is given by:

$$u(\mathbf{x}) = u_{LQR}(\mathbf{x}) = -[-0.0001 \quad -3.74 \quad -0.32 \quad -0.56]\mathbf{x} \equiv -\mathbf{K}_{LQR}\mathbf{x} \qquad (E\ 2.2.4)$$

This LQR locates the eigenvalues of $\overline{A} \equiv [A - BK_{LQR}]$ at $\lambda_{1,2} = -5.7977 \pm j10.1203$,

$\lambda_3 = -1.7890$, and $\lambda_4 = -7.6184$ in the LHP. The performance index corresponding to

(E 2.2.4) is not given in the literature.

b)   Linear Controls Resulting from LARC

To generate our LARC, we follow the guidelines given in Section 2.4. The plot of

eigenvalue ratio r_{λ_M} versus ρ in Fig. E2.2.2 is generated from our PC in approximately 2

seconds. Note that because we employ $Q = I$, all the negative eigenvalues of M are -1

and it follows that $r_{\lambda_M} = \lambda_{M1}$.

Fig. E2.2.2   A Plot of Eigenvalue Ratio Versus ρ
Symbol: $\circ$ = points where we construct and examine the corresponding LARC

From Fig. E2.2.2, we see that the eigenvalue ratio decreases when ρ increases but the

decreasing of the eigenvalue ratio becomes small for large values of ρ . We construct and

examine our LARC at $\rho = 0.05$ and 0.1 because the eigenvalue ratios corresponding to these values of ρ are small and because the eigenvalue ratio does not decrease significantly for larger values of ρ. Using the tuning guideline in Section 2.4, we start from $\rho = 0.05$ and increase ρ to 0.1:

$b1)$ The LARC:

$$u(\mathbf{x}) = u_{LARC}(\mathbf{x}) = -[-0.1036 \quad -5.2008 \quad -0.3618 \quad -0.8021]\mathbf{x} \equiv -\mathbf{K}_{LARC}\mathbf{x} \quad \text{(E 2.2.5)}$$

is applied to the nonlinear system (E 2.2.1) to satisfy the eigenvector condition with $\rho = 0.05$. This LARC locates the eigenvalues of $\overline{\mathbf{A}} \equiv [\mathbf{A} - \mathbf{BK}_{LARC}]$ at

$\lambda_{1,2} = -4.1511 \pm j2.9316$, $\lambda_3 = -29.3605$, and $\lambda_4 = -3.1120$ in the LHP.

$b2)$ The LARC:

$$u(\mathbf{x}) = u_{LARC}(\mathbf{x}) = -[-0.1791 \quad -6.9628 \quad -0.4884 \quad -1.0809]\mathbf{x} \equiv -\mathbf{K}_{LARC}\mathbf{x} \quad \text{(E 2.2.6)}$$

is applied to the nonlinear system (E 2.2.1) to satisfy the eigenvector condition with $\rho = 0.1$. This LARC locates the eigenvalues of $\overline{\mathbf{A}} \equiv [\mathbf{A} - \mathbf{BK}_{LARC}]$ at

$\lambda_{1,2} = -4.6045 \pm j2.5161$, $\lambda_3 = -43.1314$, and $\lambda_4 = -2.2981$ in the LHP.

System responses under the LQR and the LARC in (E 2.2.6) are given in Fig. E2.2.3. Notice that responses under the LARC are slower than those under the LQR but the LQR yields divergence when the system is launched from $\mathbf{x}(0) = [0.25 \quad 0.25 \quad 0.1 \quad 0.1]^T$. Now, we employ numerical simulations to estimate the attractive regions resulting from the LQR in (E 2.2.4), and the LAR controllers in (E 2.2.5) and (E 2.2.6). In these simulations, we assume that convergence had occurred if $\|\mathbf{x}(t)\| < 0.01$ for $40 \le t \le 50$, while divergence had occurred if $\exists t \, \|\mathbf{x}(t)\| > 2000$. It turns out that the attractive region

resulting from the LARC in (E 2.2.6) is the largest while that from the LQR in (E 2.2.4) is

the smallest. Attractive regions of the system under the LQR and the LARC in (E 2.2.6)

are given in Tables E2.2.2 and E2.2.3. From these tables, we notice that the dimension of

the attractive region resulting from $u_{LARC}(\mathbf{x})$ is not considerably larger than that from

$u_{LQR}(\mathbf{x})$. However, when considering the principle behind LARC and how quickly we

can generate a LAR controller, it is reasonable to employ LARC for local stabilization. In

the next chapters, LARC will be extended to obtain better results.
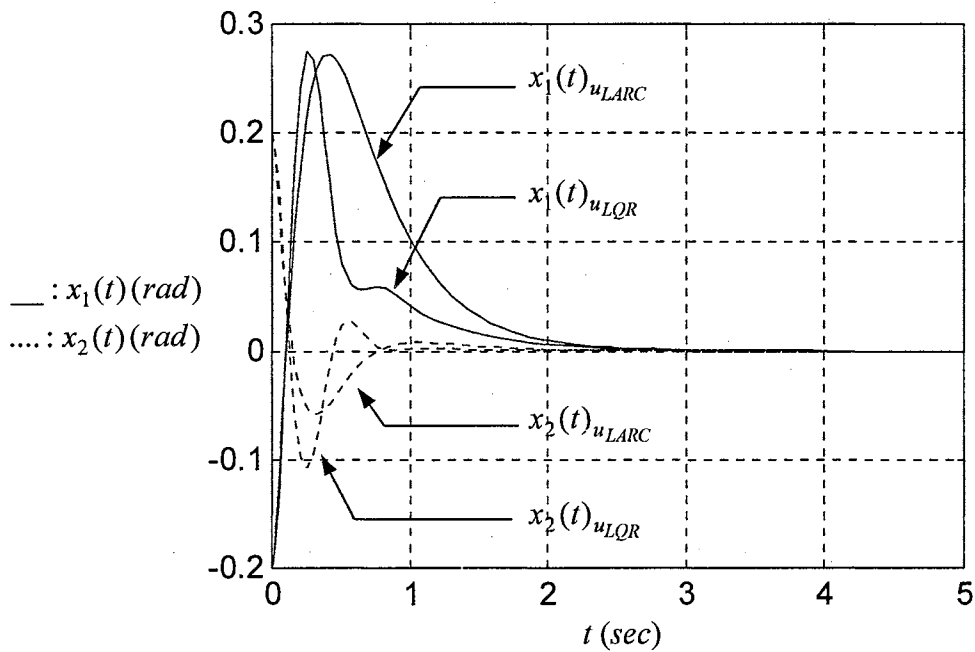
Fig. E2.2.3 (a)   Responses of the Double-Inverted-Pendulum System under $u_{LARC}(\mathbf{x})$ and

$u_{LQR}(\mathbf{x})$ with $\mathbf{x}(0) = [-0.2 \quad 0.2 \quad -0.1 \quad -0.1]^T$

Now, we demonstrate the validity of theorems in Chapter 1 and 2 while showing in details

the construction of $u_{LARC}(\mathbf{x})$ in $b1$) with $\rho = 0.05$ and $c = 1$. The selected LARC in $b2$)

having $\rho = 0.1$ and $c = 1$ can be generated in the same fashion. We solve the Riccati

equation:

$$0 = -2c\mathbf{I} - \mathbf{PA} - \mathbf{A}^T\mathbf{P} + 2\rho\,\mathbf{PB}\,\mathbf{B}^T\mathbf{P} \qquad \text{(E 2.2.7)}$$
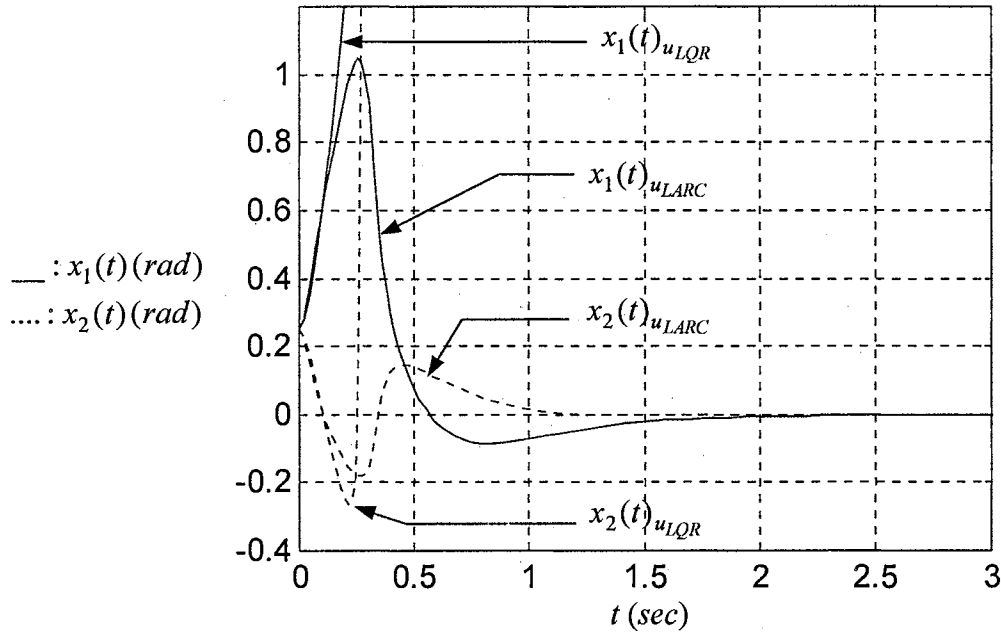
Fig. E2.2.3 (b)   Responses of the Double-Inverted-Pendulum System under $u_{LARC}(\mathbf{x})$ and
$u_{LQR}(\mathbf{x})$ with $\mathbf{x}(0) = [0.25 \quad 0.25 \quad 0.1 \quad 0.1]^T$

This yields:

$$\mathbf{P} = \begin{bmatrix} 3.8822 & 9.7644 & 1.2414 & 1.4116 \\ 9.7644 & 92.9231 & 10.0839 & 12.3278 \\ 1.2414 & 10.0839 & 1.2109 & 1.4285 \\ 1.4116 & 12.3278 & 1.4285 & 1.7592 \end{bmatrix} \qquad \text{(E 2.2.8)}$$

The corresponding LARC is:

$$\begin{aligned} u_{LARC}(\mathbf{x}) &= -\rho\mathbf{B}^T\mathbf{Px} \\ &= -[-0.1036 \quad -5.2008 \quad -0.3618 \quad -0.8021]\mathbf{x} \qquad \text{(E 2.2.6)} \\ &\equiv -\mathbf{K}_{LARC}\mathbf{x} \end{aligned}$$

where $\mathbf{K}_{LARC} = \begin{bmatrix} -0.1036 & -5.2008 & -0.3618 & -0.8021 \end{bmatrix}$. We compute further:

$$\mathbf{M} \equiv \frac{1}{2}[\mathbf{PA} + \mathbf{A}^T\mathbf{P}] = \begin{bmatrix} -0.7855 & 10.7717 & 0.7493 & 1.6613 \\ 10.7717 & 539.9765 & 37.6301 & 83.4325 \\ 0.7493 & 37.6301 & 1.6175 & 5.8035 \\ 1.6613 & 83.4325 & 5.8035 & 11.8674 \end{bmatrix} \quad \text{(E 2.2.9 a)}$$

$$\boldsymbol{\lambda}_{\mathbf{M}} \equiv \begin{bmatrix} \lambda_{M1} & \lambda_{M2} & \lambda_{M3} & \lambda_{M4} \end{bmatrix} = \begin{bmatrix} 555.6759 & -1.0000 & -1.0000 & -1.0000 \end{bmatrix} \quad \text{(E 2.2.9 b)}$$

$$\mathbf{v}_{\mathbf{M}} \equiv \begin{bmatrix} \mathbf{v}_{M1} & \mathbf{v}_{M2} & \mathbf{v}_{M3} & \mathbf{v}_{M4} \end{bmatrix} = \begin{bmatrix} 0.0196 & -0.9026 & -0.3052 & -0.0812 \\ 0.9858 & 0.0276 & 0.1254 & -0.1646 \\ 0.0686 & -0.4117 & 0.2820 & 0.4299 \\ 0.1520 & 0.1230 & -0.9009 & 0.8840 \end{bmatrix} \quad \text{(E 2.2.9 c)}$$

where $\mathbf{v}_{Mi} \in \mathfrak{R}^n$, $\|\mathbf{v}_{Mi}\| = 1, i = 1, ..., 4$.

$$\mathbf{N} = \frac{1}{2}[[\mathbf{PB}]\mathbf{K}_{LARC} + \mathbf{K}_{LARC}^T[\mathbf{PB}]^T] = \begin{bmatrix} 0.2145 & 10.7717 & 0.7493 & 1.6613 \\ 10.7717 & 540.9765 & 37.6301 & 83.4325 \\ 0.7493 & 37.6301 & 2.6175 & 5.8035 \\ 1.6613 & 83.4325 & 5.8035 & 12.8674 \end{bmatrix}$$

$$\text{(E 2.2.10 a)}$$

$$\boldsymbol{\lambda}_{\mathbf{N}} \equiv \begin{bmatrix} \lambda_{N1} & \lambda_{N2} & \lambda_{N3} & \lambda_{N4} \end{bmatrix} = \begin{bmatrix} 556.6759 & 0.0000 & 0.0000 & 0.0000 \end{bmatrix} \quad \text{(E 2.2.10 b)}$$

$$\mathbf{v}_{\mathbf{N}} \equiv \begin{bmatrix} \mathbf{v}_{N1} & \mathbf{v}_{N2} & \mathbf{v}_{N3} & \mathbf{v}_{N4} \end{bmatrix} = \begin{bmatrix} 0.0196 & -0.9026 & -0.3052 & -0.0812 \\ 0.9858 & 0.0276 & 0.1254 & -0.1646 \\ 0.0686 & -0.4117 & 0.2820 & 0.4299 \\ 0.1520 & 0.1230 & -0.9009 & 0.8840 \end{bmatrix} = \mathbf{v}_{\mathbf{M}}$$

$$\text{(E 2.2.10 c)}$$

$$[\mathbf{PB}] = \begin{bmatrix} -2.0711 & -104.0170 & -7.2354 & -16.0421 \end{bmatrix}^T \quad \text{(E 2.2.11 a)}$$

$$[\overline{\mathbf{PB}}] \equiv \frac{[\mathbf{PB}]}{\|\mathbf{PB}\|} = \begin{bmatrix} -0.0196 & -0.9858 & -0.0686 & -0.1520 \end{bmatrix}^T = \mathbf{v}_{M1} = \mathbf{v}_{N1} \quad \text{(E 2.2.11 b)}$$

$$\overline{\mathbf{K}}_{LARC}^{T} \equiv \frac{\mathbf{K}_{LARC}^{T}}{\left\|\mathbf{K}_{LARC}^{T}\right\|} = [-0.0196 \quad -0.9858 \quad -0.0686 \quad -0.1520]^{T} \quad \text{(E 2.2.12)}$$

We notice the following properties of **M** and **N** predicted by our theorems:

1) **M** has exactly one positive eigenvalue $\lambda_{\mathbf{M1}}$.

2) **N** has exactly one positive eigenvalue $\lambda_{\mathbf{N1}}$ and has no negative eigenvalue.

3) **M** and **N** share the same set of eigenvectors.

4) $\mathbf{v}_{\mathbf{M1}} = \mathbf{v}_{\mathbf{N1}}$.

5) The eigenvector $\mathbf{v}_{\mathbf{N1}}$ corresponding to the only positive eigenvalue $\lambda_{\mathbf{N1}}$ bisects the

angle between the vector **[PB]** and $\mathbf{K}_{LARC}^{T}$. Indeed:

$$\mathbf{v}_{\mathbf{N1}}.[\overline{\mathbf{PB}}] = \mathbf{v}_{\mathbf{N1}}. \overline{\mathbf{K}}_{LARC}^{T} = [\overline{\mathbf{PB}}].\overline{\mathbf{K}}_{LARC}^{T} = 1$$

6) The directions of the vectors **[PB]** and $\mathbf{K}_{LARC}^{T}$ are the same. Indeed:

$$[\overline{\mathbf{PB}}] = \overline{\mathbf{K}}_{LARC}^{T}$$

These imply that the directions of $\nabla G_{L}(\mathbf{x}) = [\mathbf{PB}]$ and of $\mathbf{v}_{\mathbf{M1}}$ are the same and the

eigenvector condition is satisfied.

			x_2																							
			.325					0.3					.275					0.25					.225				
			x_4																							
			-0.5	-.25	0	0.25	0.5	-0.5	-.25	0	0.25	0.5	-0.5	-.25	0	0.25	0.5	-0.5	-.25	0	0.25	0.5	-0.5	-.25	0	0.25	0.5
x_1	.325	x_3	-0.5																								
			-.25																								
			0																								
			0.25																								
			0.5																								
	0.3		-0.5																								
			-.25																								
			0																								
			0.25																								
			0.5																								
	.275		-0.5																								
			-.25																								
			0																								
			0.25																								
			0.5																								
	0.25		-0.5																								
			-.25																								
			0																								
			0.25																								
			0.5																								
	.225		-0.5																								
			-.25																								
			0																								
			0.25																								
			0.5																								

Table E2.2.2 Simulation Results of the Double Inverted Pendulum System in Regions farther from the Origin ($x_1 > 0$, $x_2 > 0$)

Remark: Attractive regions do not differ significantly in smaller regions about the origin.

Legends: ■ ≡ LQR and LARC systems converge, ▨ ≡ LARC system converge, □ ≡ All systems diverge

			x_2																							
			0.45					.425					0.4					.375					0.35				
			x_4																							
			-0.5	-.25	0	0.25	0.5	-0.5	-.25	0	0.25	0.5	-0.5	-.25	0	0.25	0.5	-0.5	-.25	0	0.25	0.5	-0.5	-.25	0	0.25	0.5
x_1	-0.45	x_3	-0.5																								
			-0.25																								
			0																								
			0.25																								
			0.5																								
	-.425		-0.5																								
			-0.25																								
			0																								
			0.25																								
			0.5																								
	-.40		-0.5																								
			-0.25																								
			0																								
			0.25																								
			0.5																								
	-.375		-0.5																								
			-0.25																								
			0																								
			0.25																								
			0.5																								
	-0.35		-0.5																								
			-0.25																								
			0																								
			0.25																								
			0.5																								

Table E2.2.3   Simulation Results of the Double Inverted Pendulum System in Regions farther from the Origin, ($x_1 < 0$, $x_2 > 0$)

Remark: Attractive regions do not differ significantly in smaller regions about the origin.

Legends: ■ ≡ LQR and LARC systems converge, ▨ ≡ LARC system converge, □ ≡ All systems diverge

Example 2.3   (A Cart-and-Pole System with Force Control on Cart)

We now consider a cart-and-pole system in which we use force control on the cart to stabilize the pendulum about its upright position <u>and</u> stabilize the cart about a reference position, which is set to zero. This system has one input and two outputs as in the double-inverted-pendulum system, but with less mathematical complexity. Although the system is considered in many works (Baumann, and Rugh, 1986), (Slotine, and Li, 1991), (Wang, 1994), (Ogata, 1997), we have found no controller that guarantees global stabilization for this system. Accordingly, it is common that a linear state feedback control designed by using a linearized model is employed for local stabilization.
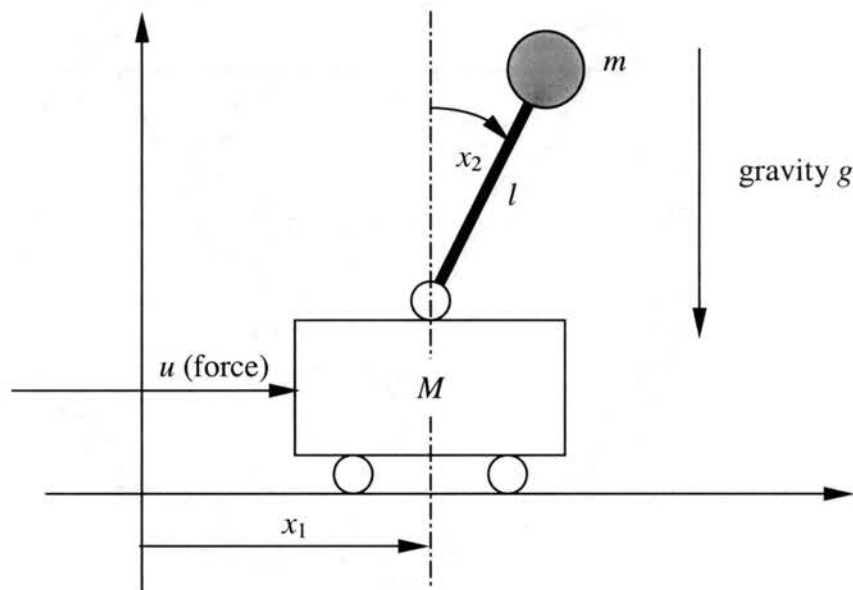
Fig. E2.3.1   A Cart-and-Pole System (Slotine, and Li, 1991), (Ogata, 1997)
Remark: $M = 2\ kg$, $m = 0.1\ kg$, $l = 0.5\ m$, and $g = 9.81\ kg.m.s^{-2}$

The nonlinear equations of motion for this system are given by (Slotine, and Li, 1991):

$$(M + m)\ddot{x}_1 + ml\ddot{x}_2 \cos x_2 - ml\dot{x}_2^2 \sin x_2 = u$$
$$m\ddot{x}_1 \cos x_2 + ml\ddot{x}_2 - mg \sin x_2 = 0$$

(E 2.3.1)

We may present the previous equation of motion in our standard form as:

$$\dot{\mathbf{x}} = \mathbf{f}(\mathbf{x}) + \mathbf{g}(\mathbf{x})u$$

(E 2.3.2 a)

where:

$$\mathbf{x} = [x_1 \quad x_2 \quad x_3 \quad x_4]^T = [x_1 \quad x_2 \quad \dot{x}_1 \quad \dot{x}_2]^T$$

(E 2.3.2 b)

$$\mathbf{f}(\mathbf{x}) = \begin{bmatrix} x_3 \\ x_4 \\ \dfrac{ml \sin(x_2)x_4^2 - mg \sin(x_2)\cos(x_2)}{(M + \sin^2(x_2)m)} \\ \dfrac{(m + M)g \sin(x_2)}{(M + \sin^2(x_2)m)l} - \dfrac{\cos(x_2)m \sin(x_2)x_4^2}{(M + \sin^2(x_2)m)} \end{bmatrix}$$

(E 2.3.2 c)

$$\mathbf{g}(\mathbf{x}) = \begin{bmatrix} 0 \\ 1 \\ \dfrac{1}{M + \sin^2(x_2)m} \\ -\dfrac{\cos(x_2)}{(M + \sin^2(x_2)m)l} \end{bmatrix}$$

(E 2.3.2 d)

Linearizing the (E 2.3.2) about the origin using the physical parameters $M = 2\ kg$, $m = 0.1$ kg, $l = 0.5\ m$, and $g = 9.81\ kg.m.s^{-2}$ produces the linearized model in (Ogata, 1997):

$$\begin{bmatrix} \dot{x}_1 \\ \dot{x}_2 \\ \dot{x}_3 \\ \dot{x}_4 \end{bmatrix} = \begin{bmatrix} 0 & 0 & 1 & 0 \\ 0 & 0 & 0 & 1 \\ 0 & -0.4905 & 0 & 0 \\ 0 & 20.6010 & 0 & 0 \end{bmatrix} \mathbf{x} + \begin{bmatrix} 0 \\ 0 \\ 0.5 \\ -1 \end{bmatrix} u$$

$$\equiv \mathbf{Ax} + \mathbf{B}u$$

(E 2.3.3)

It can be shown that (E 2.3.3) is unstable and is controllable. In the literature, we find that

(Ogata, 1997) employs pole placement to generate a linear state feedback control for

local stabilization of this system. Accordingly, we compare the dimension of the attractive regions resulting from this linear control to that resulting from LARC. Information regarding these linear controls is summarized below:

a)   *Linear Control Resulting from Pole Placement* (Ogata, 1997)

Reference (Ogata, 1997) employs a linear control based on pole placement for stabilizing this system. This is given by:

$$u(\mathbf{x}) = u_{PP}(\mathbf{x}) = -[-163.0989 \quad -298.1504 \quad -73.3945 \quad -60.6972]\mathbf{x} \equiv -\mathbf{K}_{PP}\mathbf{x}$$

$$(E2.3.4)$$

This linear control locates the eigenvalues of $\overline{\mathbf{A}} \equiv [\mathbf{A} - \mathbf{BK}_{PP}]$ at $\lambda_1 = -10$, $\lambda_2 = -10$, and $\lambda_{3,4} = -2 \pm j2\sqrt{3}$ in the LHP.

b)   *Linear Controls Resulting from LARC*

To generate our LARC, we follow the guidelines given in Section 2.4. The plot of eigenvalue ratio $r_{\lambda_{\mathbf{M}}}$ versus ρ in Fig. E2.3.2 is generated from our PC in approximately 2 seconds. Note that because we employ $\mathbf{Q} = \mathbf{I}$, all the negative eigenvalues o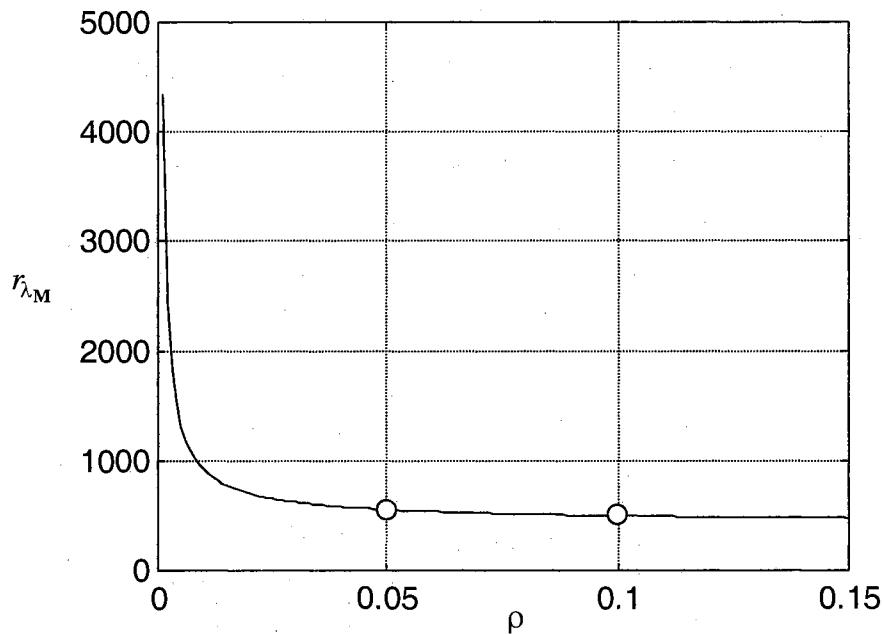f $\mathbf{M}$ are -1 and it follows that $r_{\lambda_{\mathbf{M}}} = \lambda_{\mathbf{M}1}$. From Fig. E2.3.2, we see that the eigenvalue ratio decreases when ρ increases but the decreasing of the eigenvalue ratio becomes small for large values of ρ. We construct and examine our LARC at $\rho = 300$ and 500 because the eigenvalue ratios corresponding to these values of ρ are small and because the eigenvalue ratio does not decrease significantly for larger values of ρ. Using the tuning guideline in Section 2.4, we start from $\rho = 300$ and increase ρ to 500:
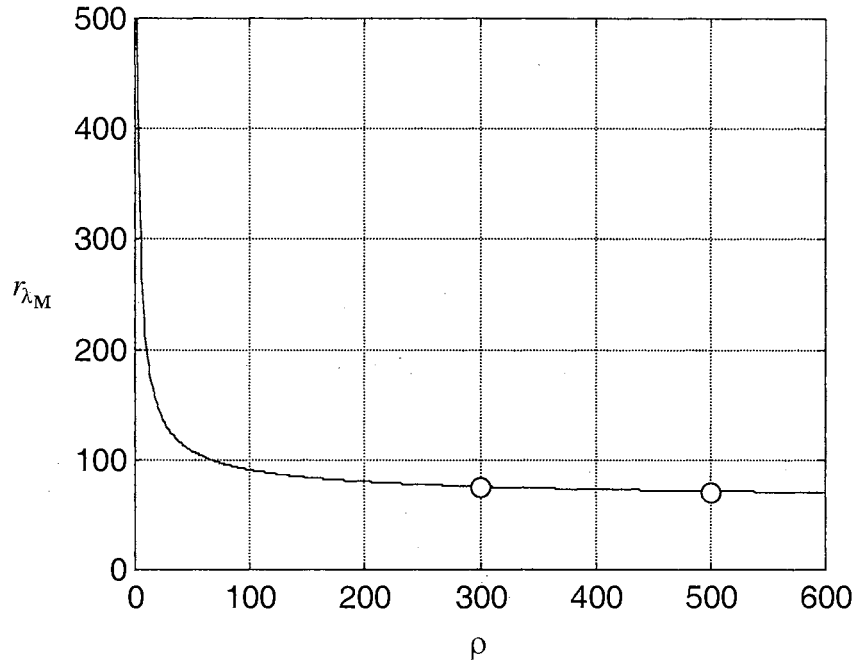
Fig. E2.3.2 A Plot of Eigenvalue Ratio Versus ρ

Symbol: $\circ$ ≡ points where we construct and examine the corresponding LARC

$b1)$ The LARC:

$$u(\mathbf{x}) = u_{LARC}(\mathbf{x}) = -\begin{bmatrix} -17.3205 & -143.6917 & -27.7674 & -36.4676 \end{bmatrix}\mathbf{x} \equiv -\mathbf{K}_{LARC}\mathbf{x}$$

(E 2.3.5)

is applied to the nonlinear system (E 2.3.1) to satisfy the eigenvector condition with

$\rho = 300$. This LARC locates the eigenvalues of $\overline{\mathbf{A}} \equiv [\mathbf{A} - \mathbf{BK}_{LARC}]$ at $\lambda_1 = -16.6600$

$\lambda_2 = -0.9139$, and $\lambda_{3,4} = -2.5050 \pm j2.2101$ in the LHP.

$b2)$ The LARC:

$$u(\mathbf{x}) = u_{LARC}(\mathbf{x}) = -\begin{bmatrix} -22.3607 & -180.0604 & -35.6916 & -46.0217 \end{bmatrix}\mathbf{x} \equiv -\mathbf{K}_{LARC}\mathbf{x}$$

(E 2.3.6)

is applied to the nonlinear system (E 2.3.1) to satisfy the eigenvector condition with

$\rho = 500$. This LARC locates the eigenvalues of $\overline{\mathbf{A}} \equiv [\mathbf{A} - \mathbf{BK}_{LARC}]$ at $\lambda_1 = -22.1829$,

$\lambda_2 = -0.9304$, and $\lambda_{3,4} = -2.5312 \pm j2.0544$ in the LHP.

By inspecting the locations of the poles of the linearized model under $u_{LARC}(\mathbf{x})$ in (E-

2.3.5), (E 2.3.6), and $u_{PP}(\mathbf{x})$ in (E 2.3.4) (Ogata, 1997), we expect that the system

responses under the LAR controllers are slower than those under $u_{PP}(\mathbf{x})$ near the origin.

In Fig. E2.3.2, we simulate the system under $u_{LARC}(\mathbf{x})$ in (E 2.3.6) and under $u_{PP}(\mathbf{x})$ in

(E 2.3.4). We notice from Fig. E2.3.2 (a) for which the system is launched from

$\mathbf{x}(0) = [0.1 \quad 0.1 \quad 0.1 \quad 0.1]^T$ that the responses under $u_{LARC}(\mathbf{x})$ are slower than those

under $u_{PP}(\mathbf{x})$, but with smaller overshoot. In Fig. E2.3.2 (b), the system is launched from

$\mathbf{x}(0) = [1 \quad 0.5 \quad 0 \quad 0]^T$. From this initial condition, we see that $u_{PP}(\mathbf{x})$ forces the system

to response quickly and yields divergence, while $u_{LARC}(\mathbf{x})$ does not force the system to

response as quick but the trajectory eventually converges to the origin.

We employ numerical simulations to estimate the attractive regions resulting from the

pole placement controller in (E 2.3.4), and from the LAR controllers in (E 2.3.5) and (E

2.3.6). In these simulations, we assume that convergence had occurred if $\|\mathbf{x}(t)\| < 0.01$ for

$40 \le t \le 50$, while divergence had occurred if $\exists t \, \|\mathbf{x}(t)\| > 2000$. It turns out that the

attractive region resulting from $u_{LARC}(\mathbf{x})$ in (E 2.3.6) is largest while that under $u_{PP}(\mathbf{x})$ is

the smallest. The attractive regions resulting from $u_{LARC}(\mathbf{x})$ in (E 2.3.6) and $u_{PP}(\mathbf{x})$ are

given in Tables E2.3.1 and E2.3.2. From these tables, we notice that the dimension of the attractive region resulting from $u_{LARC}(\mathbf{x})$ is significantly larger than that from $u_{PP}(\mathbf{x})$. Based on these investigations, we trade off in this example fast responses near the origin against a larger attractive region. This situation is common in control systems design, in which a trade-off of conflicting goals is used.
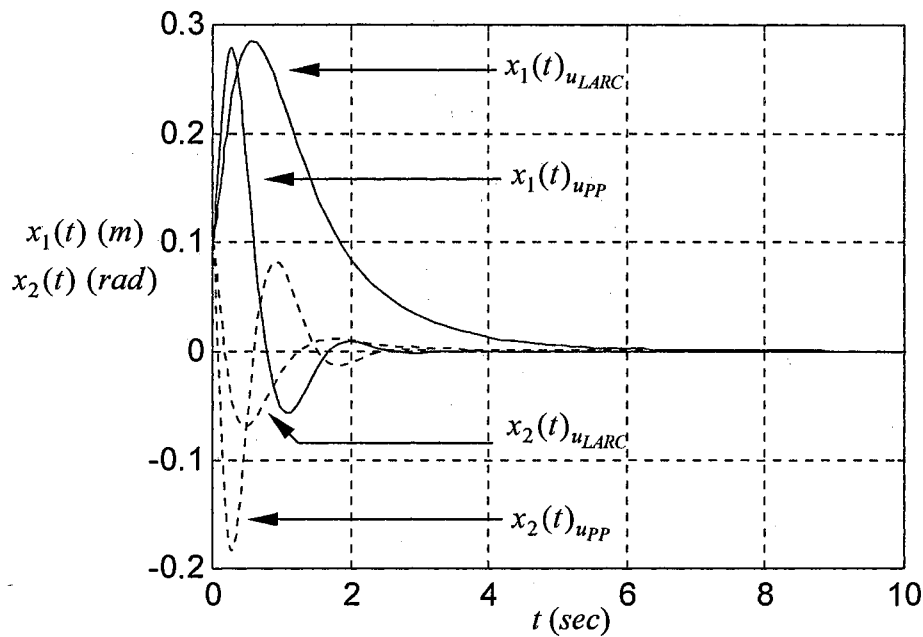
Fig. E2.3.2 (a)　Responses of the Cart-and-Pole System under $u_{LARC}(\mathbf{x})$ and $u_{PP}(\mathbf{x})$
with $\mathbf{x}(0) = [0.1 \quad 0.1 \quad 0.1 \quad 0.1]^{T}$

Now, we demonstrate the validity of theorems in Chapter 1 and 2 while showing in details the construction of $u_{LARC}(\mathbf{x})$ in (E 2.3.5). To generate a LAR controller with $\rho = 500$ and $c = 1$, we solve the Riccati equation:

$$0 = -2c\mathbf{I} - \mathbf{PA} - \mathbf{A}^{T}\mathbf{P} + 2\rho\,\mathbf{PBB}^{T}\mathbf{P} \qquad\qquad (\text{E 2.3.7})$$

This yields:

$$\mathbf{P} = \begin{bmatrix} 3.1924 & 4.1163 & 1.5478 & 0.8186 \\ 4.1163 & 20.4904 & 5.7517 & 3.2360 \\ 1.5478 & 5.7517 & 2.0509 & 1.0969 \\ 0.8186 & 3.2360 & 1.0969 & 0.6405 \end{bmatrix}$$

(E 2.3.8)
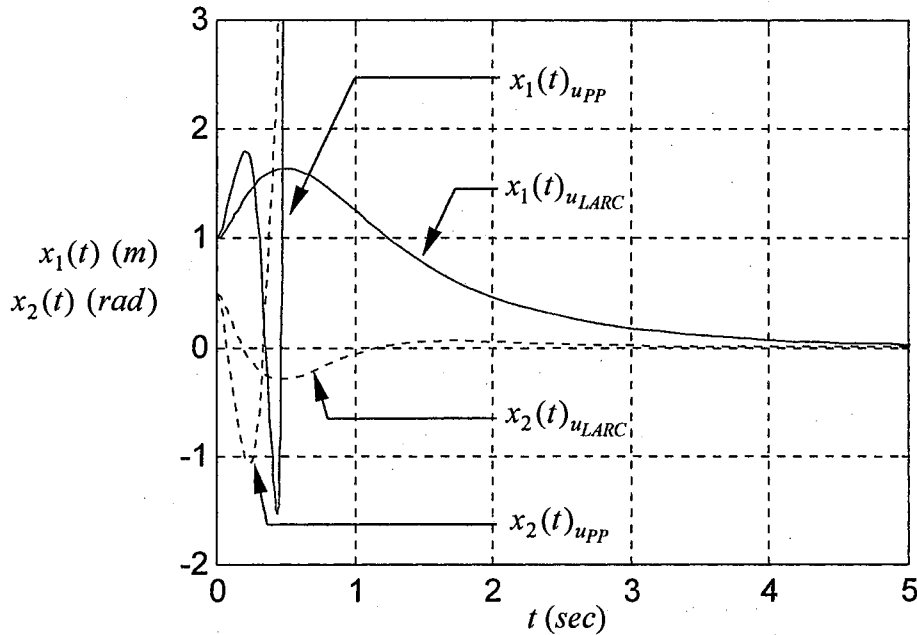
Fig. E2.3.2 (b)   Responses of the Cart-and-Pole System under $u_{LARC}(\mathbf{x})$ and $u_{PP}(\mathbf{x})$ with $\mathbf{x}(0) = [1 \quad 0.5 \quad 0 \quad 0]^T$

The corresponding LARC is:

$$\begin{aligned} u_{LARC}(\mathbf{x}) &= -\rho \mathbf{B}^T \mathbf{P} \mathbf{x} \\ &= -[-22.3607 \quad -180.0604 \quad -35.6916 \quad -46.0217]\mathbf{x} \\ &\equiv -\mathbf{K}_{LARC}\mathbf{x} \end{aligned}$$

(E 2.3.9)

where $\mathbf{K}_{LARC} = [-22.3607 \quad -180.0604 \quad -35.6916 \quad -46.0217]$. We compute further:

$$\mathbf{M} \equiv \frac{1}{2}[\mathbf{P}\mathbf{A} + \mathbf{A}^T\mathbf{P}] = \begin{bmatrix} 0 & 8.0525 & 1.5962 & 2.0582 \\ 8.0525 & 63.8435 & 12.8533 & 16.5734 \\ 1.5962 & 12.8533 & 1.5478 & 3.2852 \\ 2.0582 & 16.5734 & 3.2852 & 3.2360 \end{bmatrix}$$

(E 2.3.10 a)

$$\lambda_M \equiv [\lambda_{M1} \quad \lambda_{M2} \quad \lambda_{M3} \quad \lambda_{M4}] = [71.6272 \quad -1.0000 \quad -1.0000 \quad -1.0000] \quad \text{(E 2.3.10 b)}$$

$$\mathbf{v}_M \equiv [\mathbf{v}_{M1} \quad \mathbf{v}_{M2} \quad \mathbf{v}_{M3} \quad \mathbf{v}_{M4}] = \begin{bmatrix} 0.1173 & 0.6359 & 0.6492 & -0.4170 \\ 0.9449 & -0.0370 & 0.1229 & -0.1216 \\ 0.1873 & 0.5209 & -0.7089 & -0.2435 \\ 0.2415 & -0.5682 & -0.2465 & 0.8672 \end{bmatrix} \quad \text{(E 2.3.10 c)}$$

where $\mathbf{v}_{Mi} \in \Re^n$, $\|\mathbf{v}_{Mi}\| = 1$, $i = 1, ..., 4$.

$$\mathbf{N} = \frac{1}{2}[[\mathbf{PB}]\mathbf{K}_{LARC} + \mathbf{K}_{LARC}^T [\mathbf{PB}]^T] = \begin{bmatrix} 1.0000 & 8.0525 & 1.5962 & 2.0582 \\ 8.0525 & 64.8435 & 12.8533 & 16.5734 \\ 1.5962 & 12.8533 & 2.5478 & 3.2852 \\ 2.0582 & 16.5734 & 3.2852 & 4.2360 \end{bmatrix}$$

$$\text{(E 2.3.11 a)}$$

$$\lambda_N \equiv [\lambda_{N1} \quad \lambda_{N2} \quad \lambda_{N3} \quad \lambda_{N4}] = [72.6272 \quad 0.0000 \quad 0.0000 \quad 0.0000] \quad \text{(E 2.3.11 b)}$$

$$\mathbf{v}_N \equiv [\mathbf{v}_{N1} \quad \mathbf{v}_{N2} \quad \mathbf{v}_{N3} \quad \mathbf{v}_{N4}] = \begin{bmatrix} 0.1173 & 0.6359 & 0.6492 & -0.4170 \\ 0.9449 & -0.0370 & 0.1229 & -0.1216 \\ 0.1873 & 0.5209 & -0.7089 & -0.2435 \\ 0.2415 & --0.5682 & -0.2465 & 0.8672 \end{bmatrix} = \mathbf{v}_M$$

$$\text{(E 2.3.11 c)}$$

$$[\mathbf{PB}] = [-0.0447 \quad -0.3601 \quad -0.0714 \quad -0.0920]^T \quad \text{(E 2.3.12 a)}$$

$$[\overline{\mathbf{PB}}] \equiv \frac{[\mathbf{PB}]}{\|\mathbf{PB}\|} = [-0.1173 \quad -0.9449 \quad -0.1873 \quad -0.2415]^T = \mathbf{v}_{M1} = \mathbf{v}_{N1} \quad \text{(E 2.3.12 b)}$$

$$\overline{\mathbf{K}}_{LARC}^T \equiv \frac{\mathbf{K}_{LARC}^T}{\|\mathbf{K}_{LARC}^T\|} = [-0.1173 \quad -0.9449 \quad -0.1873 \quad -0.2415]^T \quad \text{(E 2.3.13)}$$

We notice the following properties of $\mathbf{M}$ and $\mathbf{N}$ predicted by our theorems:

1) $\mathbf{M}$ has exactly one positive eigenvalue λ_{M1}.

2) $\mathbf{N}$ has exactly one positive eigenvalue λ_{N1} and has no negative eigenvalue.

3) $\mathbf{M}$ and $\mathbf{N}$ share the same set of eigenvectors.

4) $\mathbf{v_{M1}} = \mathbf{v_{N1}}$.

5)   The eigenvector $\mathbf{v_{N1}}$ corresponding to the only positive eigenvalue λ_{N1} bisects

the angle between the vector $[\mathbf{PB}]$ and $\mathbf{K}_{LARC}^{T}$. Indeed:

$$\mathbf{v_{N1}} \cdot [\overline{\mathbf{PB}}] = \mathbf{v_{N1}} \cdot \overline{\mathbf{K}}_{LARC}^{T} = [\overline{\mathbf{PB}}] \cdot \overline{\mathbf{K}}_{LARC}^{T} = 1$$

6)   The directions of the vectors $[\mathbf{PB}]$ and $\mathbf{K}_{LARC}^{T}$ are the same. Indeed:

$$[\overline{\mathbf{PB}}] = \overline{\mathbf{K}}_{LARC}^{T}$$

These imply that the directions of $\nabla G_L(\mathbf{x}) = [\mathbf{PB}]$ and of $\mathbf{v_{M1}}$ are the same and the

eigenvector condition is satisfied.

			x_2																								
			1.25					1.00					0.75					0.50					0.25				
			x_4																								
			-1	-0.5	0	0.5	1	-1	-0.5	0	0.5	1	-1	-0.5	0	0.5	1	-1	-0.5	0	0.5	1	-1	-0.5	0	0.5	1
x_1	5	x_3 -1																									
		-0.5																									
		0																									
		0.5																									
		1																									
	4	-1																									
		-0.5																									
		0																									
		0.5																									
		1																									
	3	-1																									
		-0.5																									
		0																									
		0.5																									
		1																									
	2	-1																									
		-0.5																									
		0																									
		0.5																									
		1																									
	1	-1																									
		-0.5																									
		0																									
		0.5																									
		1																									

Table E2.3.1 Simulation Results of the Cart-and-Pole System in Regions farther from the Origin ($x_1 > 0$, $x_2 > 0$)

Remark: Attractive regions do not differ significantly in smaller regions about the origin.

Legends: ■ ≡ Pole placement and LARC systems converge, ▨ ≡ LARC system converge, □ ≡ All systems diverge

				x_2																								
				1.25					1.00					0.75					0.50					0.25				
				x_4																								
				-1	-0.5	0	0.5	1	-1	-0.5	0	0.5	1	-1	-0.5	0	0.5	1	-1	-0.5	0	0.5	1	-1	-0.5	0	0.5	1
x_1	-5	x_3	-1																									
			-0.5																									
			0																									
			0.5																									
			1																									
	-4		-1																									
			-0.5																									
			0																									
			0.5																									
			1																									
	-3		-1																									
			-0.5																									
			0																									
			0.5																									
			1																									
	-2		-1																									
			-0.5																									
			0																									
			0.5																									
			1																									
	-1		-1																									
			-0.5																									
			0																									
			0.5																									
			1																									

Table E2.3.2   Simulation Results of the Cart-and-Pole System in Regions farther from the Origin ($x_1 < 0$, $x_2 > 0$)

Remark: Attractive regions do not differ significantly in smaller regions about the origin.

Legends: ■ ≡ Pole placement and LARC systems converge, ▨ ≡ LARC system converge, □ ≡ All systems diverge

Example 2.4 (A Double-Inverted-Pendulum System with Upper-Joint Control)

We reconsider the double-inverted-pendulum system (Misawa, Arrington, and Ledgerwood, 1995) employed in Example 2.2. Now, we want to stabilize about their upright positions both links of the double-inverted- pendulum system using torque control at the <u>upper</u> joint only. The nonlinear model is obtained by substituting $[0 \quad u]^T$ for $[u \quad 0]^T$ in (E 2.2.1 a), with $\mathbf{H}_m$, $\mathbf{H}_g$, $\mathbf{H}_c$, all state variables, and all physical parameters being the same those in Example 2.2. The corresponding nonlinear model is given by:

$$\dot{\mathbf{x}} = \mathbf{f}(\mathbf{x}) + \mathbf{g}(\mathbf{x})u \qquad \text{(E 2.4.1 a)}$$

where:

$$\mathbf{f}(\mathbf{x}) = \begin{bmatrix} x_3 \\ x_4 \\ \dfrac{\left\{ \begin{array}{l} 0.9833x_3 + 1.1206\sin(x_1 - x_2)x_4^2 - 0.3165x_4 - 214.3082\sin(x_1) \\ + \cos(x_1 - x_2)\sin(x_1 - x_2)x_3^2 + 0.2824\cos(x_1 - x_2)x_3 \\ - 0.2824\cos(x_1 - x_2)x_4 + 48.2776\cos(x_1 - x_2)\sin(x_2) \end{array} \right\}}{-5.9809 + \cos(x_1 - x_2)^2} \\ \dfrac{\left\{ \begin{array}{l} -0.8774\cos(x_1 - x_2)x_3 - \cos(x_1 - x_2)\sin(x_1 - x_2)x_4^2 \\ + 0.2824\cos(x_1 - x_2)x_4 + 191.2383\cos(x_1 - x_2)\sin(x_1) \\ -5.3371\sin(x_1 - x_2)x_3^2 - 1.5071x_3 + 1.5071x_4 - 257.6614\sin(x_2) \end{array} \right\}}{-5.9809 + \cos(x_1 - x_2)^2} \end{bmatrix} \qquad \text{(E 2.4.1 b)}$$

$$\mathbf{g}(\mathbf{x}) = \begin{bmatrix} 0 \\ 0 \\ \dfrac{504.2688\cos(x_1 - x_2)}{-5.9809 + \cos(x_1 - x_2)^2} \\ \dfrac{-2691.3251}{-5.9809 + \cos(x_1 - x_2)^2} \end{bmatrix} \qquad \text{(E 2.4.1 c)}$$

Linearizing (E 2.4.1) about the equilibrium point at the origin yields:

$$\dot{\mathbf{x}} = \begin{bmatrix} 0 & 0 & 1 & 0 \\ 0 & 0 & 0 & 1 \\ 43.0258 & -9.6925 & -0.2541 & 0.1202 \\ -38.3942 & 51.7297 & 0.4787 & -0.3593 \end{bmatrix} \mathbf{x} + \begin{bmatrix} 0 \\ 0 \\ -101.2401 \\ 540.3270 \end{bmatrix} u \quad \text{(E 2.4.2)}$$

$$\equiv \mathbf{Ax} + \mathbf{B}u$$

It can be shown that (E 2.4.2) is unstable and is controllable. We have not found a reference that proposes a stabilizing controller for this system. Assuming that local stabilization is acceptable, we may employ techniques for linear systems such as pole placement, LQR, or LARC for this purpose. We now examine some specific possibilities:

a)   *Linear Controls Resulting from Pole Placement*

The linear control:

$$u(\mathbf{x}) = u_{PP}(\mathbf{x}) = -[-89.2977 \quad -8.9947 \quad -9.9560 \quad -1.6574]\mathbf{x} \equiv -\mathbf{K}_{PP}\mathbf{x} \quad \text{(E 2.4.3)}$$

is applied to the nonlinear system (E 2.4.1) to places the eigenvalues of the matrix

$\overline{\mathbf{A}} \equiv [\mathbf{A} - \mathbf{BK}_{PP}]$ at $\lambda_{1,2} = -4 \pm j4\sqrt{3}$, $\lambda_3 = -50$, and $\lambda_4 = -55$ in the LHP.

b)   *Linear Controls Resulting from LQR*

The linear control:

$$u(\mathbf{x}) = u_{LQR}(\mathbf{x}) = -[-114.0530 \quad -1.3217 \quad -18.8336 \quad -2.0673]\mathbf{x} \equiv -\mathbf{K}_{LQR}\mathbf{x} \quad \text{(E 2.4.4)}$$

is applied to the nonlinear system (E 2.1.1) to minimize the performance index:

$$J = \int_0^\infty [\mathbf{x}^T \mathbf{Ix} + 0.5u_{LQR}^2(\mathbf{x})]dt \quad \text{(E 2.4.5)}$$

This LQR locates the eigenvalues of $\overline{\mathbf{A}} \equiv [\mathbf{A} - \mathbf{BK}_{LQR}]$ at $\lambda_{1,2} = -5.91 \pm j0.5423$,

$\lambda_3 = -1.0021$ and $\lambda_4 = -777.4888$ in the LHP.

c)   *Linear Controls Resulting from LARC*

To generate our LARC, we follow the guidelines given in Section 2.4. The plot of

eigenvalue ratio r_{λ_M} versus ρ in Fig. E2.4.1 is generated from our PC in approximately

2 seconds. Note that because we employ $\mathbf{Q} = \mathbf{I}$, all the negative eigenvalues of $\mathbf{M}$ are -1

and it follows that $r_{\lambda_M} = \lambda_{M1}$. From Fig. E2.4.1, we see that the eigenvalue ratio

decreases when ρ increases but the decreasing of the eigenvalue ratio becomes small for

large values of ρ. We construct and examine our LARC at $\rho = 2.0$ because the

eigenvalue ratio corresponding to this value of ρ is small and because the eigenvalue

ratio does not decrease significantly for larger values of ρ. For this example, we examine

only one value ρ because it appears from the previous examples that a larger value of ρ

of does not produce significantly different results.
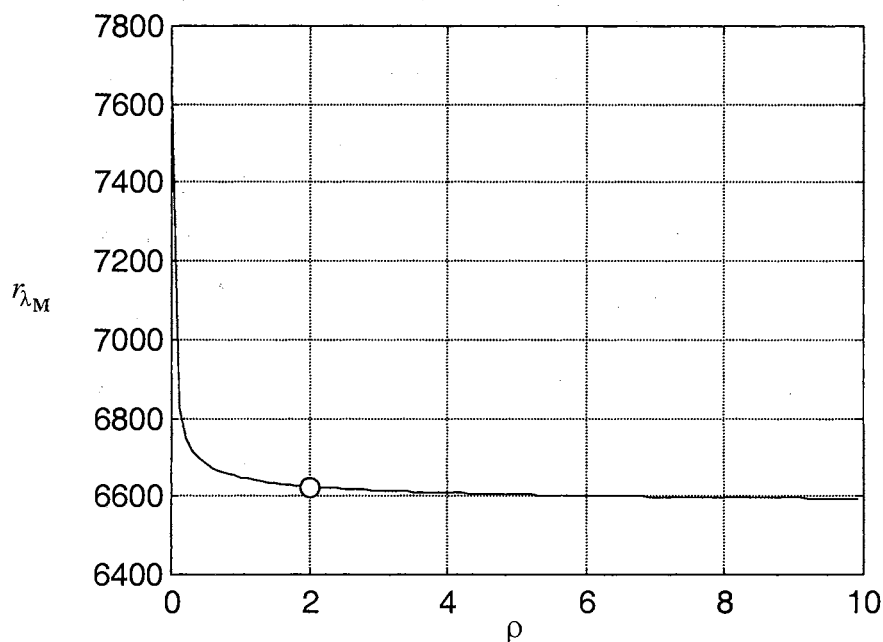
Fig. E2.4.1   A Plot of Eigenvalue Ratio Versus ρ

Symbol: $\circ$ = points where we construct and examine the corresponding LARC

The corresponding LARC is given by:

$$u(\mathbf{x}) = u_{LARC}(\mathbf{x}) = -\begin{bmatrix} -113.5510 & -1.3672 & -18.7574 & -2.0644 \end{bmatrix}\mathbf{x} \equiv -\mathbf{K}_{LARC}\mathbf{x} \quad (E\ 2.4.6)$$

This LARC locates the eigenvalues of $\overline{\mathbf{A}} \equiv [\mathbf{A} - \mathbf{BK}_{LARC}]$ at $\lambda_{1,2} = -5.8906 + j0.5772$,

$\lambda_3 = -1.0482$ and $\lambda_4 = -771.3419$ in the LHP.

We first notice that $\mathbf{K}_{LQR}$ is approximately the same as $\mathbf{K}_{LARC}$, suggesting a strong

possibility that the attractive regions corresponding to $u_{LQR}(\mathbf{x})$ and to $u_{LARC}(\mathbf{x})$ should

be approximately the same. Given a linear model, it is our experience that the situation in

which $\mathbf{K}_{LQR}$ being approximately the same as $\mathbf{K}_{LARC}$ when the quadratic performance

index is arbitrarily chosen does not occur in general. Table E2.4.1 and E2.4.2 show

simulation results from 1250 initial conditions. Convergence and divergence are defined

as those in Example 2.2. The attractive region corresponding to LQR is larger than that

corresponding to LARC. However, the difference is very small. Indeed, the number of

initial conditions from which trajectories converge under LQR is 963 while that under

LARC is 961. The attractive region corresponding to pole-placement is significantly

smaller than those under LQR and LARC. Motivated by this result, we examine further if

a larger attractive region can be obtained using a particular choice of LQR. We select

additional 25 quadratic performance indices obtained by perturbing various parameters in

the performance index in (E 2.4.5), and find that the attractive regions corresponding to a

few LQ regulators are larger than that corresponding to the LAR controller. However, the

differences are very small, ranging from 1-3 initial conditions, while the attractive

regions from most of the LQ controllers are significantly smaller than that from LARC.

Table E2.4.1   Simulation Results of the Double Inverted Pendulum System with Upper Joint Control ($x_1 > 0$, $x_2 > 0$)

Legends: ■ ≡ PP, LARC, LQR systems converge,   ▨ ≡ LARC, and LQR systems converge
▩ ≡ LQR system converges, □ ≡ All systems diverge

				x_2																								
				0.1					0.08					.06					0.04					.02				
				x_4																								
				-0.2	-0.1	0	0.1	0.2	-0.2	-0.1	0	0.1	0.2	-0.2	-0.1	0	0.1	0.2	-0.2	-0.1	0	0.1	0.2	-0.2	-0.1	0	0.1	0.2
x_1	-0.1	x_3	-0.2																									
			-0.1																									
			0																									
			0.1																									
			0.2																									
	-0.08		-0.2																									
			-0.1																									
			0																									
			0.1																									
			0.2																									
	-0.06		-0.2																									
			-0.1																									
			0																									
			0.1																									
			0.2																									
	-0.04		-0.2																									
			-0.1																									
			0																									
			0.1																									
			0.2																									
	-0.02		-0.2																									
			-0.1																									
			0																									
			0.1																									
			0.2																									

Table E2.4.2   Simulation Results of the Double Inverted Pendulum System with Upper Joint Control ($x_1 < 0$, $x_2 > 0$)

Legends: ■ ≡ PP, LARC, LQR systems converge,   ▨ ≡ LARC, and LQR systems converge
▧ ≡ LQR system converges, □ ≡ All systems diverge

2.6 Summary

1) The "eigenvector condition", which is a generalization in n-space of the relative orientation between $S_{F_L=0}$ and $S_{G_L=0}$ introduced in Section 1.4 has been established. Satisfying this eigenvector condition guarantees the symmetry of $S_{F_L=0}$ about $S_{G_L=0}$ in n-space.

2) Several properties of the functions $F_L(\mathbf{x})$ and $G_L(\mathbf{x})$ in the expression for $\dot{V}_L(\mathbf{x})$ have been discovered in this chapter. These properties imply that we can satisfy the eigenvector condition by applying a particular choice of linear control denoted by $u_{LARC}(\mathbf{x})$ to the system. By substituting $u_{LARC}(\mathbf{x})$ into the expression for $\dot{V}_L(\mathbf{x})$, we find that the $\mathbf{P}$ matrix that satisfies the eigenvector condition is the solution of a Riccati equation. Accordingly, the existence of such $\mathbf{P}$ is guaranteed provided that the conditions $C1 - C4$ in Chapter I are satisfied. We do not formulate our algorithm to solve the Riccati equation for such $\mathbf{P}$ because several algorithms are available for this task.

3) A striking result is that the eigenvector condition suggests a particular set of the quadratic performance indexes for generating LQR. Indeed, the relationship between LQR and LARC is given by $u_{LQR}(\mathbf{x}) = \frac{2}{\eta} u_{LARC}(\mathbf{x})$ when $u_{LQR}(\mathbf{x})$ is generated from such quadratic performance indexes. However, $u_{LQR}(\mathbf{x})$ does not satisfy the eigenvector condition in general.

4)   In contrast to existing linear control techniques such as pole placement and LQR, we point out that LARC has only two design parameters ρ and η to be selected. For simplicity in this introductory section, we fix $\eta = 1$. We point out a geometrical interpretation of ρ using the concept of eigenvalue ratio and illustrate how this parameter affects the size of a LAR. Finally, we show by means of examples how to select an appropriate value for ρ from the eigenvalue ratio plot such that LAR controllers can be generated using an inexpensive PC in a timely fashion. It appears from these examples that our LAR controllers yield reasonably large attractive regions when compared to those resulting from existing techniques, although we impose the restriction that $\eta = 1$.

Chapter III

Robust LARC

3.1   Introduction

In Chapter II, we establish a procedure for generating a LAR controller for SIMO time-invariant nonlinear systems (1.1) when the exact linearized model is available. In this chapter, we will extend key results from the previous chapter to establish a procedure for generating LAR controllers for SIMO time-varying systems when the models are inexact to complete our discussion on SIMO nonlinear systems. The procedures given in this chapter can be applied to SIMO time-invariant systems in the previous chapters as well.

In this chapter, the system of interest is described by:

$$\dot{\mathbf{x}} = \mathbf{f}(\mathbf{x}, t) + \mathbf{g}(\mathbf{x}, t) u(\mathbf{x}) \tag{3.1}$$

where the vectors $\mathbf{f}(\mathbf{x}, t) \in \Re^n$ and $\mathbf{g}(\mathbf{x}, t) \in \Re^n$ are uncertain, and $u(\mathbf{x}) = -\mathbf{K}\mathbf{x} \in \Re$. These are such that $\dot{\mathbf{x}}$ is piecewise continuous in t, and is locally Lipschitz in the operating region of interest in $\Re^n$ $\forall t \geq 0$. Recall from Chapter I that the above state equations can be rewritten as:

$$\begin{aligned}
\dot{\mathbf{x}} &= \mathbf{A}_n \mathbf{x} + \mathbf{B}_n u(\mathbf{x}) + [\mathbf{f}(\mathbf{x}, t) - \mathbf{A}_n \mathbf{x} + \mathbf{g}(\mathbf{x}, t) u(\mathbf{x}) - \mathbf{B}_n u(\mathbf{x})] \\
&\equiv \mathbf{A}_n \mathbf{x} + \mathbf{B}_n u(\mathbf{x}) + \mathbf{f}_\Sigma(\mathbf{x}, t, u(\mathbf{x})) \\
&\equiv \overline{\mathbf{A}}_n \mathbf{x} + \mathbf{f}_\Omega(\mathbf{x}, t)
\end{aligned} \tag{3.2}$$

where $\mathbf{A}_n \in \Re^{n \times n}$, $\mathbf{B}_n \in \Re^n$, $\overline{\mathbf{A}}_n \equiv [\mathbf{A}_n - \mathbf{B}_n \mathbf{K}] \in \Re^{n \times n}$ is a stable matrix,

$\mathbf{f}_\Sigma(\mathbf{x}, t, u(\mathbf{x})) \equiv [\mathbf{f}(\mathbf{x}, t) - \mathbf{A}_n \mathbf{x} + \mathbf{g}(\mathbf{x}, t) u(\mathbf{x}) - \mathbf{B}_n u(\mathbf{x})] \in \Re^n$, $\mathbf{f}_\Omega(\mathbf{x}, t) \equiv \mathbf{f}_\Sigma(\mathbf{x}, t, u(\mathbf{x})) \big|_{u = -\mathbf{K}\mathbf{x}}$.

To be able to employ results developed in Chapter I and II in this chapter, it is necessary that we rewrite the nonlinear model such that $\mathbf{A}_n$ is unstable, and $[\mathbf{A}_n \ \mathbf{B}_n]$ is controllable or stabilizable. In addition to this, we desire that the nominal model $\dot{\mathbf{x}} = \mathbf{A}_n \mathbf{x} + \mathbf{B}_n u(\mathbf{x})$ be chosen in a certain fashion to be able to generate a robust LARC effectively using techniques that will be developed in this chapter. Example 3.6 illustrates a guideline for choosing an appropriate nominal model, which need not be the linearized model about the origin.

3.2 Stability of Time-Invariant Linear Systems Under Time-Varying Uncertainties

In this chapter, the available "nominal" nonlinear model is given by:

$$\dot{\mathbf{x}} = \mathbf{f}_n(\mathbf{x},t) + \mathbf{g}_n(\mathbf{x},t)u(\mathbf{x}) \tag{3.3}$$

where $\mathbf{f}_n(\mathbf{x},t)$ and $\mathbf{g}_n(\mathbf{x},t) \in \mathfrak{R}^n$. By linearizing (3.3) about the origin, we obtain the "nominal" time-invariant linear model:

$$\dot{\mathbf{x}} = \mathbf{A}_n \mathbf{x} + \mathbf{B}_n u(\mathbf{x}) \tag{3.4}$$

where the linear control $u(\mathbf{x}) = -\mathbf{Kx}$ is such that $\overline{\mathbf{A}}_n \equiv [\mathbf{A}_n - \mathbf{B}_n \mathbf{K}]$ is stable. In other words, we replace $\mathbf{A}$ and $\mathbf{B}$ in the previous chapters by $\mathbf{A}_n$ and $\mathbf{B}_n$ respectively. By this replacement, we assume in our discussions that the basic conditions $C1-C4$ in Section 1.3 are satisfied. It is well known (Slotine, and Li, 1991), (Vidyasagar, 1993) that the following conditions guarantee that (3.4) approximates (3.3) about the origin uniformly in t:

$$\left.\begin{array}{c} \lim\limits_{\|\mathbf{x}\|\to 0}\left(\sup\limits_{t\geq 0}\left(\dfrac{\|\mathbf{f}_n(\mathbf{x},t)-\mathbf{A}_n\mathbf{x}\|}{\|\mathbf{x}\|}\right)\right)=0 \\[4mm] \lim\limits_{\|\mathbf{x}\|\to 0}\left(\sup\limits_{t\geq 0}\left(\dfrac{\|\mathbf{g}_n(\mathbf{x},t)-\mathbf{B}_n\|}{\|\mathbf{x}\|}\right)\right)=0 \end{array}\right\} \qquad (3.5)$$

In other words, stability about the origin of (3.4) implies that (3.3) is locally uniformly asymptotically stable when (3.5) is satisfied. In this chapter, we abbreviate "uniformly asymptotically stable" by "stable" unless otherwise stated. The context will indicate whether we are interested in the global version or the local version at the moment. Under the conditions in (3.5), the LARC developed in the previous chapters stabilizes (3.3), provided that it stabilizes (3.4). This is because when (3.5) is satisfied, (3.4) is a valid approximation of (3.3) about the origin.

3.3   Uncertainty Specifications

We exploit information about uncertainties for stability analysis and for controller generation. In each application, uncertainties are classified into two categories by the available uncertainty specifications:

Structured Uncertainty Specifications for Stability Analysis

For stability analysis, the uncertain vector $\mathbf{f}_\Omega(\mathbf{x},t)$ is "structured" if it can be written as:

$$\mathbf{f}_\Omega(\mathbf{x},t)=\sum_{j=1}^{r}[h_j(\mathbf{x},t)\,\mathbf{E}_j\mathbf{x}] \qquad (3.6)$$

where $h_j(\mathbf{x},t) \in [h_{lj}, h_{uj}] \in \Re$ are <u>uncertain</u> functions, $h_{lj} < h_{uj}$, and $\mathbf{E}_j \in \Re^{n \times n}$ $j = 1, 2,$

..., r. In this case, (3.2) can be written as:

$$\dot{\mathbf{x}} = \overline{\mathbf{A}}_n \mathbf{x} + \sum_{j=1}^{r} [h_j(\mathbf{x},t)\mathbf{E}_j \mathbf{x}] \tag{3.7}$$

The form of structured uncertainty (3.6) is adopted from (Zhou, and Khargonekar, 1987).

In addition to the structure in (3.6), we need to know h_{lj} (a lower bound of $h_j(\mathbf{x},t)$), h_{uj}

(an upper bound of $h_j(\mathbf{x},t)$), and $\mathbf{E}_j$ $j = 1, \ldots, r$ for stability analysis.

Unstructured Uncertainty Specifications for Stability Analysis

When the only available uncertainty specification is a bound on $\dfrac{\|\mathbf{f}_\Omega(\mathbf{x},t)\|}{\|\mathbf{x}\|}$, we say that the

uncertainty is "unstructured". In this case, the system is described by (3.2).

Structured Uncertainty Specifications for Controller Generation

The structured uncertainty specifications for controller generation are obtained by

rewriting (3.6) to include the linear state feedback gain matrix explicitly. Indeed, we

substitute $-\mathbf{Kx}$ for $u(\mathbf{x})$, and $\displaystyle\sum_{j=1}^{r} [h_j(\mathbf{x},t)\mathbf{E}_j \mathbf{x}]$ for $\mathbf{f}_\Omega(\mathbf{x},t)$ in (3.2) to produce:

$$\dot{\mathbf{x}} = \left[\mathbf{A}_n - \mathbf{B}_n \mathbf{K} + \sum_{j=1}^{r} [h_j(\mathbf{x},t)\mathbf{E}_j] \right] \mathbf{x} \tag{3.8}$$

Because $\mathbf{A}_n$, $[\mathbf{B}_n \mathbf{K}]$, and $\mathbf{E}_j$ belong to $\Re^{n \times n}$, it appears from (3.8) that the term

$\displaystyle\sum_{j=1}^{r} [h_j(\mathbf{x},t)\mathbf{E}_j]$ represents uncertainties in $\mathbf{A}_n$ and $[\mathbf{B}_n \mathbf{K}]$. Accordingly, we can describe

the dynamics of the uncertain system by:

$$\dot{\mathbf{x}} = \left[\mathbf{A}_n - \mathbf{B}_n \mathbf{K} + \sum_{j=1}^{r} [h_j(\mathbf{x},t)\mathbf{E}_j] \right] \mathbf{x}$$

$$= \left[[\mathbf{A}_n + \sum_{\alpha=1}^{r_{A_n}} [h_\alpha^{A_n}(\mathbf{x},t)\mathbf{E}_\alpha^{A_n}]] + [-\mathbf{B}_n \mathbf{K} + \sum_{\beta=1}^{r_{B_n}} [h_\beta^{B_n}(\mathbf{x},t)\mathbf{E}_\beta^{B_n}]] \right] \mathbf{x} \qquad (3.9)$$

$$\equiv \left[[\mathbf{A}_n + \Delta\mathbf{A}_n(\mathbf{x},t)] + [-[\mathbf{B}_n + \Delta\mathbf{B}_n(\mathbf{x},t)]\mathbf{K}] \right] \mathbf{x}$$

where

1) $r = r_{A_n} + r_{B_n}$, $1 \le r_{A_n} \le n \times n$, $1 \le r_{B_n} \le n$

2) $h_j(\mathbf{x},t) = h_\alpha(\mathbf{x},t)$, $\mathbf{E}_j = \mathbf{E}_\alpha^{A_n} \in \Re^{n \times n}$, $j = 1,2,\ldots,r_{A_n}$

3) $h_j(\mathbf{x},t) = h_\beta(\mathbf{x},t)$, $\mathbf{E}_j = \mathbf{E}_\beta^{B_n} \in \Re^{n \times n}$, $j = r_{A_n} + 1, r_{A_n} + 2, \ldots, r$

4) $\Delta\mathbf{A}_n(\mathbf{x},t) \equiv \sum_{\alpha=1}^{r_{A_n}} [h_\alpha^{A_n}(\mathbf{x},t)\mathbf{E}_\alpha^{A_n}]$

5) $-\Delta\mathbf{B}_n(\mathbf{x},t)\mathbf{K} \equiv \sum_{\beta=1}^{r_{B_n}} [h_\beta^{B_n}(\mathbf{x},t)\mathbf{E}_\beta^{B_n}]$

6) $\sum_{j=1}^{r} [h_j(\mathbf{x},t)\mathbf{E}_j] = \sum_{\alpha=1}^{r_{A_n}} [h_\alpha^{A_n}(\mathbf{x},t)\mathbf{E}_\alpha^{A_n}] + \sum_{\beta=1}^{r_{B_n}} [h_\beta^{B_n}(\mathbf{x},t)\mathbf{E}_\beta^{B_n}]$

Note that the uncertain matrix $-[\Delta\mathbf{B}_n(\mathbf{x},t)]\mathbf{K}$ depends on $\mathbf{K}$ while the uncertain matrix

$\Delta\mathbf{A}_n(\mathbf{x},t)$ does not. We assume for simplicity that the uncertainties in $\mathbf{K}$ are negligible.

This is a valid assumption, because we can usually construct an amplifier with a precise

gain. We see from (3.2) and (3.9) that:

$$[\Delta\mathbf{A}_n(\mathbf{x},t)]\mathbf{x} = \mathbf{f}(\mathbf{x},t) - \mathbf{A}_n\mathbf{x} \qquad (3.10)$$

$$\Delta\mathbf{B}_n(\mathbf{x},t) = \mathbf{g}(\mathbf{x},t) - \mathbf{B}_n \qquad (3.11)$$

where the (i, j) elements of $\Delta\mathbf{A}_n(\mathbf{x},t)$ and of $\Delta\mathbf{B}_n(\mathbf{x},t)$ are zero if there is no uncertainty

in such elements. The information on the elements of $\Delta\mathbf{A}_n(\mathbf{x},t)$ and $\Delta\mathbf{B}_n(\mathbf{x},t)$ are

structured uncertainty specifications for controller generation. Note that writing

$\Delta A_n(\mathbf{x}, t)\mathbf{x}$ as $\sum_{\alpha=1}^{r_{A_n}} [h_\alpha^{A_n}(\mathbf{x}, t)\mathbf{E}_\alpha^{A_n}]\mathbf{x}$ is obvious because $\Delta A_n(\mathbf{x}, t), \mathbf{E}_\alpha^{A_n} \in \Re^{n \times n}$. We note

that:

$$\Delta B_n(\mathbf{x}, t) = \sum_{\beta=1}^{r_{B_n}} [h_\beta^{B_n}(\mathbf{x}, t)\mathbf{E}_\beta^{\Delta B n}]\mathbf{x} \tag{3.12}$$

where $\mathbf{E}_\beta^{\Delta Bn} \in \Re^{n \times m}$. Using this notation, we write:

$$-[\Delta B_n(\mathbf{x}, t)]\mathbf{Kx} = \sum_{\beta=1}^{r_{B_n}} [h_\beta^{B_n}(\mathbf{x}, t)[-\mathbf{E}_\beta^{\Delta Bn}\mathbf{K}]]\mathbf{x} = \sum_{\beta=1}^{r_{B_n}} [h_\beta^{B_n}(\mathbf{x}, t)\mathbf{E}_\beta^{B_n}]\mathbf{x} \tag{3.13}$$

where $\mathbf{E}_\beta^{B_n} = [-\mathbf{E}_\beta^{\Delta Bn}\mathbf{K}] \in \Re^{n \times n}$.

Unstructured Uncertainty Specifications for Controller Generation

When the uncertainties are unstructured, we have that:

$$\begin{aligned}\mathbf{f}_\Omega(\mathbf{x}, t) &= [\mathbf{f}(\mathbf{x}, t) - \mathbf{A}_n\mathbf{x}] + [\mathbf{g}(\mathbf{x}, t) - \mathbf{B}_n]u(\mathbf{x})\,|_{u=-\mathbf{Kx}} \\ &= \Delta\mathbf{f}(\mathbf{x}, t) + \Delta\mathbf{g}(\mathbf{x}, t)u(\mathbf{x})\end{aligned} \tag{3.14}$$

where $\Delta\mathbf{f}(\mathbf{x}, t) \equiv \mathbf{f}(\mathbf{x}, t) - \mathbf{A}_n\mathbf{x}$ and $\Delta\mathbf{g}(\mathbf{x}, t) \equiv \mathbf{g}(\mathbf{x}, t) - \mathbf{B}_n$. The specifications for

unstructured uncertainties are bounds on $\dfrac{\|\Delta\mathbf{f}(\mathbf{x}, t)\|}{\|\mathbf{x}\|}$ and $\|\Delta\mathbf{g}(\mathbf{x}, t)\|$ denoted by

$\max\left(\dfrac{\|\Delta\mathbf{f}(\mathbf{x}, t)\|}{\|\mathbf{x}\|}\right)$ and $\max(\|\Delta\mathbf{g}(\mathbf{x}, t)\|)$ respectively. We can employ these specifications

to bound $\dfrac{\|\mathbf{f}_\Omega(\mathbf{x}, t)\|}{\|\mathbf{x}\|}$:

$$\frac{\left\|\mathbf{f}_{\Omega}(\mathbf{x},t)\right\|}{\left\|\mathbf{x}\right\|} = \frac{\left\|\Delta\mathbf{f}(\mathbf{x},t) + \Delta\mathbf{g}(\mathbf{x},t)u\mid_{u=-\mathbf{Kx}}\right\|}{\left\|\mathbf{x}\right\|}$$

$$\leq \frac{\left\|\Delta\mathbf{f}(\mathbf{x},t)\right\|}{\left\|\mathbf{x}\right\|} + \frac{\left\|\Delta\mathbf{g}(\mathbf{x},t)\right\|}{\left\|\mathbf{x}\right\|}\left\|u\mid_{u=-\mathbf{Kx}}\right\| \qquad (3.15)$$

$$\leq \frac{\left\|\Delta\mathbf{f}(\mathbf{x},t)\right\|}{\left\|\mathbf{x}\right\|} + \left\|\Delta\mathbf{g}(\mathbf{x},t)\right\|\left\|\mathbf{K}\right\|$$

We assume for simplicity that the uncertainties in **K** are negligible. This is a valid assumption because we can usually construct an amplifier with a precise gain.

3.4   Theorems

In this section, we state three fundamental theorems. We will employ them for both stability analysis and controller generation. Most of the results in this section are based on continuity of eigenvalues of symmetric matrices. Accordingly, we state a symmetric perturbation theorem based on the Courant-Fischer min-max representation (Ortega, 1990):

Theorem 3.1   (Continuity of Eigenvalues of Symmetric Matrices)

Let **A** and **A+E** in $\mathfrak{R}^{n\times n}$ be symmetric with eigenvalues $\lambda_1 \geq ... \geq \lambda_n$ and $\mu_1 \geq ... \geq \mu_n$ respectively. Then:

$$\left|\lambda_i - \mu_i\right| \leq \left\|\mathbf{E}\right\| \qquad (3.16)$$

where $i = 1, ..., n$.

A proof for Theorem 3.1 can be found in (Ortega, 1990). In words, Theorem 3.1 says that small changes in elements of a symmetric matrix **A** causes correspondingly small changes in the eigenvalues of **A**. Next, we state a theorem that allows us to obtain structured uncertainty bounds for stability of (3.7) in an operating region about the origin.

Theorem 3.2 (Structured Uncertainty Bound)

Let $\overline{\mathbf{A}}_n$ be a stable matrix and Γ be a region in state space where the bounded uncertainties can be described by (3.6). The time derivative of the quadratic Lyapunov function (1.5) along trajectories of the structured uncertain nonlinear system (3.7) is negative definite in Γ if:

$$\lambda_{\max}(\mathbf{\Phi}) < 0 \tag{3.17 a}$$

$$\lambda_{\max}(\mathbf{Z}) < 0 \tag{3.17 b}$$

where $\lambda_{\max}(\Xi)$ is the maximum eigenvalue of $\Xi \in \mathfrak{R}^n$, and Ξ denotes $\mathbf{\Phi}$, $\mathbf{Z}$. Matrices $\mathbf{\Phi}$ and $\mathbf{Z}$ are computed by applying the following equations in order:

$$-2\mathbf{Q} = \mathbf{P}\overline{\mathbf{A}}_n + \overline{\mathbf{A}}_n^T \mathbf{P} \tag{3.18 a}$$

where $\mathbf{Q}$, and $\mathbf{P}$ are $n \times n$ symmetric positive definite matrices. The existence of such $\mathbf{Q}$ and $\mathbf{P}$ is guaranteed by Lyapunov stability because $\overline{\mathbf{A}}_n$ is stable.

$$\overline{\mathbf{A}}_l \equiv \overline{\mathbf{A}}_n + \sum_{j=1}^{r} h_{lj} \mathbf{E}_j \tag{3.18 b}$$

where the subscript "*l*" denotes "lower bound".

$$\mathbf{\Phi} \equiv \mathbf{P}\overline{\mathbf{A}}_l + \overline{\mathbf{A}}_l^T \mathbf{P} \tag{3.18 c}$$

where $\boldsymbol{\Phi}$ is a symmetric matrix because $[\mathbf{P}\overline{\mathbf{A}}_l]^T = \overline{\mathbf{A}}_l^T\mathbf{P}$ due to the symmetry of $\mathbf{P}$.

$$\boldsymbol{\Psi}_j \equiv [\mathbf{P}\mathbf{E}_j + \mathbf{E}_j^T\mathbf{P}] = \boldsymbol{\Psi}_j^T \qquad (3.18\ d)$$

$$\boldsymbol{\Psi}_j^D = \mathbf{T}_{\boldsymbol{\Psi}_j}^T\boldsymbol{\Psi}_j\mathbf{T}_{\boldsymbol{\Psi}_j} = \mathrm{diag}[\lambda_{1j}(\boldsymbol{\Psi}_j) \quad \ldots \quad \lambda_{nj}(\boldsymbol{\Psi}_j)] \qquad (3.18\ e)$$

where $\mathbf{T}_{\boldsymbol{\Psi}_j} = [\mathbf{v}_{1j}(\boldsymbol{\Psi}_j) \mid \ldots \mid \mathbf{v}_{nj}(\boldsymbol{\Psi}_j)]$, $\mathbf{T}_{\boldsymbol{\Psi}_j}^T\mathbf{T}_{\boldsymbol{\Psi}_j} = \mathbf{I}$, $\{\mathbf{v}_{1j}(\boldsymbol{\Psi}_j) \quad \ldots \quad \mathbf{v}_{nj}(\boldsymbol{\Psi}_j)\}$ is the set

of n orthonormal eigenvectors of $\boldsymbol{\Psi}_j$, the superscript "D" denotes that $\boldsymbol{\Psi}_j^D$ is diagonal,

and the subscript j denotes that $\boldsymbol{\Psi}_j^D$ is associated with $\mathbf{E}_j$.

$$\boldsymbol{\Psi}_j^{D,\,0+} = \boldsymbol{\Psi}_j^D \Big|_{[\boldsymbol{\Psi}_j^D(i,i)<0]\rightarrow[\boldsymbol{\Psi}_j^D(i,i)=0]} \qquad (3.18\ f)$$

where the subscript on the RHS of (3.18 f) means that we obtain the diagonal matrix

$\boldsymbol{\Psi}_j^{D,0+}$ from the diagonal matrix $\boldsymbol{\Psi}_j^D$ by setting all negative diagonal elements of $\boldsymbol{\Psi}_j^D$ to

zero, and $\boldsymbol{\Psi}_j^D(i,i)$ denotes the (i,i) element of $\boldsymbol{\Psi}_j^D$. The superscript "0+" is employed

with the superscript "D" to designate that $\boldsymbol{\Psi}_j^{D,\,0+}$ is diagonal, and is either positive

semidefinite or positive definite. This is because a diagonal element of the diagonal matrix

$\boldsymbol{\Psi}_j^{D,0+}$ is either zero or positive, because of the operation in (3.18 f).

$$\boldsymbol{\Psi}_j^{0+} = [\mathbf{T}_{\boldsymbol{\Psi}_j}^{-1}]^T[\boldsymbol{\Psi}_j^{D,0+}]\mathbf{T}_{\boldsymbol{\Psi}_j}^T = \mathbf{T}_{\boldsymbol{\Psi}_j}[\boldsymbol{\Psi}_j^{D,0+}]\mathbf{T}_{\boldsymbol{\Psi}_j}^T \qquad (3.18\ g)$$

In $\boldsymbol{\Psi}_j^{0+}$, the superscript "D" is not employed with "0+" and we designate that $\boldsymbol{\Psi}_j^{0+}$ is

positive semidefinite or is positive definite but need not be diagonal. Finally,

$$\mathbf{Z} \equiv \boldsymbol{\Phi} + \sum_{j=1}^{r}[(h_{uj} - h_{lj})\boldsymbol{\Psi}_j^{0+}] \qquad (3.18\ h)$$

Proof

Our nonlinear system with structured uncertainty is given by (3.7) and is reproduced for convenience:

$$\dot{\mathbf{x}} = \overline{\mathbf{A}}_n \mathbf{x} + \sum_{j=1}^{r} [h_j(\mathbf{x},t)\mathbf{E}_j \mathbf{x}] \tag{3.7}$$

Now, we write for $j = 1, 2, ..., r$:

$$\begin{aligned} h_j(\mathbf{x},t) &= h_{lj} + h_j(\mathbf{x},t) - h_{lj} \\ &\equiv h_{lj} + l_j(\mathbf{x},t) \end{aligned} \tag{3.19}$$

where

$$l_j(\mathbf{x},t) \equiv h_j(\mathbf{x},t) - h_{lj} \tag{3.20}$$

Since $h_j(\mathbf{x},t) \in [h_{lj}, h_{uj}] \in \mathfrak{R}$, it follows from (3.20) that $l_j(\mathbf{x}) \in [0, h_{uj} - h_{lj}]$ where $h_{uj} - h_{lj} > 0 \; \forall j$. Substituting $h_{lj} + l_j(\mathbf{x})$ for $h_j(\mathbf{x},t)$ in (3.7) yields:

$$\begin{aligned} \dot{\mathbf{x}} &= \overline{\mathbf{A}}_n \mathbf{x} + \sum_{j=1}^{r} h_{lj}\mathbf{E}_j\mathbf{x} + \sum_{j=1}^{r} l_j(\mathbf{x},t)\mathbf{E}_j\mathbf{x} \\ &= [\overline{\mathbf{A}}_n + \sum_{j=1}^{r} h_{lj}\mathbf{E}_j]\mathbf{x} + \sum_{j=1}^{r} l_j(\mathbf{x},t)\mathbf{E}_j\mathbf{x} \\ &= \overline{\mathbf{A}}_l \mathbf{x} + \sum_{j=1}^{r} l_j(\mathbf{x},t)\mathbf{E}_j\mathbf{x} \end{aligned} \tag{3.21}$$

where $\overline{\mathbf{A}}_l \equiv \overline{\mathbf{A}}_n + \sum_{j=1}^{r} h_{lj}\mathbf{E}_j$. Because $\overline{\mathbf{A}}_n$ is stable, we know by Lyapunov stability the existence of symmetric positive definite matrices $\mathbf{Q}$ and $\mathbf{P}$ satisfying the Lyapunov equation (3.18 a). To examine effects of structured uncertainties, consider the time derivative of the quadratic Lyapunov function (1.5) along trajectories of the structured uncertain nonlinear system (3.21):

(Proof of Theorem 3.2 (Cont.))

$$\dot{V}(\mathbf{x},t) = \frac{1}{2}\mathbf{x}^T[\mathbf{P}\overline{\mathbf{A}}_l + \overline{\mathbf{A}}_l^T\mathbf{P}]\mathbf{x} + \frac{1}{2}\sum_{j=1}^{r} l_j(\mathbf{x},t)\mathbf{x}^T[\mathbf{P}\mathbf{E}_j + \mathbf{E}_j^T\mathbf{P}]\mathbf{x}$$

$$= \frac{1}{2}\mathbf{x}^T\mathbf{\Phi}\mathbf{x} + \frac{1}{2}\sum_{j=1}^{r} l_j(\mathbf{x},t)\mathbf{x}^T\mathbf{\Psi}_j\mathbf{x}$$

(3.22)

where $\mathbf{Q}$ is specified and $\mathbf{P}$ is determined from (3.18 a), $\mathbf{\Phi}$ is given by (3.18 c), and $\mathbf{\Psi}_j$ by (3.18 d). Since $\dot{V}(\mathbf{x},t) = \frac{1}{2}\mathbf{x}^T\mathbf{\Phi}\mathbf{x}$ when $l_j(\mathbf{x},t) = 0$ $\forall j$, a necessary condition for $\dot{V}(\mathbf{x},t)$ to be negative definite is that $\mathbf{\Phi}$ be negative definite. Note that because $\mathbf{\Phi} = \mathbf{\Phi}^T$, a sufficient condition guaranteeing that $\mathbf{\Phi}$ is negative definite is given by (3.17 a) (Orgeta, 1990). To examine $\mathbf{\Phi}$, we notice from (3.18 b) that $\overline{\mathbf{A}}_l\big|_{h_{lj}=0\ \forall j} = \overline{\mathbf{A}}_n$.

Accordingly, $\mathbf{\Phi}\big|_{h_{lj}=0\ \forall j} = [\mathbf{P}\mathbf{A}_n + \mathbf{A}_n^T\mathbf{P}] = -2\mathbf{Q}$ and it follows that $\lambda_i(\mathbf{\Phi}\big|_{h_{lj}=0\ \forall j}) < 0$, $j = 1,\ldots,r$, $i = 1,\ldots,n$ because $\overline{\mathbf{A}}_n$ is stable. Now, we substitute the given numerical values for h_{lj}, $j = 1,\ldots,r$ into (3.18 b) and compute the corresponding $\overline{\mathbf{A}}_l$. Then employ the resulting $\overline{\mathbf{A}}_l$ to obtain $\mathbf{\Phi}$ using (3.18 c), and examine the negative definiteness of $\mathbf{\Phi}$ using (3.17 a).

To guarantee that $\dot{V}(\mathbf{x},t)$ is negative definite in the region Γ where the structured uncertainties are valid, we need to examine the quadratic terms $\mathbf{x}^T\mathbf{\Psi}_j\mathbf{x}$ in (3.22) $\forall j$. We assume the general case in which $\mathbf{\Psi}_j$ is not diagonal. Since $\mathbf{\Psi}_j = [\mathbf{P}\mathbf{E}_j + \mathbf{E}_j^T\mathbf{P}]$, it follows that $\mathbf{\Psi}_j^T = [\mathbf{E}_j^T\mathbf{P}^T + \mathbf{P}^T\mathbf{E}_j] = [\mathbf{E}_j^T\mathbf{P} + \mathbf{P}\mathbf{E}_j] = \mathbf{\Psi}_j$ and we conclude that $\mathbf{\Psi}_j = \mathbf{\Psi}_j^T$ $\forall j$.

(Proof of Theorem 3.2 (Cont.))

Accordingly, Ψ_j has a set of n orthonormal eigenvectors $\{v_{1j}(\Psi_j) \quad \dots \quad v_{nj}(\Psi_j)\}$

(Hagan et al, 1996). We now reduce $x^T \Psi_j x$ to the principal axes by using the linear

transformation:

$$x = T_{\Psi_j} z = [v_{1j}(\Psi_j) \mid v_{2j}(\Psi_j) \mid \dots \mid v_{nj}(\Psi_j)]z \tag{3.23}$$

where $T_{\Psi_j} = [v_{1j}(\Psi_j) \mid v_{2j}(\Psi_j) \mid \dots \mid v_{nj}(\Psi_j)]$. Accordingly,

$$\begin{aligned}
x^T \Psi_j x &= z^T [T_{\Psi_j}^T \Psi_j T_{\Psi_j}]z \\
&\equiv z^T \Psi_j^D z
\end{aligned} \tag{3.24}$$

where $\Psi_j^D \equiv T_{\Psi_j}^T \Psi_j T_{\Psi_j} = \text{diag}[\lambda_{1j}(\Psi_j) \quad \lambda_{2j}(\Psi_j) \quad \dots \quad \lambda_{nj}(\Psi_j)]$. Applying (3.18 f),

we now obtain the diagonal matrix $\Psi_j^{D, \, 0+}$ from the diagonal matrix Ψ_j^D by setting all

negative diagonal elements of Ψ_j^D to zeros $\forall j$. Accordingly, we have that:

$$z^T [\Psi_j^{D, \, 0+}]z \geq 0 \tag{3.25}$$

$$z^T [\Psi_j^{D, 0+}]z \geq z^T \Psi_j^D z = x^T \Psi_j x \tag{3.26}$$

Now, we change the basis back to the original using (3.23):

$$\begin{aligned}
z^T [\Psi_j^{D, \, 0+}]z &= x^T [T_{\Psi_j}^{-1}]^T [\Psi_j^{D, \, 0+}][T_{\Psi_j}^{-1}]x \\
&= x^T T_{\Psi_j} [\Psi_j^{D, \, 0+}]T_{\Psi_j}^T x \\
&\equiv x^T \Psi_j^{0+} x \geq 0
\end{aligned} \tag{3.27}$$

where $\Psi_j^{0+} = T_{\Psi_j} [\Psi_j^{D, \, 0+}]T_{\Psi_j}^T$. We note in addition that:

$$T_{\Psi_j}^{-1} = T_{\Psi_j}^T \tag{3.28 a}$$

$$\Psi_j^{0+} = [\Psi_j^{0+}]^T \tag{3.28 b}$$

(Proof of Theorem 3.2 (Cont.))

To see that (3.28 a) is valid, we observe that $[\mathbf{T}_{\Psi_j}^T][\mathbf{T}_{\Psi_j}] = \mathbf{I}$ by (3.23). We need to show

further that $[\mathbf{T}_{\Psi_j}][\mathbf{T}_{\Psi_j}^T] = \mathbf{I}$. Assume that $[\mathbf{T}_{\Psi_j}][\mathbf{T}_{\Psi_j}^T] \neq \mathbf{I}$, it follows that

$[\mathbf{T}_{\Psi_j}^T][\mathbf{T}_{\Psi_j}][\mathbf{T}_{\Psi_j}^T] \neq [\mathbf{T}_{\Psi_j}^T] \Rightarrow \mathbf{I}[\mathbf{T}_{\Psi_j}^T] \neq [\mathbf{T}_{\Psi_j}^T] \Rightarrow [\mathbf{T}_{\Psi_j}^T] \neq [\mathbf{T}_{\Psi_j}^T]$. A contradiction arises

and we conclude that $[\mathbf{T}_{\Psi_j}][\mathbf{T}_{\Psi_j}^T] = \mathbf{I}$. To see that (3.28 b) is valid, we transpose both

sides of (3.28 b) to obtain $[\mathbf{\Psi}_j^{0+}]^T = [\mathbf{T}_{\Psi_j}[\mathbf{\Psi}_j^{D,\,0+}]\mathbf{T}_{\Psi_j}^T]^T = \mathbf{T}_{\Psi_j}[\mathbf{\Psi}_j^{D,\,0+}]^T \mathbf{T}_{\Psi_j}^T$

$= \mathbf{T}_{\Psi_j}[\mathbf{\Psi}_j^{D,\,0+}]\mathbf{T}_{\Psi_j}^T = \mathbf{\Psi}_j^{0+}$.

Because $(h_{uj} - h_{lj}) \geq l_j(\mathbf{x}) > 0$, it follows from (3.26) and (3.27) that:

$$l_j(\mathbf{x},t)[\mathbf{x}^T\mathbf{\Psi}_j\mathbf{x}] \leq l_j(\mathbf{x},t)[\mathbf{x}^T\mathbf{\Psi}_j^{0+}\mathbf{x}] \leq (h_{uj} - h_{lj})[\mathbf{x}^T\mathbf{\Psi}_j^{0+}\mathbf{x}] \ \forall \mathbf{x} \qquad (3.29)$$

Applying the inequality (3.29) to (3.22) yields the key result:

$$\dot{V}(\mathbf{x},t) = \frac{1}{2}\mathbf{x}^T\mathbf{\Phi}\mathbf{x} + \frac{1}{2}\sum_{j=1}^r l_j(\mathbf{x},t)\mathbf{x}^T\mathbf{\Psi}_j\mathbf{x} \leq \frac{1}{2}\mathbf{x}^T\mathbf{\Phi}\mathbf{x} + \frac{1}{2}\sum_{j=1}^r ((h_{uj} - h_{lj})[\mathbf{x}^T\mathbf{\Psi}_j^{0+}\mathbf{x}]) \quad (3.30)$$

Since $\mathbf{\Phi} = \mathbf{\Phi}^T$ and $\mathbf{\Psi}_j^{0+} = [\mathbf{\Psi}_j^{0+}]^T$, it follows from (3.30) that the following conditions

guarantees that $\dot{V}(\mathbf{x},t)$ is negative definite in regions where the structured uncertain

specifications hold:

$$\lambda_{\max}(\mathbf{\Phi}) < 0 \qquad (3.17\ \text{a})$$

$$\lambda_{\max}(\mathbf{Z}) < 0 \qquad (3.17\ \text{b})$$

where $\mathbf{Z} \equiv \mathbf{\Phi} + \sum_{j=1}^r ((h_{uj} - h_{lj})\mathbf{\Psi}_j^{0+}$, and $i = 1, 2, \ldots, n$. This completes the proof of

Theorem 3.2.

We note for Theorem 3.2 that:

1)   (3.17 b) implies (3.17 a) because $\sum_{j=1}^{r}((h_{uj} - h_{lj})\Psi_j^{0+})$ is either symmetric

positive semidefinite or symmetric positive definite. The condition (3.17 a) is

given explicitly because it can be checked easily and failure to satisfy (3.17 a)

implies that (3.17 b) can never be satisfied.

2)   Theorem 3.2 can handle both symmetric and asymmetric uncertainties, where the

uncertainties in $h_j(\mathbf{x})$ are "symmetric" when $h_j(\mathbf{x}) \in [h_{lj}, h_{uj}]$ and $h_{lj} = -h_{uj}$.

1)   If we can decrease $(h_{ui} - h_{li})$, then $(h_{uj} - h_{lj})$ $j \neq i$ can often be increased.

2)   Substituting a relationship among the upper bounds h_{uj} $j = 1, \ldots r$ into (3.17 b)

can often reduce conservatism of the resulting allowable uncertainty bounds.

These observations will be illustrated in Example 3.1 and 3.2. In Corollary 3.1, we point

out a special case in which the structured uncertainty is single-term:

Corollary 3.1   (Single-Term Structured Uncertainty Bound)

If the structured uncertainty in (3.7) is single-term ($r = 1$) or:

$$\mathbf{f}_\Omega(\mathbf{x}, t) = h(\mathbf{x}, t)\mathbf{E}\mathbf{x} \tag{3.31}$$

where $h(\mathbf{x}, t) \in [h_l, h_u] \in \mathfrak{R}$, and $\mathbf{E} \in \mathfrak{R}^{n \times n}$ then the time derivative of the quadratic

Lyapunov function (1.5) along trajectories of the structured uncertain system (3.7) is

negative definite in region Γ where the uncertainty specifications are valid if:

$$\lambda_{\max}(\mathbf{\Phi}) < 0 \tag{3.32 a}$$

$$\lambda_{\max}(\mathbf{\Phi} + (h_u - h_l)\mathbf{\Psi}) < 0 \tag{3.32 b}$$

where $\boldsymbol{\Phi} = \boldsymbol{\Phi}^T$ is determined from (3.18 c) using:

$$\overline{\mathbf{A}}_l \equiv \overline{\mathbf{A}}_n + h_l \mathbf{E} \tag{3.33 a}$$

$$\boldsymbol{\Psi} \equiv [\mathbf{PE} + \mathbf{E}^T \mathbf{P}] = \boldsymbol{\Psi}^T \tag{3.33 b}$$

Proof

The necessity of (3.32 a) follows directly from the proof of Theorem 3.1. Now we draw

from (3.30) that for this single-term structured uncertainty:

$$\dot{V}(\mathbf{x},t) = \frac{1}{2}\mathbf{x}^T \boldsymbol{\Phi}\mathbf{x} + \frac{1}{2}l(\mathbf{x},t)\mathbf{x}^T \boldsymbol{\Psi}\mathbf{x}$$

$$\equiv \frac{1}{2}\mathbf{x}^T \boldsymbol{\Phi}\mathbf{x} + \frac{1}{2}l(\mathbf{x},t)w(\mathbf{x}) \tag{3.34}$$

where $l(\mathbf{x},t) \in [0, h_u - h_l]$ is nonnegative, and $w(\mathbf{x}) \equiv \mathbf{x}^T \boldsymbol{\Psi}\mathbf{x}$. We assume that $\boldsymbol{\Psi} = \boldsymbol{\Psi}^T$

has at least one positive eigenvalue. Otherwise, $l(\mathbf{x})\mathbf{x}^T \boldsymbol{\Psi}\mathbf{x} \leq 0$ and (3.32 a) implies

(3.32 b), guaranteeing that $\dot{V}(\mathbf{x},t)$ is negative definite in Γ. Consider the regions

$R_{w \leq 0} \equiv \{\mathbf{x} \mid w(\mathbf{x}) \leq 0\}$ and $R_{w > 0} \equiv \{\mathbf{x} \mid w(\mathbf{x}) > 0\}$. We see that:

1) $R_{w \leq 0} \cap R_{w > 0} = \varnothing$ because $w(\mathbf{x})$ is a function and thus must have a single value at

     a given point.

2) $\Gamma \subseteq R_{w \leq 0} \cup R_{w > 0} = \mathfrak{R}^n$ because $w(\mathbf{x})$ is defined $\forall \mathbf{x}$.

We now examine $\dot{V}(\mathbf{x},t)$ in $R_{w \leq 0}$ and in $R_{w > 0}$:

1)   For a given point in $R_{w \leq 0}$, we see that $\dot{V}(\mathbf{x},t) = \frac{1}{2}\mathbf{x}^T \boldsymbol{\Phi}\mathbf{x} + \frac{1}{2}l(\mathbf{x},t)w(\mathbf{x})$ is negative

     definite provided that (3.32 a) is satisfied. This is because $l(\mathbf{x})w(\mathbf{x}) \leq 0$ in $R_{w \leq 0}$,

     and (3.32 a) implies that $\mathbf{x}^T \boldsymbol{\Phi}\mathbf{x}$ is globally negative definite.

2)   For a given point in $R_{w>0}$, we see that $l(\mathbf{x})w(\mathbf{x}) \le (h_u - h_l)w(\mathbf{x})$. This is because

$h_u - h_l > l(\mathbf{x},t) \ge 0$ and $w(\mathbf{x}) \equiv \mathbf{x}^T \mathbf{\Psi} \mathbf{x} > 0$ in $R_{w>0}$. Accordingly, we see that in

$R_{w>0}$:

$$\dot{V}(\mathbf{x},t) = \frac{1}{2}\mathbf{x}^T \mathbf{\Phi}\mathbf{x} + \frac{1}{2}l(\mathbf{x},t)\mathbf{x}^T \mathbf{\Psi}\mathbf{x} \le \frac{1}{2}\mathbf{x}^T \mathbf{\Phi}\mathbf{x} + \frac{1}{2}(h_u - h_l)\mathbf{x}^T \mathbf{\Psi}\mathbf{x} \qquad (3.35)$$

Thus, satisfying (3.32 b) guarantees that $\dot{V}(\mathbf{x},t)$ is negative definite in $R_{w>0}$. Since

$\dot{V}(\mathbf{x},t)$ is negative definite in $R_{w\le0}$ when (3.32 a) is satisfied, it follows that satisfying

both (3.32 a) and (3.32 b) guarantees that $\dot{V}(\mathbf{x},t)$ is negative definite in $R_{w\le0}$ and in

$R_{w>0}$. This implies that $\dot{V}(\mathbf{x},t)$ is negative definite in Γ and completes the proof.

For single-term structured uncertainties, we note that (3.32 b) does not imply (3.32 a)

because the quadratic function $(h_u - h_l)\mathbf{x}^T \mathbf{\Psi}\mathbf{x}$ may be negative at infinitely many points.

Accordingly, both (3.32 a) and (3.32 b) must be satisfied to guarantee stability of (3.7)

under the single-term structured uncertainty. The bound obtained for single-term

structured uncertainties using Corollary 3.1 is equally or less conservative than that from

Theorem 3.1 because:

$$\dot{V}(\mathbf{x}) = \frac{1}{2}\mathbf{x}^T \mathbf{\Phi}\mathbf{x} + \frac{1}{2}l(\mathbf{x})\mathbf{x}^T \mathbf{\Psi}\mathbf{x} \le \frac{1}{2}\mathbf{x}^T \mathbf{\Phi}\mathbf{x} + \frac{1}{2}(h_u - h_l)\mathbf{x}^T \mathbf{\Psi}\mathbf{x} \le \frac{1}{2}(h_u - h_l)\mathbf{x}^T \mathbf{\Psi}^{0+}\mathbf{x} \quad (3.36)$$

We now show that our bounds for quadratic functions employed in Theorem 3.2 are

equally or less conservative than those derived from the spectral-norm:

Lemma 3.1   (Reduced Conservatism of Structured Uncertainty Bounds)

The following inequality holds for all $\mathbf{\Psi}_j = \mathbf{\Psi}_j^T \in \mathfrak{R}^{n \times n}$:

$$\mathbf{x}^T \mathbf{\Psi}_j \mathbf{x} \le \mathbf{x}^T \mathbf{\Psi}_j^{0+} \mathbf{x} \le \mathbf{x}^T \left\| \mathbf{\Psi}_j \right\| \mathbf{x} \tag{3.37}$$

where $\mathbf{\Psi}_j$ is determined from (3.18 d), $\mathbf{\Psi}_j^{0+}$ from (3.18 f) and $\mathbf{x}^T \mathbf{\Psi}_j^{0+} \mathbf{x} \ge 0$.

proof

Since $\mathbf{\Psi}_j = \mathbf{\Psi}_j^T \in \mathfrak{R}^{n \times n}$, we have that (Lancaster, 1969):

$$\left\| \mathbf{\Psi}_j \right\| = \max_{i=1,\dots,n} (\lambda_i^{1/2}(\mathbf{\Psi}_j^T \mathbf{\Psi}_j)) = \max_{i=1,\dots,n} (\lambda_i^{1/2}(\mathbf{\Psi}_j^2)) = \max_{i=1,\dots,n} (\mid \lambda_i(\mathbf{\Psi}_j) \mid) \tag{3.38}$$

where $\mid \lambda_i(\mathbf{\Psi}_j) \mid$ denotes the absolute value of $\lambda_i(\mathbf{\Psi}_j)$. Accordingly, we have:

$$\mathbf{x}^T \left\| \mathbf{\Psi}_j \right\| \mathbf{x} = (\max_{i=1,\dots,n} \mid \lambda_i(\mathbf{\Psi}_j) \mid) [\mathbf{x}^T \mathbf{x}] \tag{3.39}$$

Now, recall the steps in the proof of Theorem 3.1. In the proof, we reduce $\mathbf{x}^T \mathbf{\Psi}_j \mathbf{x}$ to the

principal axes using the linear transformation $\mathbf{x} = \mathbf{T}_{\mathbf{\Psi}_j} \mathbf{z}$ in (3.23), and proceed from (3.24)

to (3.26). For convenience, we reproduce (3.26) from the proof of Theorem 3.1:

$$\mathbf{z}^T [\mathbf{\Psi}_j^{D, 0+}] \mathbf{z} \ge \mathbf{z}^T \mathbf{\Psi}_j^D \mathbf{z} = \mathbf{x}^T \mathbf{\Psi}_j \mathbf{x} \tag{3.26}$$

where $\mathbf{\Psi}_j^D$ is a diagonal matrix whose n diagonal elements are $\lambda_i(\mathbf{\Psi}_j)$, $i = 1, \dots, n$, and

$\mathbf{\Psi}_j^{D, 0+}$ is a diagonal matrix obtained from (3.18 f) by replacing all negative elements

along the diagonal of $\mathbf{\Psi}_j^D$ by zeros. Accordingly, all the nonzero diagonal elements of the

diagonal matrix $\mathbf{\Psi}_j^{D, 0+}$ are positive eigenvalues of $\mathbf{\Psi}_j$. We denote these positive

eigenvalues of $\mathbf{\Psi}_j$ by $\lambda_i^+(\mathbf{\Psi}_j)$ for some $i \in \{1, 2, \dots, n\}$. Now, we change the basis of

$\mathbf{z}^T [\mathbf{\Psi}_j^{D,\,0+}] \mathbf{z}$ in (3.26) back to the original basis to produces (3.27). We recall from the proof of Theorem 3.2 that:

$$\mathbf{z}^T [\mathbf{\Psi}_j^{D,\,0+}] \mathbf{z} = \mathbf{x}^T \mathbf{\Psi}_j^{\,0+} \mathbf{x} \geq 0 \tag{3.27}$$

where $\mathbf{\Psi}_j^{\,0+} = \mathbf{T}_{\mathbf{\Psi}_j} [\mathbf{\Psi}_j^{D,\,0+}] \mathbf{T}_{\mathbf{\Psi}_j}^T$. Substituting $\mathbf{x}^T \mathbf{\Psi}_j^{\,0+} \mathbf{x}$ for $\mathbf{z}^T [\mathbf{\Psi}_j^{D,\,0+}] \mathbf{z}$ in (3.26) yields:

$$\mathbf{x}^T \mathbf{\Psi}_j^{\,0+} \mathbf{x} \geq \mathbf{x}^T \mathbf{\Psi}_j \mathbf{x} \tag{3.40}$$

This completes the first part of the proof. Now, we substitute $\mathbf{T}_{\mathbf{\Psi}_j} \mathbf{z}$ for $\mathbf{x}$ in (3.39) to produce:

$$
\begin{aligned}
\mathbf{x}^T \left\| \mathbf{\Psi}_j \right\| \mathbf{x} &= (\max_{i=1,\dots,n} |\lambda_i(\mathbf{\Psi}_j)|)[\mathbf{x}^T \mathbf{x}] \\
&= (\max_{i=1,\dots,n} |\lambda_i(\mathbf{\Psi}_j)|)[\mathbf{z}^T [\mathbf{T}_{\mathbf{\Psi}_j}^T][\mathbf{T}_{\mathbf{\Psi}_j}]\mathbf{z}] \\
&= (\max_{i=1,\dots,n} |\lambda_i(\mathbf{\Psi}_j)|)[\mathbf{z}^T \mathbf{I}\, \mathbf{z}] \\
&= \mathbf{z}^T \mathrm{diag}[\max_{i=1,\dots,n} |\lambda_i(\mathbf{\Psi}_j)|, \quad \dots, \quad \max_{i=1,\dots,n} |\lambda_i(\mathbf{\Psi}_j)|]\,\mathbf{z}
\end{aligned}
\tag{3.41}
$$

From (3.31) and the construction of $\mathbf{\Psi}_j^{D,\,0+}$, we see that:

$$\mathbf{x}^T \left\| \mathbf{\Psi}_j \right\| \mathbf{x} = \mathbf{z}^T \mathrm{diag}[\max_{i=1,\dots,n} |\lambda_i(\mathbf{\Psi}_j)|, \quad \dots, \quad \max_{i=1,\dots,n} |\lambda_i(\mathbf{\Psi}_j)|]\,\mathbf{z} \geq \mathbf{z}^T [\mathbf{\Psi}_j^{D,\,0+}]\mathbf{z} \tag{3.42}$$

Since $\mathbf{z}^T [\mathbf{\Psi}_j^{D,\,0+}]\mathbf{z} = \mathbf{x}^T \mathbf{\Psi}_j^{\,0+} \mathbf{x}$, we have shown that:

$$\mathbf{x}^T \mathbf{\Psi}_j \mathbf{x} \leq \mathbf{x}^T \mathbf{\Psi}_j^{\,0+} \mathbf{x} \leq \mathbf{x}^T \left\| \mathbf{\Psi}_j \right\| \mathbf{x}$$

This completes the proof.

To compare the bounds resulting from Theorem 3.2 to the existing ones, we now employ two common examples employed in several references. Example 3.1 is given as a review of Theorem 3.2 while we proceed quickly in Example 3.2.

Example 3.1   (A Second-Order Uncertain System)

We consider a system drawn from (Vedavalli, 1985), (Vedavalli, and Liang, 1986), (Zhou, and Khargonekar, 1987):

$$\dot{\mathbf{x}} = \overline{\mathbf{A}}_n \mathbf{x} + h(\mathbf{x})\mathbf{E}\mathbf{x} \qquad \text{(E 3.1.1)}$$

where $\mathbf{x} = [x_1 \quad x_2]^T$, $\overline{\mathbf{A}}_n = \begin{bmatrix} -3 & -2 \\ 1 & 0 \end{bmatrix}$ is a stable matrix, $\mathbf{E} = \begin{bmatrix} -1 & 1 \\ 0 & 0 \end{bmatrix}$, the uncertain function $h(\mathbf{x}) \in [h_l, h_u] \in \Re$, and $h_l < h_u$. We see that the uncertainty is single-term and thus we may apply either Corollary 3.1 or Theorem 3.2. However, it can be shown that these produce the same conclusions <u>for this particular example</u>. Since Theorem 3.2 is more complicated to apply, we illustrate this in detail.

It can be shown that the eigenvalues of $\overline{\mathbf{A}}_n$ are $\lambda_1 = -2$ and $\lambda_2 = -1$ indicating stability of the nominal linear model $\dot{\mathbf{x}} = \overline{\mathbf{A}}_n \mathbf{x}$. Because $\overline{\mathbf{A}}_n$ is stable, we know by Lyapunov stability the existence of symmetric positive definite matrices $\mathbf{Q}$ and $\mathbf{P}$ satisfying the Lyapunov equation (3.18 a). For this example, we choose $\mathbf{Q} = \mathbf{I}$ for simplicity. This produces:

$$\mathbf{P} = \begin{bmatrix} 0.5 & 0.5 \\ 0.5 & 2.5 \end{bmatrix} \qquad \text{(E 3.1.2)}$$

In practice, we usually know h_l and h_u when the model is constructed. <u>In this example, we assume that the objective is to find h_l and h_u such that the system is globally stable for any</u> $h(\mathbf{x}) \in [h_l, h_u]$. Clearly, we desire that $h_u - h_l$ is as large as possible. Now, we write:

$$\begin{aligned} h(\mathbf{x}) &= h_l + h(\mathbf{x}) - h_l \\ &\equiv h_l + l(\mathbf{x}) \end{aligned} \qquad \text{(E 3.1.3)}$$

where

$$l(\mathbf{x}) \equiv h(\mathbf{x}) - h_l \qquad\qquad \text{E 3.1.4)}$$

Since $h(\mathbf{x}) \in [h_l, h_u]$, it follows from (E 3.1.4) that $l(\mathbf{x}) \in [0, h_u - h_l]$. Substituting

$h_l + l(\mathbf{x})$ for $h(\mathbf{x})$ in (E 3.1.1) yields:

$$
\begin{aligned}
\dot{\mathbf{x}} &= \overline{\mathbf{A}}_n \mathbf{x} + h_l \mathbf{E}\mathbf{x} + l(\mathbf{x})\mathbf{E}\mathbf{x} \\
&= \begin{bmatrix} -3 & -2 \\ 1 & 0 \end{bmatrix} \mathbf{x} + h_l \begin{bmatrix} -1 & 1 \\ 0 & 0 \end{bmatrix} \mathbf{x} + l(\mathbf{x})\mathbf{E}\mathbf{x} \\
&= \overline{\mathbf{A}}_l \mathbf{x} + l(\mathbf{x})\mathbf{E}\mathbf{x}
\end{aligned}
\qquad \text{(E 3.1.5)}
$$

where we employ (3.18 b):

$$\overline{\mathbf{A}}_l = \overline{\mathbf{A}}_n + h_l \mathbf{E} = \begin{bmatrix} -3 & -2 \\ 1 & 0 \end{bmatrix} + h_l \begin{bmatrix} -1 & 1 \\ 0 & 0 \end{bmatrix} \qquad \text{(E 3.1.6)}$$

To examine effects of uncertainties, consider the time derivative of the quadratic

Lyapunov function along trajectories of the uncertain system (E 3.1.5):

$$
\begin{aligned}
\dot{V}(\mathbf{x}) &= \frac{1}{2}\mathbf{x}^T [\mathbf{P}\overline{\mathbf{A}}_l + \overline{\mathbf{A}}_l^T \mathbf{P}]\mathbf{x} + \frac{1}{2}l(\mathbf{x})\mathbf{x}^T [\mathbf{P}\mathbf{E} + \mathbf{E}^T \mathbf{P}]\mathbf{x} \\
&= \frac{1}{2}\mathbf{x}^T \mathbf{\Phi}\mathbf{x} + \frac{1}{2}l(\mathbf{x})\mathbf{x}^T \mathbf{\Psi}\mathbf{x}
\end{aligned}
\qquad \text{(E 3.1.7)}
$$

where $\mathbf{Q} = \mathbf{I}$ and $\mathbf{P}$ is given by (E 3.1.2), $\mathbf{\Phi} = [\mathbf{P}\overline{\mathbf{A}}_l + \overline{\mathbf{A}}_l^T \mathbf{P}]$ by (3.18 c), and

$\mathbf{\Psi} = [\mathbf{P}\mathbf{E} + \mathbf{E}^T \mathbf{P}]$ by (3.18 d). Since $\dot{V}(\mathbf{x}) = \frac{1}{2}\mathbf{x}^T \mathbf{\Phi}\mathbf{x}$ when $l(\mathbf{x}) = 0$, a necessary condition

for $\dot{V}(\mathbf{x})$ to be negative definite is that $\mathbf{\Phi}$ be negative definite as in (3.17 a). To examine

this, we notice from (E 3.1.6) that $\overline{\mathbf{A}}_l \big|_{h_l=0} = \overline{\mathbf{A}}_n$ and it follows from the Lyapunov

equation (3.18 a) that $\lambda_i(\mathbf{\Phi}\big|_{h_l=0}) < 0$ $i = 1,2$. Thus, we gradually vary h_l from zero and

examine the sign of $\lambda_{\max}(\mathbf{\Phi})$ to find the largest magnitude of the allowable lower bound

of the structured uncertainty for which $\mathbf{\Phi}$ remains negative definite. In this example, we

decrease h_l from zero to negative values although the opposite is possible. This is because

we want to compare our result to those from the references in which h_l is negative. Under

the particular pair of $\mathbf{Q} = \mathbf{I}$ and $\mathbf{P}$ in (E 3.1.2), we have that $\lambda_i(\overline{\mathbf{A}}_l \mid_{-2 < h_l \leq 0}) < 0$ $\forall i$ and:

$$\Phi\mid_{h_l = -2^+} = \begin{bmatrix} 0^- & 0 \\ 0 & -4^+ \end{bmatrix} \qquad (E\ 3.1.8)$$

where $c^- = c - \varepsilon$, $c^+ = c + \varepsilon$, $c \in \Re$, and $\varepsilon \in \Re^+$ is infinitesimally small. This shows that

Φ is negative definite under such pair of $\mathbf{Q}$ and $\mathbf{P}$ when $0 \geq h_l > -2$. Next, we want to

find the largest value for h_u such that (3.17 b) is satisfied. We employ (3.18 d) to obtain:

$$\Psi = \begin{bmatrix} -1 & 0 \\ 0 & 1 \end{bmatrix} \qquad (E\ 3.1.9)$$

The matrix Ψ is diagonal but this cannot be expected in general. To illustrate the step

involving (3.18 e) in Theorem 3.2, we execute a reduction to principal axes although this

is not required for this particular problem. Since $\Psi = \Psi^T$, Ψ has a set of n orthonormal

eigenvectors $\{\mathbf{v}_1(\Psi) \ \dots \ \mathbf{v}_n(\Psi)\}$ (Hagan et al, 1996). In this example, $n = 2$ and we

reduce $\mathbf{x}^T\Psi\mathbf{x}$ to the principal axes by using the linear transformation:

$$\mathbf{x} = \mathbf{T}_\Psi \mathbf{z} = [\mathbf{v}_1(\Psi) \quad \mathbf{v}_2(\Psi)]\mathbf{z} = \begin{bmatrix} 0 & 1 \\ 1 & 0 \end{bmatrix} \mathbf{z} \qquad (E\ 3.1.10)$$

where $\mathbf{T}_\Psi = [\mathbf{v}_1(\Psi) \quad \mathbf{v}_2(\Psi)]$, $\mathbf{v}_1(\Psi) = [0 \ \ 1]^T$ and $\mathbf{v}_2(\Psi) = [1 \ \ 0]^T$. Accordingly,

$$\begin{aligned} \mathbf{x}^T\Psi\mathbf{x} &= \mathbf{z}^T [\mathbf{T}_\Psi^T \Psi \mathbf{T}_\Psi]\mathbf{z} \\ &\equiv \mathbf{z}^T \Psi^D \mathbf{z} \end{aligned} \qquad (E\ 3.1.11)$$

where Ψ^D is determined from (3.18 e):

$$\Psi^D = T_\Psi^T \Psi T_\Psi$$

$$= \text{diag}[\lambda_1(\Psi) \quad \ldots \quad \lambda_n(\Psi)] \qquad \text{(E 3.1.12)}$$

$$= \begin{bmatrix} 1 & 0 \\ 0 & -1 \end{bmatrix}$$

Applying (3.18 f), we now obtain the diagonal matrix $\Psi^{D,0+}$ from the diagonal matrix Ψ^D by setting negative diagonal elements of Ψ^D to zero:

$$\Psi^{D,0+} = \Psi^D \Big|_{[\Psi^D(i,i)<0]\to[\Psi^D(i,i)=0]} = \begin{bmatrix} 1 & 0 \\ 0 & 0 \end{bmatrix} \qquad \text{(E 3.1.13)}$$

Accordingly, we have that:

$$\mathbf{z}^T[\Psi^{D,0+}]\mathbf{z} \geq 0 \qquad \text{(E 3.1.14 a)}$$

$$\mathbf{z}^T[\Psi^{D,0+}]\mathbf{z} \geq \mathbf{z}^T\Psi^D\mathbf{z} = \mathbf{x}^T\Psi\mathbf{x} \qquad \text{(E 3.1.14 b)}$$

Now, we change the basis to the original using (E 3.1.10):

$$\mathbf{z}^T[\Psi^{D,0+}]\mathbf{z} = \mathbf{x}^T[T_\Psi^{-1}]^T[\Psi^{D,0+}][T_\Psi^{-1}]\mathbf{x}$$

$$= \mathbf{x}^T T_\Psi[\Psi^{D,0+}]T_\Psi^T\mathbf{x} \qquad \text{(E 3.1.15)}$$

$$\equiv \mathbf{x}^T\Psi^{0+}\mathbf{x}$$

where

$$\Psi^{0+} = T_\Psi[\Psi^{D,0+}]T_\Psi^T = \begin{bmatrix} 0 & 0 \\ 0 & 1 \end{bmatrix} \qquad \text{(E 3.1.16 a)}$$

$$T_\Psi^{-1} = T_\Psi^T \qquad \text{(E 3.1.16 b)}$$

Because $(h_u - h_l) \geq l(\mathbf{x}) > 0$, it follows from (E 3.1.14) and (E 3.1.15) that:

$$l(\mathbf{x})[\mathbf{x}^T\Psi\mathbf{x}] \leq l(\mathbf{x})[\mathbf{x}^T\Psi^{0+}\mathbf{x}] \leq [h_u - h_l][\mathbf{x}^T\Psi^{0+}\mathbf{x}] \quad \forall \mathbf{x} \qquad \text{(E 3.1.17)}$$

Applying the inequality in (E 3.1.17) to (E 3.1.7) yields the key result:

$$\dot{V}(\mathbf{x}) = \frac{1}{2}\mathbf{x}^T\Phi\mathbf{x} + \frac{1}{2}l(\mathbf{x})[\mathbf{x}^T\Psi\mathbf{x}] \leq \frac{1}{2}\mathbf{x}^T\Phi\mathbf{x} + \frac{1}{2}[h_u - h_l][\mathbf{x}^T\Psi^{0+}\mathbf{x}] \quad \forall \mathbf{x} \quad \text{(E 3.1.18)}$$

Now we recall from the proof of Theorem 3.2 that $\mathbf{\Phi} = \mathbf{\Phi}^T$ and $\mathbf{\Psi}^{0+} = [\mathbf{\Psi}^{0+}]^T$. It follows

from (E 3.1.18) that the following conditions guarantees that $\dot{V}(\mathbf{x})$ is negative definite:

$$\lambda_i(\mathbf{\Phi}) < 0 \qquad\qquad (3.17\text{ a})$$

$$\lambda_i(\mathbf{\Phi} + (h_u - h_l)\mathbf{\Psi}^{0+}) < 0 \qquad\qquad (3.17\text{ b})$$

where $i = 1, 2$. To find the upper bound h_u of $h(\mathbf{x})$, we determine the largest value of

$(h_u - h_l)\big|_{h_l = -2^+} \in \mathfrak{R}^+$ such that (3.17 b) holds. For convenience, we let

$(h_u - h_l)\big|_{h_l = -2^+} \equiv c \in \mathfrak{R}^+$ and invoke (3.17 b):

$$\lambda_i\left(\begin{bmatrix} 0^- & 0 \\ 0 & -4^+ \end{bmatrix} + c\begin{bmatrix} 0 & 0 \\ 0 & 1 \end{bmatrix}\right) < 0 \qquad\qquad (\text{E }3.1.19)$$

For this example with the particular choices of $\mathbf{Q}$ and $\mathbf{P}$, both $\mathbf{\Phi}$ and $\mathbf{\Psi}^{0+}$ are diagonal.

Thus, it is clear that (E 3.1.19) holds when $0 < c < 4$. Since (3.17 a) holds when

$-2 < h_l \le 0$ and (3.17 b) holds when $0 < c = (h_u - h_l)\big|_{h_l = -2^+} < 4^-$, it follows that $\dot{V}(\mathbf{x})$ is

globally negative definite when:

$$h(\mathbf{x}) \in (-2, 2) \qquad\qquad (\text{E }3.1.20)$$

where we choose $h_l = -2^+$ and $h_u = 2^-$. The bound (E 3.1.20) is the same as that from

(Zhou, and Khargonekar, 1987), which is the largest bound we found in the literature for

this particular problem. In general, we need to tune the initial $\mathbf{Q}$ to demonstrate a large

allowable uncertainty bound. However, this example is a special case where the simple

initial choice of $\mathbf{Q} = \mathbf{I}$ works well. It can be shown numerically that an inappropriate

choice of $\mathbf{Q}$ can lead to a very conservative allowable uncertainty bound. Note that when

the uncertain function $h(\mathbf{x})$ is fixed at extreme values, we have:

1)   When $h(\mathbf{x}) = -1.9999$, the eigenvalues of $[\overline{\mathbf{A}}_n - 1.9999\mathbf{E}]$ are

$\lambda_{1,2} = -0.5 \pm j1.9365$.

2)   When $h(\mathbf{x}) = 1.9999$, the eigenvalues of $[\overline{\mathbf{A}}_n + 1.9999\mathbf{E}]$ are at $\lambda_1 = -4.9999$ and

$\lambda_2 = -0.00002$.

Given a set of uncertainty specifications, trading off among these specifications may be

possible. In this particular example, decreasing the upper bound h_u yields a less

conservative lower bound h_l. Indeed, it can be shown by using Corollary 3.1 that the

system is stable when $h(\mathbf{x}) \in [-2.6, 1.1]$ using $\mathbf{Q} = \begin{bmatrix} 40 & -9 \\ -9 & 9 \end{bmatrix}$. These uncertainty

specifications and this choice of $\mathbf{Q}$ produce $\max(\lambda(\mathbf{Z})) = -0.415 < 0$ and

$\lambda_{\max}(\mathbf{\Phi}) = -0.9243 < 0$, implying that h_u can be greater than 1.1 and/or h_l can be less

than –2.6. However, we do not pursue this further because the present result is sufficient

to demonstrate the trade off between the allowable upper bound and the allowable lower

bound. For this choice of $\mathbf{Q}$ and these new uncertainty specification, we note that

Theorem 3.2 cannot be employed to demonstrate stability of the system because (3.17) is

not satisfied. The shows that the bound resulting from Corollary 3.1 is less conservative

than that resulting from Theorem 3.2 as pointed out at after the proof of Corollary 3.1.

When the uncertain function $h(\mathbf{x})$ is fixed at the new extreme values, we have:

1)   When $h(\mathbf{x}) = -2.6$, the eigenvalues of $[\overline{\mathbf{A}}_n - 2.6\mathbf{E}]$ are $\lambda_{1,2} = -0.2 \pm j2.1354$.

3)   When $h(\mathbf{x}) = 1.1$, the eigenvalues of $[\overline{\mathbf{A}}_n + 1.1\mathbf{E}]$ are $\lambda_1 = -3.8673$ and

$\lambda_2 = -0.2327$.

Example 3.2 (A Third-Order Uncertain System)

Consider the uncertain system from (Zhou, and Khargonekar, 1987), (Lee et al, 1996),

(Olas, and Ahmadkhanlou, 1994):

$$\dot{\mathbf{x}} = \begin{bmatrix} -2 & 0 & -1 \\ 0 & -3 & 0 \\ -1 & -1 & 4 \end{bmatrix} \mathbf{x} + \begin{bmatrix} h_1(\mathbf{x}) & 0 & h_1(\mathbf{x}) \\ 0 & h_2(\mathbf{x}) & 0 \\ h_1(\mathbf{x}) & h_2(\mathbf{x}) & h_1(\mathbf{x}) \end{bmatrix} \mathbf{x}$$

$$= \begin{bmatrix} -2 & 0 & -1 \\ 0 & -3 & 0 \\ -1 & -1 & 4 \end{bmatrix} \mathbf{x} + h_1(\mathbf{x}) \begin{bmatrix} 1 & 0 & 1 \\ 0 & 0 & 0 \\ 1 & 0 & 1 \end{bmatrix} \mathbf{x} + h_2(\mathbf{x}) \begin{bmatrix} 0 & 0 & 0 \\ 0 & 1 & 0 \\ 0 & 1 & 0 \end{bmatrix} \mathbf{x} \qquad (\text{E } 3.2.1)$$

$$= \overline{\mathbf{A}}_n \mathbf{x} + \sum_{j=1}^{2} [h_j(\mathbf{x}) \mathbf{E}_j \mathbf{x}]$$

where $\overline{\mathbf{A}}_n = \begin{bmatrix} -2 & 0 & -1 \\ 0 & -3 & 0 \\ -1 & -1 & 4 \end{bmatrix}$ is a stable matrix, $\mathbf{E}_1 = \begin{bmatrix} 1 & 0 & 1 \\ 0 & 0 & 0 \\ 1 & 0 & 1 \end{bmatrix}$, and $\mathbf{E}_2 = \begin{bmatrix} 0 & 0 & 0 \\ 0 & 1 & 0 \\ 0 & 1 & 0 \end{bmatrix}$.

The objective is to find the upper bounds h_{uj} and lower bounds h_{lj} of $h_j(\mathbf{x})$, $j = 1,\ 2$ for

which the system remains stable. Because this example originally appears in (Zhou, and

Khargonekar, 1987), we follow (Zhou, and Khargonekar, 1987) to restrict that h_{lj} are

negative and h_{uj} are positive although this is not required for Theorem 3.2. According to

this reference, stability of (E 3.2.1) is guaranteed if one of the following conditions are

satisfied:

$$h_1^2(\mathbf{x}) + h_2^2(\mathbf{x}) < 0.8158 \qquad (\text{E } 3.2.2 \text{ a})$$

$$0.6052 |h_1(\mathbf{x})| + 0.3512 |h_2(\mathbf{x})| < 1 \qquad (\text{E } 3.2.2 \text{ b})$$

$$|h_j(\mathbf{x})| < 1.5532,\ j = 1, 2 \qquad (\text{E } 3.2.2 \text{ c})$$

By direct computation, it can be shown that (E 3.2.2) does not include the case in which:

$$h_1(\mathbf{x}) \in [-3 * 10^5, 1.74] \qquad (\text{E } 3.2.3 \text{ a})$$

$$h_2(\mathbf{x}) \in [-6*10^5,\ 2.99] \qquad\qquad \text{(E 3.2.3 b)}$$

where the bounds in (E 3.2.3) are obtained by using the univariate optimization technique,

which will be discussed in detail when we generate LAR controllers for uncertain

nonlinear systems. Note that Theorem 3.2 accepts both symmetric and asymmetric

uncertainties. Uncertainties in $h_j(\mathbf{x}) \in [h_{lj},\ h_{uj}]$ are called "symmetric" if $-h_{lj} = h_{uj}$, and

"asymmetric" otherwise. Using Theorem 3.2, we want to show that (E 3.2.1) is stable

$\forall h_j(\mathbf{x})$ satisfying (E 3.2.3). To show this, we choose:

$$\mathbf{Q} = \begin{bmatrix} 0.2511 & 0.0175 & 0.0784 \\ 0.0175 & 2.2850*10^6 & 0.0093 \\ 0.0784 & 0.0093 & 0.5202 \end{bmatrix} \qquad\qquad \text{(E 3.2.4)}$$

This choice of $\mathbf{Q}$ is obtained by using the univariate optimization technique. Starting from

$\mathbf{Q} = \begin{bmatrix} 1 & 0.1 & 0.1 \\ 0.1 & 1 & 0.1 \\ 0.1 & 0.1 & 1 \end{bmatrix}$, the univariate technique takes less than 1 minute on our computer to

produce (E 3.2.4). The initial value for $\mathbf{Q}$ was arbitrarily selected. Other choices of initial

value may or may not produce the same result. We now follow the procedure listed in

Theorem 3.2:

1)   Following (3.18 a), we obtain:

$$\mathbf{P} = \begin{bmatrix} 0.1350 & 0.0145 & -0.0188 \\ 0.0145 & 7.6167*10^5 & -0.0187 \\ -0.0188 & -0.0187 & 0.1348 \end{bmatrix} \qquad\qquad \text{(E 3.2.5)}$$

2)   Following (3.18 b), we obtain:

$$\overline{\mathbf{A}}_l = \begin{bmatrix} -2 & 0 & -1 \\ 0 & -3 & 0 \\ -1 & -1 & 4 \end{bmatrix} - 3*10^5 \begin{bmatrix} 1 & 0 & 1 \\ 0 & 0 & 0 \\ 1 & 0 & 1 \end{bmatrix} - 6*10^5 \begin{bmatrix} 0 & 0 & 0 \\ 0 & 1 & 0 \\ 0 & 1 & 0 \end{bmatrix}$$

(E 3.2.6)

$$= \begin{bmatrix} -300002 & 0 & -300001 \\ 0 & -600003 & 0 \\ -300001 & -600001 & -300004 \end{bmatrix}$$

3)   Following (3.18 c), we obtain:

$$\mathbf{\Phi} = \begin{bmatrix} -6.9685*10^4 & 3.8437*10^3 & -6.9623*10^4 \\ 3.8437*10^3 & -9.1400*10^{11} & -6.8404*10^4 \\ -6.9623*10^4 & -6.8404*10^4 & -6.9562*10^4 \end{bmatrix}$$

(E 3.2.7)

Note that (3.18 a) is satisfied because the eigenvalues of $\mathbf{\Phi}$ are $\lambda_1 = -0.585$,

$\lambda_2 = -1.3925*10^5$, and $\lambda_3 = -9.1400*10^{11}$. Since $\mathbf{\Phi} = \mathbf{\Phi}^T \in \mathfrak{R}^{n \times n}$, this implies

that $\mathbf{\Phi}$ is negative definite.

4)   Following (3.18 d), we obtain:

$$\mathbf{\Psi}_1 = \begin{bmatrix} 0.2323 & -4.1678*10^{-3} & 0.2321 \\ -4.1678*10^{-3} & 0 & -4.1678*10^{-3} \\ 0.2321 & -4.1678*10^{-3} & 0.2319 \end{bmatrix}$$

(E 3.2.8 a)

$$\mathbf{\Psi}_2 = \begin{bmatrix} 0 & -4.3223*10^{-3} & 0 \\ -4.3223*10^{-3} & 1.5233*10^6 & 0.1161 \\ 0 & 0.1161 & 0 \end{bmatrix}$$

(E 3.2.8 b)

5)   Following (3.18 e), we obtain:

$$\mathbf{T}_{\mathbf{\Psi}_1} = \begin{bmatrix} -0.7074 & 0.7067 & -0.0156 \\ 0.0127 & 0.0347 & 0.9993 \\ -0.7067 & -0.7067 & 0.0335 \end{bmatrix}$$

(E 3.2.9 a)

$$\mathbf{T_{\Psi_2}} = \begin{bmatrix} 0.9993 & 0 & -0.0372 \\ 0 & -1 & 0 \\ 0.0372 & 0 & 0.9993 \end{bmatrix}$$ (E 3.2.9 b)

$$\mathbf{\Psi}_1^D = \text{diag}[0.4642 \quad 0 \quad -7.493*10^{-5}]$$ (E 3.2.9 c)

$$\mathbf{\Psi}_2^D = \text{diag}[0 \quad 1.5233*10^6 \quad -1*10^{-8}]$$ (E 3.2.9 d)

6)   Following (3.18 f), we obtain:

$$\mathbf{\Psi}_1^{D,0+} = \text{diag}[0.4642 \quad 0 \quad 0]$$ (E 3.2.10 a)

$$\mathbf{\Psi}_2^{D,0+} = \text{diag}[0 \quad 1.5233*10^6 \quad 0]$$ (E 3.2.10 b)

7)   Following (3.18 g), we obtain:

$$\mathbf{\Psi}_1^{0+} = \begin{bmatrix} 0.2323 & -4.1690*10^{-3} & 0.2321 \\ -4.1690*10^{-3} & 7.4824*10^{-5} & -4.1653*10^{-3} \\ 0.2321 & -4.1653*10^{-3} & 0.2319 \end{bmatrix}$$ (E 3.2.11 a)

$$\mathbf{\Psi}_2^{0+} = \begin{bmatrix} 1.2264*10^{-11} & -4.3223*10^{-3} & -3.294*10^{-10} \\ -4.3223*10^{-3} & 1.5233*10^6 & 0.1161 \\ -3.294*10^{-10} & 0.1161 & 8.847*10^{-9} \end{bmatrix}$$ (E 3.2.11 b)

8)   Following (3.18 h), we obtain:

$$\mathbf{Z} \equiv \mathbf{\Phi} + \sum_{j=1}^{2}[(h_{uj} - h_{lj})\mathbf{\Psi}_i^{0+}] = \begin{bmatrix} -9.2578*10^{-2} & -0.4049 & 0.2351 \\ -0.4049 & -1.5211*10^4 & 1.0745 \\ 0.2351 & 1.0745 & -0.6064 \end{bmatrix}$$ (E 3.2.12 a)

It can be shown that the eigenvalues of $\mathbf{Z}$ are $\lambda_1 = -1.2499*10^{-3}$, $\lambda_2 = -0.6976$, and

$\lambda_3 = -1.5211*10^4$ showing that (3.17 b) is satisfied. Since (3.11 a) and (3.11 b) are

satisfied, we conclude that the system is stable when the uncertain functions $h_j(\mathbf{x})$ are

within the bounds given in (E 3.2.3) $\forall j$. Now, we notice that

$\lambda_{\max}(\mathbf{Z}) = -1.2499 * 10^{-3} < 0$. This suggests that the allowable uncertainty bound can be greater than (E 3.2.3). Indeed, reapplying the same procedure shows that the lower bounds of $h_j(\mathbf{x})$, $j = 1, 2$ can be expanded beyond $-3 * 10^5$ and $-6 * 10^5$ respectively. However, we omit this because the present results are sufficient to demonstrate the effectiveness of Theorem 3.2. When $h_1(\mathbf{x})$ and $h_2(\mathbf{x})$ are fixed at their extreme values, we have:

1)   When $h_1(\mathbf{x}) = -3 * 10^5$ and $h_2(\mathbf{x}) = -6 * 10^5$, the eigenvalues of

$[\overline{\mathbf{A}}_n - 3 * 10^5 \mathbf{E}_1 - 6 * 10^5 \mathbf{E}_2]$ are $\lambda_1 = -2$, $\lambda_2 = -6 * 10^5$, and $\lambda_3 = -6 * 10^5$.

2)   When $h_1(\mathbf{x}) = 1.74$ and $h_2(\mathbf{x}) = 2.99$, the eigenvalues of $[\overline{\mathbf{A}}_n + 1.74\mathbf{E}_1 + 2.99\mathbf{E}_2]$

are $\lambda_1 = -1.5974 * 10^{-2}$, $\lambda_2 = -1 * 10^{-2}$, and $\lambda_3 = -2.5040$.

3)   When $h_1(\mathbf{x}) = -3 * 10^5$ and $h_2(\mathbf{x}) = 2.99$, the eigenvalues of

$[\overline{\mathbf{A}}_n - 3 * 10^5 \mathbf{E}_1 + 2.99\mathbf{E}_2]$ are $\lambda_1 = -2$, $\lambda_2 = -0.01$, and $\lambda_3 = -6 * 10^5$.

4)   When $h_1(\mathbf{x}) = 1.74$ and $h_2(\mathbf{x}) = -6 * 10^5$, the eigenvalues of

$[\overline{\mathbf{A}}_n + 1.74\mathbf{E}_1 - 6 * 10^5 \mathbf{E}_2]$ are $\lambda_1 = -2.5040$, $\lambda_2 = -0.016$, and $\lambda_3 = -6 * 10^5$.

Figure E3.2.1 compares our allowable uncertainty bounds to those from (Zhou, and Khargonekar, 1987) $\equiv$ (ZK), (Lee et al, 1996) $\equiv$ (L), (Olas, and Ahmadkhanlou, 1994) $\equiv$ (OA). We see from Fig. E3.2.1 that our upper bounds are approximately the same as those in the references. However, the lower bounds in these references are significantly smaller than ours.
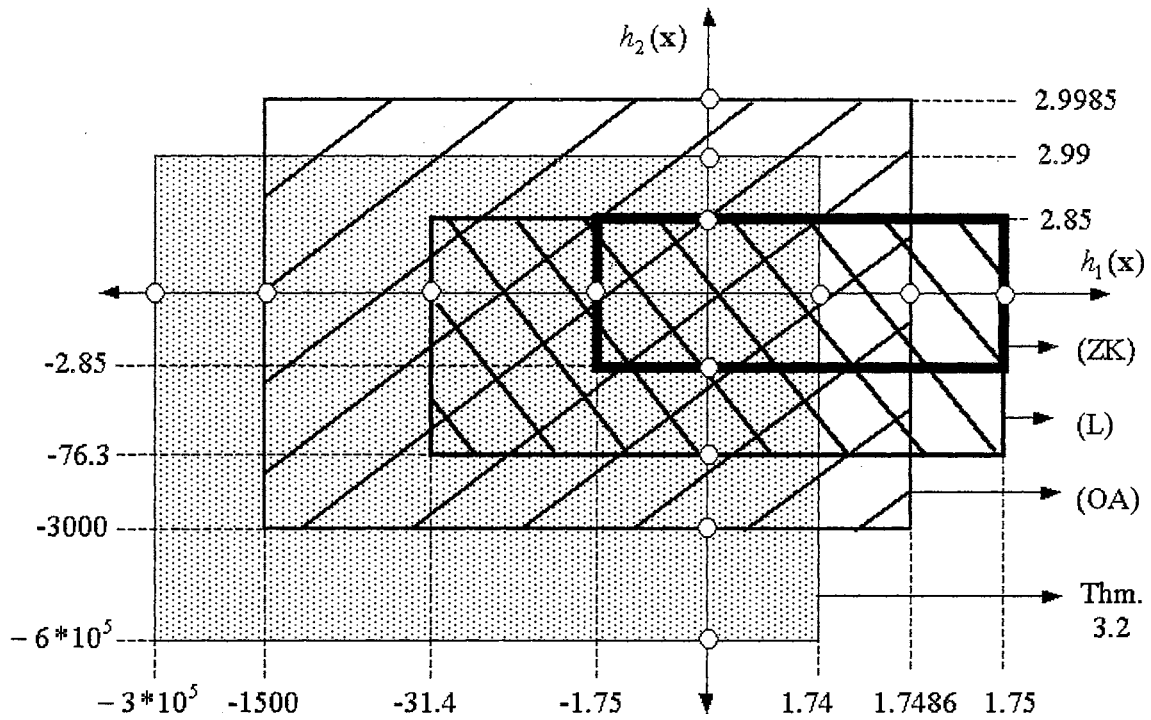
Fig. E3.2.1   Area of Allowable Uncertainties Resulting from
(ZK), (L), (OA), and Theorem 3.2 (not to scale)
Legends: ☐ ≡ (ZK), ◩ ≡ (L), ▨ ≡ (OA), ▤ ≡ Theorem 3.2

While the "areas" of allowable uncertainties resulting from Theorem 3.2 and (Olas, and

Ahmadkhanlou, 1994) are larger than those from (Zhou, and Khargonekar, 1987) and

(Lee et al, 1996), the formers require considerably more computations than the latters.

The amount of computation required for computing the bounds in Theorem 3.2 and in

(Olas, and Ahmadkhanlou, 1994) depends significantly on the order of the system (n) and

the number of uncertainty matrices (r). This will be discussed when we give an algorithm

for generating a LARC in the presence of uncertainties.

When the structure of the uncertain vector $f_\Omega(x,t)$ is unknown and the only known

uncertainty specification is a bound on $\dfrac{\|f_\Omega(x,t)\|}{\|x\|}$, Theorem 3.2 is inapplicable and the

uncertainty is called unstructured. In this case, we adopt a theorem from (Kim, 1995) as

Theorem 3.3 for such unstructured uncertainties. This theorem is the latest we have found

in the literature for this subject. By means of common examples, the author (Kim, 1995)

shows that the resulting allowable bound is less conservative than those in (Patel, Toda,

and Sridhar, 1977) and (Chen, and Han, 1994).

Theorem 3.3 (Unstructured Uncertainty Bound)

The system:

$$\dot{\mathbf{x}} = \overline{\mathbf{A}}_n \mathbf{x} + \mathbf{f}_\Omega(\mathbf{x}, t) \tag{3.2}$$

is stable if:

$$\frac{\|\mathbf{f}_\Omega(\mathbf{x}, t)\|}{\|\mathbf{x}\|} \le \mu \equiv \lambda_{\min}^{1/2}(2\varepsilon\mathbf{Q} - \varepsilon^2\mathbf{PP}) \tag{3.43}$$

where the symmetric positive definite matrices $\mathbf{P}$ and $\mathbf{Q}$ satisfy the Lyapunov equation

$-2\mathbf{Q} = \mathbf{P}\overline{\mathbf{A}}_n + \overline{\mathbf{A}}_n^T\mathbf{P}$ with $\overline{\mathbf{A}}_n$ being a stable matrix and:

$$0 < \varepsilon < \frac{2}{\sigma_{\max}^2(\mathbf{Q}^{-1/2}\mathbf{P})} \equiv \varepsilon_{\max} \tag{3.44 a}$$

$$\mu = \lambda_{\min}^{1/2}(2\varepsilon\mathbf{Q} - \varepsilon^2\mathbf{PP}) > 0 \tag{3.44 b}$$

where $\mathbf{Q}^{-1/2} = [\mathbf{Q}^{1/2}]^{-1}$, $\mathbf{Q}^{1/2}\mathbf{Q}^{1/2} = \mathbf{Q}$, $\sigma_{\max}(\mathbf{Q}^{-1/2}\mathbf{P})$ is the maximum singular value of

$[\mathbf{Q}^{-1/2}\mathbf{P}]$. The proof of Theorem 3.3 can be found in (Kim, 1995). The time derivative of

the quadratic Lyapunov function (1.5) along trajectories of (3.2) is given by:

$$\dot{V}(\mathbf{x}, t) = \frac{1}{2}\mathbf{x}^T[\mathbf{PA}_n + \mathbf{A}_n^T\mathbf{P}]\mathbf{x} + \mathbf{f}_\Omega^T(\mathbf{x}, t)\mathbf{Px} \tag{3.45}$$

The function $\dot{V}(\mathbf{x},t)$ is guaranteed to be negative definite in a region Γ where (3.43) is satisfied. Given a triplet of $\overline{\mathbf{A}}_n$, $\mathbf{P}$ and $\mathbf{Q}$, we search over the interval of ε given in (3.44-a) to find $\max(\mu) \equiv \mu_{max}$ in (3.44 c) because this is the least conservative allowable uncertainty bound on $\dfrac{\|\mathbf{f}_\Omega(\mathbf{x},t)\|}{\|\mathbf{x}\|}$ that guarantees the negative definiteness of $\dot{V}(\mathbf{x},t)$ in Γ.

We now apply Theorem 3.3 to Example 3.1 and 3.2, and compare the resulting allowable uncertainty bounds to those resulting from Theorem 3.2.

Example 3.1 (Cont.)

If the structure of the uncertainty in Example 3.1 is unknown, then we represent the system by (3.2):

$$\dot{\mathbf{x}} = \overline{\mathbf{A}}_n \mathbf{x} + \mathbf{f}_\Omega(\mathbf{x}) \tag{3.2}$$

where $\overline{\mathbf{A}}_n = \begin{bmatrix} -3 & -2 \\ 1 & 0 \end{bmatrix}$ is a stable matrix. The objective is to find a large allowable bound on $\dfrac{\|\mathbf{f}_\Omega(\mathbf{x})\|}{\|\mathbf{x}\|}$ such that the time derivative of the quadratic Lyapunov function along trajectories of (3.2) is globally negative definite to establish global stability. It appears in (Kim, 1995) that:

$$\mathbf{Q} = \begin{bmatrix} 2.3 & 1 \\ 1 & 5 \end{bmatrix} \tag{E 3.1.18}$$

Applying (3.18 a), we obtain:

$$\mathbf{P} = \begin{bmatrix} 1.6000 & 2.5000 \\ 2.5000 & 8.7000 \end{bmatrix} \tag{E 3.1.19}$$

Applying (3.44 a), we obtain:

$$\frac{2}{\sigma_{max}^2 (\mathbf{Q}^{-1/2} \mathbf{P})} \equiv \varepsilon_{max} = 0.1183 \tag{E 3.1.20}$$

Now, we employ (3.44 c) and plot μ as a function of ε in Fig. E3.1.1. It can be shown

that the maximum value of μ and the corresponding ε are given by:

$$\mu_{max} = 0.5351 \tag{E 3.1.21 a}$$

$$\varepsilon_{\mu_{max}} = 0.0753 \tag{E 3.1.21 b}$$

For stability of (3.2), we must have that:

$$\max\left(\frac{\|\mathbf{f}_\Omega(\mathbf{x})\|}{\|\mathbf{x}\|}\right) \leq \mu_{max} = 0.5351 \tag{E 3.1.22}$$

Indeed, we can employ the univariate optimization technique presented in Section 3.6 to

obtain $\mu_{max} = 0.5401$ using:

$$\mathbf{Q} = \begin{bmatrix} 3.4633 & 2.1302 \\ 2.1302 & 6.6823 \end{bmatrix} \tag{E 3.1.23}$$
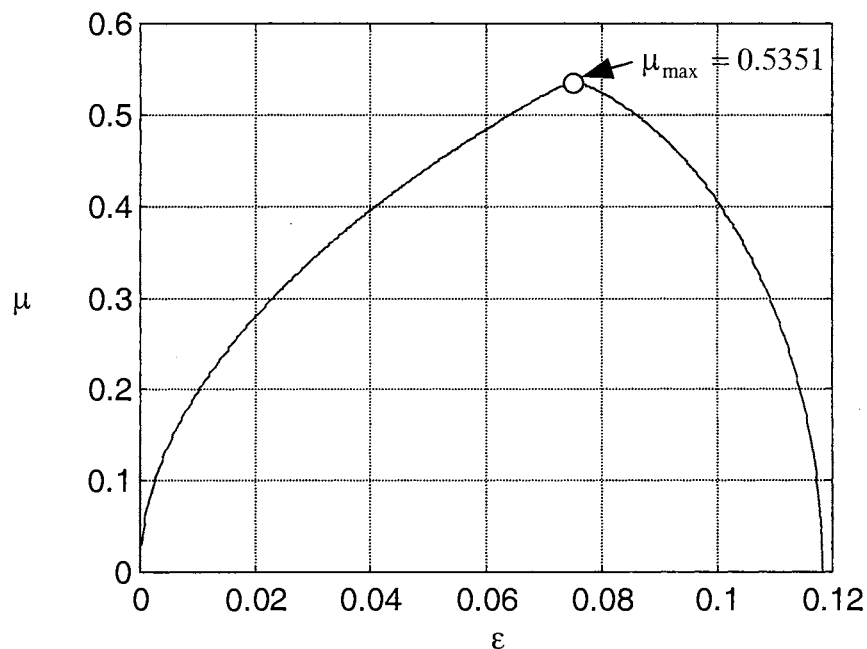
Fig. E3.1.1 Uncertainty Bound μ for Stability as a Function of ε

To compare the resulting bound in (E 3.1.22) with that when the uncertainty is structured, we examine:

$$\mathbf{f}_\Omega(\mathbf{x}) = h(\mathbf{x})\mathbf{Ex} \qquad \text{(E 3.1.24 a)}$$

$$\max\left(\frac{\|\mathbf{f}_\Omega(\mathbf{x})\|}{\|\mathbf{x}\|}\right) = \max\left(\frac{\|h(\mathbf{x})\mathbf{Ex}\|}{\|\mathbf{x}\|}\right) = h_u \max\left(\frac{\|\mathbf{Ex}\|}{\|\mathbf{x}\|}\right) = h_u\|\mathbf{E}\| = 2.8284^- > \mu_{max} \qquad \text{(E 3.1.24 b)}$$

According to (E 3.1.22) and (E 3.1.24 b) we see that when the structure of uncertainty is known, the uncertainty bound is <u>significantly larger</u> than that when the structure of the uncertainty is unknown.

Example 3.2 (Cont.)

If the structure of the uncertainty in Example 3.2 is unknown, then we represent the system by (3.2). The original paper in which this example appears (Zhou, and Khargonekar, 1987) does not consider unstructured uncertainties. In addition, the reference from which Theorem 3.3 is drawn (Kim, 1995) does not employ this example, and does not propose a technique to find $\mathbf{Q}$ for obtaining a large allowable uncertainty bound. Accordingly, we find $\mathbf{Q}$ for this problem at this point by using trial-and-error. We start by using $\mathbf{Q} = \mathbf{I}$, find the corresponding μ_{max} and tune the diagonal elements of $\mathbf{Q}$ accordingly. For simplicity, we restrict $\mathbf{Q}$ to be diagonal, although this does not necessarily yield the best result. The largest μ_{max} we can find under this restriction corresponds to:

$$\mathbf{Q} = \begin{bmatrix} 1 & 0 & 0 \\ 0 & 1.95 & 0 \\ 0 & 0 & 1 \end{bmatrix} \qquad \text{(E 3.2.13)}$$

Applying (3.12 a), we obtain:

$$\mathbf{P} = \begin{bmatrix} 0.5714 & 0.0378 & -0.1429 \\ 0.0378 & 0.6654 & -0.0462 \\ -0.1429 & -0.0462 & 0.2857 \end{bmatrix} \qquad \text{(E 3.2.14)}$$

Applying (3.44 a), we obtain:

$$\frac{2}{\sigma_{\max}^2 [\mathbf{Q}^{-1/2}\mathbf{P}]} \equiv \varepsilon_{\max} = 4.8372 \qquad \text{(E 3.2.15)}$$

Now, we employ (3.44 c) and plot μ as a function of ε in Fig. E3.2.2. It can be shown

that the maximum value of μ and the corresponding ε are given by:

$$\mu_{\max} = 1.5679 \qquad \text{(E 3.2.16 a)}$$

$$\varepsilon_{\mu_{\max}} = 2.4427 \qquad \text{(E 3.2.16 b)}$$

Note that a very similar result can be obtained using a different choice for $\mathbf{Q}$. Indeed, we

can employ the univariate optimization to obtain $\mu_{\max} = 1.5680$ with:

$$\mathbf{Q} = \begin{bmatrix} 0.9135 & 0.0960 & 0.0886 \\ 0.0960 & 0.9797 & 0.0951 \\ 0.0886 & 0.0951 & 1.0829 \end{bmatrix} \qquad \text{(E 3.2.17)}$$

To compare the resulting bound with that when the uncertainty is structured, we examine:

$$\mathbf{f}_{\Omega}(\mathbf{x}) = \sum_{j=1}^{2} [h_j(\mathbf{x})\mathbf{E}_j \mathbf{x}] \qquad \text{(E 3.2.18 a)}$$

$$\max\left(\frac{\|\mathbf{f}_{\Omega}(\mathbf{x})\|}{\|\mathbf{x}\|}\right) > \max\left(\frac{[h_{u1}\mathbf{E}_1 + h_{u2}\mathbf{E}_2]\mathbf{x}}{\|\mathbf{x}\|}\right) = \|h_{u1}\mathbf{E}_1 + h_{u2}\mathbf{E}_2\| = 4.7852 > \mu_{\max} \qquad \text{(E 3.2.18 b)}$$

According to (E 3.1.16 a) and (E 3.2.18), we see that when the structure of uncertainty is

known, the resulting uncertainty bound is <u>significantly larger</u> than that when the structure

of the uncertainty is unknown. This conclusion is the same as that for Example 3.1.
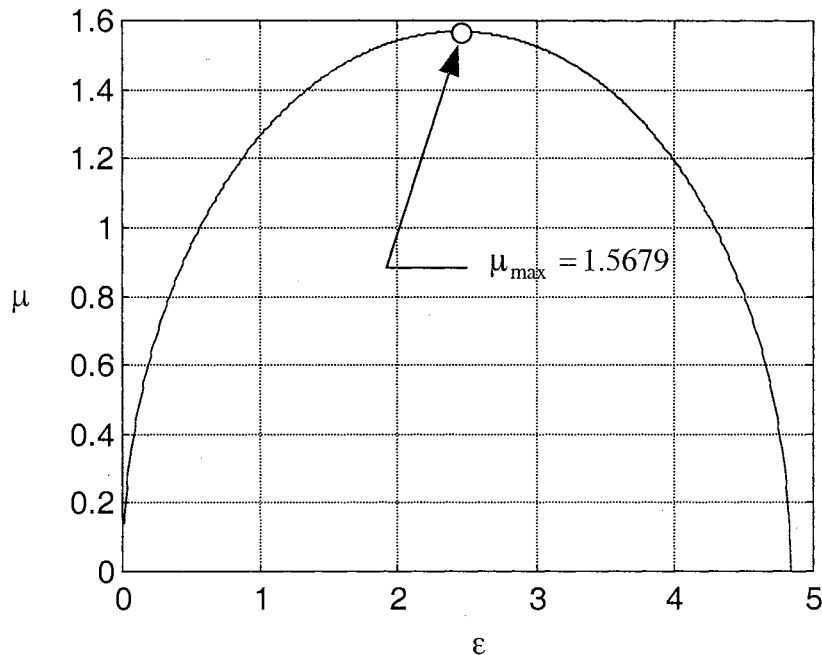
Fig. E3.2.2 Uncertainty Bound μ for Stability as a Function of ε

3.5   Controller Selection

A stabilizing linear controller can be generated by substituting the given uncertainty

specifications into Theorem 3.2 (for structured uncertainties) and into Theorem 3.3 (for

unstructured uncertainties), and solve for a set of $\{\mathbf{K}, \mathbf{Q}, \mathbf{P}\}$ that satisfies relevant

theorems. We desire that $\{\mathbf{K}, \mathbf{Q}, \mathbf{P}\}$ is such that the relevant theorem is satisfied in a

radially large region about the origin because this produces a large LAR. It would be ideal

if we could solve for such $\{\mathbf{K}, \mathbf{Q}, \mathbf{P}\}$ algebraically. However, we do not expect this to

happen when we deal with practical problems because of the nonlinearities involved. In

this research work, we propose to solve for such $\{\mathbf{K}, \mathbf{Q}, \mathbf{P}\}$ using numerical optimization.

We find that at least two existing optimization techniques (Fox, 1971), (Olas, 1994),

(Olas, and Ahmadkhanlou, 1994) can be employed to find a stabilizing controller.

However, the amount of computation required for these optimization techniques grows

significantly as the order of the system increases. When the uncertainties are structured,

considerably more computations are required as the number of uncertain terms (r)

increases. Accordingly, it is crucial that we start the optimization routine from a

"reasonably good" initial value. By "reasonably good", we mean that the initial value is

such that the allowable uncertainty bound is large or is at a local maximum with respect to

Theorem 3.2 and 3.3 in a feasible domain.

By generating a set of LAR controllers for the nominal linear model (3.4), we obtain the

corresponding set of initial values for such optimization. Then we select from this set a

"reasonably good" initial value based on Theorem 3.2 (for structured uncertainties),

Theorem 3.3 (for unstructured uncertainties), and the available control energy. We employ

such an initial value for the optimization because it satisfies the eigenvector condition. To

see why this is desirable, we rewrite (3.2) as:

$$\dot{\mathbf{x}} = [\mathbf{A}_n \mathbf{x} + \mathbf{f}_\Sigma(\mathbf{x},t,u)] + \mathbf{B}_n\, u_{LARC}(\mathbf{x}) \tag{3.2}$$

It can be shown that the time derivative of the quadratic Lyapunov function (1.5) along

trajectories of (3.2) is:

$$
\begin{aligned}
\dot{V}(\mathbf{x},t) &= \frac{1}{2}\mathbf{x}^T\left[\mathbf{PA}_n + [\mathbf{PA}_n]^T\right]\mathbf{x} + \mathbf{x}^T\mathbf{Pf}_\Sigma(\mathbf{x},t,u_{LARC}(\mathbf{x})) + \mathbf{x}^T\mathbf{PB}_n u_{LARC}(\mathbf{x}) \\
&\equiv \mathbf{x}^T\mathbf{M}_n\mathbf{x} + \mathbf{x}^T\mathbf{Pf}_\Sigma(\mathbf{x},t,u_{LARC}(\mathbf{x})) + \mathbf{x}^T\mathbf{PB}_n u_{LARC}(\mathbf{x}) \\
&\equiv F_{Ln}(\mathbf{x}) + F_\Sigma(\mathbf{x},t,u_{LARC}(\mathbf{x})) + G_{Ln}(\mathbf{x})u_{LARC}(\mathbf{x}) \\
&\equiv F_\Delta(\mathbf{x},t,u_{LARC}(\mathbf{x})) + G_{Ln}(\mathbf{x})u_{LARC}(\mathbf{x})
\end{aligned}
\tag{3.45}
$$

where $\mathbf{M}_n \equiv \dfrac{1}{2}\left[\mathbf{PA}_n + [\mathbf{PA}_n]^T\right]$, $F_\Sigma(\mathbf{x},t,u_{LARC}(\mathbf{x})) \equiv \mathbf{x}^T\mathbf{Pf}_\Sigma(\mathbf{x},t,u_{LARC}(\mathbf{x}))$,

$F_{Ln}(\mathbf{x}) \equiv \mathbf{x}^T\mathbf{M}_n\mathbf{x}$, $G_{Ln}(\mathbf{x}) \equiv \mathbf{x}^T\mathbf{PB}_n$, and $F_\Delta(\mathbf{x},t,u_{LARC}(\mathbf{x})) \equiv F_{Ln}(\mathbf{x}) + F_\Sigma(\mathbf{x},t,u_{LARC}(\mathbf{x}))$.

We define $S_{F_{Ln}=0} \equiv \{\mathbf{x} \mid F_{Ln}(\mathbf{x}) = 0\}$, $S_{G_{Ln}=0} \equiv \{\mathbf{x} \mid G_{Ln}(\mathbf{x}) = 0\}$, and $S_{F_\Delta=0} \equiv \{\mathbf{x} \mid F_\Delta(\mathbf{x},t,$ $u(\mathbf{x})) = 0\}$. From the expression for $u_{LARC}(\mathbf{x})$ in (2.16), we note that $S_{G_{Ln}=0} = S_{u_{LARC}=0}$.

We recall from Lemma 2.3 that the matrix $\mathbf{P}$ corresponding to a LAR controller is such that the eigenvector condition is satisfied and it follows from the definition of the eigenvector condition that $S_{F_{Ln}=0}$ is symmetric about $S_{G_{Ln}=0}$ such that $S_{G_{Ln}=0} \subset$ $R_{[F_{Ln}<0]\cup\{0\}}$. From the expression for $\dot{V}(\mathbf{x},t)$, we see that $S_{F_{Ln}=0}$ is the same as $S_{F_\Delta=0}$ when there is no uncertainty $(\mathbf{f}_\Sigma(\mathbf{x},t,u(\mathbf{x})) = \mathbf{0})$. In this situation, it follows from the definition of the eigenvector condition that $S_{F_\Delta=0}$ is symmetric about $S_{G_{Ln}=0}$ such that $S_{G_{Ln}=0} \subset R_{[F_\Delta<0]\cup\{0\}}$. Because of the uncertain vector $\mathbf{f}_\Sigma(\mathbf{x},t,u(\mathbf{x}))$, $S_{F_\Delta=0}$ deviates from $S_{F_{Ln}=0}$ and can be time-varying. However, Theorem 3.2 and 3.3 implies that $S_{F_\Delta=0}$ does not intersects $S_{G_{Ln}=0}$ when $\mathbf{f}_\Sigma(\mathbf{x},t,u(\mathbf{x}))$ is sufficiently small $\forall t$. Indeed, if $S_{F_\Delta=0}$ intersects $S_{G_{Ln}=0}$ at a particular t, then $\dot{V}(\mathbf{x},t)$ is not globally uniformly negative definite. This leads to a contradiction because we know from Theorem 3.2 and 3.3 that $\dot{V}(\mathbf{x},t)$ is globally uniformly negative definite under sufficiently small uncertainties. Since $S_{G_{Ln}=0}$ is fixed in the state space for all possible uncertainties and t, this implies that $S_{F_\Delta=0}$ is in a small neighborhood about $S_{F_{Ln}=0}$ for sufficiently small uncertainties $\forall t$. We emphasize that the deviations of $S_{F_\Delta=0}$ from $S_{F_{Ln}=0}$ can occur arbitrarily close to the origin because of the uncertainties.

Next, we illustrate graphically in Fig. 3.1 how these deviations can affect the dimension of the LAR when the eigenvector condition is both dissatisfied and not satisfied. In this illustration, we employ the following representations:

1) $\diamond \equiv$ the intersection point between the surfaces $S_{G_{Ln}=0}$ and $S_{F_{\Delta}=0}$ corresponding

to the exact nonlinear model (3.2)

2)   —— $\equiv$ the surface $S_{F_{Ln}=0}$, which is the same as $S_{F_{\Delta}=0}$ when $\mathbf{f}_{\Sigma}(\mathbf{x},t,u(\mathbf{x})) = \mathbf{0}$.

3)   ▬▬ $\equiv$ the surface $S_{F_{\Delta}=0}$

5)   ▬ ▬ $\equiv$ the surface $S_{G_{Ln}=0}$

5)   ▢ $\equiv$ regions of uncertainties.
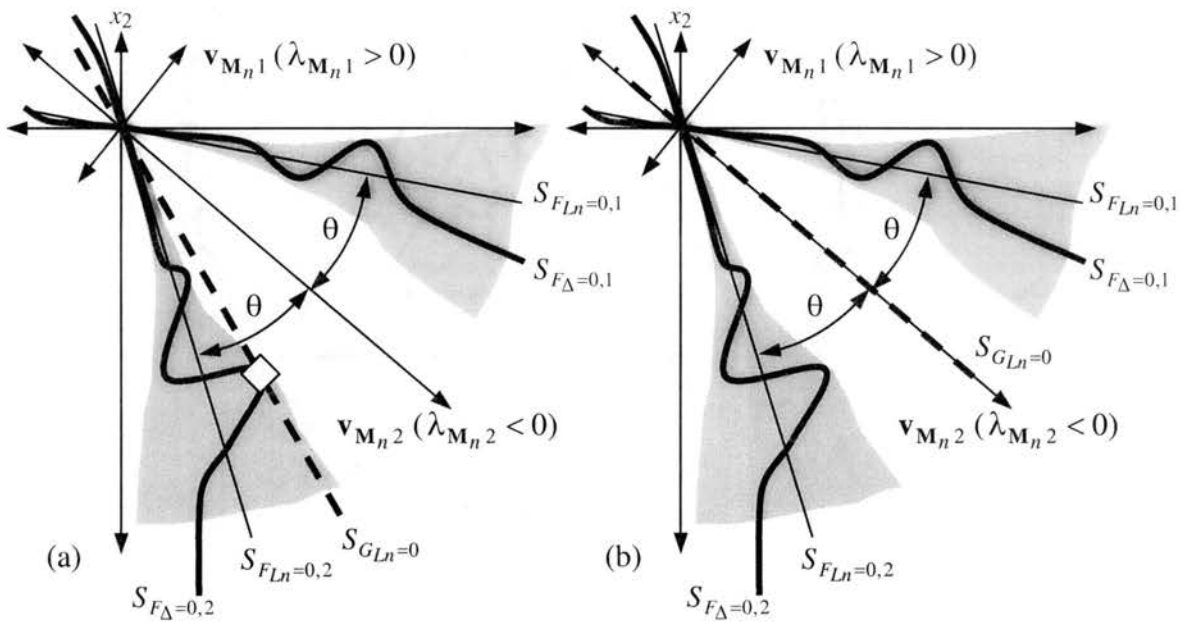
Fig. 3.1   Effects of Nonlinear Uncertainties on the Possible Intersection between $S_{G_{Ln}=0}$
and $S_{F_{\Delta}=0}$ when the Eigenvector Condition is not Satisfied (a) and is Satisfied (b)
a) $S_{G_{Ln}=0}$ runs close to $S_{F_{Ln}=0,2}$ and far from $S_{F_{Ln}=0,1}$, locating the intersection
between $S_{F_{\Delta}=0}$ and $S_{G_{Ln}=0}$ (denoted by $\diamond$) undesirably close to the origin.
b) $S_{G_{Ln}=0}$ runs midway between the lines $S_{F_{Ln}=0,1}$ and $S_{F_{Ln}=0,2}$

When the eigenvector condition is not satisfied, $S_{G_{Ln}=0}$ may be located close to a

particular portion of $S_{F_{Ln}=0}$. Accordingly, small deviations of $S_{F_{\Delta}=0}$ from $S_{F_{Ln}=0}$ can

result in an intersection between $S_{G_{Ln}=0}$ and $S_{F_{\Delta}=0}$ corresponding to the <u>exact nonlinear model</u> arbitrarily close to the origin. At such intersection point, $\dot{V}(\mathbf{x},t) = 0$ for all possible choices of $u(\mathbf{x})$ including $u(\mathbf{x}) = u_{LARC}(\mathbf{x})$. Since it is necessary that $\dot{V}(\mathbf{x},t)\big|_{\mathbf{x}\neq 0} < 0$ in a LAR, it follows that such small deviations can lead to an arbitrarily small LAR when the eigenvector condition is dissatisfied. This situation is illustrated in Fig. 3.1 (a).

In Fig. 3.1 (b), the eigenvector condition is satisfied and $S_{F_{Ln}=0}$ is symmetric about $S_{G_{Ln}=0}$. Accordingly, $S_{G_{Ln}=0}$ does not run close to a particular portion of $S_{F_{Ln}=0}$. When the uncertainties are sufficiently small, we have seen that $S_{F_{\Delta}=0}$ is in a small neighborhood about $S_{F_{Ln}=0}$ and thus $S_{F_{\Delta}=0}$ does not intersect $S_{G_{Ln}=0}$. In this situation,

$S_{G_{Ln}=0} \subset R_{[F_{\Delta}<0]\cup\{0\}}$ and the expression for $\dot{V}(\mathbf{x},t)$ in (3.45) implies that we can force the LAR to be as large as we like by manipulating $u_{LARC}(\mathbf{x})$. When the eigenvalue ratio $r_{\lambda_{M_n}}$ corresponding to the time derivative of the Lyapunov function along the nominal linear model (3.4) is large, the additional adverse effects are straightforward from Proposition 1.2 and the above discussions. These arguments are the same as those given in Section 1.4 except that the possible adverse effects resulting from uncertainties are now added to those resulting from nonlinearities.

Remark: A special case of the situation discussed previously occurs when the nominal linear model $\dot{\mathbf{x}} = \mathbf{A}_n\mathbf{x} + \mathbf{B}_n u(\mathbf{x})$ is exactly the linearized model about the origin of the exact time-varying nonlinear system $\dot{\mathbf{x}} = \mathbf{f}(\mathbf{x},t) + \mathbf{g}(\mathbf{x},t)u(\mathbf{x})$, implying that

$$\lim_{\|\mathbf{x}\|\to 0}\left(\sup_{t\geq 0}\left(\frac{\|\mathbf{f}(\mathbf{x},t)-\mathbf{A}_n\mathbf{x}\|}{\|\mathbf{x}\|}\right)\right)=0 \text{ and } \lim_{\|\mathbf{x}\|\to 0}\left(\sup_{t\geq 0}\left(\frac{\|\mathbf{g}(\mathbf{x},t)-\mathbf{B}_n\|}{\|\mathbf{x}\|}\right)\right)=0.$$ Under these

conditions, $\dfrac{\|\mathbf{f}_\Omega(\mathbf{x},t)\|}{\|\mathbf{x}\|}$ is negligible in sufficiently small regions about the origin, and it

follows from Theorem 3.3 that the nonlinear system is locally uniformly asymptotically

stable when $\mathbf{K}$ is such that $\overline{\mathbf{A}}_n \equiv [\mathbf{A}_n - \mathbf{B}_n\mathbf{K}]$ is stable. In addition, it can be drawn from

the previous argument that $S_{F_{Ln}=0} = S_{F_L=0}$ and the deviations of $S_{F_\Delta=0}$ from these

surfaces are negligible in sufficiently small region about the origin. In this special case,

we see that LARC in Chapter I and II can be employed to stabilize the system

$\dot{\mathbf{x}} = \mathbf{f}(\mathbf{x},t) + \mathbf{g}(\mathbf{x},t)u(\mathbf{x})$ such that the origin is locally uniformly asymptotically stable

with a reasonably large attractive region by regarding $\mathbf{A}_n$ as $\mathbf{A}$, and $\mathbf{B}_n$ as $\mathbf{B}$. Note that

when $\dfrac{\|\mathbf{f}_\Omega(\mathbf{x},t)\|}{\|\mathbf{x}\|}$ is not negligible in sufficiently small regions about the origin, we need

information about $\dfrac{\|\mathbf{f}_\Omega(\mathbf{x},t)\|}{\|\mathbf{x}\|}$ to generate a stabilizing LARC. This is discussed in the next

section.

3.6   Controller Generation

Given (3.2) with specifications for uncertainties, we want to determine for stabilization of

(3.2) the solution $\mathbf{K} = \mathbf{K}_{LARC}$, $\mathbf{Q}$, and $\mathbf{P}$ such that $\dot{V}(\mathbf{x},t)$ is negative definite in an

operating region Θ about the origin where such specifications are valid. We restrict our

LARC to be linear for simplicity, although this does not necessarily produce the best

result. Note that:

1)   We say that the controller "meets" the given uncertainty specifications in the

region Θ when $\dot{V}(\mathbf{x}, t)$ is negative definite in the same region. Clearly, we desire

that the uncertainties are met in a radially large region about the origin.

2)   We need not write $\mathbf{P}$ explicitly in the solution, because $\mathbf{K} = \mathbf{K}_{LARC}$ and $\mathbf{Q}$ implies

$\mathbf{P}$.

A choice of $\mathbf{Q}$ in Theorem 3.2 and 3.3 do not affect physical properties of the system

because $\mathbf{Q}$ does not represent any components in a physical system. However, it turns out

that some particular choices of $\mathbf{Q}$ can be employed to demonstrate that uncertainty

specifications are met under a particular linear controller using Theorem 3.2 and 3.3. Note

that Theorem 3.2 and 3.3 demonstrate global stability by showing that the time derivative

of the quadratic Lyapunov function along system trajectories is globally negative definite

and the LAR is radially unbounded for sufficiently small uncertainties. However, we need

not restrict the applications of Theorem 3.2 and 3.3 to the case in which a LAR is radially

unbounded. As we have seen from Chapters I and II, we desire only that a LAR be

radially large when local stabilization is acceptable. We emphasize that the LARC

developed in the previous chapters is primarily for systems that can be approximated in Θ

by linear time-invariant models. In this chapter, such LARC is integrated with Theorem

3.2 and 3.3 to remove such restriction. Procedures for generating a LARC in the presence

of uncertainties using Theorem 3.2 and 3.3 are now given:

Systems with Structured Uncertainties

To generate a LAR controller for the system (3.2) with structured uncertainties, we find

under the given structured uncertain specifications a particular pair of $\mathbf{K}_{LARC}$ and $\mathbf{Q}$ such

that in an operating region Θ about the origin:

$$\lambda_{max}(\mathbf{Z}(\mathbf{K}_{LARC}, \mathbf{Q})) < 0 \qquad (3.46)$$

where the uncertainty specifications and the relevant notations are given in the section

"Structured Uncertainty Specifications for Controller Generations". The procedure begins

by choosing a region $\{(\rho, \eta) \mid 0 < \rho_l \leq \rho \leq \rho_u, 1 \leq \eta \leq \eta_u\}$ and compute $\mathbf{K} = \mathbf{K}_{LARC}$ and $\mathbf{Q}$

at points distributed evenly in this region using (2.12) and (2.16). Knowing $\mathbf{K} = \mathbf{K}_{LARC}$

and $\mathbf{Q}$ at these points, we plot $\lambda_{max}(\mathbf{Z}(\mathbf{K}_{LARC}(\rho, \eta), \mathbf{Q}(\rho, \eta))) = \lambda_{max}(\mathbf{Z}(\rho, \eta))$ versus ρ

and η using Theorem 3.2. If $\lambda_{max}(\mathbf{Z}) < 0$ at any point in this region, $\mathbf{K}_{LARC}$

corresponding to such point meets the uncertainty specifications and we terminate the

procedure. Otherwise, we obtain from this plot a coordinate (ρ, η) corresponding to a

small value of $\lambda_{max}(\mathbf{Z})$ and we employ this (ρ, η) to obtain $\{\mathbf{K}_{LARC}, \mathbf{Q}\}$ as the initial

value for the next optimization routine. Generally, selecting such (ρ, η) is possible

because we can visualize clearly a plot in three dimensions.

Starting from the feasible initial value $\{\mathbf{K}_{LARC}, \mathbf{Q}\}$ determined previously, we want to find

a particular pair of $\mathbf{K}_{LARC}$ and $\mathbf{Q}$ such that $\lambda_{max}(\mathbf{Z}(\mathbf{K}_{LARC}, \mathbf{Q})) < 0$ under the given

uncertainty specifications. This problem can be cast as a constrained optimization problem

in which the objective is to minimize $\lambda_{max}(\mathbf{Z}(\mathbf{K}_{LARC}, \mathbf{Q}))$ and the constraints are

$Re(\lambda_i (\mathbf{A}_n - \mathbf{B}_n \mathbf{K}_{LARC})) < 0 \; \forall i$, $\mathbf{Q} = \mathbf{Q}^T$ and $\lambda_{\min}(\mathbf{Q}) > 0$. The latter is required to guarantee that the quadratic Lyapunov function is negative definite. We call a point satisfying these constraints a "feasible" point, and denote a solution for $\mathbf{K}_{LARC}$ by $\mathbf{K}_{OLARC}$ where the subscript "OLARC" designates that the LAR gain matrix is obtained by using optimization. In this phase of the procedure, $\mathbf{K}_{LARC}$ and $\mathbf{Q}$ are to be updated by an optimization routine, not by (2.12) and (2.16). We emphasize that the feasible initial value $\{\mathbf{K}_{LARC}, \mathbf{Q}\}$ for the optimization selected previously from the plot of $\lambda_{\max}(\mathbf{Z}(\rho, \eta))$ is reasonably good. This is in the sense that such an initial value corresponds to a small value of $\lambda_{\max}(\mathbf{Z})$ in a certain set of $\{\mathbf{K}_{LARC}, \mathbf{Q}\}$ satisfying the eigenvector condition.

For simplicity, we employ the "univariate" optimization technique (Fox, 1971) to find a solution $\{\mathbf{K}_{LARC}, \mathbf{Q}\}$ such that $\lambda_{\max}(\mathbf{Z}(\mathbf{K}_{LARC}, \mathbf{Q})) < 0$ while we understand that other techniques may produce better results. Using the univariate technique, we perturb one variable in the objective function at a time and update the solution $\{\mathbf{K}_{LARC}, \mathbf{Q}\}$ if such perturbation decreases $\lambda_{\max}(\mathbf{Z})$. The procedure is terminated when the decrement in $\lambda_{\max}(\mathbf{Z})$ is less than a prescribed value after all variables in the objective function are perturbed. In general, the solution can be as close to a local minimum as we like but it is likely not the minimum because this approach does not include a mechanism to compute the gradient. Except for pathological cases, this seems to be acceptable for our purpose because we need not obtain a true minimum. Indeed, it is sufficient to admit any solution such that $\lambda_{\max}(\mathbf{Z}) < 0$. Of course, obtaining the solution $\{\mathbf{K}_{LARC}, \mathbf{Q}\}$ that meets the given uncertainty specifications may not be possible for some strong specifications.

We emphasize that the univariate technique is not the only possible technique for this optimization problem. Indeed, we have seen in Example 3.3 that the results obtained from the gradient-based technique in (Olas, 1994) and (Olas, and Ahmadkhanlou 1994) are satisfactory. Given a fixed linear gain matrix $\mathbf{K}$ such that $\text{Re}(\lambda_i(\mathbf{A}_n - \mathbf{B}_n\mathbf{K})) < 0 \ \forall i$, this technique requires us to compute eigenvalues of $C_\lambda = 2^r$ matrices of dimension $n \times n$ to update $\mathbf{Q}$, where r is the number of uncertainty matrices $\mathbf{E}_j$ and is bounded by $1 \le r \le \dim(\mathbf{A}_n) + \dim(\mathbf{B}_n) = (n^2 + mn)$. For the univariate technique, we know by inspecting Theorem 3.2 that we need to compute the eigenvalues and eigenvectors of $\mathbf{\Psi}_j$, $j = 1, 2, ..., r$ and the eigenvalues of $\mathbf{Z}$ to see if a change in an element of $\mathbf{Q}$ decreases $\lambda_{\max}(\mathbf{Z})$. Since $\lambda_{\max}(\mathbf{Z})$ <u>may</u> decrease when we decrease or increase an element of $\mathbf{Q}$, and $\mathbf{Q} = \mathbf{Q}^T$ contains $1 + 2 + ... + n = \frac{1}{2}n(n+1)$ different elements, it follows that we need to compute $\lambda_{\max}(\mathbf{Z})$ at least once and at most $n(n+1)$ times to update the solution for $\mathbf{Q}$. Thus, we are required to compute eigenvalues of <u>at most</u> $C_\lambda = (r+1)n(n+1)$ matrices of dimension $n \times n$ to update $\mathbf{Q}$. When r is small, the technique in (Olas, 1994) and (Olas, and Ahmadkhanlou, 1994) generally requires less computation than the univariate technique. However, the former requires more computation than the latter does when r is large.

For these optimization techniques, it is clear that the required computation grows very rapidly as the order of the system n and the number of uncertainty matrices r increase. Accordingly, <u>it is crucial for a high dimensional system with a large number of uncertainty matrices that the initial value be reasonably good</u>. In our case, we obtain this

initial value from the plot generated previously using (2.12), (2.16) and Theorem 3.2.

Procedure 2 is now given (Procedure 1 was given in Chapter II):

Step 1 Choose a region $\{(\rho,\eta)\,|\,0<\rho_l \leq \rho \leq \rho_u, 1 \leq \eta \leq \eta_u\}$ and compute $\mathbf{K} = \mathbf{K}_{LARC}$

and $\mathbf{Q}$ at points distributed evenly in this region using (2.12) and (2.16). Then

plot $\lambda_{max}(\mathbf{Z}(\rho,\eta))$ versus ρ and η in three dimensions using Theorem 3.2 and

the given structured uncertainty specifications, and find a region of (ρ,η)

where $\lambda_{max}(\mathbf{Z}(\rho,\eta))$ is small or is negative from such plot. For each of our

example problems to follow, less than 3 minutes were required to accomplish

this.

Step 2 If we find from the plot in Step 1 that $\lambda_{max}(\mathbf{Z}(\rho,\eta)) < 0$ at a particular (ρ,η),

then the matrix $\mathbf{K}_{LARC}$ corresponding to such (ρ,η) meets the uncertainty

specifications and we terminate the procedure. In this case, we usually select

$\{\mathbf{K}_{LARC}, \mathbf{Q}\}$ corresponding to the minimum of $\lambda_{max}(\mathbf{Z}(\rho,\eta))$ in the plots as our

solution although we can accept any solutions such that $\lambda_{max}(\mathbf{Z}(\rho,\eta)) < 0$. If

the minimum of $\lambda_{max}(\mathbf{Z}(\rho,\eta))$ in the plot is positive, we obtain from this plot

an initial value $\{\mathbf{K}_{LARC}, \mathbf{Q}\}$ such that the corresponding $\lambda_{max}(\mathbf{Z}(\rho,\eta))$ is small

for the optimization in Step 3.

When the available control energy is limited, it is preferable to start the

optimization from an initial value in which $\mathbf{K}_{LARC}$ is small. This usually forces

us to admit an initial value $\{\mathbf{K}_{LARC}, \mathbf{Q}\}$ corresponding to a larger

$\lambda_{max}(Z(\rho,\eta))$. In this case, we select the initial value from a "flat" portion of

the plot where decreasing (ρ,η) does not increase $\lambda_{max}(Z(\rho,\eta))$ significantly.

Step 3   Starting from the feasible initial value in Step 2, we employ an optimization

technique to search for $\{K_{LARC}, Q\}$ such that $\lambda_{max}(Z(K_{LARC}, Q)) < 0$. There

are several applicable optimization techniques but we employ the

straightforward "univariate" technique (Fox, 1971) for simplicity. We regard

the elements of K_{LARC} and Q as our variables in the objective function

$\lambda_{max}(Z(K_{LARC}, Q))$. Then we perturb these variables one at a time and

examine the corresponding $\lambda_{max}(Z(K_{LARC}, Q))$. Our perturbations must be

such that $\{K_{LARC}, Q\}$ remains feasible. If the objective function decreases, we

continue to perturb this variable in the same direction. Otherwise, we reverse

the direction of the perturbation and repeat the above sequences. When the

decrement in $\lambda_{max}(Z(K_{LARC}, Q))$ is less than a prescribed value, we perturb a

new variable and repeat the above sequences. These nested loops terminate

when computation time is expired or when the decrement in

$\lambda_{max}(Z(K_{LARC}, Q))$ is less than a prescribed value after all the variables are

perturbed in this fashion. All the "prescribed" values and the perturbations are

determined by using heuristics. In the examples herein, we set these to be

between 0.5% - 1% of the previous values.

Systems with Unstructured Uncertainties

To generate a LAR controller for the system (3.2) with unstructured uncertainties, we find

under the given unstructured uncertainty specifications a particular pair of $\mathbf{K}_{LARC}$ and $\mathbf{Q}$

such that in an operating region Θ about the origin:

$$\max\left(\frac{\|\Delta\mathbf{f}(\mathbf{x},t)\|}{\|\mathbf{x}\|}\right) + \|\mathbf{K}_{LARC}\|\max(\|\Delta\mathbf{g}(\mathbf{x},t)\|) \leq \mu_{\max} \tag{3.47}$$

where the uncertainty specifications and the relevant notations are given in the section

"Unstructured Uncertainty Specifications for Controller Generations". Given a known pair

of unstructured uncertainty specifications $\max\left(\dfrac{\|\Delta\mathbf{f}(\mathbf{x},t)\|}{\|\mathbf{x}\|}\right)$ and $\max(\|\Delta\mathbf{g}(\mathbf{x},t)\|)$, it follows

from (3.47) that we want to find $\mathbf{K}_{LARC}$ such that:

$$\delta \equiv \max\left(\frac{\|\Delta\mathbf{f}(\mathbf{x},t)\|}{\|\mathbf{x}\|}\right) + \|\mathbf{K}_{LARC}\|\max(\|\Delta\mathbf{g}(\mathbf{x},t)\|) - \mu_{\max} \leq 0 \tag{3.48}$$

Note that defining δ as in (3.48) allows us to obtain the corresponding optimization

algorithm from that for structured uncertainties quickly. To see this, notice that the

problem statement for structured uncertainties in (3.46) is similar to that for unstructured

uncertainties in (3.48). We now introduce a procedure for generating a LARC under

unstructured uncertainties. Except that we employ Theorem 3.3 instead of Theorem 3.2,

this procedure is the same as Procedure 2 given previously. This procedure begins by

choosing a region $\{(\rho,\eta) \mid 0 < \rho_l \leq \rho \leq \rho_u, 1 \leq \eta \leq \eta_u\}$ and compute $\mathbf{K} = \mathbf{K}_{LARC}$ and $\mathbf{Q}$ at

points distributed evenly in this region using (2.12) and (2.16). Knowing $\mathbf{K} = \mathbf{K}_{LARC}$ and

$\mathbf{Q}$ at these points, we plot $\delta(\mathbf{K}_{LARC}(\rho,\eta),\mathbf{Q}(\rho,\eta)) = \delta(\rho,\eta)$ versus ρ and η using

Theorem 3.3 and (3.48). If $\delta(\rho,\eta) \leq 0$ at any point in this region, $\mathbf{K}_{LARC}$ corresponding to

such point meets the uncertainty specifications and we terminate the procedure. Otherwise, we obtain from this plot a coordinate (ρ, η) corresponding to a small value of $\delta(\rho, \eta)$ and we employ this (ρ, η) to obtain $\{\mathbf{K}_{LARC}, \mathbf{Q}\}$ as the initial value for the next optimization routine. Generally, selecting such (ρ, η) is possible because we can visualize clearly a plot in three dimensions.

Starting from the feasible initial value $\{\mathbf{K}_{LARC}, \mathbf{Q}\}$ determined previously, we want to find a particular pair of $\mathbf{K}_{LARC}$ and $\mathbf{Q}$ such that $\delta(\mathbf{K}_{LARC}, \mathbf{Q}) < 0$ under the given uncertainty specifications. This problem can be cast as a constrained optimization problem in which the objective is to minimize $\delta(\mathbf{K}_{LARC}, \mathbf{Q})$ and the constraints are

$\mathrm{Re}(\lambda_i(\mathbf{A}_n - \mathbf{B}_n\mathbf{K}_{LARC})) < 0 \ \forall i$, $\mathbf{Q} = \mathbf{Q}^T$ and $\lambda_{\min}(\mathbf{Q}) > 0$. The latter is required to guarantee that the quadratic Lyapunov function is negative definite. We call a point satisfying these constraints a "feasible" point, and denote a solution for $\mathbf{K}_{LARC}$ by $\mathbf{K}_{OLARC}$ where the subscript "OLARC" designates that the LAR gain matrix is obtained by using optimization. In this phase of the procedure, $\mathbf{K}_{LARC}$ and $\mathbf{Q}$ are to be updated by an optimization routine, but not by (2.12) and (2.16). We emphasize that the feasible initial value $\{\mathbf{K}_{LARC}, \mathbf{Q}\}$ for the optimization selected previously from the plot of $\delta(\rho, \eta)$ is reasonably good. This is in the sense that such an initial value corresponds to a small value of δ in a certain set of $\{\mathbf{K}_{LARC}, \mathbf{Q}\}$ satisfying the eigenvector condition.

By inspecting Theorem 3.3, it is clear that the required computation grows very rapidly as the order of the system n increases. Accordingly, it is crucial for a high dimensional

system that the initial value be reasonably good. In our case, we obtain this initial value by using (2.12), (2.16) and Theorem 3.3. Procedure 3 is now given:

Step 1 Choose a region $\{(\rho, \eta) \,|\, 0 < \rho_l \leq \rho \leq \rho_u, 1 \leq \eta \leq \eta_u\}$ and compute $\mathbf{K} = \mathbf{K}_{LARC}$

and $\mathbf{Q}$ at points distributed evenly in this region using (2.12) and (2.16). Then

plot $\delta(\rho, \eta)$ versus ρ and η in three dimensions using Theorem 3.3 and the

given unstructured uncertainty specifications. The objective of this step is to

find a region of (ρ, η) where $\delta(\rho, \eta)$ is small or is negative. Although it is not

clear where this region is when we start this step, the shape of the first plot will

guide us to a better selection of this region for the second plot and so on. In the

examples herein, the time required for this is approximately the same as that

when the uncertainties are structured.

Step 2 If we find from the plot in Step 1 that $\delta(\rho, \eta) \leq 0$ at a particular (ρ, η), then

the matrix $\mathbf{K}_{LARC}$ corresponding to such (ρ, η) meets the uncertainty

specifications and we terminate the procedure. In this case, we usually select

$\{\mathbf{K}_{LARC}, \mathbf{Q}\}$ corresponding to the minimum of $\delta(\rho, \eta)$ in the plot as our

solution, although we can accept any solutions such that $\delta(\rho, \eta) \leq 0$. If the

minimum of $\delta(\rho, \eta)$ in the plot is positive, we obtain from this plot an initial

value $\{\mathbf{K}_{LARC}, \mathbf{Q}\}$ such that the corresponding $\delta(\rho, \eta)$ is small for the

optimization in Step 3.

When the available control energy is limited, it is preferable to start the optimization from an initial value in which $\mathbf{K}_{LARC}$ is small. This usually forces us to admit an initial value $\{\mathbf{K}_{LARC}, \mathbf{Q}\}$ corresponding to a larger $\delta(\rho, \eta)$. In this case, we select the initial value from a "flat" portion of the plot where decreasing (ρ, η) does not increase $\delta(\rho, \eta)$ significantly.

Step 3   Starting from the feasible initial value in Step 2, we employ an optimization technique to search for $\{\mathbf{K}_{LARC}, \mathbf{Q}\}$ such that $\delta(\mathbf{K}_{LARC}, \mathbf{Q}) \leq 0$. There are several applicable optimization techniques but we employ the straightforward "univariate" technique (Fox, 1971) for simplicity. We regard the elements of $\mathbf{Q}$ and $\mathbf{K}$ as our variables in the objective function $\delta(\mathbf{K}_{LARC}, \mathbf{Q})$. Then we perturb these variables one at a time and examine the corresponding $\delta(\mathbf{K}_{LARC}, \mathbf{Q})$. Our perturbations must be such that $\{\mathbf{K}_{LARC}, \mathbf{Q}\}$ remains feasible. If the objective function decreases, we continue to perturb this variable in the same direction. Otherwise, we reverse the direction of the perturbation and repeat the above sequences. When the decrement in $\delta(\mathbf{K}_{LARC}, \mathbf{Q})$ is less than a prescribed value, we perturb a new variable and repeat the above sequences. These nested loops terminate when computation time is expired or when the decrement in $\delta(\mathbf{K}_{LARC}, \mathbf{Q})$ is less than a prescribed value after all the variables are perturbed in this fashion. All the "prescribed" values and the perturbations are determined by using heuristics. In examples herein, we set these to be between 0.5% - 1% of the previous values.

Example 3.3 (The Double-Inverted-Pendulum System with Lower-Joint Control)

In this example, we draw the double-inverted-pendulum system from Example 2.2 to

demonstrate how to generate a LARC in the presence of structured uncertainties.

Nonlinearities are treated as "pseudo" structured uncertainties entering the nominal

linearized model. Additional structured uncertainties can be augmented to these pseudo

uncertainties as in (3.7), and we can apply the same procedure to generate LAR

controllers for such systems. Recall from Example 2.2 the equation of motion of the

system is:

$$\dot{\mathbf{x}} = \mathbf{f}(\mathbf{x}) + \mathbf{g}(\mathbf{x})u \qquad\qquad \text{(E 2.2.2 a)}$$

where:

$$\mathbf{x} = [x_1 \quad x_2 \quad x_3 \quad x_4]^T = [x_1 \quad x_2 \quad \dot{x}_1 \quad \dot{x}_2]^T \qquad\qquad \text{(E 2.2.2 b)}$$

$$\mathbf{f}(\mathbf{x}) = \begin{bmatrix} x_3 \\ x_4 \\ \dfrac{\left\{ \begin{array}{l}(\sin(x_1 - x_2)x_3^2 + 0.2824x_3 - 0.2824x_4 + 48.2776\sin(x_2))\cos(x_1 - x_2) \\ + 0.9833x_3 + 1.1206\sin(x_1 - x_2)x_4^2 - 0.3165x_4 - 214.3082\sin(x_1) \end{array} \right\}}{-5.9809 + \cos^2(x_1 - x_2)} \\ \dfrac{\left\{ \begin{array}{l}(-0.8774x_3 - \sin(x_1 - x_2)x_4^2 + 0.2824x_4 + 191.2383\sin(x_1))\cos(x_1 - x_2) \\ - 5.3371\sin(x_1 - x_2)x_3^2 - 1.5071x_3 + 1.5071x_4 - 257.6614\sin(x_2) \end{array} \right\}}{-5.9809 + \cos^2(x_1\text{-}x_2)} \end{bmatrix}$$

$$\text{(E 2.2.2 c)}$$

$$\mathbf{g}(\mathbf{x}) = \begin{bmatrix} 0 \\ 0 \\ \dfrac{-565.1008}{-5.9809 + \cos^2(x_1 - x_2)} \\ \dfrac{504.2688\cos(x_1\text{-}x_2)}{-5.9809 + \cos^2(x_1 - x_2)} \end{bmatrix} \qquad\qquad \text{(E 2.2.2 d)}$$

For the singular point at the origin of this system, the linearized model of (E 2.2.2) is

given by:

$$\dot{\mathbf{x}} = \begin{bmatrix} 0 & 0 & 1 & 0 \\ 0 & 0 & 0 & 1 \\ 43.0258 & -9.6925 & -0.2541 & 0.1202 \\ -38.3942 & 51.7297 & 0.4787 & -0.3593 \end{bmatrix} \mathbf{x} + \begin{bmatrix} 0 \\ 0 \\ 113.4531 \\ -101.2401 \end{bmatrix} u \qquad \text{(E 2.2.3)}$$

$$\equiv \mathbf{A}_n \mathbf{x} + \mathbf{B}_n u$$

By inspecting (E 2.2.2), we see that the system cannot be described globally by (3.9).

However, it appears that (3.9) can approximate (E 2.2.2) better than (E 2.2.3) in a

region about the origin because (3.9) represents a family of infinitely many models

including (E 2.2.3). We then employ (3.9) to generate a LARC for (E 2.2.2). To obtain

reasonable structured uncertainty specifications for (3.9), we notice that the nominal

linearized model (E 2.2.3) does not include the effects of the following nonlinear terms in

(E 2.2.2 c):

1) $w_1(\mathbf{x}) \equiv \dfrac{\sin(x_1 - x_2)\cos(x_1 - x_2)x_3^2}{-5.9809 + \cos^2(x_1 - x_2)}$ in the third component of $\mathbf{f}(\mathbf{x})$

2) $w_2(\mathbf{x}) \equiv \dfrac{1.1206\sin(x_1 - x_2)x_4^2}{-5.9809 + \cos^2(x_1 - x_2)}$ in the third component of $\mathbf{f}(\mathbf{x})$

3) $w_3(\mathbf{x}) \equiv \dfrac{-\sin(x_1 - x_2)\cos(x_1 - x_2)x_4^2}{-5.9809 + \cos^2(x_1 - x_2)}$ in the forth component of $\mathbf{f}(\mathbf{x})$

4) $w_4(\mathbf{x}) \equiv \dfrac{-5.3371\sin(x_1 - x_2)x_3^2}{-5.9809 + \cos^2(x_1 - x_2)}$ in the forth component of $\mathbf{f}(\mathbf{x})$

This is because linearizing them about the origin produces zeros. It is possible to consider

other nonlinear terms but we omit these because $w_i(\mathbf{x})$, $i = 1,2,3,4$ are sufficient for

demonstrating how to generate a LARC. We are interested in $w_i(\mathbf{x})$ because we know

from numerical simulations in Example 2.2 that when trajectories converge, x_3 (joint

velocity of the lower link) and x_4 (joint velocity of the upper link) are relatively large

when compared to x_1 (joint angle of the lower link) and to x_2 (joint angle of the upper

link). Assuming that this is true for the system under our LARC, we see that neglecting

$w_i(\mathbf{x})$, $i = 1,2,3,4$ can lead to significant modeling error. Based on this assumption, we

now assume a crude operating region in which we desire convergence:

$$\Theta \equiv \{\mathbf{x} \mid \mid x_1 \mid < \frac{\pi}{40}, \mid x_2 \mid < \frac{\pi}{40}, \mid x_3 \mid < 0.5, \text{and} \mid x_4 \mid < 0.5\} \qquad \text{(E 3.3.1)}$$

where we note that $\frac{\pi}{40} = 0.0785 = 4.5°$. After we obtain the LARC and perform numerical

simulations, we shall see that this assumption is valid. Now, we write $w_i(\mathbf{x})$, $i = 1,2,3,4$

as structured uncertainties:

1)   For $w_1(\mathbf{x})$, we obtain:

$$\begin{bmatrix} 0 \\ 0 \\ w_1(\mathbf{x}) \\ 0 \end{bmatrix} = \frac{\sin(x_1 - x_2)\cos(x_1 - x_2)x_3}{-5.9809 + \cos^2(x_1 - x_2)} \begin{bmatrix} 0 & 0 & 0 & 0 \\ 0 & 0 & 0 & 0 \\ 0 & 0 & 1 & 0 \\ 0 & 0 & 0 & 0 \end{bmatrix} \begin{bmatrix} x_1 \\ x_2 \\ x_3 \\ x_4 \end{bmatrix} \qquad \text{(E 3.3.2 a)}$$

$$\equiv h_1^{An}(\mathbf{x})\mathbf{E}_1^{An}\mathbf{x}$$

where $h_1^{An}(\mathbf{x}) \in [h_{l1}^{An}, h_{u1}^{An}]$, $h_{l1}^{An} = \dfrac{\dfrac{1}{2}\sin(\dfrac{\pi}{20})\cos(\dfrac{\pi}{20})}{-5.9809 + \cos^2(\dfrac{\pi}{20})} = -0.0154$,

$$h_{u1}^{An} = \frac{\dfrac{1}{2}\sin(-\dfrac{\pi}{20})\cos(-\dfrac{\pi}{20})}{-5.9809 + \cos^2(-\dfrac{\pi}{20})} = 0.0154, \text{ and } \mathbf{E}_1^{An} \equiv \mathbf{E}_1 = \begin{bmatrix} 0 & 0 & 0 & 0 \\ 0 & 0 & 0 & 0 \\ 0 & 0 & 1 & 0 \\ 0 & 0 & 0 & 0 \end{bmatrix}.$$

2)   For $w_2(\mathbf{x})$, we obtain:

$$
\begin{bmatrix} 0 \\ 0 \\ w_2(\mathbf{x}) \\ 0 \end{bmatrix} = \frac{1.1206\sin(x_1 - x_2)x_4}{-5.9809 + \cos^2(x_1 - x_2)} \begin{bmatrix} 0 & 0 & 0 & 0 \\ 0 & 0 & 0 & 0 \\ 0 & 0 & 0 & 1 \\ 0 & 0 & 0 & 0 \end{bmatrix} \begin{bmatrix} x_1 \\ x_2 \\ x_3 \\ x_4 \end{bmatrix} \qquad \text{(E 3.3.2 b)}
$$

$$
\equiv h_2^{An}(\mathbf{x})\mathbf{E}_2^{An}\mathbf{x}
$$

where $h_2^{An}(\mathbf{x}) \in [h_{l2}^{An}, h_{u2}^{An}]$, $h_{l2}^{An} = \dfrac{\frac{1}{2}1.1206\sin(\frac{\pi}{20})}{-5.9809 + \cos^2(\frac{\pi}{20})} = -0.0175$, and

$$
h_{u2}^{An} = \frac{\frac{1}{2}1.1206\sin(-\frac{\pi}{20})}{-5.9809 + \cos^2(-\frac{\pi}{20})} = 0.0175, \text{ and } \mathbf{E}_2^{An} \equiv \mathbf{E}_2 = \begin{bmatrix} 0 & 0 & 0 & 0 \\ 0 & 0 & 0 & 0 \\ 0 & 0 & 0 & 1 \\ 0 & 0 & 0 & 0 \end{bmatrix}.
$$

3)   For $w_3(\mathbf{x})$, we obtain:

$$
\begin{bmatrix} 0 \\ 0 \\ 0 \\ w_3(\mathbf{x}) \end{bmatrix} = \frac{-\sin(x_1 - x_2)\cos(x_1 - x_2)x_4}{-5.9809 + \cos^2(x_1 - x_2)} \begin{bmatrix} 0 & 0 & 0 & 0 \\ 0 & 0 & 0 & 0 \\ 0 & 0 & 0 & 0 \\ 0 & 0 & 0 & 1 \end{bmatrix} \begin{bmatrix} x_1 \\ x_2 \\ x_3 \\ x_4 \end{bmatrix} \qquad \text{(E 3.3.2 c)}
$$

$$
\equiv h_3^{An}(\mathbf{x})\mathbf{E}_3^{An}\mathbf{x}
$$

where $h_3^{An}(\mathbf{x}) \in [h_{l3}^{An}, h_{u3}^{An}]$, $h_{l3}^{An} = \dfrac{-\frac{1}{2}\sin(-\frac{\pi}{20})\cos(-\frac{\pi}{20})}{-5.9809 + \cos^2(-\frac{\pi}{20})} = -0.0154$,

$$
h_{u3}^{An} = \frac{-\frac{1}{2}\sin(\frac{\pi}{20})\cos(\frac{\pi}{20})}{-5.9809 + \cos^2(\frac{\pi}{20})} = 0.0154, \text{ and } \mathbf{E}_3^{An} \equiv \mathbf{E}_3 = \begin{bmatrix} 0 & 0 & 0 & 0 \\ 0 & 0 & 0 & 0 \\ 0 & 0 & 0 & 0 \\ 0 & 0 & 0 & 1 \end{bmatrix}.
$$

4)   For $w_4(\mathbf{x})$, we obtain:

$$\begin{bmatrix} 0 \\ 0 \\ 0 \\ w_4(\mathbf{x}) \end{bmatrix} = \frac{-5.3371\sin(x_1 - x_2)x_3}{-5.9809 + \cos^2(x_1 - x_2)} \begin{bmatrix} 0 & 0 & 0 & 0 \\ 0 & 0 & 0 & 0 \\ 0 & 0 & 0 & 0 \\ 0 & 0 & 1 & 0 \end{bmatrix} \begin{bmatrix} x_1 \\ x_2 \\ x_3 \\ x_4 \end{bmatrix} \qquad \text{(E 3.3.2 d)}$$

$$\equiv h_4^{An}(\mathbf{x})\mathbf{E}_4^{An}\mathbf{x}$$

where $h_4^{An}(\mathbf{x}) \in [h_{l4}^{An}, h_{u4}^{An}]$, $h_{l4}^{An} = \dfrac{-\dfrac{1}{2}5.3371\sin(-\dfrac{\pi}{20})}{-5.9809 + \cos^2(-\dfrac{\pi}{20})} = -0.0834$,

$$h_{u4}^{An} = \frac{-\dfrac{1}{2}0.0834\sin(\dfrac{\pi}{20})}{-5.9809 + \cos^2(\dfrac{\pi}{20})} = 0.0834, \text{ and } \mathbf{E}_4^{An} \equiv \mathbf{E}_4 = \begin{bmatrix} 0 & 0 & 0 & 0 \\ 0 & 0 & 0 & 0 \\ 0 & 0 & 0 & 0 \\ 0 & 0 & 1 & 0 \end{bmatrix}.$$

Note that $w_i(\mathbf{x})$, $i = 1, 2, 3, 4$ are treated as uncertainties entering $\mathbf{A}_n$:

$$[\Delta\mathbf{A}_n(\mathbf{x})]\mathbf{x} = \sum_{\alpha=1}^{4} [h_\alpha^{An}(\mathbf{x})\mathbf{E}_\alpha^{An}]\mathbf{x} \qquad \text{(E 3.3.3)}$$

To generate a LARC, we want to include the nonlinearities in $\mathbf{g}(\mathbf{x})$ into our considerations. This is because while it is reasonable to employ $\mathbf{B}_n$ in the nominal linearized model to approximate $\mathbf{g}(\mathbf{x})$ in Θ, $[\mathbf{g}(\mathbf{x}) - \mathbf{B}]\mathbf{K}_{LARC} = [\Delta\mathbf{B}_n(\mathbf{x})]\mathbf{K}_{LARC}\mathbf{x}$ may be large in Θ because of the possibility that the resulting $\mathbf{K}_{LARC}$ may be large. To include this possibility into our controller generation, we augment $[\Delta\mathbf{B}_n(\mathbf{x})]\mathbf{K}_{LARC}\mathbf{x}$ to the nominal linearized model as additional structured uncertainties entering $\mathbf{B}_n$. We recall from (3.11):

$$\Delta \mathbf{B}_n(\mathbf{x}) = \begin{bmatrix} 0 \\ 0 \\ \dfrac{-565.1008}{-5.9809 + \cos^2(x_1 - x_2)} - 113.4531 \\ \dfrac{504.2688\cos(x_1 - x_2)}{-5.9809 + \cos^2(x_1 - x_2)} + 101.2401 \end{bmatrix} \equiv \sum_{\beta=1}^{2} [h_\beta^{Bn}(\mathbf{x},t)\mathbf{E}_\beta^{\Delta Bn}]\mathbf{x} \quad \text{(E 3.3.4)}$$

where $h_1^{Bn}(\mathbf{x},t) = \Delta\mathbf{B}_n(\mathbf{x})(3,1)$, $h_2^{Bn}(\mathbf{x},t) = \Delta\mathbf{B}_n(\mathbf{x})(4,1)$, $\mathbf{E}_1^{\Delta Bn} = [0\ 0\ 1\ 0]^T$, and

$\mathbf{E}_2^{\Delta Bn} = [0\ 0\ 0\ 1]^T$. It follows that:

$$-[\Delta\mathbf{B}_n(\mathbf{x})]\mathbf{K}\mathbf{x} = \left[h_1^{Bn}(\mathbf{x},t) \begin{bmatrix} \mathbf{0} \\ \mathbf{0} \\ -\mathbf{K} \\ \mathbf{0} \end{bmatrix} + h_2^{Bn}(\mathbf{x},t) \begin{bmatrix} \mathbf{0} \\ \mathbf{0} \\ \mathbf{0} \\ -\mathbf{K} \end{bmatrix} \right]\mathbf{x} = \sum_{\beta=1}^{2} [h_\beta^{Bn}(\mathbf{x})\mathbf{E}_\beta^{Bn}]\mathbf{x} \quad \text{(E 3.3.5)}$$

where

1) $h_1^{Bn}(\mathbf{x}) \in [h_{l1}^{Bn}, h_{u1}^{Bn}]$

2) $h_2^{Bn}(\mathbf{x}) \in [h_{l2}^{Bn}, h_{u2}^{Bn}]$

3) $h_{l1}^{Bn} = \dfrac{-565.1008}{-5.9809 + \cos^2(\frac{\pi}{20})} - 113.4531 = -0.5547$

4) $h_{u1}^{Bn} = \dfrac{-565.1008}{-5.9809 + \cos^2(0)} - 113.4531 = 0$

5) $h_{l2}^{Bn} = \dfrac{504.2688\cos(0)}{-5.9809 + \cos^2(0)} + 101.2401 = 0,$

6) $h_{u2}^{Bn} = \dfrac{504.2688\cos(\frac{\pi}{20})}{-5.9809 + \cos^2(\frac{\pi}{20})} + 101.2401 = 1.7353$

7) $\mathbf{E}_1^{Bn} = [\mathbf{0}\ \ \mathbf{0}\ \ -\mathbf{K}^T\ \ \mathbf{0}]^T$

8) $\mathbf{E}_2^{Bn} = [\mathbf{0}\ \ \mathbf{0}\ \ \mathbf{0}\ \ -\mathbf{K}^T]^T$.

Using the uncertainty specifications obtained previously, we approximate (E 2.2.2) in Θ

by:

$$\dot{\mathbf{x}} = \left[[\mathbf{A}_n + \sum_{\alpha=1}^{4} [h_\alpha^{A_n}(\mathbf{x})\mathbf{E}_\alpha^{A_n}]] + [-\mathbf{B}_n \mathbf{K} + \sum_{\beta=1}^{2} [h_\beta^{B_n}(\mathbf{x})\mathbf{E}_\beta^{B_n}]] \right] \mathbf{x} \qquad \text{(E 3.3.6)}$$

$$\equiv \left[[\mathbf{A}_n + \Delta\mathbf{A}_n(\mathbf{x})] + [-[\mathbf{B}_n + \Delta\mathbf{B}_n(\mathbf{x})]\mathbf{K}] \right] \mathbf{x}$$

where $\Delta\mathbf{A}_n(\mathbf{x})$ and $-\Delta\mathbf{B}_n(\mathbf{x})\mathbf{K}$ are given by (E 3.3.3) and (E 3.3.5) respectively. Note

that (E 3.3.6) does not represent (E 2.2.2) exactly in Θ but we expect that it approximates

(E 2.2.2) better than (E 2.2.3) does in the same region because of the augmented nonlinear

structured pseudo-uncertainties. We emphasize that $h_\alpha^{A_n}(\mathbf{x})$, $\alpha = 1, 2, 3, 4$ and $h_\beta^{A_n}(\mathbf{x})$,

$\beta = 1, 2$ need not be the corresponding functions given previously. Rather, they can be any

functions that obey the corresponding bounds $[h_{l\alpha}^{A_n}, h_{u\alpha}^{A_n}]$ and $[h_{l\beta}^{B_n}, h_{u\beta}^{B_n}]$. Accordingly,

we see that (E 3.3.6) includes not only the pseudo-uncertainties, but also any uncertainties

obeying such bounds. To generate a LARC for (E 3.3.6), we follow the procedure given in

Section 3.5. Using (2.12), (2.16), and Theorem 3.2, we plot $\lambda_{max}(\mathbf{Z})$ versus $\rho \in \mathfrak{R}^+$ and

$\eta \geq 1$, and determine the minimum of $\lambda_{max}(\mathbf{Z})$ in this plot. We realize that the values of

ρ and η corresponding to this minimum may produce a LARC that requires a large

amount of control energy but we assume in this example that we are not limited by this

factor. When the availability of control energy is limited, we usually want to choose small

values of ρ and η that correspond to a small value of $\lambda_{max}(\mathbf{Z})$ from such plot because

small values of ρ and η usually produce a small $\mathbf{K}_{LARC}$. This will be illustrated in

Example 3.4.

Because we do not know where the minimum of $\lambda_{max}(\mathbf{Z})$ is, we first generate the plot in

a large region of $0.001 \leq \rho \leq 100$ and $1 \leq \eta \leq 100$ using large grids as shown in Fig

E3.3.1. From Fig. E3.3.1, we find that $\lambda_{max}(\mathbf{Z})$ has a local minimum when ρ and η are

small. Accordingly, we reduce the plotting domain to $0.001 \leq \rho \leq 0.1$ and $1 \leq \eta \leq 2.5$, and

plot $\lambda_{max}(\mathbf{Z})$ versus ρ and η as in Fig. E3.3.2. From Fig. E3.3.2, we find that

$\min(\lambda_{max}(\mathbf{Z})) = 0.7220$ occurs at $(\rho, \eta) = (\rho^*, \eta^*) = (0.031, 1.65)$. The plot of $\lambda_{max}(\mathbf{Z})$

versus η when $\rho = \rho^* = 0.031$ is given in Fig. E3.3.3. Using our computer, the

computation time is less than 1 minute.
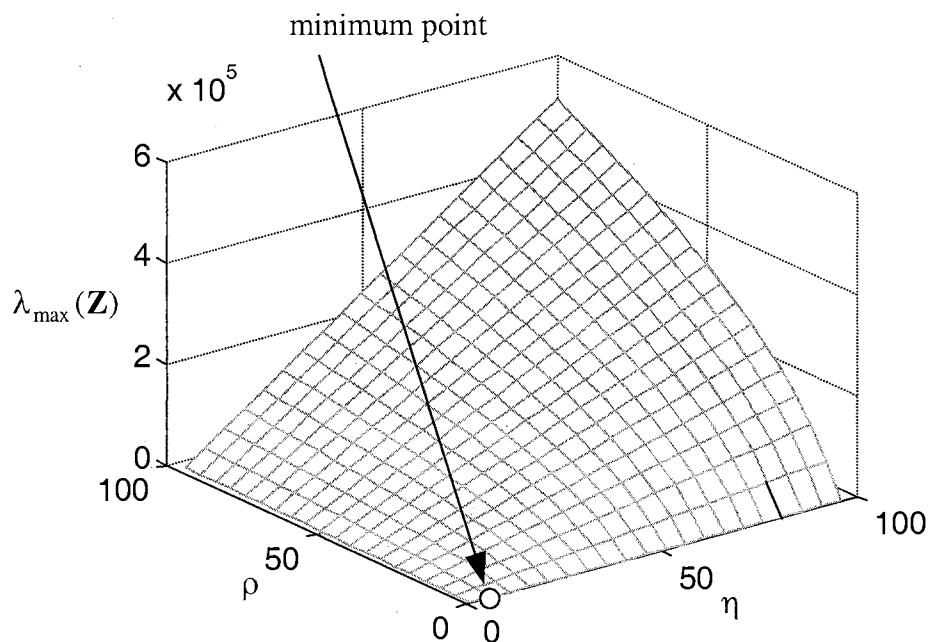
Fig. E3.3.1　A Plot of $\lambda_{max}(\mathbf{Z})$ versus $\rho \in [0.001, 100]$ and $\eta \in [1, 100]$
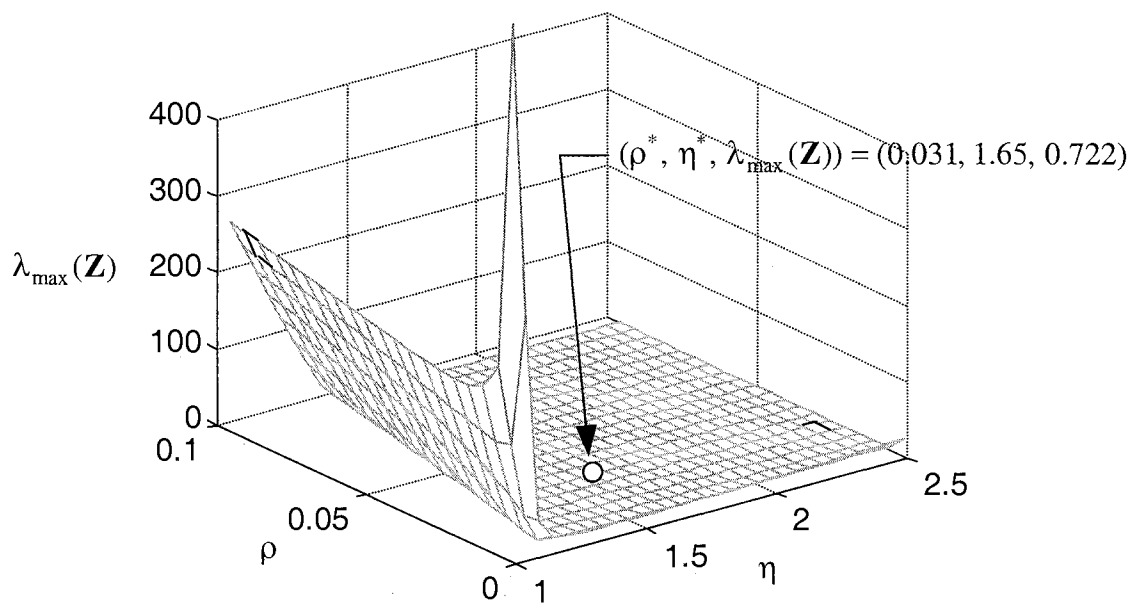
Fig. E3.3.2   A Plot of $\lambda_{max}(\mathbf{Z})$ versus $\rho \in [0.001, 0.1]$ and $\eta \in [1, 2.5]$
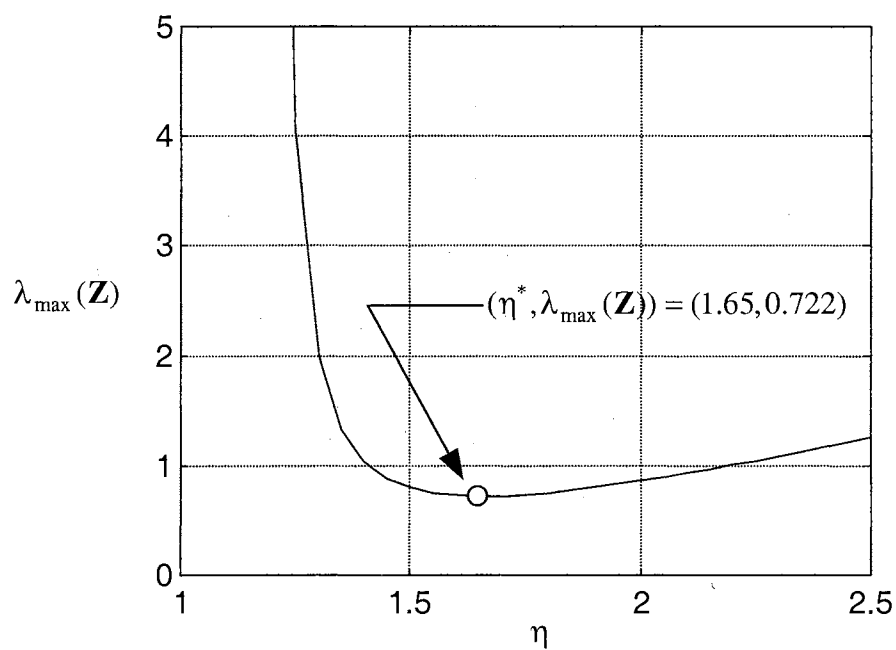
Fig. E3.3.3   A Plot of $\lambda_{max}(\mathbf{Z})$ versus $\eta \in [1, 2.5]$ when $\rho = \rho^* = 0.031$

The minimum point $\lambda_{max}(\mathbf{Z}) = 0.7220$ corresponds to the following matrices:

$$\mathbf{K}_{LARC} = [-0.1141 \quad -7.1286 \quad -0.4935 \quad -1.0932] \qquad \text{(E 3.3.7)}$$

$$\mathbf{Q} = \begin{bmatrix} 1.1002 & 6.2628 & 0.4335 & 0.9604 \\ 6.2628 & 392.3790 & 27.0938 & 60.0187 \\ 0.4335 & 27.0938 & 2.8756 & 4.1549 \\ 0.9604 & 60.0187 & 4.1549 & 10.2040 \end{bmatrix} \qquad \text{(E 3.3.8)}$$

$$\mathbf{P} \equiv \mathbf{P}_{(E3.3.9)} = \begin{bmatrix} 4.5672 & 11.4836 & 1.4703 & 1.6697 \\ 11.4836 & 101.9292 & 10.9763 & 13.6770 \\ 1.4703 & 10.9763 & 1.3090 & 1.5622 \\ 1.6697 & 13.6770 & 1.5622 & 1.9617 \end{bmatrix} \qquad \text{(E 3.3.9)}$$

$$\overline{\mathbf{A}}_n \equiv [\mathbf{A}_n - \mathbf{B}_n \mathbf{K}_{LARC}] = \begin{bmatrix} 0 & 0 & 1 & 0 \\ 0 & 0 & 0 & 1 \\ 55.9675 & 799.0742 & 55.7340 & 124.1461 \\ -49.9428 & -669.9749 & -49.4824 & -111.0340 \end{bmatrix} \quad \text{(E 3.3.10)}$$

where the eigenvalues of $\overline{\mathbf{A}}_n$ are at $\lambda_1 = -43.3035$, $\lambda_{2,3} = -5.0925 \pm j\,2.1912$, and

$\lambda_4 = -1.8116$ in the LHP. Because $\lambda_{max}(\mathbf{Z}) > 0$, the time derivative of the quadratic

Lyapunov function $V(\mathbf{x}) = \dfrac{1}{2}\mathbf{x}^T \mathbf{P}_{(E3.3.9)}\mathbf{x}$ along trajectories of (E 3.3.6) is not

negative definite in Θ. Accordingly, we continue with the simple univariate optimization

technique to search for $\mathbf{K}_{LARC}$ that meets the structured uncertainty specifications. We

start the univariate technique with the initial value for $\mathbf{K}_{LARC}$ and $\mathbf{Q}$ taken from (E 3.3.7)

and (E 3.3.8) respectively. In less than 10 seconds on our computer, the univariate

technique gives a linear gain matrix $\mathbf{K}_{LARC}$ and $\mathbf{Q}$ such that $\lambda_{max}(\mathbf{Z}) < 0$, implying that

the uncertainty specifications are met under such $\mathbf{K}_{LARC}$ and $\mathbf{Q}$. However, we continue to

run the optimization algorithm to decrease $\lambda_{max}(\mathbf{Z})$ further. The algorithm does not

produce better results after it runs for approximately 2 minutes on our computer. At this

point, we obtain:

$$\lambda_{max}(\mathbf{Z}) = -1.7797 \qquad\qquad (E\ 3.3.11)$$

The corresponding matrices are given by:

$$\mathbf{K}_{LARC} \equiv \mathbf{K}_{OLARC} = [-0.0804 \quad -8.6189 \quad -0.5572 \quad -1.1748] \qquad (E\ 3.3.12)$$

$$\mathbf{Q} = \begin{bmatrix} 1.6119 & 13.1838 & 1.2758 & 1.7495 \\ 13.1838 & 332.1778 & 30.3678 & 49.3434 \\ 1.2758 & 30.3678 & 4.7783 & 4.6135 \\ 1.7495 & 49.3434 & 4.6135 & 9.1941 \end{bmatrix} \qquad (E\ 3.3.13)$$

$$\mathbf{P} \equiv \mathbf{P}_{(E3.3.14)} = \begin{bmatrix} 4.6236 & 12.4067 & 1.4066 & 1.6109 \\ 12.4067 & 157.1118 & 17.1767 & 20.6637 \\ 1.4066 & 17.1767 & 2.0826 & 2.4550 \\ 1.6109 & 20.6637 & 2.4550 & 2.9956 \end{bmatrix} \qquad (E\ 3.3.14)$$

$$\overline{\mathbf{A}}_n \equiv [\mathbf{A}_n - \mathbf{B}_n \mathbf{K}_{OLARC}] = \begin{bmatrix} 0 & 0 & 1 & 0 \\ 0 & 0 & 0 & 1 \\ 52.1474 & 968.1484 & 62.9620 & 133.4049 \\ -46.5339 & -820.8486 & -55.9323 & -119.2962 \end{bmatrix} \qquad (E\ 3.3.15)$$

where the eigenvalues of $\overline{\mathbf{A}}_n$ are $\lambda_1 = -39.7642$, $\lambda_2 = -11.8991$, $\lambda_3 = -3.1758$, and

$\lambda_4 = -1.4951$ in the LHP. Because $\lambda_{max}(\mathbf{Z}) < 0$, it follows that the region about the

origin in which the time derivative of the quadratic Lyapunov function $V = \frac{1}{2}\mathbf{x}^T \mathbf{P}_{(E3.3.14)}\mathbf{x}$

along trajectories of (E 3.3.6) is negative definite contains Θ. When $\lambda_{max}(\mathbf{Z}) = 0^-$, we

know from the fundamental idea of LARC that the corresponding LAR is the largest β_C

that can be contained in Θ. For this particular example, $\lambda_{max}(\mathbf{Z}) < 0^-$. Accordingly, the

corresponding LAR is larger than the largest β_C that can be contained in Θ. Note that the

initial value is extremely important for obtaining a solution of the optimization problem.

Indeed, our univariate optimization cannot find a solution $\mathbf{K}_{OLARC}$ that meets the given uncertainty specifications when we employ the same initial value $\mathbf{K}_{LARC}$ in (E 3.3.7) but replace the initial value $\mathbf{Q}$ in (E 3.3.8) by the feasible matrix:

$$\mathbf{Q} = \begin{bmatrix} 1 & 0.1 & 0.1 & 0.1 \\ 0.1 & 1 & 0.1 & 0.1 \\ 0.1 & 0.1 & 1 & 0.1 \\ 0.1 & 0.1 & 0.1 & 1 \end{bmatrix}$$

To estimate the attractive regions corresponding to $\mathbf{K}_{LARC}$ (E 3.3.7) and to $\mathbf{K}_{OLARC}$ (E-3.3.12), we employ numerical simulations. We define convergence and divergence to be the same as those in Example 2.2. These attractive regions are displayed in Table E3.3.1 and E3.3.2 with the attractive region corresponding to $\mathbf{K}_{LQR}$ (Misawa, Arrington, and Ledgerwood, 1995) in Example 2.2. From these tables, it appears that the attractive region corresponding to $\mathbf{K}_{OLARC}$ is the largest while the attractive region corresponding to $\mathbf{K}_{LARC}$ is larger than that corresponding to $\mathbf{K}_{LQR}$. From the tables, we see that the attractive regions corresponding to $\mathbf{K}_{OLARC}$ is larger than Θ. Since a LAR must be contained in Θ, this agrees with a known fact that the attractive region must contain every LAR. We do not present the application of the unstructured uncertainty bound from Theorem 3.3 in this example because the resulting allowable bound is very conservative. This result agrees with those in Example 3.1 and 3.2.

Using the matrices resulting from the univariate technique, we now illustrate the application of Theorem 3.2. Note that internal computing precision is 16 decimal digits but we display only 4 decimal digits for conveniences:

1)   Following (3.18 b), we obtain:

$$\overline{\mathbf{A}}_l \equiv \overline{\mathbf{A}}_n + \sum_{j=1}^{6} h_{lj} \mathbf{E}_j$$

$$= \mathbf{A}_n - \mathbf{B}_n \mathbf{K} + \sum_{\alpha=1}^{4} [h_\alpha^{A_n}(\mathbf{x})\mathbf{E}_\alpha^{A_n}]\mathbf{x} + \sum_{\beta=1}^{2} [h_\beta^{A_n}(\mathbf{x})\mathbf{E}_\beta^{A_n}]\mathbf{x} \qquad \text{(E 3.3.16)}$$

$$= \begin{bmatrix} 0 & 0 & 1 & 0 \\ 0 & 0 & 0 & 1 \\ 52.1028 & 963.3675 & 62.6375 & 132.7357 \\ -46.5339 & -820.8486 & -56.0157 & -119.3116 \end{bmatrix}$$

2)   Following (3.18 c), we obtain:

$$\mathbf{\Phi} = \begin{bmatrix} -3.3493 & -33.8584 & -3.2352 & -4.5745 \\ -33.8584 & -828.5962 & -77.9894 & -122.2360 \\ -3.2352 & -77.9894 & -11.3176 & -11.7048 \\ -4.5745 & -122.2360 & -11.7048 & -21.7660 \end{bmatrix} \qquad \text{(E 3.3.17)}$$

The eigenvalues of $\mathbf{\Phi}$ are $\lambda_1 = -855.4701$, $\lambda_2 = -4.0113$, $\lambda_3 = -3.6898$, and

$\lambda_4 = -1.8579$. So we have $\lambda_{max}(\mathbf{\Phi}) = -1.8579$ and the condition in (3.17 a) is satisfied.

3)   Following (3.18 d), we obtain:

$$\mathbf{\Psi}_1 = \begin{bmatrix} 0 & 0 & 1.4066 & 0 \\ 0 & 0 & 17.1767 & 0 \\ 1.4066 & 17.1767 & 4.1653 & 2.4550 \\ 0 & 0 & 2.4550 & 0 \end{bmatrix} \qquad \text{(E 3.3.18 a)}$$

$$\mathbf{\Psi}_2 = \begin{bmatrix} 0 & 0 & 0 & 1.4066 \\ 0 & 0 & 0 & 17.1767 \\ 0 & 0 & 0 & 2.0826 \\ 1.4066 & 17.1767 & 2.0826 & 4.9099 \end{bmatrix} \qquad \text{(E 3.3.18 b)}$$

$$\mathbf{\Psi}_3 = \begin{bmatrix} 0 & 0 & 0 & 1.6109 \\ 0 & 0 & 0 & 20.6637 \\ 0 & 0 & 0 & 2.4550 \\ 1.6109 & 20.6637 & 2.4550 & 5.9912 \end{bmatrix} \qquad \text{(E 3.3.18 c)}$$

$$\mathbf{\Psi}_4 = \begin{bmatrix} 0 & 0 & 1.6109 & 0 \\ 0 & 0 & 20.6637 & 0 \\ 1.6109 & 20.6637 & 4.9099 & 2.9956 \\ 0 & 0 & 2.9956 & 0 \end{bmatrix} \qquad \text{(E 3.3.18 d)}$$

$$\mathbf{\Psi}_5 = \begin{bmatrix} 0.2262 & 13.5043 & 0.9512 & 1.8498 \\ 13.5043 & 296.0890 & 27.5210 & 41.3384 \\ 0.9512 & 27.5210 & 2.3209 & 3.8146 \\ 1.8498 & 41.3384 & 3.8146 & 5.7682 \end{bmatrix} \qquad \text{(E 3.3.18 e)}$$

$$\mathbf{\Psi}_6 = \begin{bmatrix} 0.2590 & 15.5457 & 1.0950 & 2.1334 \\ 15.5457 & 356.1974 & 32.6730 & 50.0945 \\ 1.0950 & 32.6730 & 2.7358 & 4.5532 \\ 2.1334 & 50.0945 & 4.5532 & 7.0385 \end{bmatrix} \qquad \text{(E 3.3.18 f)}$$

4)   Following (3.18 e), we obtain:

$$\mathbf{T}_{\mathbf{\Psi}_1} = \begin{bmatrix} -0.9967 & 0.0536 & 0.0604 & 0.0000 \\ 0.0800 & 0.6550 & 0.7380 & -0.1415 \\ 0.0000 & 0.7479 & -0.6638 & 0.0000 \\ 0.0114 & 0.0936 & 0.1055 & 0.9899 \end{bmatrix} \qquad \text{(E 3.3.19 a)}$$

$$\mathbf{T}_{\mathbf{\Psi}_2} = \begin{bmatrix} -0.9967 & 0.0531 & -0.0612 & 0.0000 \\ 0.0804 & 0.6488 & -0.7470 & -0.1204 \\ 0.0098 & 0.0787 & -0.0906 & 0.9927 \\ 0.0000 & 0.7550 & 0.6557 & 0.0000 \end{bmatrix} \qquad \text{(E 3.3.19 b)}$$

$$\mathbf{T}_{\mathbf{\Psi}_3} = \begin{bmatrix} -0.9970 & 0.0506 & -0.0583 & 0.0000 \\ 0.0766 & 0.6484 & -0.7482 & -0.1180 \\ 0.0091 & 0.0770 & -0.0889 & 0.9930 \\ 0.0000 & 0.7557 & 0.6550 & 0.0000 \end{bmatrix} \qquad \text{(E 3.3.19 c)}$$

$$\mathbf{T}_{\mathbf{\Psi}_4} = \begin{bmatrix} -0.9970 & 0.0511 & 0.0575 & 0.0000 \\ 0.0761 & 0.6558 & 0.7372 & -0.1435 \\ 0.0000 & 0.7471 & -0.6647 & 0.0000 \\ 0.0110 & 0.0951 & 0.1069 & 0.9897 \end{bmatrix} \qquad \text{(E 3.3.19 d)}$$

$$\mathbf{T_{\Psi_5}} = \begin{bmatrix} 0.0448 & 0.7860 & 0.6160 & 0.1613 \\ 0.9852 & -0.1002 & 0.0504 & -0.1077 \\ 0.0914 & 0.6073 & -0.7851 & -0.3155 \\ 0.1375 & 0.0581 & -0.0396 & 0.9289 \end{bmatrix}$$ (E 3.3.19 e)

$$\mathbf{T_{\Psi_6}} = \begin{bmatrix} 0.0429 & 0.7809 & -0.5095 & 0.0337 \\ 0.9853 & -0.1018 & 0.0221 & 0.1265 \\ 0.0903 & 0.6104 & 0.7208 & 0.1148 \\ 0.1386 & 0.0848 & -0.4694 & -0.9847 \end{bmatrix}$$ (E 3.3.19 f)

$$\mathbf{\Psi}_1^D = \mathrm{diag}\,[0 \quad 19.6150 \quad -15.4497 \quad 0]$$ (E 3.3.20 a)

$$\mathbf{\Psi}_2^D = \mathrm{diag}\,[0 \quad 19.9873 \quad -15.0774 \quad 0]$$ (E 3.3.20 b)

$$\mathbf{\Psi}_3^D = \mathrm{diag}\,[0 \quad 24.0808 \quad -18.0896 \quad 0]$$ (E 3.3.20 c)

$$\mathbf{\Psi}_4^D = \mathrm{diag}\,[0 \quad 23.5402 \quad -18.6302 \quad 0]$$ (E 3.3.20 d)

$$\mathbf{\Psi}_5^D = \mathrm{diag}\,[305.0279 \quad -0.6236 \quad 0 \quad 0]$$ (E 3.3.20 e)

$$\mathbf{\Psi}_6^D = \mathrm{diag}\,[366.9107 \quad -0.6800 \quad 0 \quad 0]$$ (E 3.3.20 f)

5)   Following (3.18 f), we obtain:

$$\mathbf{\Psi}_1^{D,0+} = \mathrm{diag}\,[0 \quad 19.6150 \quad 0 \quad 0]$$ (E 3.3.21 a)

$$\mathbf{\Psi}_2^{D,0+} = \mathrm{diag}\,[0 \quad 19.9873 \quad 0 \quad 0]$$ (E 3.3.21 b)

$$\mathbf{\Psi}_3^{D,0+} = \mathrm{diag}\,[0 \quad 24.0808 \quad 0 \quad 0]$$ (E 3.3.21 c)

$$\mathbf{\Psi}_4^{D,0+} = \mathrm{diag}\,[0 \quad 23.5402 \quad 0 \quad 0]$$ (E 3.3.21 d)

$$\mathbf{\Psi}_5^{D,0+} = \mathrm{diag}\,[305.0279 \quad 0 \quad 0 \quad 0]$$ (E 3.3.21 e)

$$\mathbf{\Psi}_6^{D,0+} = \mathrm{diag}\,[366.9107 \quad 0 \quad 0 \quad 0]$$ (E 3.3.21 f)

6)   Following (3.18 g), we obtain:

$$\mathbf{\Psi}_1^{0+} = \begin{bmatrix} 0.0564 & 0.6890 & 0.7868 & 0.0985 \\ 0.6890 & 8.4142 & 9.6086 & 1.2026 \\ 0.7868 & 9.6086 & 10.9725 & 1.3733 \\ 0.0985 & 1.2026 & 1.3733 & 0.1719 \end{bmatrix}$$ (E 3.3.22 a)

$$\mathbf{\Psi}_2^{0+} = \begin{bmatrix} 0.0564 & 0.6890 & 0.0835 & 0.8018 \\ 0.6890 & 8.4142 & 1.0202 & 9.7910 \\ 0.0835 & 1.0202 & 0.1237 & 1.1871 \\ 0.8018 & 9.7910 & 1.1871 & 11.3930 \end{bmatrix} \tag{E 3.3.22 b}$$

$$\mathbf{\Psi}_3^{0+} = \begin{bmatrix} 0.0615 & 0.7894 & 0.0938 & 0.9199 \\ 0.7894 & 10.1254 & 1.2030 & 11.7997 \\ 0.0938 & 1.2030 & 0.1429 & 1.4019 \\ 0.9199 & 11.7997 & 1.4019 & 13.7510 \end{bmatrix} \tag{E 3.3.22 c}$$

$$\mathbf{\Psi}_4^{0+} = \begin{bmatrix} 0.0615 & 0.7894 & 0.8992 & 0.1144 \\ 0.7894 & 10.1254 & 11.5348 & 1.4679 \\ 0.8992 & 11.5348 & 13.1405 & 1.6722 \\ 0.1144 & 1.4679 & 1.6722 & 0.2128 \end{bmatrix} \tag{E 3.3.22 d}$$

$$\mathbf{\Psi}_5^{0+} = \begin{bmatrix} 0.6114 & 13.4552 & 1.2489 & 1.8783 \\ 13.4552 & 296.0953 & 27.4830 & 41.3347 \\ 1.2489 & 27.4830 & 2.5509 & 3.8366 \\ 1.8783 & 41.3347 & 3.8366 & 5.7703 \end{bmatrix} \tag{E 3.3.22 e}$$

$$\mathbf{\Psi}_6^{0+} = \begin{bmatrix} 0.6737 & 15.4916 & 1.4191 & 2.1784 \\ 15.4916 & 356.2044 & 32.6307 & 50.0886 \\ 1.4191 & 32.6307 & 2.9892 & 4.5885 \\ 2.1784 & 50.0886 & 4.5885 & 7.0433 \end{bmatrix} \tag{E 3.3.22 f}$$

7)   Following (3.18 h), we obtain:

$$\mathbf{Z} \equiv \mathbf{\Phi} + \sum_{j=1}^{6} [(h_{uj} - h_{lj})\mathbf{\Psi}_j^{0+}] = \begin{bmatrix} -1.8251 & 0.6891 & 0.1002 & 0.3261 \\ 0.6891 & -43.6762 & -3.8277 & -11.4009 \\ 0.1002 & -3.8277 & -2.1770 & -1.2084 \\ 0.3261 & -11.4009 & -1.2084 & -5.4798 \end{bmatrix} \tag{E 3.3.23}$$

It can be shown that the eigenvalues of $\mathbf{Z}$ are $\lambda_1 = -47.1905$, $\lambda_2 = -2.4052$,

$\lambda_3 = -1.7827$, and $\lambda_4 = -1.7797$. Accordingly, we have that $\lambda_{\max}(\mathbf{Z}) = -1.7797 < 0$ and

(3.17 b) is satisfied.

			x_2																							
			.325					0.3					.275					0.25					.225				
			x_4																								
			-0.5	-.25	0	0.25	0.5	-0.5	-.25	0	0.25	0.5	-0.5	-.25	0	0.25	0.5	-0.5	-.25	0	0.25	0.5	-0.5	-.25	0	0.25	0.5
x_1	.325	x_3	-0.5																									
			-.25																									
			0																									
			0.25																									
			0.5																									
	0.3		-0.5																									
			-.25																									
			0																									
			0.25																									
			0.5																									
	.275		-0.5																									
			-.25																									
			0																									
			0.25																									
			0.5																									
	0.25		-0.5																									
			-.25																									
			0																									
			0.25																									
			0.5																									
	.225		-0.5																									
			-.25																									
			0																									
			0.25																									
			0.5																									

Table E3.3.1 Simulation Results of the Double Inverted Pendulum System in Regions farther from the Origin ($x_1 > 0$, $x_2 > 0$)

Remark: Attractive regions do not differ significantly in small regions about the origin.

Legends: ■ ≡ LQR, LARC, and OLARC systems converge, ▨ ≡ LARC, and OLARC systems converge
▧ ≡ OLARC system converges, □ ≡ All system diverge

				x_2																					
				0.45					.425					0.4					.375					0.35				
				x_4																					
x_1		x_3		-0.5	-.25	0	0.25	0.5	-0.5	-.25	0	0.25	0.5	-0.5	-.25	0	0.25	0.5	-0.5	-.25	0	0.25	0.5	-0.5	-.25	0	0.25	0.5
	-0.45		-0.5																									
			-0.25																									
			0																									
			0.25																									
			0.5																									
	-.425		-0.5																									
			-0.25																									
			0																									
			0.25																									
			0.5																									
	-.40		-0.5																									
			-0.25																									
			0																									
			0.25																									
			0.5																									
	-.375		-0.5																									
			-0.25																									
			0																									
			0.25																									
			0.5																									
	-0.35		-0.5																									
			-0.25																									
			0																									
			0.25																									
			0.5																									

Table E3.3.2 Simulation Results of the Double Inverted Pendulum System in Regions farther from the Origin ($x_1 < 0$, $x_2 > 0$)

Remark: Attractive regions do not differ significantly in small regions about the origin.

Legends: ■ ≡ LQR, LARC, and OLARC systems converge, ▨ ≡ LARC, and OLARC systems converge
▩ ≡ OLARC system converges, □ ≡ All system diverge

Example 3.4   (A Fighter Aircraft)

In this example, we consider the problem of stabilizing the longitudinal short period

mode of a fighter aircraft about two operating points (Schmitendorf, 1988), (Chen, and

Chen, 1991). We assume that the available control energy is limited and thus we require

that every element of our linear state-feedback gain matrix be small. The dynamics at

mach = 0.5 and altitude = 5000 feet, and at mach = 0.9 and altitude = 35,000 feet are

given by (E 3.4.1 a) and (E 3.4.1 b) respectively:

$$\dot{x} = [\mathbf{A}_n + \Delta\mathbf{A}_C]\mathbf{x} + [\mathbf{B}_n + \Delta\mathbf{B}_C]u \qquad\qquad \text{(E 3.4.1 a)}$$

$$\dot{x} = [\mathbf{A}_n - \Delta\mathbf{A}_C]\mathbf{x} + [\mathbf{B}_n - \Delta\mathbf{B}_C]u \qquad\qquad \text{(E 3.4.1 b)}$$

where $\mathbf{x} = [x_1 \quad x_2 \quad x_3]^T$, x_1 = normal acceleration, x_2 = pitch rate, x_3 = elevator

angle, u = elevator control, $\mathbf{A}_n = \begin{bmatrix} -0.8251 & 17.76 & 90.245 \\ 0.1734 & -0.7549 & -11.1 \\ 0 & 0 & -250 \end{bmatrix}$ is unstable,

$$\Delta\mathbf{A}_C = \begin{bmatrix} -0.1645 & -0.35 & 5.905 \\ 0.0914 & -0.0963 & -0.29 \\ 0 & 0 & 0 \end{bmatrix}, \mathbf{B}_n = \begin{bmatrix} -91.44 \\ 0 \\ 250 \end{bmatrix}, \text{and } \Delta\mathbf{B}_C = \begin{bmatrix} -6.34 \\ 0 \\ 0 \end{bmatrix}.$$

In (Schmitendorf, 1988), the system is modeled as:

$$\dot{x} = [\mathbf{A}_n + \Delta\mathbf{A}_n(\mathbf{x})]\mathbf{x} + [\mathbf{B}_n + \Delta\mathbf{B}_n(\mathbf{x})]u \qquad\qquad \text{(E 3.4.2 a)}$$

$$\Delta\mathbf{A}_n(\mathbf{x}) = h_1^{An}(\mathbf{x},t)\mathbf{E}_1^{An} + h_2^{An}(\mathbf{x},t)\mathbf{E}_2^{An} \qquad\qquad \text{(E 3.4.2 b)}$$

$$\Delta\mathbf{B}_n(\mathbf{x}) = h_1^{Bn}(\mathbf{x},t)\mathbf{E}_1^{\Delta Bn} \qquad\qquad \text{(E 3.4.2 c)}$$

where $\mathbf{E}_1^{An} = \begin{bmatrix} -0.1645 & -0.35 & 5.905 \\ 0 & 0 & 0 \\ 0 & 0 & 0 \end{bmatrix}, \mathbf{E}_2^{An} = \begin{bmatrix} 0 & 0 & 0 \\ 0.0914 & -0.0963 & -0.29 \\ 0 & 0 & 0 \end{bmatrix},$

$$\mathbf{E}_1^{\Delta Bn} = \begin{bmatrix} -6.34 \\ 0 \\ 0 \end{bmatrix}, \ h_1^{An}(\mathbf{x},t) \in [-1,1], \ h_2^{An}(\mathbf{x},t) \in [-1,1], \text{ and } h_1^{Bn}(\mathbf{x},t) \in [-1,1]. \text{ When the}$$

system is modeled as (E3.4.2), we see that the uncertainties in $\mathbf{A}_n$ are assumed to enter

each row of $\mathbf{A}_n$ proportionally. The solution from (Schmitendorf, 1988) is:

$$\mathbf{K}_{[Sch]} = [0.593 \quad 1.8965 \quad -0.642] \tag{E 3.4.3}$$

Reference (Chen, and Chen, 1991) refers to (Schmitendorf, 1988) and reports the

stabilizing solution gain matrix:

$$\mathbf{K}_{[CC]} = [0.2556 \quad 0.3595 \quad 0.1370] \tag{E 3.4.4}$$

We say that $\mathbf{K}_{[CC]}$ is "smaller" than $\mathbf{K}_{[Sch]}$ because each element of $\mathbf{K}_{[CC]}$ is smaller

than the respective one in $\mathbf{K}_{[Sch]}$. In this particular example, $\mathbf{K}_{[CC]}$ is preferable because

the control energy is limited. <u>Our objective is to show that our LARC can handle more</u>

<u>general and stronger uncertainties with a smaller gain matrix</u>. We now cast the problem

in a more general form, allowing the uncertainties to enter $\mathbf{A}_n$ independently. In this

case, the dynamics of the uncertain system are:

$$\begin{aligned}
\dot{\mathbf{x}} &= [\mathbf{A}_n + \sum_{\alpha=1}^{6} [h_\alpha^{An}(\mathbf{x},t)\mathbf{E}_\alpha^{An}]]\mathbf{x} - [\mathbf{B}_n + h_1^{Bn}(\mathbf{x},t)\mathbf{E}_1^{\Delta Bn}]\mathbf{K}\mathbf{x} \\
&= [\mathbf{A}_n + \sum_{\alpha=1}^{6} [h_\alpha^{An}(\mathbf{x},t)\mathbf{E}_\alpha^{An}]]\mathbf{x} + [-\mathbf{B}_n\mathbf{K} + h_1^{Bn}(\mathbf{x},t)\mathbf{E}_1^{Bn}]\mathbf{x}
\end{aligned} \tag{E 3.4.5}$$

where $\mathbf{E}_1^{An} = \begin{bmatrix} 1 & 0 & 0 \\ 0 & 0 & 0 \\ 0 & 0 & 0 \end{bmatrix}, \ \mathbf{E}_2^{An} = \begin{bmatrix} 0 & 1 & 0 \\ 0 & 0 & 0 \\ 0 & 0 & 0 \end{bmatrix}, \ \mathbf{E}_3^{An} = \begin{bmatrix} 0 & 0 & 1 \\ 0 & 0 & 0 \\ 0 & 0 & 0 \end{bmatrix}, \ \mathbf{E}_4^{An} = \begin{bmatrix} 0 & 0 & 0 \\ 1 & 0 & 0 \\ 0 & 0 & 0 \end{bmatrix},$

$\mathbf{E}_5^{An} = \begin{bmatrix} 0 & 0 & 0 \\ 0 & 1 & 0 \\ 0 & 0 & 0 \end{bmatrix}, \ \mathbf{E}_6^{An} = \begin{bmatrix} 0 & 0 & 0 \\ 0 & 0 & 1 \\ 0 & 0 & 0 \end{bmatrix}, \ \mathbf{E}_1^{\Delta Bn} = \begin{bmatrix} 1 \\ 0 \\ 0 \end{bmatrix}, \ \mathbf{E}_1^{Bn} = \begin{bmatrix} -\mathbf{K} \\ 0 \\ 0 \end{bmatrix}, \ h_1^{An}(\mathbf{x},t) \in [-0.1645,$

$,0.1645]$, $h_2^{A_n}(\mathbf{x},t) \in [-0.35, 0.35]$, $h_3^{A_n}(\mathbf{x},t) \in [-5.905, 5.905]$, $h_4^{A_n}(\mathbf{x},t) \in [-0.0914,$

$,0.0914]$, $h_5^{A_n}(\mathbf{x},t) \in [-0.0963, 0.0963]$, $h_6^{A_n}(\mathbf{x},t) \in [-0.29, 0.29]$, and $h_1^{B_n}(\mathbf{x},t) \in [-6.34$

$,6.34]$.

To generate a LARC for this uncertain system, we start the "second" procedure by

generating a three-dimension plot of $\lambda_{max}(\mathbf{Z})$ versus ρ and η, and determine from this

plot if there exists a particular (ρ, η) such that $\lambda_{max}(\mathbf{Z}) < 0$. A plot of $\lambda_{max}(\mathbf{Z})$ in a

region of ρ and η is shown in Fig. E3.4.1, from which we see that the minimum of

$\lambda_{max}(\mathbf{Z})$ is nonnegative. We emphasize that the sign of $\lambda_{max}(\mathbf{Z})$ for large values of ρ

and η need not be examined because these correspond to large gain matrices.
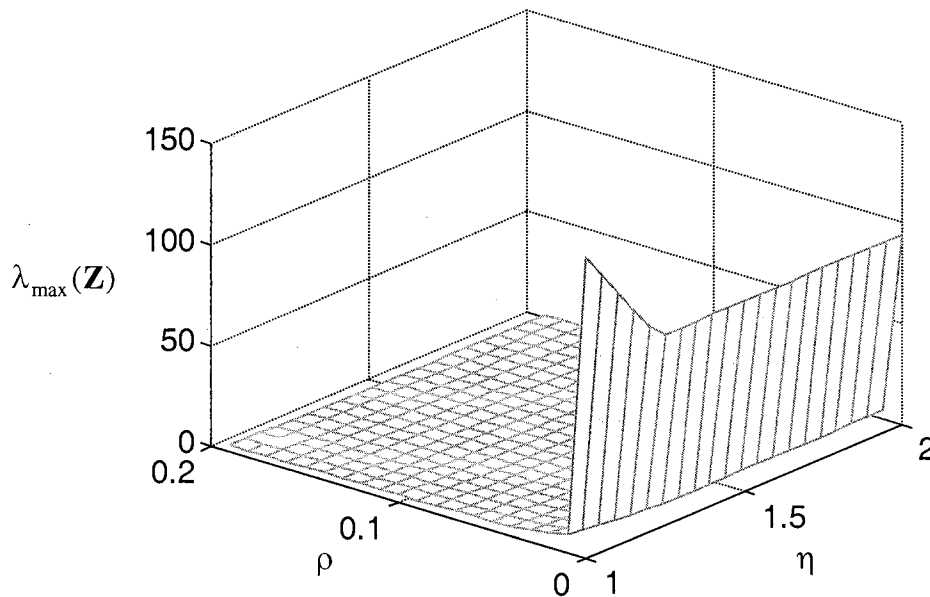
Fig. E3.4.1 A Plot of $\lambda_{max}(\mathbf{Z})$ versus $\rho \in [0.0001, 0.2]$ and $\eta \in [1,2]$

Because the minimum of $\lambda_{\max}(\mathbf{Z})$ in Fig. E3.4.1 is nonnegative, we enter the second

phase of the procedure in which optimization is employed to find a gain matrix that meets

the given uncertainty specifications. To find an initial value for such optimization, we

normally select from this plot (ρ,η) at which $\lambda_{\max}(\mathbf{Z})$ is small because we want to

minimize $\lambda_{\max}(\mathbf{Z})$. Fig. E3.4.1 shows that $\lambda_{\max}(\mathbf{Z})$ is small when (ρ,η) is large.

However, direct computations show that a large (ρ,η) corresponds to a large $\mathbf{K}_{LARC}$.

Since the solution $\mathbf{K}_{LARC}$ for this problem is required to be small, we need to trade a

larger $\lambda_{\max}(\mathbf{Z})$ for a smaller (ρ,η). Now, we notice from Fig. E3.4.1 that $\lambda_{\max}(\mathbf{Z})$

decreases sharply in regions where ρ and η are small. This suggests that we examine the

plot in such regions to do the trade-off. Using our computer, it takes approximately 5

seconds to produce the plot of $\lambda_{\max}(\mathbf{Z})$ shown in Fig. E3.4.2 and Fig. E3.4.3.
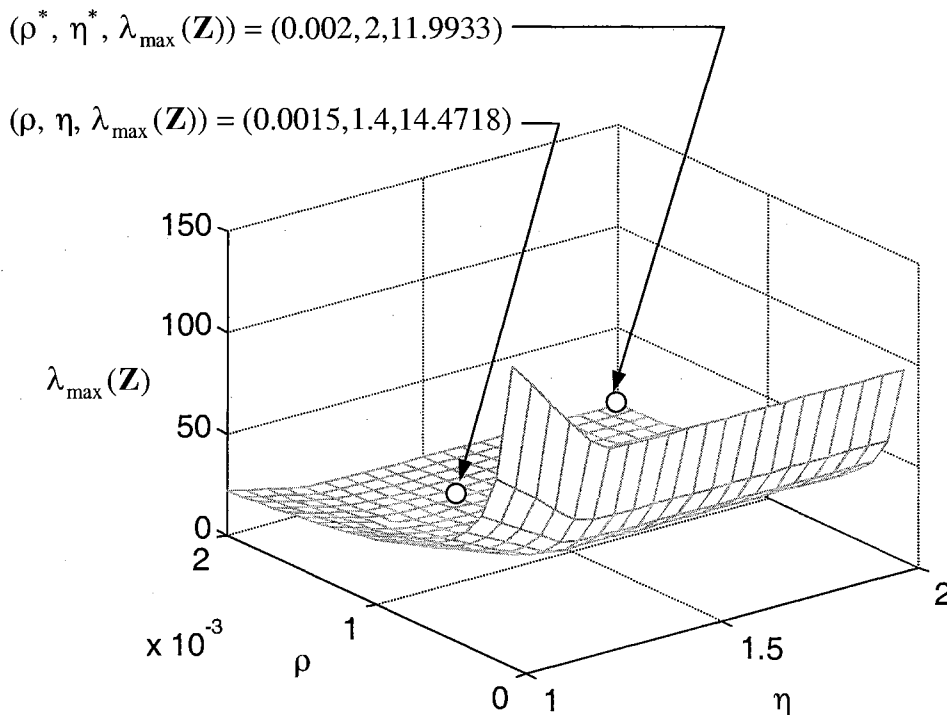
Fig. E3.4.2 A Plot of $\lambda_{max}(\mathbf{Z})$ versus $\rho \in [0.0001, 0.002]$ and $\eta \in [1, 2]$
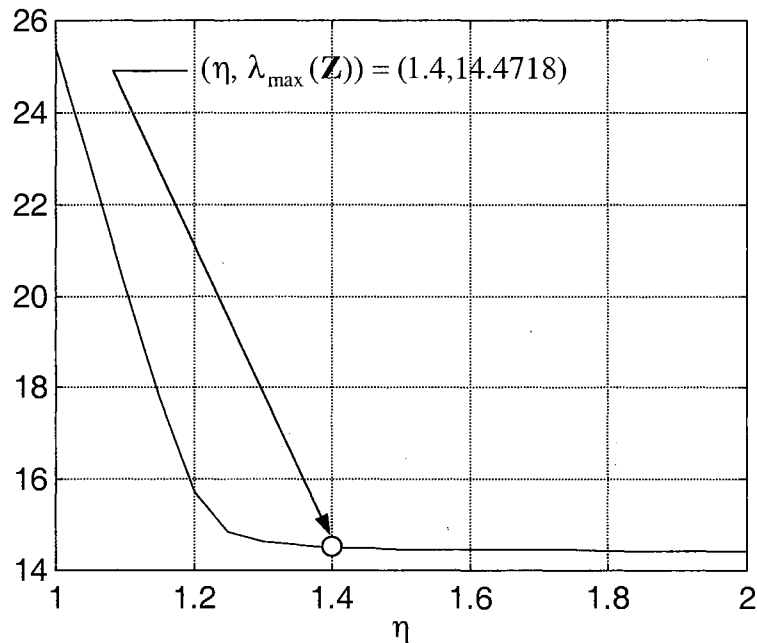
Fig. E3.4.3 A Plot of $\lambda_{max}(\mathbf{Z})$ versus $\eta \in [1, 2]$ when $\rho = 0.0015$

The minimum value of $\lambda_{max}(\mathbf{Z}) = 11.9933$ in Fig. E3.4.2 is at $(\rho^*, \eta^*) = (0.002, 2)$. We

examine Fig. E3.4.2 and find that a portion of the plot is flat. In this flat portion, reducing

the values of ρ and η does not increase the value of $\lambda_{max}(\mathbf{Z})$ significantly. Accordingly,

we select from this flat portion $(\rho, \eta) = (0.0015, 1.4)$ corresponding to

$\lambda_{max}(\mathbf{Z}) = 14.4718$ and employ this (ρ, η) to generate $\{\mathbf{K}_{LARC}, \mathbf{Q}\}$ as an initial value for

our optimization routine. Other points in this flat portion having small $\lambda_{max}(\mathbf{Z})$ can be

selected for this purpose as well. To investigate effects of different initial values, we start

our optimization routine from the initial values corresponding to $(\rho^*, \eta^*) = (0.002, 2)$ and

to $(\rho, \eta) = (0.0015, 1.4)$. Using Lemma 2.3, the initial value $\{\mathbf{K}_{LARC,1}, \mathbf{Q}\}$ corresponding

to $(\rho^*, \eta^*) = (0.002, 2)$ is given by:

$$\mathbf{K}_{LARC,1} = [-0.0817 \quad -0.4451 \quad -0.0055] \qquad \text{(E 3.4.6 a)}$$

$$\mathbf{Q} = \begin{bmatrix} 1.8342 & 4.5452 & 0.0559 \\ 4.5452 & 25.7659 & 0.3046 \\ 0.0559 & 0.3046 & 1.0037 \end{bmatrix} \qquad \text{(E 3.4.6 b)}$$

In the same fashion, the initial value $\{\mathbf{K}_{LARC,2}, \mathbf{Q}\}$ corresponding to

$(\rho, \eta) = (0.0015, 1.4)$ is given by:

$$\mathbf{K}_{LARC,2} = [-0.0500 \quad -0.2886 \quad -0.0030] \qquad \text{(E 3.4.7 a)}$$

$$\mathbf{Q} = \begin{bmatrix} 1.3398 & 1.9624 & 0.0204 \\ 1.9624 & 12.3335 & 0.1177 \\ 0.0204 & 0.1177 & 1.0012 \end{bmatrix} \qquad \text{(E 3.4.7 b)}$$

Notice that the gain matrix corresponding to $(\rho^*, \eta^*) = (0.002, 2)$ is relatively larger than

that corresponding to $(\rho, \eta) = (0.0015, 1.4)$. Applying the univariate optimization to

Theorem 3.2, it takes our PC approximately 1 minute to find a solution corresponding to

the initial value in (E 3.4.6):

$$\mathbf{K}_{OLARC,1} = [-0.0825 \quad -0.4451 \quad -0.0055] \qquad \text{(E 3.4.8 a)}$$

$$\mathbf{Q} = \begin{bmatrix} 0.2336 & 0.6211 & 0.0396 \\ 0.6211 & 4.0120 & 0.2410 \\ 0.0396 & 0.2410 & 0.9833 \end{bmatrix} \qquad \text{(E 3.4.8 b)}$$

The solution $\mathbf{K}_{OLARC,1}$ in (E 3.4.8) corresponds to $\lambda_{\max}(\mathbf{Z}) = -0.0101$. In the same

fashion, it takes our PC approximately 1 minute to find a solution corresponding to the

initial value in (E 3.4.7). This solution is given by:

$$\mathbf{K}_{OLARC,2} = [-0.0715 \quad -0.2886 \quad -0.0030]$$

(E 3.4.9 a)

$$\mathbf{Q} = \begin{bmatrix} 0.1209 & 0.2316 & 0.0090 \\ 0.2316 & 0.9881 & 0.0188 \\ 0.0090 & 0.0188 & 0.5874 \end{bmatrix}$$

(E 3.4.9 b)

The solution $\mathbf{K}_{OLARC,2}$ in (E 3.4.9) corresponds to $\lambda_{\max}(\mathbf{Z}) = -0.0108$. Notice that the

solution $\mathbf{K}_{OLARC,2}$ is smaller than $\mathbf{K}_{[65]}$ in (E 3.4.3), $\mathbf{K}_{[60]}$ in (E 3.4.4), and $\mathbf{K}_{OLARC,1}$

(E 3.4.8 a). We see from this particular example that a small initial gain matrix can lead

to a small solution gain matrix.

For this particular example, we want to show further that our "second" procedure can

generate a LARC to meet increased uncertainty specifications with a small state-feedback

gain matrix. For this purpose, we assume that the variations in $h_\alpha^{An}(\mathbf{x},t)$, $\alpha = 1, 2, \ldots, 6$

and $h_1^{Bn}(\mathbf{x},t)$ increase by 25 %. We now have:

$$h_1^{An}(\mathbf{x},t) \in 1.25[-0.1645, 0.1645], \quad h_2^{An}(\mathbf{x},t) \in 1.25[-0.35, 0.35], \ldots,$$

$$h_6^{An}(\mathbf{x},t) \in 1.25[-0.29, 0.29], \text{ and } h_1^{Bn}(\mathbf{x},t) \in 1.25[-6.34, 6.34]$$

(E 3.4.10)

We reapply the second procedure by plotting $\lambda_{\max}(\mathbf{Z})$ versus ρ and η according to the

increased structured uncertainty specifications. The plot is given in Fig. E3.4.4. It is clear

that the minimum of $\lambda_{\max}(\mathbf{Z})$ in this plot is greater than zero and thus we employ

optimization to find a small gain matrix that meets the increased specifications. In the

same fashion, we see that this plot has a flat portion, and we select from this portion a

point at which ρ, η, and $\lambda_{\max}(\mathbf{Z})$ are small to generate an initial value for the optimization

routine. We select from this portion the same coordinate $(\rho, \eta) = (0.0015, 1.4)$, which

now corresponds to $\lambda_{max}(\mathbf{Z}) = 18.7552$.

$(\rho, \eta, \lambda_{max}(\mathbf{Z})) = (0.0015, 1.4, 18.7552)$
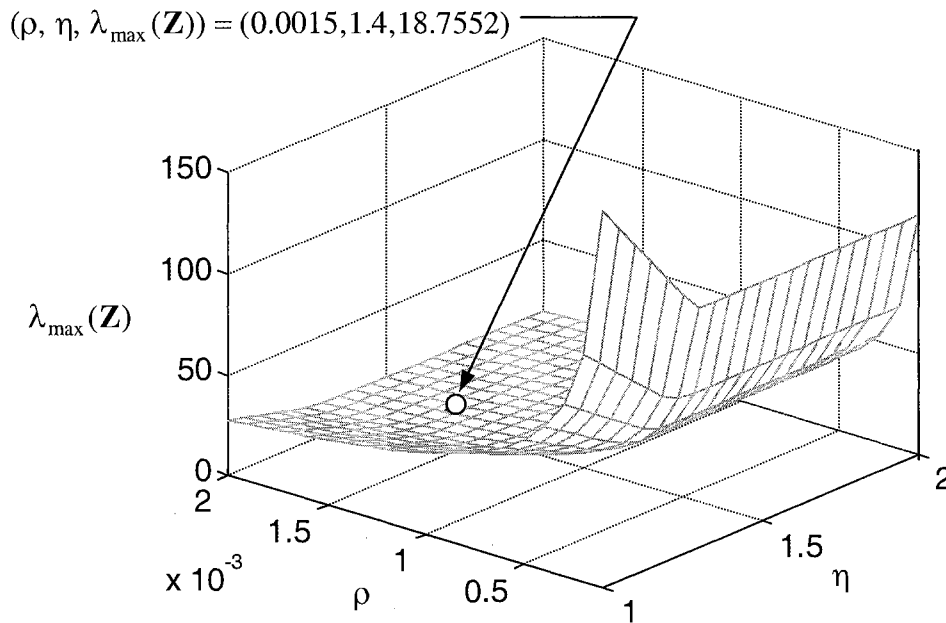
Fig. E3.4.4   A Plot of $\lambda_{max}(\mathbf{Z})$ versus $\rho \in [0.0001, 0.002]$ and $\eta \in [1, 2]$

We have seen that $(\rho, \eta) = (0.0015, 1.4)$ corresponds to the initial value $\{\mathbf{K}_{LARC,2}, \mathbf{Q}\}$ in

(E 3.4.7). Using this initial value, we apply the univariate optimization to Theorem 3.2

and obtain the solution:

$$\mathbf{K}_{OLARC,3} = [-0.0939 \quad -0.4451 \quad -0.0055] \qquad \text{(E 3.4.11 a)}$$

$$\mathbf{Q} = \begin{bmatrix} 0.2623 & 0.5707 & 0.0327 \\ 0.5707 & 2.2043 & 0.1089 \\ 0.0327 & 0.1089 & 1.1397 \end{bmatrix} \qquad \text{(E 3.4.11 b)}$$

This solution corresponds to $\lambda_{max}(\mathbf{Z}) = -0.0101$ and a computation time of

approximately 1 minute. Continue running the optimization routine yields the minimum

value of $\lambda_{max}(\mathbf{Z}) = -0.1403$, which corresponds to:

$$\mathbf{K}_{OLARC,4} = [-0.1635 \quad -0.5303 \quad -0.4297]$$

(E 3.4.12 a)

$$\mathbf{Q} = \begin{bmatrix} 0.3498 & 0.5817 & 0.0399 \\ 0.5817 & 1.6964 & 0.0043 \\ 0.0399 & 0.0043 & 0.9250 \end{bmatrix}$$

(E 3.4.12 b)

The total computation time is approximately 2 minutes. Since we require that the linear gain matrix be small, we select the solution $\mathbf{K}_{OLARC,3}$ in (E 3.4.11 a) for the increased uncertainties. Because the gain matrices $\mathbf{K}_{OLARC,3}$ and $\mathbf{K}_{OLARC,4}$ are such that $\lambda_{max}(\mathbf{Z}) < 0$, we know that they can stabilize the system when the uncertainties are increased by more than 25 %. We do not pursue this further because it appears that the present results are satisfactory.

Example 3.5 (The Cart-and-Pole System with Force Control on Cart)

In this example, we generate a robust LARC for stabilizing the cart-and-pole system in Example 2.2 about the origin. We treat nonlinearities as "pseudo" structured uncertainties entering the nominal linearized model as in Example 3.3. Additional structured uncertainties can be augmented to these pseudo uncertainties as in (3.7), and we can apply the same procedure to generate LAR controllers for such systems. Recall the equation of motion of the system from (E 2.3.2):

$$\dot{\mathbf{x}} = \mathbf{f}(\mathbf{x}) + \mathbf{g}(\mathbf{x})u \qquad \text{(E 2.3.2 a)}$$

where:

$$\mathbf{x} = [x_1 \quad x_2 \quad x_3 \quad x_4]^T = [x_1 \quad x_2 \quad \dot{x}_1 \quad \dot{x}_2]^T \qquad \text{(E 2.3.2 b)}$$

$$\mathbf{f}(\mathbf{x}) = \begin{bmatrix} x_3 \\ x_4 \\ \dfrac{ml\sin(x_2)x_4^2 - mg\sin(x_2)\cos(x_2)}{(M+\sin^2(x_2)m)} \\ \dfrac{(m+M)g\sin(x_2)}{(M+\sin^2(x_2)m)l} - \dfrac{\cos(x_2)m\sin(x_2)x_4^2}{(M+\sin^2(x_2)m)} \end{bmatrix} \qquad \text{(E 2.3.2 c)}$$

$$\mathbf{g}(\mathbf{x}) = \begin{bmatrix} 0 \\ 1 \\ \dfrac{1}{M+\sin^2(x_2)m} \\ -\dfrac{\cos(x_2)}{(M+\sin^2(x_2)m)l} \end{bmatrix} \qquad \text{(E 2.3.2 d)}$$

Linearizing the (E 2.3.2) about the origin using the physical parameters $M = 2\ kg$, $m = 0.1$ kg, $l = 0.5\ m$, and $g = 9.81\ kg.m.s^{-2}$ produces the linearized model in (Ogata, 1997):

$$
\begin{bmatrix} \dot{x}_1 \\ \dot{x}_2 \\ \dot{x}_3 \\ \dot{x}_4 \end{bmatrix} = \begin{bmatrix} 0 & 0 & 1 & 0 \\ 0 & 0 & 0 & 1 \\ 0 & -0.4905 & 0 & 0 \\ 0 & 20.6010 & 0 & 0 \end{bmatrix} \mathbf{x} + \begin{bmatrix} 0 \\ 0 \\ 0.5 \\ -1 \end{bmatrix} u
$$
(E 2.3.3)

$$
\equiv \mathbf{A}_n \mathbf{x} + \mathbf{B}_n u
$$

By inspecting (E 2.2.2), we see that the system cannot be described globally by (3.9).

However, it appears that (3.9) can approximate (E 2.3.2) better than (E 2.3.3) in a

region about the origin because (3.9) represents a family of infinitely many models

including (E 2.3.3). We then employ (3.9) to generate a LARC for (E 2.3.2). To obtain

reasonable structured uncertainty specifications for (3.9), we notice that the nominal

linearized model (E 2.2.3) does not include the effects of the following nonlinear terms in

(E 2.3.2 c):

1) $\quad w_1(\mathbf{x}) = \dfrac{ml\sin(x_2)x_4^2}{(M+\sin^2(x_2)m)}$ in the third component of $\mathbf{f}(\mathbf{x})$

2) $\quad w_2(\mathbf{x}) = -\dfrac{\cos(x_2)m\sin(x_2)x_4^2}{(M+\sin^2(x_2)m)}$ in the forth component of $\mathbf{f}(\mathbf{x})$

This is because linearizing them about the origin produces zeros. We are interested in

$w_i(\mathbf{x})$, $i = 1,2$ because we know from numerical simulations in Example 2.3 that when

trajectories converge, x_4 (joint velocity of the pole) is relatively large when compared to

x_2 (joint angle of the pole). Assuming that this is true for the system under our LARC,

we see that neglecting $w_i(\mathbf{x})$, $i = 1,2$ can lead to significant modeling error. Based on this

assumption, we now assume a crude operating region in which we desire convergence:

$$
\Theta \equiv \{\mathbf{x} \mid |x_2| < 0.5, \text{ and } |x_4| < 1.5\}
$$
(E 3.5.1)

After we obtain the LARC and perform numerical simulations, we shall see that this

assumption is valid. Now, we write $w_i(\mathbf{x})$, $i = 1, 2$ as structured uncertainties:

1) For $w_1(\mathbf{x})$, we obtain:

$$\begin{bmatrix} 0 \\ 0 \\ w_1(\mathbf{x}) \\ 0 \end{bmatrix} = \frac{ml\sin(x_2)x_4}{(M+\sin^2(x_2)m)} \begin{bmatrix} 0 & 0 & 0 & 0 \\ 0 & 0 & 0 & 0 \\ 0 & 0 & 0 & 1 \\ 0 & 0 & 0 & 0 \end{bmatrix} \begin{bmatrix} x_1 \\ x_2 \\ x_3 \\ x_4 \end{bmatrix} \qquad \text{(E 3.5.2 a)}$$

$$\equiv h_1^{An}(\mathbf{x})\mathbf{E}_1^{An}\mathbf{x}$$

where $h_1^{An}(\mathbf{x}) \in [h_{l1}^{An}, h_{u1}^{An}]$, $h_{l1}^{An} = \dfrac{ml\sin(-0.5)x_4}{(M+\sin^2(-0.5)m)} = -0.01778$,

$h_{u1}^{An} = \dfrac{ml\sin(-0.5)x_4}{(M+\sin^2(-0.5)m)} = 0.01778$, and $\mathbf{E}_1^{An} \equiv \mathbf{E}_1 = \begin{bmatrix} 0 & 0 & 0 & 0 \\ 0 & 0 & 0 & 0 \\ 0 & 0 & 0 & 1 \\ 0 & 0 & 0 & 0 \end{bmatrix}$.

2) For $w_2(\mathbf{x})$, we obtain:

$$\begin{bmatrix} 0 \\ 0 \\ 0 \\ w_2(\mathbf{x}) \end{bmatrix} = -\frac{\cos(x_2)m\sin(x_2)x_4}{(M+\sin^2(x_2)m)} \begin{bmatrix} 0 & 0 & 0 & 0 \\ 0 & 0 & 0 & 0 \\ 0 & 0 & 0 & 0 \\ 0 & 0 & 0 & 1 \end{bmatrix} \begin{bmatrix} x_1 \\ x_2 \\ x_3 \\ x_4 \end{bmatrix} \qquad \text{(E 3.5.2 b)}$$

$$\equiv h_2^{An}(\mathbf{x})\mathbf{E}_2^{An}\mathbf{x}$$

where $h_2^{An}(\mathbf{x}) \in [h_{l2}^{An}, h_{u2}^{An}]$, $h_{l2}^{An} = -\dfrac{\cos(0.5)m\sin(0.5)x_4}{(M+\sin^2(0.5)m)} = -0.0312$, and

$h_{u2}^{An} = -\dfrac{\cos(-0.5)m\sin(-0.5)x_4}{(M+\sin^2(-0.5)m)} = 0.0312$, and $\mathbf{E}_2^{An} \equiv \mathbf{E}_2 = \begin{bmatrix} 0 & 0 & 0 & 0 \\ 0 & 0 & 0 & 0 \\ 0 & 0 & 0 & 0 \\ 0 & 0 & 0 & 1 \end{bmatrix}$.

Note that $w_i(\mathbf{x})$, $i = 1, 2$ are treated as uncertainties entering $\mathbf{A}_n$:

$$[\Delta \mathbf{A}_n(\mathbf{x})]\mathbf{x} = \sum_{\alpha=1}^{2} [h_\alpha^{A_n}(\mathbf{x})\mathbf{E}_\alpha^{A_n}]\mathbf{x} \qquad \text{(E 3.5.3)}$$

To generate a LARC, we want to include the nonlinearities in $\mathbf{g}(\mathbf{x})$ into our considerations. This is because while it is reasonable to employ $\mathbf{B}_n$ in the nominal linearized model to approximate $\mathbf{g}(\mathbf{x})$ in Θ, $[\mathbf{g}(\mathbf{x}) - \mathbf{B}]\mathbf{K}_{LARC} = [\Delta \mathbf{B}_n(\mathbf{x})]\mathbf{K}_{LARC}\mathbf{x}$ may be large in Θ because of the possibility that the resulting $\mathbf{K}_{LARC}$ may be large. To include this possibility into our controller generation, we augment $[\Delta \mathbf{B}_n(\mathbf{x})]\mathbf{K}_{LARC}\mathbf{x}$ to the nominal linearized model as additional structured uncertainties entering $\mathbf{B}_n$. We recall from (3.11):

$$\Delta \mathbf{B}_n(\mathbf{x}) = \begin{bmatrix} 0 \\ 1 \\ \dfrac{1}{M + \sin^2(x_2)m} - 0.5 \\ -\dfrac{\cos(x_2)}{(M + \sin^2(x_2)m)l} + 1 \end{bmatrix} \equiv \sum_{\beta=1}^{2} [h_\beta^{B_n}(\mathbf{x},t)\mathbf{E}_\beta^{\Delta B_n}]\mathbf{x} \qquad \text{(E 3.5.4)}$$

where $h_1^{B_n}(\mathbf{x},t) = \Delta \mathbf{B}_n(\mathbf{x})(3,1)$, $h_2^{B_n}(\mathbf{x},t) = \Delta \mathbf{B}_n(\mathbf{x})(4,1)$, $\mathbf{E}_1^{\Delta B_n} = [0 \ 0 \ 1 \ 0]^T$, and $\mathbf{E}_2^{\Delta B_n} = [0 \ 0 \ 0 \ 1]^T$. It follows that:

$$-[\Delta \mathbf{B}_n(\mathbf{x})]\mathbf{K}\mathbf{x} = \begin{bmatrix} h_1^{B_n}(\mathbf{x},t)\begin{bmatrix} 0 \\ 0 \\ -\mathbf{K} \\ 0 \end{bmatrix} + h_2^{B_n}(\mathbf{x},t)\begin{bmatrix} 0 \\ 0 \\ 0 \\ -\mathbf{K} \end{bmatrix} \end{bmatrix}\mathbf{x} = \sum_{\beta=1}^{2} [h_\beta^{B_n}(\mathbf{x})\mathbf{E}_\beta^{B_n}]\mathbf{x} \qquad \text{(E 3.5.5)}$$

where

1) $h_1^{B_n}(\mathbf{x}) \in [h_{l1}^{B_n}, h_{u1}^{B_n}]$

2) $h_2^{B_n}(\mathbf{x}) \in [h_{l2}^{B_n}, h_{u2}^{B_n}]$

3) $\quad h_{l1}^{Bn} = \dfrac{1}{M + \sin^2(0.5)m} - 0.5 = -0.0057$

4) $\quad h_{u1}^{Bn} = \dfrac{1}{M + \sin^2(0)m} - 0.5 = 0$

5) $\quad h_{l2}^{Bn} = -\dfrac{\cos(0)}{(M + \sin^2(0)m)l} + 1 = 0$

6) $\quad h_{u2}^{Bn} = -\dfrac{\cos(0.5)}{(M + \sin^2(0.5)m)l} + 1 = 0.1324$

7) $\quad \mathbf{E}_1^{Bn} = [\mathbf{0} \quad \mathbf{0} \quad -\mathbf{K}^T \quad \mathbf{0}]^T$

8) $\quad \mathbf{E}_2^{Bn} = [\mathbf{0} \quad \mathbf{0} \quad \mathbf{0} \quad -\mathbf{K}^T]^T.$

Using the uncertainty specifications obtained previously, we approximate (E 2.3.2) in Θ by:

$$\dot{\mathbf{x}} = [\mathbf{A}_n + \sum_{\alpha=1}^{2} [h_{\alpha}^{An}(\mathbf{x})\mathbf{E}_{\alpha}^{An}]]\mathbf{x} + [-\mathbf{B}_n\mathbf{K} + \sum_{\beta=1}^{2}[h_{\beta}^{Bn}(\mathbf{x})\mathbf{E}_{\beta}^{Bn}]]\mathbf{x}$$
$$\equiv [[\mathbf{A}_n + \Delta\mathbf{A}_n(\mathbf{x})] + [-[\mathbf{B}_n + \Delta\mathbf{B}_n(\mathbf{x})]\mathbf{K}]\,\mathbf{x} \qquad \text{(E 3.5.6)}$$

where $\Delta\mathbf{A}_n(\mathbf{x})$ and $-\Delta\mathbf{B}_n(\mathbf{x})\mathbf{K}$ are given by (E 3.5.3) and (E 3.5.5) respectively. Note

that (E 3.5.6) does not represent (E 2.3.2) exactly in Θ but we expect that it approximates

(E 2.3.2) better than (E 2.3.3) does in the same region because of the augmented

nonlinear structured pseudo-uncertainties. We emphasize that $h_{\alpha}^{An}(\mathbf{x})$, $\alpha = 1, 2$ and

$h_{\beta}^{An}(\mathbf{x})$, $\beta = 1, 2$ need not be the corresponding functions given previously. Rather, they

can be any functions that obey the corresponding bounds $[h_{l\alpha}^{An}, h_{u\alpha}^{An}]$ and $[h_{l\beta}^{Bn}, h_{u\beta}^{Bn}]$.

Accordingly, we see that (E 3.5.6) includes not only the pseudo-uncertainties, but also

any uncertainties obeying such bounds. To generate a LARC for (E 3.5.6), we follow the

procedure given in Section 3.5. Using (2.12), (2.16), and Theorem 3.2, we plot $\lambda_{max}(\mathbf{Z})$

versus $\rho \in \mathfrak{R}^+$ and $\eta \geq 1$, and determine the minimum of $\lambda_{max}(\mathbf{Z})$ in this plot. We realize

that the values of ρ and η corresponding to this minimum may produce a LARC that

requires a large amount of control energy but we assume in this example that we are not

limited by this factor.

Because we do not know where the minimum of $\lambda_{max}(\mathbf{Z})$ is, we first generate the plot in

a large region of $0.2 \leq \rho \leq 100$ and $1 \leq \eta \leq 100$ using large grids as shown in Fig E3.5.1.

From Fig. E3.5.1, we find that $\lambda_{max}(\mathbf{Z})$ has a local minimum when ρ and η are small.

Accordingly, we reduce the plotting domain to $0.2 \leq \rho \leq 3$ and $1.35 \leq \eta \leq 4$, and plot

$\lambda_{max}(\mathbf{Z})$ versus ρ and η as in Fig. E3.5.2. From Fig. E3.5.2, we find that

$min(\lambda_{max}(\mathbf{Z})) = -0.4803$ occurs at $(\rho, \eta) = (\rho^*, \eta^*) = (1.95, 1.8)$. The plot of $\lambda_{max}(\mathbf{Z})$

versus η when $\rho = \rho^* = 1.95$ is given in Fig. E3.5.3. Using our computer, the

computation time is less than 1 minute. Since $min(\lambda_{max}(\mathbf{Z})) < 0$, no optimization is

called to generate a LARC. Using ρ^* and η^*, we solve the Riccati equation (2.12) for $\mathbf{P}$

and generate LARC according to (2.16). This produces:

$$\mathbf{K}_{LARC} = [-2.5136 \quad -57.4749 \quad -5.1254 \quad -13.0073] \qquad (E\ 3.5.7)$$
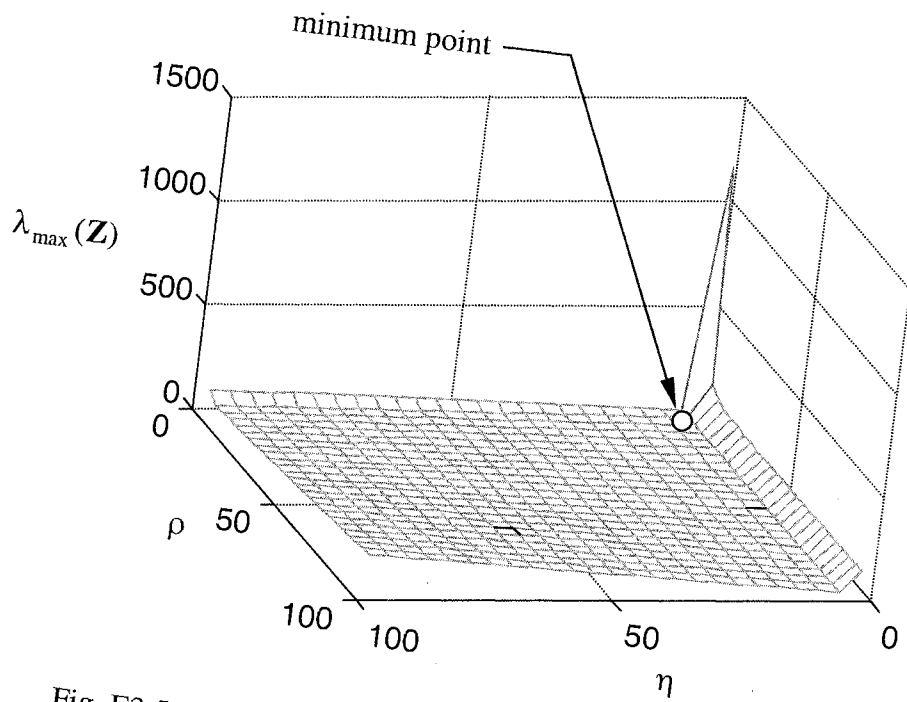
Fig. E3.5.1   A Plot of $\lambda_{max}(\mathbf{Z})$ versus $\rho \in [0.2, 100]$ and $\eta \in [1, 100]$
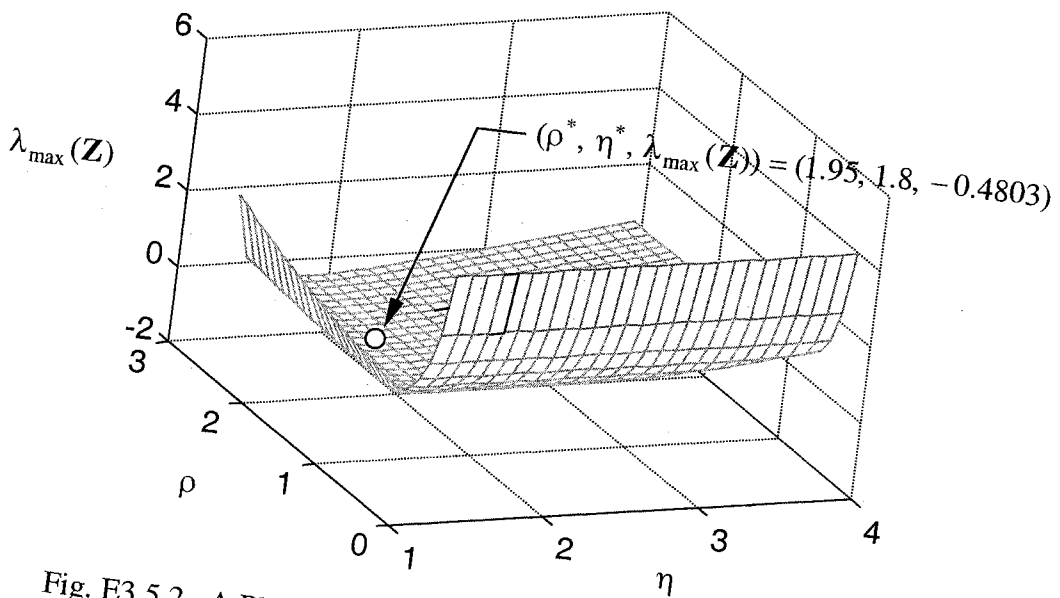
Fig. E3.5.2   A Plot of $\lambda_{max}(\mathbf{Z})$ versus $\rho \in [0.2, 3]$ and $\eta \in [1.35, 4]$
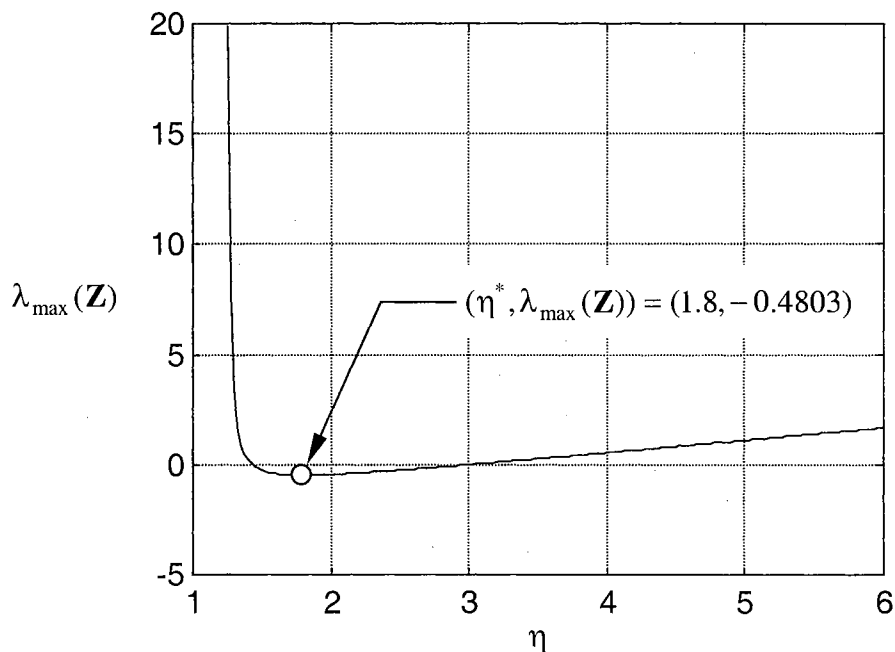
Fig. E3.5.3 A Plot of $\lambda_{max}(\mathbf{Z})$ versus $\eta \in [1, 6]$ when $\rho = \rho^* = 1.95$

$$\mathbf{Q} = \begin{bmatrix} 1.8000 & 18.2927 & 1.6313 & 4.1399 \\ 18.2927 & 419.2795 & 37.3006 & 94.6621 \\ 1.6313 & 37.3006 & 4.3263 & 8.4416 \\ 4.1399 & 94.6621 & 8.4416 & 22.4233 \end{bmatrix} \qquad \text{(E 3.5.8)}$$

$$\mathbf{P} \equiv \mathbf{P}_{(E3.5.9)} = \begin{bmatrix} 4.0782 & 10.3497 & 3.1579 & 2.2951 \\ 10.3497 & 119.5777 & 18.8090 & 25.7791 \\ 3.1579 & 18.8090 & 5.3843 & 4.1524 \\ 2.2951 & 25.7791 & 4.1524 & 5.7820 \end{bmatrix} \qquad \text{(E 3.5.9)}$$

$$\overline{\mathbf{A}}_n \equiv [\mathbf{A}_n - \mathbf{B}_n \mathbf{K}_{LARC}] = \begin{bmatrix} 0 & 0 & 1 & 0 \\ 0 & 0 & 0 & 1 \\ 1.2568 & 28.2469 & 2.5627 & 6.5037 \\ -2.5136 & -36.8739 & -5.1254 & -13.0073 \end{bmatrix} \text{(E 3.5.10)}$$

where the eigenvalues of $\overline{\mathbf{A}}_n$ are at $\lambda_1 = -5.4495$, $\lambda_{2,3} = -1.9466 \pm j\, 0.5630$, and

$\lambda_4 = -1.1020$ in the LHP. Because $\lambda_{max}(\mathbf{Z}) > 0$, it follows from Theorem 3.2 that the

time derivative of the quadratic Lyapunov function $V(\mathbf{x}) = \frac{1}{2}\mathbf{x}^T\mathbf{P}_{(E3.5.9)}\mathbf{x}$ along trajectories of (E 3.5.6) is negative definite in Θ. In addition, the corresponding LAR contains the largest β_C that can be contained in Θ.

To estimate the attractive regions corresponding to $\mathbf{K}_{LARC}$ (with uncertainty specifications), we employ numerical simulations. The corresponding attractive region is displayed in Table E3.5.1 and E3.5.2 with those corresponding to $\mathbf{K}_{PP}$ (Ogata, 1997) and to $\mathbf{K}_{LARC}$ (without uncertainty specifications) in Example 2.3. In the same fashion as in previous examples, we assume that a trajectory converges to the origin if $\|\mathbf{x}(t)\| < 0.01$ for $40 \leq t \leq 50$, and diverges from the origin if $\exists t$ such that $\|\mathbf{x}(t)\| > 2000$. From these tables, it appears that the attractive region corresponding to $\mathbf{K}_{LARC}$ (with uncertainty specifications) and to $\mathbf{K}_{LARC}$ (without uncertainty specifications) are approximately the same while the attractive region corresponding to $\mathbf{K}_{PP}$ is significantly smaller. From these tables, we see that the attractive regions corresponding to $\mathbf{K}_{LARC}$ (with uncertainty specifications) is larger than Θ. Since a LAR must be contained in Θ, this agrees with a known fact that the attractive region must contain every LAR. We do not present the application of the unstructured uncertainty bound from Theorem 3.3 in this example because the resulting allowable bound is very conservative. This result agrees with those in Example 3.1 and 3.2.

				x_2																								
				1.25					1.00					0.75					0.50					0.25				
				x_4																								
				-1	-0.5	0	0.5	1	-1	-0.5	0	0.5	1	-1	-0.5	0	0.5	1	-1	-0.5	0	0.5	1	-1	-0.5	0	0.5	1
x_1		x_3	-1																									
	5		-0.5																									
			0																									
			0.5																									
			1																									
	4		-1																									
			-0.5																									
			0																									
			0.5																									
			1																									
	3		-1																									
			-0.5																									
			0																									
			0.5																									
			1																									
	2		-1																									
			-0.5																									
			0																									
			0.5																									
			1																									
	1		-1																									
			-0.5																									
			0																									
			0.5																									
			1																									

Table E3.5.1 Simulation Results of the Cart-and-Pole System in Regions farther from the Origin ($x_1 > 0$, $x_2 > 0$)

Legends: ■ ≡ Pole placement and LARC (with and without uncertainty specifications) converge,

▨ ≡ LARC (with and without uncertainty specifications) converge, ▦ ≡ LARC (<u>with</u> uncertainty specifications) converges

▥ ≡ LARC (<u>without</u> uncertainty specifications) converges, □ ≡ All systems diverge

				x_2																						
			1.25					1.00					0.75					0.50					0.25				
			x_4																								
			-1	-0.5	0	0.5	1	-1	-0.5	0	0.5	1	-1	-0.5	0	0.5	1	-1	-0.5	0	0.5	1	-1	-0.5	0	0.5	1
x_1	-5	x_3 -1																									
		-0.5																									
		0																									
		0.5																									
		1																									
	-4	-1																									
		-0.5																									
		0																									
		0.5																									
		1																									
	-3	-1																									
		-0.5																									
		0																									
		0.5																									
		1																									
	-2	-1																									
		-0.5																									
		0																									
		0.5																									
		1																									
	-1	-1																									
		-0.5																									
		0																									
		0.5																									
		1																									

Table E3.5.2   Simulation Results of the Cart-and-Pole System in Regions farther from the Origin ($x_1 < 0$, $x_2 > 0$)

Legends: ▨ ≡ Pole placement and LARC (with and without uncertainty specifications) converge,
▨ ≡ LARC (with and without uncertainty specifications) converge, ▨ ≡ LARC (<u>with</u> uncertainty specifications) converges
▥ ≡ LARC (<u>without</u> uncertainty specifications) converges, □ ≡ All systems diverge

Example 3.6 (Choosing an Appropriate Nominal Model)

Given a nominal linear time-invariant model and the associated structured uncertainty

specifications, it appears from the previous common examples that we can generate a

LARC systematically to obtain satisfactorily large attractive regions when compared to

those in the literature. In each of those examples, the linearized model about the origin is

employed as the nominal model for simplicity, but this need not be the best choice. While

it is true that properties of a system should not change because of different

representations, we note that Theorem 3.2 is based on the sufficiency of the Lyapunov

stability, and thus we do not expect it to yield the same result for all possible

representations. Indeed, some representations allow us to find a stabilizing LAR

controller using Theorem 3.2 very easily, while others do not. A nominal model that

forces us to employ special treatments to obtain a stabilizing LAR controller is said to be

"poor". When a sufficiently poor nominal is employed, we may not be able to find a

stabilizing controller using Theorem 3.2, although one may exist. Indeed, we illustrate in

this example effects of a poor nominal model. The nonlinear system of interest is now

represented as a nominal model subjected to time-varying nonlinear structured

uncertainties:

$$\dot{\mathbf{x}} = \mathbf{A}_n\mathbf{x} + \mathbf{B}_n u + \sum_{j=1}^{2}(h_j(\mathbf{x},t)\mathbf{E}_j)\mathbf{x}$$
$$\equiv \mathbf{A}_n\mathbf{x} + \mathbf{B}_n u + \mathbf{f}_\Omega(\mathbf{x},t)$$

(E 3.6.1 a)

where $\mathbf{x} = [x_1 \quad x_2]^T$, and $\mathbf{f}_\Omega(\mathbf{x},t) \equiv [f_{\Omega1}(\mathbf{x},t) \quad f_{\Omega2}(\mathbf{x},t)]^T = \sum_{j=1}^{2}(h_j(\mathbf{x},t)\mathbf{E}_j)\mathbf{x}$. The

nominal model $\dot{\mathbf{x}} = \mathbf{A}_n\mathbf{x} + \mathbf{B}_n u$ and the associated uncertainty specifications are

given by:

$$\left.\begin{array}{l} \mathbf{A}_n = \begin{bmatrix} 44 & 0 \\ 0 & 1 \end{bmatrix}, \; \mathbf{B}_n = \begin{bmatrix} 1 \\ 1 \end{bmatrix} \\[2em] \mathbf{E}_1 = \begin{bmatrix} 1 & 0 \\ 0 & 0 \end{bmatrix}, \; \mathbf{E}_2 = \begin{bmatrix} 0 & 0 \\ 1 & 0 \end{bmatrix} \\[2em] h_1(\mathbf{x},t) \in [-41.5, -38.5] \equiv [h_{l1}, h_{u1}] \\[0.5em] h_2(\mathbf{x},t) \in [0, -1] \equiv [h_{l2}, h_{u2}] \end{array}\right\} \qquad \text{(E 3.6.1 b)}$$

Note that the nominal model in (E 3.6.1) is not a linearized model. Otherwise, we must be

have $\displaystyle \lim_{\|\mathbf{x}\| \to 0}\left(\sup_{t \ge 0}\left(\frac{\|\mathbf{f}_\Omega(\mathbf{x},t)\|}{\|\mathbf{x}\|} \right) \right) = 0$ for some $(\mathbf{x}, t)$ because this is the definition of a

linearized model (Vidyasagar, 1993). Clearly, this is not true for (E 3.6.1). To find a

simple guideline for choosing a nominal model, we examine the proof of Theorem 3.2.

To apply Theorem 3.2, $\mathbf{K}$ must be such that $\overline{\mathbf{A}}_n \equiv [\mathbf{A}_n - \mathbf{B}_n\mathbf{K}]$ is stable because this

represents dynamics of the nominal model. In addition, we desire that $\lambda_{\max}(\mathbf{Z}) < 0$ to

assure the negative definiteness of the Lyapunov time derivative in the region where

uncertainty specifications are valid. By examining (3.18 h), $\lambda_{\max}(\mathbf{Z}) < 0$ if and only if

the symmetric matrix $\mathbf{\Phi} \in \Re^{n \times n}$ is negative definite, because the symmetric matrix

$\displaystyle \sum_{j=1}^{r}[(h_{uj} - h_{lj})\mathbf{\Psi}_j^{0+}] \in \Re^{n \times n}$ is either positive definite or positive semidefinite by

construction. From (3.18 c), the conditions that $\mathbf{\Phi}$ is negative definite and $\mathbf{P}$ is positive

definite can be satisfied simultaneously if and only if $\overline{\mathbf{A}}_l$ is stable, because (3.18 c) is a

Lyapunov equation. Now, we recall from (3.18 b) that $\overline{\mathbf{A}}_l \equiv \overline{\mathbf{A}}_n + \displaystyle\sum_{j=1}^{r} h_{lj}\mathbf{E}_j$. It follows

from Theorem 3.1 that $\overline{\mathbf{A}}_l$ is stable if the h_{lj} are sufficiently small $\forall j$, because $\mathbf{K}$ is such

that $\overline{\mathbf{A}}_n$ is stable. Notice that that we cannot reduce effects of $\displaystyle\sum_{j=1}^{r}[(h_{uj} - h_{lj})\mathbf{\Psi}_j^{0+}]$ on

$\lambda_{\max}(\mathbf{Z})$ by recasting the model such that $(h_{uj} - h_{lj}) > 0$ are smaller $\forall j$. However, we

can recast the model such that magnitudes of h_{lj} are smaller $\forall j$ to suppress the effect of

$\displaystyle\sum_{j=1}^{r} h_{lj}\mathbf{E}_j$ on $\overline{\mathbf{A}}_l$. Indeed, we can decrease the magnitude of h_{l1} by recasting the model as:

$$\dot{\mathbf{x}} = \mathbf{A}_n \mathbf{x} + \mathbf{B}_n u + \sum_{j=1}^{2} (h_j(\mathbf{x},t)\mathbf{E}_j)\mathbf{x}$$

$$\equiv \mathbf{A}_n \mathbf{x} + \mathbf{B}_n u + \mathbf{f}_\Omega(\mathbf{x},t)$$

(E 3.6.2 a)

where the nominal model $\dot{\mathbf{x}} = \mathbf{A}_n \mathbf{x} + \mathbf{B}_n u$ and the associated uncertainty specifications in

(E 3.6.2 a) are determined from:

$$\mathbf{A}_n = \begin{bmatrix} 44 - 40 & 0 \\ 0 & 1 \end{bmatrix} = \begin{bmatrix} 4 & 0 \\ 0 & 1 \end{bmatrix}, \ \mathbf{B}_n = \begin{bmatrix} 1 \\ 1 \end{bmatrix}$$

$$\mathbf{E}_1 = \begin{bmatrix} 1 & 0 \\ 0 & 0 \end{bmatrix}, \ \mathbf{E}_2 = \begin{bmatrix} 0 & 0 \\ 1 & 0 \end{bmatrix}$$

$$h_1(\mathbf{x},t) \in [-41.5 + 40, -38.5 + 40] = [-1.5, 1.5] \equiv [h_{l1}, h_{u1}]$$

$$h_2(\mathbf{x},t) \in [-1, 0] = [h_{l2}, h_{u2}]$$

(E 3.6.2 b)

The new representation is obtained by subtracting $40x_1$ from the first state equation

$\dot{x}_1 = 44x_1 + u$, and adding $40x_1$ to the first uncertain component $f_{\Omega 1}(\mathbf{x},t) = h_1(\mathbf{x},t)x_1$.

We now employ Theorem 3.2 to find a LAR stabilizing controller. The plots of $\lambda_{max}(\mathbf{Z})$

versus ρ and η corresponding to the representations in (E 3.6.1) and (E 3.6.2) are given

in Fig. E3.6.1 and E3.6.2 respectively. The plotting data in Fig. E3.6.1 show that there is

no coordinate (ρ, η) such that $\lambda_{max}(\mathbf{Z}) < 0$. Moreover, extending the plotting domain

produces the same result that we see from Fig. E 3.6.1, namely that the plot is flat for

large values of ρ and η. This is in contrast to Fig. E3.6.2, in which there are many

coordinates (ρ, η) such that $\lambda_{max}(\mathbf{Z}) < 0$.

Fig. E3.6.1 A Plot of $\lambda_{max}(\mathbf{Z})$ versus $\rho \in [1,96]$ and $\eta \in [1,20]$
Using the Representation in (E 3.6.1)
Remark: 1) There is no (ρ,η) such that $\lambda_{max}(\mathbf{Z}) < 0$.
2) The plot is flat for large values of ρ and η.

$(\rho, \eta, \lambda_{max}(\mathbf{Z})) = (50, 10, -0.1227)$
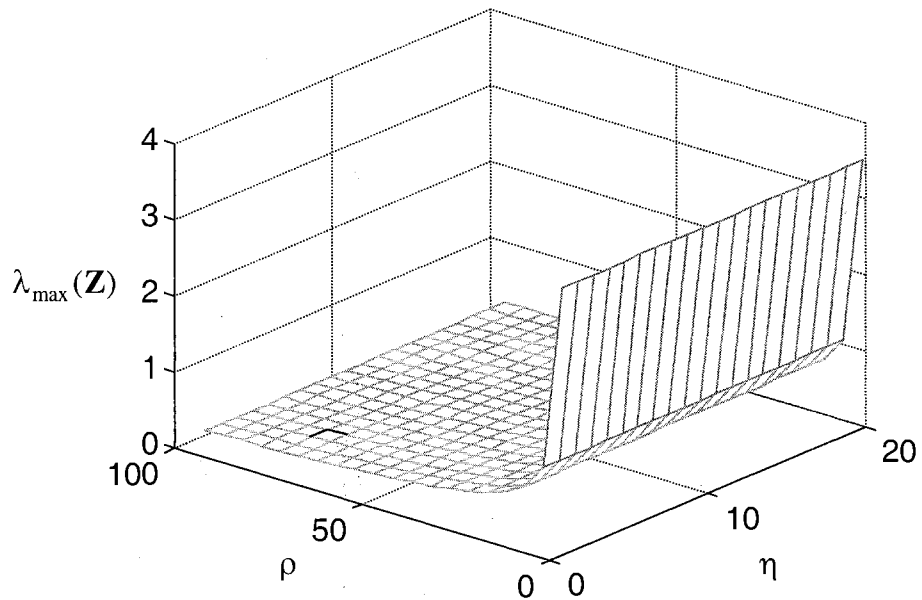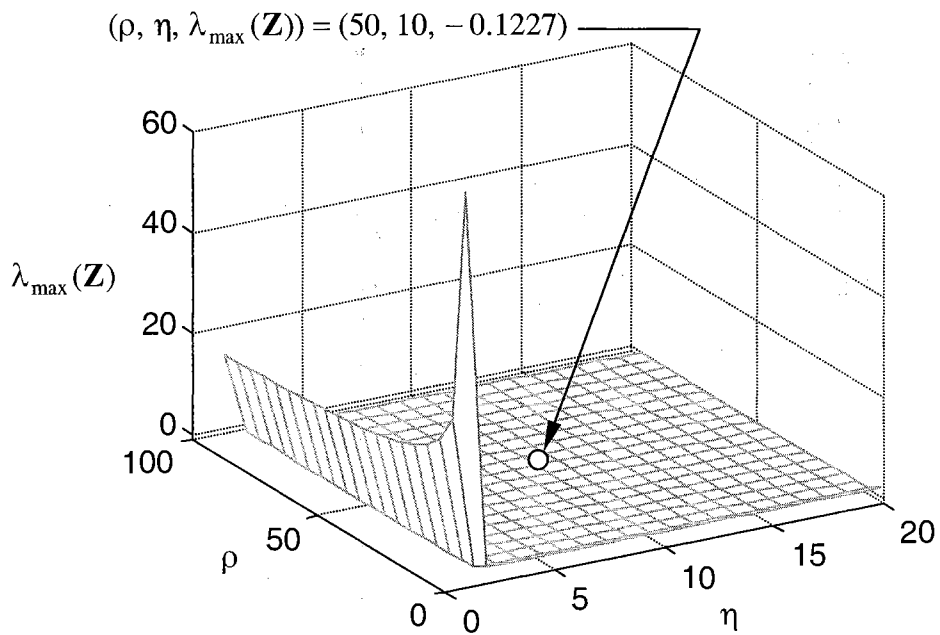
Fig. E3.6.2 A Plot of $\lambda_{max}(\mathbf{Z})$ versus $\rho \in [1,96]$ and $\eta \in [1,20]$

For the representation in (E 3.6.2), we arbitrarily select $(\rho, \eta) = (50, 10)$ in Fig. E3.6.2 to obtain $\lambda_{\max}(\mathbf{Z}) = -0.1227$. This corresponds to:

$$\mathbf{K}_{LARC} = [278.1184 \quad -137.5878] \tag{E 3.6.3}$$

$$\mathbf{Q} = \begin{bmatrix} 140.2298 & -68.8783 \\ -68.8783 & 35.0747 \end{bmatrix} \tag{E 3.6.4}$$

We note that it may be possible to find other coordinates to produce other gain matrices whose absolute value of each element is smaller than the respective ones in (E 3.6.3). However, we do not pursue this because the present result is sufficient to demonstrate effects of a "poor" nominal model. Note that the nominal model in (E 3.6.1) is very poor. Indeed, our optimization routine cannot find a solution $\{\mathbf{K}, \mathbf{Q}\}$ to meet the uncertainty specifications in (E 3.6.1), although we start the routine from initial values corresponding to small values of $\lambda_{\max}(\mathbf{Z})$ in Fig. E3.6.1. The criteria for choosing an appropriate nominal model presented in this example can be applied in the situation in which a linearized model is given as well. We emphasize that an unnecessarily poor nominal model may not allow us to employ Theorem 3.2 to generate a stabilizing LAR controller, although one may exist. Now, suppose that the nominal model $\dot{\mathbf{x}} = \mathbf{A}_n \mathbf{x} + \mathbf{B}_n u$ and the associated uncertainty specifications are determined from:

$$\left.\begin{aligned} \mathbf{A}_n &= \begin{bmatrix} 44 - 41.5 & 0 \\ 0 - 1 & 1 \end{bmatrix} = \begin{bmatrix} 2.5 & 0 \\ -1 & 1 \end{bmatrix}, \ \mathbf{B}_n = \begin{bmatrix} 1 \\ 1 \end{bmatrix} \\ \mathbf{E}_1 &= \begin{bmatrix} 1 & 0 \\ 0 & 0 \end{bmatrix}, \ \mathbf{E}_2 = \begin{bmatrix} 0 & 0 \\ 1 & 0 \end{bmatrix} \\ h_1(\mathbf{x}, t) \in [-41.5 + 41.5, -38.5 + 41.5] &= [0, 3] \equiv [h_{l1}, h_{u1}] \\ h_2(\mathbf{x}, t) \in [-1 + 1, 0 + 1] = [0, 1] &= [h_{l2}, h_{u2}] \end{aligned}\right\} \tag{E 3.6.5}$$

The new representation in (E 3.6.5) is obtained by subtracting $41.5x_1$ from the first state

equation $\dot{x}_1 = 44x_1 + u$, subtracting x_1 from the second state equation $\dot{x}_1 = x_2 + u$,

adding $41.5x_1$ to the first uncertain component $f_{\Omega 1}(\mathbf{x}, t) = h_1(\mathbf{x}, t)x_1$, and adding x_1 to

the second uncertain component $f_{\Omega 2}(\mathbf{x}, t) = h_2(\mathbf{x}, t)x_1$. Using Theorem 3.2, we plot

$\lambda_{max}(\mathbf{Z})$ versus ρ and η in Fig. E3.6.3 to find a stabilizing LARC for the representation

in (E 3.6.5). According to the plotting data, there are many coordinates (ρ, η) such that

$\lambda_{max}(\mathbf{Z}) < 0$. One such coordinate is the coordinate $(\rho, \eta) = (50, 10)$ employed earlier for

the representation in (E 3.6.2). Because the model has been recast, we now have

$\lambda_{max}(\mathbf{Z}) = -0.0657$ and:

$$\mathbf{K}_{LARC} = [280.7107 \quad -75.9225] \tag{E 3.6.6}$$

$$\mathbf{Q} = \begin{bmatrix} 142.8373 & -75.9225 \\ -75.9225 & 41.6397 \end{bmatrix} \tag{E 3.6.7}$$
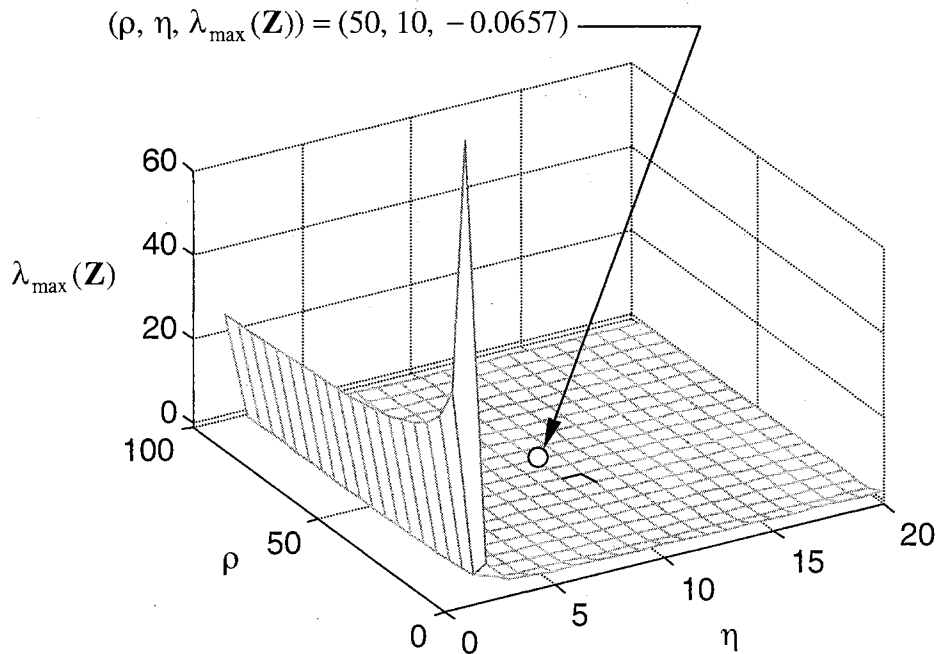
Fig. E3.6.3 A Plot of $\lambda_{max}(\mathbf{Z})$ versus $\rho \in [1, 96]$ and $\eta \in [1, 20]$

Notice that $\lambda_{max}(\mathbf{Z})$ corresponding to (E 3.6.2) is less than that corresponding to (E 3.6.5) under the same coordinate $(\rho,\eta) = (50,10)$, although the magnitudes of h_{1j} $j = 1,2$ in (E 3.6.5) are zero. This suggests that it is unnecessary to choose a nominal model such that the magnitudes of h_{1j} are zero $\forall j$, and it is sufficient that these are small. We do not examine how an appropriate nominal model should be chosen when the uncertainties are unstructured. This is because it has been our experience that unstructured uncertainty bounds are too conservative to be employed in actual practice.

3.7 Summary

1) In this chapter, we state explicitly in Theorems 3.2 and 3.3 two numerical bounds on the uncertain nonlinear function $\dfrac{\|\mathbf{f}_\Omega(\mathbf{x},t)\|}{\|\mathbf{x}\|}$ that guarantee the negative definiteness of $\dot{V}(\mathbf{x},t)$ in operating regions about the origin where such bounds are obeyed. We desire that $\dot{V}(\mathbf{x},t)$ is negative definite in a radially large region about the origin because this implies a large LAR.

2) In the first portion of this chapter, we propose a new structured uncertainty bound and draw an unstructured uncertainty bound from the literature for analyzing (3.2). Our focus is at the former because we find from our preliminary studies that unstructured uncertainty bounds usually produce conservative results. For system analysis, we apply our structured uncertainty bound to common examples employed in the literature. It appears that our allowable uncertainty bound is equally or less conservative than the existing ones. For controller generation, the concept of eigenvector condition is combined with our structured uncertainty bound and an optimization technique. It appears that when the initial value for the optimization is generated from the eigenvector condition and our structured uncertainty bound, a simple optimization technique is sufficient to produce robust LAR controllers. The allowable uncertainty bounds resulting from our procedure are less conservative than those in (Chen, and Chen, 1991), which are the least conservative results for the common examples we draw from the literature. In

addition, results from such common examples show that our LAR linear gain

matrices are smaller than the corresponding ones from (Chen, and Chen, 1991).

3)   We emphasize that the optimization phase is not always needed when generating

our robust LARC. It is employed only when needed to ensure that computing

resources and time are not consumed unnecessarily. When such an optimization is

needed, our Procedures 2 and 3 indicate this and provide a plot for determining

reasonably good initial values for the optimization. By means of examples, it

appears that these initial values result in fast convergence to solutions, with

appropriate choices for initial values. However, convergence does not occur if

inappropriate initial values are employed.

4)   Theorem 3.2 and 3.3 can be employed to guarantee global stability of (3.2) when

$\dfrac{\left\| \mathbf{f}_\Omega(\mathbf{x},t) \right\|}{\left\| \mathbf{x} \right\|}$ is sufficiently small.

Chapter IV

LARC for MIMO Systems

4.1   Linearized Model Case

Our primary objective in this chapter is to obtain a MIMO version of LARC developed in

Chapter II. The available mathematical description is assumed to be:

$$\dot{\mathbf{x}} = \mathbf{f}(\mathbf{x}) + \mathbf{g}(\mathbf{x})\mathbf{u}(\mathbf{x}) \qquad (4.1)$$

where the vector $\mathbf{f}(\mathbf{x}) \in \mathfrak{R}^n$, and matrix $\mathbf{g}(\mathbf{x}) \in \mathfrak{R}^{n \times m}$ can be uncertain. In our discussions,

$\mathbf{f}(\mathbf{x})$, $\mathbf{g}(\mathbf{x})$, and the control $\mathbf{u}(\mathbf{x}) = -\mathbf{K}\mathbf{x} \in \mathfrak{R}^m$ are such that $\dot{\mathbf{x}}$ is locally Lipschitz in the

operating region of interest in $\mathfrak{R}^n$ $\forall t \geq 0$. We assume that the linearized model of (4.1)

exists about the origin and is given by:

$$\dot{\mathbf{x}} = \mathbf{A}\mathbf{x} + \mathbf{B}\mathbf{u}(\mathbf{x}) \qquad (4.2)$$

where $\mathbf{A} \in \mathfrak{R}^{n \times n}$, and $\mathbf{B} \in \mathfrak{R}^{n \times m}$ are known, and [$\mathbf{A}$ $\mathbf{B}$] is controllable or stabilizable. An

uncertain nonlinear system having a known linearized model can be found in Section 1.1.

The gain matrix $\mathbf{K}$ is such that $\overline{\mathbf{A}} \equiv [\mathbf{A} - \mathbf{B}\mathbf{K}]$ is stable. In the Chapter I and II, we

explore several key properties of the functions $F_L(\mathbf{x}) = \mathbf{x}^T \mathbf{P}\mathbf{A}\mathbf{x}$ and $G_L(\mathbf{x}) = \mathbf{x}^T \mathbf{P}\mathbf{B}$.

Using these properties, we establish the concepts of eigenvector condition, eigenvalue

ratio, and formulate LARC for SIMO systems when the linearized model is available. In

this chapter, these known properties will be extended to formulate LARC for MIMO

systems. We shall see that some theorems for SIMO systems can be applied to MIMO

systems immediately while some require slight changes. Indeed, the formulation of LARC for MIMO systems is straightforward from that for SIMO systems.

Eigenvector Condition

Most of our notations in this section are derived from those in Chapter I, and II. In this chapter, we provide statements and recall mathematical objects from the previous chapters, with the understanding that we replace $\mathbf{g}(\mathbf{x}) \in \Re^n$, $\mathbf{B} \in \Re^n$,

$G(\mathbf{x}) \equiv \mathbf{x}^T \mathbf{P} \mathbf{g}(\mathbf{x}) \in \Re$, $G_L(\mathbf{x}) \equiv \mathbf{x}^T \mathbf{P} \mathbf{B} \in \Re$, and $u(\mathbf{x}) \in \Re$ in the previous chapters by

$\mathbf{g}(\mathbf{x}) \in \Re^{n \times m}$, $\mathbf{B} \in \Re^{n \times m}$, $\mathbf{G}(\mathbf{x}) \equiv \mathbf{x}^T \mathbf{P} \mathbf{g}(\mathbf{x}) \in \Re^{1 \times m}$, $\mathbf{G}_L(\mathbf{x}) \in \Re^{1 \times m}$, and $\mathbf{u}(\mathbf{x}) \in \Re^m$ respectively.

It is well-known that Lyapunov stability is applicable to MIMO systems as well as SIMO systems. Thus, the fundamental idea of LARC presented in Section 1.2 applies to MIMO systems. Now, consider the time derivative of the quadratic Lyapunov function (1.5) along trajectories of the nonlinear system (4.1):

$$\begin{aligned} \dot{V}(\mathbf{x}) &= \mathbf{x}^T \mathbf{P} \mathbf{f}(\mathbf{x}) + \mathbf{x}^T \mathbf{P} \mathbf{g}(\mathbf{x}) \mathbf{u}(\mathbf{x}) \\ &\equiv F(\mathbf{x}) + \mathbf{G}(\mathbf{x}) \mathbf{u}(\mathbf{x}) \end{aligned} \tag{4.3}$$

According to the fundamental idea of LAR, we desire that the region B_L defined in (1.6) be radially large to obtain a large LAR. The existence of B_L about the origin is guaranteed because $\mathbf{K}$ stabilizes the linear model (4.2). From the definitions of $\mathbf{x}_{C_{Si}}$ in section 1.3, we see that the dimensions of B_L and LAR are limited by the existence of $\mathbf{x}_{C_{Si}}$. At $\mathbf{x}_{C_{Si}}$, we have that $F(\mathbf{x}_{C_{Si}}) = 0$ and $\mathbf{G}(\mathbf{x}_{C_{Si}}) = \mathbf{0}$. It is clear from (4.3) that the

control $\mathbf{u}(\mathbf{x})$ cannot force $\dot{V}(\mathbf{x})$ to be negative at $\mathbf{x}_{C_{Si}}$ so we require that $\mathbf{x}_{C_{Si}}$ be removed or be as far from the origin as possible. To accomplish this, we consider first a MIMO version of Lemma 1.1

Lemma 4.1   (Relationship between $S_{\mathbf{G}_L=\mathbf{0}}$ and $R_{[F_L<0]\cup\{0\}}$)

If the basic conditions $C1$–$C4$ in Lemma 1.1 are satisfied then:

$$S_{\mathbf{G}_L=\mathbf{0}} \subset R_{[F_L<0]\cup\{0\}}$$

where $R_{[F_L<0]\cup\{0\}} \equiv \{\mathbf{x} \mid F_L(\mathbf{x}) < 0\} \cup \{\mathbf{0}\}$, $F_L(\mathbf{x}) \equiv \mathbf{x}^T\mathbf{PAx}$, $S_{\mathbf{G}_L=\mathbf{0}} \equiv \{\mathbf{x} \mid \mathbf{G}_L(\mathbf{x}) = \mathbf{0}\}$,

$\mathbf{G}_L(\mathbf{x}) \equiv \mathbf{x}^T\mathbf{PB} \in \mathfrak{R}^{1\times m}$, and $\mathbf{P}$ and $\mathbf{Q}$ are symmetric positive definite matrices.

Proof

Consider the time derivative of the quadratic Lyapunov function (1.5) along the trajectories of the <u>linearized model</u> (4.2) under a linear control $\mathbf{u}(\mathbf{x})$:

$$\begin{aligned}
\dot{V}_L(\mathbf{x}) &= \mathbf{x}^T\mathbf{PAx} + \mathbf{x}^T\mathbf{PBu}(\mathbf{x}) \\
&\equiv F_L(\mathbf{x}) + \mathbf{G}_L(\mathbf{x})\mathbf{u}(\mathbf{x})
\end{aligned} \tag{4.4}$$

where $\mathbf{G}_L(\mathbf{x}) \equiv \mathbf{x}^T\mathbf{PB} \in \mathfrak{R}^{1\times m}$, and $F_L(\mathbf{x}) \equiv \mathbf{x}^T\mathbf{PAx} \in \mathfrak{R}$. The subscript "$L$" in $\dot{V}_L(\mathbf{x})$,

$\mathbf{G}_L(\mathbf{x})$ and $F_L(\mathbf{x})$ denotes that they are defined with respect to the linearized model.

Notice that the system of linear equations $\mathbf{G}_L(\mathbf{x}) = \mathbf{x}^T\mathbf{PB} = \mathbf{0}$ can be written as:

$$[\mathbf{B}^T\mathbf{P}]_{m\times n}\mathbf{x} = [\mathbf{0}]_{m\times 1} \tag{4.5}$$

From basic linear algebra, the dimension of the solution space of (4.5) is:

$$\dim(S_{\mathbf{G}_L=\mathbf{0}}) \equiv \gamma = n - r \tag{4.6}$$

where $r \equiv \text{rank}(\mathbf{B}^T \mathbf{P})$ and $S_{\mathbf{G}_L=0}$ is the solution space of (4.5). Depending on the point

we want to discuss, we alternatively denote the set $\{\mathbf{x} \mid \mathbf{G}_L(\mathbf{x}) = 0\}$ by $S_{\mathbf{G}_L=0}$ or by

$S_{\mathbf{G}_L=0}$ when we want to consider it as a subspace or as a surface, respectively. Given a

nonzero $\mathbf{B}$, we have that $1 \le r \le n$ and thus $0 \le \gamma \le (n-1)$. By Lyapunov stability, the

existence of the stabilizing linear gain matrix $\mathbf{K}$ implies the existence of a symmetric

positive definite matrix $\mathbf{P}$ such that $\dot{V}_L(\mathbf{x})$ is globally negative definite. The coexistence

of the $S_{\mathbf{G}_L=0}$ and the globally negative definite function $\dot{V}_L(\mathbf{x})$ implies that:

1) The region $R_{[F_L<0] \cup \{0\}}$ exists.

2) $S_{\mathbf{G}_L=0} \subset R_{[F_L<0] \cup \{0\}}$

When $\text{rank}(\mathbf{PB}) = n$, we have that $\gamma = 0$. In this case, $S_{\mathbf{G}_L=0} = \{0\}$ and Lemma 4.1 is

trivially satisfied. This completes the proof.

From Lemma 4.1, we see that $S_{\mathbf{G}_L=0}$ in MIMO systems is analogous to $S_{G_L=0}$ in SIMO

systems except that $0 \le \dim(S_{\mathbf{G}_L=0}) \le (n-1)$ while $\dim(S_{G_L=0}) = (n-1)$. Referring to

the discussions given in Chapter I for SIMO systems, it is conceivable for MIMO

systems that $\mathbf{x}_{C_{Si}}$ can be located reasonably far from the origin by locating $S_{\mathbf{G}_L=0}$ on the

symmetry plane of $S_{F_L=0}$ such that $F_L(\mathbf{x})\mid_{\mathbf{x}\neq 0} < 0$ on $S_{\mathbf{G}_L=0}$. This relative orientation is

the eigenvector condition for MIMO systems.

By examining the proof of Theorem 1.2, we see that this theorem does not restrict the

dimension of $\mathbf{B}$. Accordingly, it is immediate that the symmetry axes of $S_{F_L=0}$ for MIMO

systems are the n orthonormal eigenvectors of $\mathbf{M} \equiv \dfrac{1}{2}[\mathbf{PA} + \mathbf{A}^T\mathbf{P}]$. Because of this and

because $\mathbf{x}^T\mathbf{Mx} = F_L(\mathbf{x})$, the eigenvector condition for MIMO systems is satisfied if

$S_{\mathbf{G}_{L}=\mathbf{0}}$ is spanned by γ eigenvectors of $\mathbf{M}$ such that the corresponding γ eigenvalues of

$\mathbf{M}$ are negative. Lemma 4.1 guarantees that $\mathbf{M}$ has <u>at least</u> γ negative eigenvalues

because $S_{\mathbf{G}_{L}=\mathbf{0}} \subset R_{[F_L<0]\cup\{\mathbf{0}\}}$. The following questions are immediate from the definition

of eigenvector conditions:

1)   Under what condition can the eigenvector condition for MIMO systems be

       satisfied by a particular choice of $\mathbf{P}$?

2)   Suppose the eigenvector condition can be satisfied by a particular choice of $\mathbf{P}$,

       how can we obtain such $\mathbf{P}$?

It turns out that the existence of $\mathbf{P}$ satisfying the eigenvector condition for MIMO systems

is guaranteed when $[\mathbf{A}, \mathbf{B}]$ is controllable or stabilizable, and such $\mathbf{P}$ is the unique

symmetric positive definite solution of a Riccati equation. In addition, it gives rise to the

control law $\mathbf{u}_{LARC}(\mathbf{x}) = -\eta\rho\mathbf{B}^T\mathbf{Px}$ where $\eta \geq 1$ and $\rho \in \Re^+$. These are the same results

we obtained for SIMO systems.

Theorem 4.1   (Generating $\mathbf{P}$ to satisfy the Eigenvector Condition)

The symmetric positive definite matrix $\mathbf{P}$ generated from Theorem 2.3 satisfies the

eigenvector condition for MIMO systems

Proof

Recall the Riccati equation in Theorem 2.3:

(Proof of Theorem 4.1 (Cont.))

$$0 = -2\mathbf{Q} - [\mathbf{PA} + \mathbf{A}^T\mathbf{P}] + 2\rho\,\mathbf{PB}\,\mathbf{B}^T\mathbf{P}$$
$$= -c\mathbf{I} - \mathbf{M} + \overline{\mathbf{N}}$$

(4.7)

where $\mathbf{M} \equiv \dfrac{1}{2}[\mathbf{PA} + \mathbf{A}^T\mathbf{P}]$, $\overline{\mathbf{N}} \equiv \dfrac{1}{2}[[\mathbf{PB}]\mathbf{K} + \mathbf{K}^T[\mathbf{PB}]^T\,]\big|_{\mathbf{K}^T = \rho[\mathbf{PB}]} = \rho\,[\mathbf{PB}\,\mathbf{B}^T\mathbf{P}]$, and

$\mathbf{Q} = c\mathbf{I}$. We emphasize that now $\mathbf{B} \in \mathfrak{R}^{n\times m}$. Because Theorem 2.3 does not restrict the

dimension of $\mathbf{B}$, the existence of the symmetric positive definite solution $\mathbf{P}$ of the Riccati

equation (4.7) is guaranteed when $[\mathbf{A}, \mathbf{B}]$ is controllable or stabilizable. By

Lyapunov stability, the existence of such $\mathbf{P}$ guarantees that $\overline{\mathbf{A}} \equiv [\mathbf{A} - \mathbf{BK}]\big|_{\mathbf{K}^T = \rho[\mathbf{PB}]}$ is

stable. It remains to show that such $\mathbf{P}$ satisfies the eigenvector condition.

Now, we notice that the function $\mathbf{G}_L(\mathbf{x})\mathbf{u}(\mathbf{x})$ in (4.4) with $\mathbf{u}(\mathbf{x}) = -\mathbf{Kx} = -\rho\mathbf{B}^T\mathbf{Px}$ is:

$$\mathbf{G}_L(\mathbf{x})\mathbf{u}(\mathbf{x}) = -[\mathbf{x}^T\mathbf{PB}][\rho\mathbf{B}^T\mathbf{Px}] = -\mathbf{x}^T\rho[\mathbf{PBB}^T\mathbf{P}]\mathbf{x} = -\mathbf{x}^T\overline{\mathbf{N}}\mathbf{x} = -\rho[\mathbf{x}^T\mathbf{PB}][\mathbf{x}^T\mathbf{PB}]^T \le 0$$

(4.9)

where $\mathbf{G}_L(\mathbf{x}) \equiv \mathbf{x}^T\mathbf{PB}$, $\overline{\mathbf{N}} \equiv \rho[\mathbf{PBB}^T\mathbf{P}] = \rho[\mathbf{PBB}^T\mathbf{P}]^T = \overline{\mathbf{N}}^T$, and $\mathbf{x}^T\overline{\mathbf{N}}\mathbf{x} \ge 0$. We know

that:

1) The real symmetric matrix $\overline{\mathbf{N}}$ has a set of n orthonormal eigenvectors

   $V_{\overline{\mathbf{N}}} \equiv \{\mathbf{v}_{\overline{\mathbf{N}}1}, \mathbf{v}_{\overline{\mathbf{N}}2}, ..., \mathbf{v}_{\overline{\mathbf{N}}n}\}$ spanning $\mathfrak{R}^n$ (Hagan et al, 1996).

2) For $i = 1, 2, ... n$, $\lambda_{\mathbf{N}i} \ge 0$ because $\mathbf{x}^T\overline{\mathbf{N}}\mathbf{x} \ge 0$ and $\overline{\mathbf{N}} = \overline{\mathbf{N}}^T$.

3) A basis for generating $S_{\mathbf{G}_L=0}$ contains $\gamma \equiv (n - r)$ linearly independent vectors.

   Indeed, we know from Lemma 4.1 that $0 \le \dim(S_{\mathbf{G}_L=0}) \equiv \gamma \le (n - 1)$, where

   $n \ge r \equiv rank(\mathbf{PB}) \ge 1$ for a nonzero $\mathbf{B}$.

(Proof of Theorem 4.1 (Cont.))

Now, we notice from (4.9) that when $\mathbf{K}^T = \rho[\mathbf{PB}]$:

$$S_{\mathbf{G}_{L=0}} = \{\mathbf{x} \mid \mathbf{x}^T \overline{\mathbf{N}} \mathbf{x} = 0\} \tag{4.10}$$

Because $0 \le \dim(S_{\mathbf{G}_{L=0}}) \equiv \gamma \le (n-1)$ and because the n eigenvectors of $\overline{\mathbf{N}}$ are orthonormal, we know that a basis of $S_{\mathbf{G}_{L=0}}$ is a set of γ orthonormal eigenvectors of $\overline{\mathbf{N}}$.

For convenience, we arrange the vectors in this basis as $\{\mathbf{v}_{\overline{\mathbf{N}}(r+1)}, \mathbf{v}_{\overline{\mathbf{N}}(r+2)}, \ldots, \mathbf{v}_{\overline{\mathbf{N}}n}\} \equiv V_{\overline{\mathbf{N}}\gamma}$ and denote the set of the corresponding eigenvalues by $\lambda_{\overline{\mathbf{N}}\gamma} \equiv \{\lambda_{\overline{\mathbf{N}}(r+1)}, \lambda_{\overline{\mathbf{N}}(r+2)}, \ldots, \lambda_{\overline{\mathbf{N}}n}\}$.

For each of the basis vector, it follows from (4.10) that:

$$\mathbf{v}_{\overline{\mathbf{N}}i}^T \overline{\mathbf{N}} \mathbf{v}_{\overline{\mathbf{N}}i} = \mathbf{v}_{\overline{\mathbf{N}}i}^T \lambda_{\overline{\mathbf{N}}i} \mathbf{v}_{\overline{\mathbf{N}}i} = \lambda_{\overline{\mathbf{N}}i} \left\| \mathbf{v}_{\overline{\mathbf{N}}i} \right\|^2 = 0 \tag{4.11}$$

for $i = (r+1), (r+2), \ldots, n$. This implies that $\lambda_{\overline{\mathbf{N}}i} = 0$ for $i = (r+1), (r+2), \ldots, n$ and we have shown that $\overline{\mathbf{N}}$ has at least γ zero eigenvalues. Now, we claim that $\overline{\mathbf{N}}$ has exactly γ zero eigenvalues. Indeed, if $\overline{\mathbf{N}}$ has more than γ zero eigenvalues then $\mathbf{x}^T \overline{\mathbf{N}} \mathbf{x} = 0$ along the corresponding orthonormal eigenvectors, implying that there are more than γ linearly independent vectors belonging to $S_{\mathbf{G}_{L=0}}$. This is a contradiction because we know that $\dim(S_{\mathbf{G}_{L=0}}) = \gamma$. Thus, $\overline{\mathbf{N}}$ has exactly γ zero eigenvalues. The remaining r eigenvalues of $\overline{\mathbf{N}}$ are positive because $\mathbf{x}^T \overline{\mathbf{N}} \mathbf{x} \ge 0$.

By examining the proof of Theorem 2.1, we see that this theorem applies to MIMO systems immediately. Accordingly, we know that the matrices $\mathbf{M}$ and $\overline{\mathbf{N}}$ in (4.7) share the same set of orthonormal eigenvectors when $\mathbf{Q} = c\mathbf{I}$. Using these results, we can reduce (4.7) to the principal axes of $\mathbf{M}$:

(Proof of Theorem 4.1 (Cont.))

$$-c\mathbf{I} = \Lambda_{\mathbf{M}} - \Lambda_{\overline{\mathbf{N}}}$$

$$\equiv \begin{bmatrix} \Lambda_{\mathbf{M}\overline{\mathbf{N}}u} & \mathbf{0} \\ \mathbf{0} & \Lambda_{\mathbf{M}\overline{\mathbf{N}}l} \end{bmatrix} \qquad (4.12\text{ a})$$

where

$$\Lambda_{\mathbf{M}} = \text{diag}[\lambda_{\mathbf{M}1} \ \lambda_{\mathbf{M}2} \ \dots \ \lambda_{\mathbf{M}n}] \qquad (4.12\text{ b})$$

$$\Lambda_{\overline{\mathbf{N}}} = \text{diag}[\lambda_{\overline{\mathbf{N}}1} \ \lambda_{\overline{\mathbf{N}}2} \ \dots \ \lambda_{\overline{\mathbf{N}}n}] \qquad (4.12\text{ c})$$

$$\Lambda_{\mathbf{M}\overline{\mathbf{N}}u} = \text{diag}[\lambda_{\mathbf{M}1} - \lambda_{\overline{\mathbf{N}}1} \ \ \lambda_{\mathbf{M}2} - \lambda_{\overline{\mathbf{N}}2} \ \dots \ \lambda_{\mathbf{M}r} - \lambda_{\overline{\mathbf{N}}r}] \qquad (4.12\text{ d})$$

$$\Lambda_{\mathbf{M}\overline{\mathbf{N}}l} = \text{diag}[\lambda_{\mathbf{M}(r+1)} - \lambda_{\overline{\mathbf{N}}(r+1)} \ \ \lambda_{\mathbf{M}(r+2)} - \lambda_{\overline{\mathbf{N}}(r+2)} \ \dots \ \lambda_{\mathbf{M}n} - \lambda_{\overline{\mathbf{N}}n}]$$
$$= \text{diag}[\lambda_{\mathbf{M}(r+1)} \ \ \lambda_{\mathbf{M}(r+2)} \ \dots \ \lambda_{\mathbf{M}n}] \qquad (4.12\text{ e})$$

By inspecting (4.12), we see that $\lambda_{\mathbf{M}i} = -c < 0$ because $\lambda_{\overline{\mathbf{N}}i} = 0$, $i = r+1$, $r+2$, ..., n.

Accordingly, $\mathbf{x}^T\overline{\mathbf{N}}\mathbf{x} = 0$ on the space spanned by $\{\mathbf{v}_{\mathbf{M}i}\}$, $i = r+1$, $r+2$, ..., n. Since

$\{\mathbf{x} \mid \mathbf{x}^T\overline{\mathbf{N}}\mathbf{x} = 0\} = S_{\mathbf{G}_L=0}$, it follows that $\{\mathbf{v}_{\mathbf{M}i}\}$, $i = r+1$, $r+2$, ..., n spans $S_{\mathbf{G}_L=0}$ such

that $\lambda_{\mathbf{M}i} < 0$. This shows that the eigenvector condition is satisfied by the solution $\mathbf{P}$ of

the Riccati equation (4.7) and completes the proof.

To conclude this section, we have shown that the eigenvector condition for MIMO

systems can be satisfied by the unique symmetric positive definite solution $\mathbf{P}$ of the

Riccati equation (4.7). Notice that the set $\{\lambda_{\mathbf{M}1}, \lambda_{\mathbf{M}2}, \dots, \lambda_{\mathbf{M}r}\}$ contains at least one

positive number because $\mathbf{A}$ is unstable, but it may or may not contain a negative number.

Note in addition that when the eigenvector condition is satisfied, we can draw from

Theorem 4.1 that:

1) $\lambda_{\mathbf{M}i} > \lambda_{\mathbf{M}j}$ $\forall i \in \{1, 2, \ldots, r\}$ and $\forall j \in \{r+1, r+2, \ldots, n\}$.

2) $0 > \lambda_{\mathbf{M}(r+1)} = \lambda_{\mathbf{M}(r+2)} = \ldots = \lambda_{\mathbf{M}n} = -c$.

These statements are immediate from (4.12). For convenience, we denoted the maximum

positive eigenvalue of $\mathbf{M}$ by $\lambda_{\mathbf{M}1}$.

Eigenvalue Ratio

When the eigenvector condition is satisfied, we recall from Proposition 1.2 and from

Chapter II that the eigenvalue-ratio plot allows us to select a value for ρ to generate $\mathbf{P}$

from the Riccati equation (2.12) such that the "angle" between $S_{F_L=0}$ and $S_{G_L=0}$ is large,

and $\mathbf{x}_{C_{Si}}$ is reasonably far from the origin. Using such ρ and the corresponding $\mathbf{P}$, in

Chapter II we generate quickly LAR controllers using (2.16). We see from examples in

Chapter II that such LAR controllers yield satisfactorily large attractive regions when

compared to those resulting from pole placement and from LQR.

For MIMO systems, we employ the eigenvalue-ratio plot to generate LAR controllers in a

similar fashion. The only major difference is the definition of eigenvalue ratio. This will

be drawn from Theorem 4.2, which is a straightforward extension of Theorem 1.3. All the

notations employed in Theorem 4.2 are immediate from those in Proposition 1.2 and in

Theorem 1.3.

Theorem 4.2 (Implication of Eigenvalue Ratio)

Let the set of n orthonormal eigenvectors $\{\mathbf{v}_{\mathbf{M}1},\ldots,\mathbf{v}_{\mathbf{M}r},\mathbf{v}_{\mathbf{M}(r+1)},\ldots,\mathbf{v}_{\mathbf{M}n}\}$ of

$\mathbf{M} \equiv \dfrac{1}{2}[\mathbf{PA} + \mathbf{A}^{T}\mathbf{P}]$ be employed for generating $\mathfrak{R}^{n}$. If the basic conditions $C1 - C4$ are

satisfied, then the angle θ between a vector $[z_1 \quad z_2 \quad \ldots \quad z_n]^{T} \equiv \mathbf{z}^{F_L=0}_{\{\mathbf{v}_{\mathbf{M}1},\mathbf{v}_{\mathbf{M}2},\ldots,\mathbf{v}_{\mathbf{M}n}\}} \in S_{F_L=0}$

and its projection $[0 \quad \ldots \quad 0 \quad z_{r+1} \quad \ldots \quad z_n]^{T} \equiv \mathbf{z}_{\{\mathbf{v}_{\mathbf{M}(r+1)},\mathbf{v}_{\mathbf{M}(r+2)},\ldots,\mathbf{v}_{\mathbf{M}n}\}}$ onto the plane spanned

by $\{\mathbf{v}_{\mathbf{M}(r+1)},\mathbf{v}_{\mathbf{M}(r+2)},\ldots,\mathbf{v}_{\mathbf{M}n}\}$ is the smallest when $z_2 = \ldots = z_r = z_{r+2} = \ldots = z_n = 0$ or

when:

$$\mathbf{z}^{F_L=0}_{\{\mathbf{v}_{\mathbf{M}1},\mathbf{v}_{\mathbf{M}2},\ldots,\mathbf{v}_{\mathbf{M}n}\}} = \begin{bmatrix} z_1 & 0 & \ldots & 0 & z_{r+1} & 0 & \ldots & 0 \end{bmatrix}^{T} \equiv \mathbf{z}^{F_L=0}_{\{\mathbf{v}_{\mathbf{M}1},\mathbf{v}_{\mathbf{M}(r+1)}\}}$$

where the eigenvalues of $\mathbf{M}$ are arranged as $\lambda_{\mathbf{M}1} \geq \ldots \geq \lambda_{\mathbf{M}r} > \lambda_{\mathbf{M}(r+1)} \geq \ldots \geq \lambda_{\mathbf{M}n}$,

$\lambda_{\mathbf{M}1} > 0$, $0 > \lambda_{\mathbf{M}(r+1)} \geq \ldots \geq \lambda_{\mathbf{M}n}$ and $\mathbf{z}^{F_L=0}_{\{\mathbf{v}_{\mathbf{M}1},\mathbf{v}_{\mathbf{M}2},\ldots,\mathbf{v}_{\mathbf{M}n}\}} \neq \mathbf{0}$.

Proof

The projection of $\mathbf{z}^{F_L=0}_{\{\mathbf{v}_{\mathbf{M}1},\mathbf{v}_{\mathbf{M}2},\ldots,\mathbf{v}_{\mathbf{M}n}\}} = [z_1 \quad z_2 \quad \ldots \quad z_n]^{T} \in S_{F_L=0}$ onto the plane spanned

by $\{\mathbf{v}_{\mathbf{M}(r+1)},\mathbf{v}_{\mathbf{M}(r+2)},\ldots,\mathbf{v}_{\mathbf{M}n}\}$ is the vector:

$$\mathbf{z}_{\{\mathbf{v}_{\mathbf{M}(r+1)},\mathbf{v}_{\mathbf{M}(r+2)},\ldots,\mathbf{v}_{\mathbf{M}n}\}} = [0 \quad \ldots \quad 0 \quad z_{r+1} \quad \ldots \quad z_n]^{T}$$

Note that we do not consider the cases in which $z_1 = z_2 = \ldots = z_r = 0$. To see this,

consider the expression for $F_L(\mathbf{x}) = \mathbf{x}^{T}\mathbf{Mx} = 0$ in the principal-axes coordinate:

$$F_L(\mathbf{x})\big|_{\mathbf{x}=\mathbf{T_M z}} = F_{L_T}(\mathbf{z}) = \lambda_{\mathbf{M}1}z_1^{2} + \ldots + \lambda_{\mathbf{M}r}z_r^{2} + \lambda_{\mathbf{M}(r+1)}z_{(r+1)}^{2} + \ldots + \lambda_{\mathbf{M}n}z_n^{2} = 0 \quad (4.11)$$

where the z_i – axis is along $\mathbf{v}_{\mathbf{M}i}$, $i = 1,2,\ldots,n$ and $\mathbf{T_M} = [\mathbf{v}_{\mathbf{M}1} \mid \mathbf{v}_{\mathbf{M}2} \mid \ldots \mid \mathbf{v}_{\mathbf{M}n}]$. We see

that if $z_1 = z_2 = \ldots = z_r = 0$ then (4.11) is satisfied only at the origin because

(Proof of Theorem 4.2 (Cont.))

$0 > \lambda_{M(r+1)} \geq \ldots \geq \lambda_{Mn}$. Since Theorem 4.2 does not apply at the origin, this special case is irrelevant. Our original problem is to find $\mathbf{z}^{FL=0}_{\{v_{M1}, v_{M2}, \ldots, v_{Mn}\}}$ such that the angle between

$\mathbf{z}^{FL=0}_{\{v_{M1}, v_{M2}, \ldots, v_{Mn}\}}$ and the corresponding projection $\mathbf{z}_{\{v_{M(r+1)}, v_{M(r+2)}, \ldots, v_{Mn}\}}$ is <u>minimized</u>

over all possible $\mathbf{z}^{FL=0}_{\{v_{M1}, v_{M2}, \ldots, v_{Mn}\}} \neq \mathbf{0}$. From basic geometry, the cosine of the angle θ

between $\mathbf{z}^{FL=0}_{\{v_{M1}, v_{M2}, \ldots, v_{Mn}\}}$ and $\mathbf{z}_{\{v_{M(r+1)}, v_{M(r+2)}, \ldots, v_{Mn}\}}$ is given by:

$$
\begin{aligned}
\cos(\theta) &= \frac{[\mathbf{z}^{FL=0}_{\{v_{M1}, v_{M2}, \ldots, v_{Mn}\}}]^T \, \mathbf{z}_{\{v_{M(r+1)}, v_{M(r+2)}, \ldots, v_{Mn}\}}}{\left\| [\mathbf{z}^{FL=0}_{\{v_{M1}, v_{M2}, \ldots, v_{Mn}\}}]^T \right\| \left\| \mathbf{z}_{\{v_{M(r+1)}, v_{M(r+2)}, \ldots, v_{Mn}\}} \right\|} \\[2mm]
&= \frac{z_{r+1}^2 + z_{r+2}^2 + \ldots + z_n^2}{\sqrt{z_1^2 + z_2^2 + \ldots + z_r^2 + z_{r+1}^2 + \ldots + z_n^2} \, \sqrt{z_{r+1}^2 + z_{r+2}^2 + \ldots + z_n^2}} \\[2mm]
&= \frac{\sqrt{z_{r+1}^2 + z_{r+2}^2 + \ldots + z_n^2}}{\sqrt{z_1^2 + z_2^2 + \ldots + z_r^2 + z_{r+1}^2 + \ldots + z_n^2}}
\end{aligned} \tag{4.12}
$$

Notice from (4.12) that for MIMO systems, $\cos(\theta)$ can be zero at infinitely many points other than the origin because $\lambda_{M1}, \lambda_{M2}, \ldots, \lambda_{Mr}$ need not be all-positive. Example of such

points are $[z_1 \;\; z_2 \;\; \ldots \;\; z_{r-1} \;\; z_r \;\; z_{r+1} \;\; \ldots \;\; z_n]^T = [c \;\; 0 \;\; \ldots \;\; 0 \;\; c\sqrt{\dfrac{\lambda_{M1}}{|\lambda_{Mr}|}} \;\; 0 \;\; \ldots \;\; 0]^T$

where $c \in \Re$, $\lambda_{M1} > 0$, and $\lambda_{Mr} < 0$. Because $\mathbf{z}^{FL=0}_{\{v_{M1}, v_{M2}, \ldots, v_{Mn}\}} \neq \mathbf{0}$, the denominator in

(4.12) is greater than zero, while we see that the numerator in (4.12) is nonnegative. These implies that $0 \leq \cos(\theta) < 1$ and $0 < \theta \leq (\pi/2)$. In this range, we have that $\cos(\theta)$

monotonically increases as θ decreases. Accordingly, the original problem can be cast as

an optimization problem for which the objective is to find $\mathbf{z}^{FL=0}_{\{v_{M1}, v_{M2}, \ldots, v_{Mn}\}} \neq \mathbf{0}$ that

<u>maximizes</u> the right-hand side of (4.12), with constraints given by (4.11) and by Theorem

4.1:

(Proof of Theorem 4.2 (Cont.))

$$\text{Maximize}: J_1 = \frac{\sqrt{z_{r+1}^2 + z_{r+2}^2 + \ldots + z_n^2}}{\sqrt{z_1^2 + z_2^2 + \ldots + z_r^2 + z_{r+1}^2 + \ldots + z_n^2}}$$

Subjected to: 1) $\lambda_{M1}z_1^2 + \ldots + \lambda_{Mr}z_r^2 + \lambda_{M(r+1)}z_{(r+1)}^2 + \ldots + \lambda_{Mn}z_n^2 = 0$

: 2) $\lambda_{M1} \geq \ldots \geq \lambda_{Mr} > \lambda_{M(r+1)} \geq \ldots \geq \lambda_{Mn}$ (4.13)

: 3) $0 > \lambda_{M(r+1)} \geq \ldots \geq \lambda_{Mn}$

: 4) $\lambda_{M1} > 0$

We notice that the numerator and the denominator of the objective function are nonnegative. Accordingly, squaring the objective function does not change the solution. For simplicity, we now convert (4.13) to:

$$\text{Maximize}: J_2 = J_1^2 = \frac{z_{r+1}^2 + z_{r+2}^2 + \ldots + z_n^2}{(z_1^2 + z_2^2 + \ldots + z_r^2) + (z_{r+1}^2 + \ldots + z_n^2)}$$

Subjected to: 1) $\lambda_{M1}z_1^2 + \ldots + \lambda_{Mr}z_r^2 + \lambda_{M(r+1)}z_{(r+1)}^2 + \ldots + \lambda_{Mn}z_n^2 = 0$

: 2) $\lambda_{M1} \geq \ldots \geq \lambda_{Mr} > \lambda_{M(r+1)} \geq \ldots \geq \lambda_{Mn}$ (4.14)

: 3) $0 > \lambda_{M(r+1)} \geq \ldots \geq \lambda_{Mn}$

: 4) $\lambda_{M1} > 0$

where the range of the objective function is $0 \leq J_2 < 1$. This is equivalent to:

$$\text{Minimize}: J_3 = J_2^{-1} = \frac{z_1^2 + z_2^2 + \ldots + z_r^2}{z_{r+1}^2 + z_{r+2}^2 + \ldots + z_n^2} + 1$$

Subjected to: 1) $\lambda_{M1}z_1^2 + \ldots + \lambda_{Mr}z_r^2 + \lambda_{M(r+1)}z_{(r+1)}^2 + \ldots + \lambda_{Mn}z_n^2 = 0$

: 2) $\lambda_{M1} \geq \ldots \geq \lambda_{Mr} > \lambda_{M(r+1)} \geq \ldots \geq \lambda_{Mn}$ (4.15)

: 3) $0 > \lambda_{M(r+1)} \geq \ldots \geq \lambda_{Mn}$

: 4) $\lambda_{M1} > 0$

where the range of the objective function is now $1 < J_3 \leq \infty$. We emphasize that the signs of λ_{Mi}, $i = 2,3,\ldots,r$ need not be the same. To find the solution $z_{\{v_{M1}, v_{M2}, \ldots, v_{Mn}\}}^{F_L = 0}$

$= [z_1 \ldots z_r \; z_{r+1} \ldots z_n]^T \neq 0$ for (4.15), we consider the following arguments:

(Proof of Theorem 4.2 (Cont.))

1)   The set $\{z_1, z_2, \ldots, z_r\}$ corresponding to the solution vector contains at least one

nonzero element z_i such that $\lambda_{\mathbf{M}i} > 0$. Otherwise, the first constraint in (4.15) is

satisfied only at the origin, or the first constraint and the third constraint cannot be

satisfied at the same time. This leads to a contradiction since we omit the origin

and we require that all constraints be satisfied.

2)   The set $\{z_{r+1}, z_{r+2}, \ldots, z_n\}$ corresponding to the solution vector contains at least

one nonzero element. Otherwise we see from the objective function in (4.15) that

the objective function is at the maximum of infinity. Since we seek a minimum, it

follows that $\{z_{r+1}, z_{r+2}, \ldots, z_n\}$ must contain at least one nonzero element.

3)   The constraints in (4.15) implies that:

$$\lambda_{\mathbf{M}1}(z_1^2 + \ldots + z_r^2) \geq \lambda_{\mathbf{M}1}z_1^2 + \ldots + \lambda_{\mathbf{M}r}z_r^2 = -(\lambda_{\mathbf{M}(r+1)}z_{r+1}^2 + \ldots + \lambda_{\mathbf{M}n}z_n^2) > 0$$

$$z_1^2 + \ldots + z_r^2 \geq \frac{\lambda_{\mathbf{M}1}z_1^2 + \ldots + \lambda_{\mathbf{M}r}z_r^2}{\lambda_{\mathbf{M}1}} = \frac{-(\lambda_{\mathbf{M}(r+1)}z_{r+1}^2 + \ldots + \lambda_{\mathbf{M}n}z_n^2)}{\lambda_{\mathbf{M}1}} > 0$$

where $-(\lambda_{\mathbf{M}(r+1)}z_{r+1}^2 + \ldots + \lambda_{\mathbf{M}n}z_n^2) > 0$ because of the third constraint in (4.15).

Notice that $z_1^2 + \ldots + z_r^2 = \dfrac{\lambda_{\mathbf{M}1}z_1^2 + \ldots + \lambda_{\mathbf{M}r}z_r^2}{\lambda_{\mathbf{M}1}}$ when $z_i = 0$, $i = 2, 3, \ldots, r$.

Accordingly, $z_1^2 + \ldots + z_r^2$ is minimum for a given $\{z_{r+1}, \ldots, z_n\}$ when $z_i = 0$,

$i = 2, 3, \ldots, r$.

4)   The constraints in (4.15) implies that:

$$0 > \lambda_{\mathbf{M}(r+1)}(z_{r+1}^2 + \ldots + z_n^2) \geq \lambda_{\mathbf{M}(r+1)}z_{r+1}^2 + \ldots + \lambda_{\mathbf{M}n}z_n^2 = -(\lambda_{\mathbf{M}1}z_1^2 + \ldots + \lambda_{\mathbf{M}r}z_r^2)$$

$$0 < z_{r+1}^2 + \ldots + z_n^2 \leq \frac{\lambda_{\mathbf{M}(r+1)}z_{r+1}^2 + \ldots + \lambda_{\mathbf{M}n}z_n^2}{\lambda_{\mathbf{M}(r+1)}} = \frac{-(\lambda_{\mathbf{M}1}z_1^2 + \ldots + \lambda_{\mathbf{M}r}z_r^2)}{\lambda_{\mathbf{M}(r+1)}}$$

(Proof of Theorem 4.2 (Cont.))

where the inequalities are reversed because $\lambda_{M(r+1)} < 0$. Notice that

$$z_{r+1}^2 + \ldots + z_n^2 = \frac{\lambda_{M(r+1)} z_{r+1}^2 + \ldots + \lambda_{Mn} z_n^2}{\lambda_{M(r+1)}} \quad \text{when } z_i = 0, \ i = r+2, r+3, \ldots, n.$$

Accordingly, $z_{r+1}^2 + \ldots + z_n^2$ is maximum for a given $\{z_1, \ldots, z_r\}$ when $z_i = 0$,

$i = r+2, r+3, \ldots, n$.

It follows from the arguments in 1 – 4 that the solution of (4.15) is given by:

$$\mathbf{z}_{\{\mathbf{v_{M1}}, \mathbf{v_{M2}}, \ldots, \mathbf{v_{Mn}}\}}^{F_L=0} = \begin{bmatrix} z_1 & 0 & \ldots & 0 & z_{r+1} & 0 & \ldots & 0 \end{bmatrix}^T \equiv \mathbf{z}_{\{\mathbf{v_{M1}}, \mathbf{v_{M(r+1)}}\}}^{F_L=0}$$

At the solution $\mathbf{z}_{\{\mathbf{v_{M1}}, \mathbf{v_{M(r+1)}}\}}^{F_L=0}$, the minimum of the objective function in (4.15) is given

by:

$$J_3^* = \frac{z_1^2}{z_{r+1}^2} + 1 \tag{4.16}$$

To find the minimum of J_3, we substitute $\mathbf{z}_{\{\mathbf{v_{M1}}, \mathbf{v_{M(r+1)}}\}}^{F_L=0}$ into the first constraint in (4.15)

to produce:

$$\lambda_{M1} z_1^2 + \lambda_{M(r+1)} z_{(r+1)}^2 = 0$$

$$z_1^2 = -\frac{\lambda_{M(r+1)} z_{(r+1)}^2}{\lambda_{M1}} > 0 \tag{4.17}$$

where we recall that $\lambda_{M1} > 0$ and $\lambda_{M(r+1)} < 0$. Notice that we can always find a value of

z_1 for every set of $\{\lambda_{M1}, \lambda_{M(r+1)}, z_{r+1}\}$ where $\lambda_{M1} > 0$ and $\lambda_{M(r+1)} < 0$ such that the

first constraint is satisfied. Now, we substitute $-\dfrac{\lambda_{M(r+1)} z_{(r+1)}^2}{\lambda_{M1}}$ for z_1^2 in (4.16). This

produces the minimum values for J_3:

(Proof of Theorem 4.2 (Cont.))

$$J_3^* = -\frac{\lambda_{M(r+1)}}{\lambda_{M1}} + 1 = \frac{\lambda_{M1} - \lambda_{M(r+1)}}{\lambda_{M1}} > 1 \qquad (4.18\ a)$$

where we note that $\dfrac{\lambda_{M1} - \lambda_{M(r+1)}}{\lambda_{M1}} > 1$ because $\lambda_{M1} > 0$ and $\lambda_{M(r+1)} < 0$. This solution

corresponds to the <u>maximum</u> value of J_2 and J_1:

$$0 < J_2^* = (J_3^*)^{-1} = \frac{\lambda_{M1}}{\lambda_{M1} - \lambda_{M(r+1)}} < 1 \qquad (4.18\ b)$$

$$0 < J_1^* = \sqrt{J_2^*} = \sqrt{\frac{\lambda_{M1}}{\lambda_{M1} - \lambda_{M(r+1)}}} < 1 \qquad (4.18\ c)$$

This completes the proof of Theorem 4.2.

We recall from (1.23) that the eigenvalue ratio is defined as:

$$r_{\lambda_M} \equiv \left| \frac{\max(\lambda_{Mi}^+)}{\max(\lambda_{Mj}^-)} \right| \qquad (1.23)$$

where λ_{Mi}^+ are positive eigenvalues of $\mathbf{M}$, λ_{Mj}^- are the negative eigenvalues of $\mathbf{M}$ such

that $\mathbf{v}_{Mj}$ spans $S_{G_L=0}$ when the eigenvector condition is satisfied. Using the arrangement

of eigenvalues of $\mathbf{M}$ in (4.15), we have that $i = 1$ and $j = r+1, r+2, \ldots, n$. <u>Thus, the</u>

<u>eigenvalue ratio for MIMO systems is given by</u> $r_{\lambda_M} = \left| \dfrac{\lambda_{M1}}{\lambda_{M(r+1)}} \right| = -\dfrac{\lambda_{M1}}{\lambda_{M(r+1)}}$. By

inspecting (4.18), a small r_{λ_M} corresponds to a large J_3, to a small J_2, and to a small

J_1. Since $J_1 = \cos(\theta)$, a small J_1 implies that the angle between a vector belonging to

$S_{F_L=0}$ and its projection onto $S_{G_L=0}$ is large by Theorem 4.2. By satisfying the

eigenvector condition with a small r_{λ_M}, we not only locate $S_{F_L=0}$ symmetrically about

$S_{\mathbf{G}_{L}=0}$, but also force $S_{F_{L}=0}$ away from $S_{\mathbf{G}_{L}=0}$. In view of Proposition 1.1 and 1.2, this implies that a possible intersection point $\mathbf{x}_{C_{Si}}$ between $S_{F=0}$ and $S_{\mathbf{G}=0}$ is located "reasonably far" from the origin.

Generating LARC Using a Linearized Model

In this section, we are interested in generating a LARC for (4.1) when the linearized model about the origin is known. The fundamental idea of LARC is to force $\dot{V}(\mathbf{x})$ to be negative definite in radially large regions about the origin. We see that this cannot be accomplished at intersection points between $S_{F=0}$ and $S_{\mathbf{G}=0}$, and between $S_{F=0}$ and $S_{\mathbf{u}=0}$. When the relative orientations of these surfaces are poor, these intersection points can occur arbitrarily close to the origin, and result in an arbitrarily small LAR in the presence of small nonlinearities. Now, we reexamine a local approximation of $\dot{V}(\mathbf{x})$ about the origin:

$$
\begin{aligned}
\dot{V}_L(\mathbf{x}) &= \mathbf{x}^T \mathbf{P} \mathbf{A} \mathbf{x} + \mathbf{x}^T \mathbf{P} \mathbf{B} \mathbf{u}(\mathbf{x}) \\
&\equiv F_L(\mathbf{x}) + \mathbf{G}_L(\mathbf{x}) \mathbf{u}(\mathbf{x})
\end{aligned}
\tag{4.4}
$$

where $\mathbf{P}$ is obtained from Theorem 4.1 to satisfy the eigenvector condition. Now, we recall from the definition of eigenvector condition that $S_{F_L=0}$ is symmetric about $S_{\mathbf{G}_L=0}$ such that $S_{\mathbf{G}_L=0} \subset R_{[F_L<0] \cup \{0\}}$. By examining (4.4), it is reasonable that we orient $S_{\mathbf{u}=0}$ and $S_{\mathbf{G}_L=0}$ in the same fashion such that $S_{F_L=0}$ is symmetric about $S_{\mathbf{u}=0}$, and $S_{\mathbf{u}=0} \subset R_{[F_L<0] \cup \{0\}}$. This particular relative orientation follows from the same reasoning we employ to establish the eigenvector condition. Indeed, if $S_{\mathbf{u}=0}$ is close to a particular

portion of $S_{F_L=0}$ then the deviations of $S_{F=0}$ from $S_{F_L=0}$ may locate an intersection

between $S_{u=0}$ and $S_{F=0}$ arbitrarily close to the origin. At such an intersection, it is clear

that we cannot force $\dot{V}$ to be negative because $\mathbf{u} = \mathbf{0}$ and $F = 0$, and the resulting LAR

is then small. We see that such linear control corresponds to the linear gain matrix

$\mathbf{K} = \rho[\mathbf{PB}]^T = \rho\mathbf{B}^T\mathbf{P}$ employed in the Riccati equation (4.7) to solve for $\mathbf{P}$.

Corresponding to such linear gain matrix is the linear control:

$$\mathbf{u}(\mathbf{x}) = -\rho\mathbf{B}^T\mathbf{P}\mathbf{x} \tag{4.19}$$

where $\rho \in \mathfrak{R}^+$. These results are the same as those obtained in Chapter II for SIMO

systems.

To obtain the general form of LARC for MIMO systems, we examine the proof of

Lemma 2.3 in which the general from of LARC for SIMO systems is derived. We see

that Lemma 2.3 does not assume a specific dimension for $\mathbf{B}$. Accordingly, the general

form of LARC for MIMO systems is immediate from Lemma 2.3:

$$\mathbf{u}_{LARC}(\mathbf{x}) = -\eta\rho\mathbf{B}^T\mathbf{P}\mathbf{x} \equiv -\mathbf{K}_{LARC}\mathbf{x} \tag{4.20}$$

where $\mathbf{P}$ is the solution of the Riccati equation in Theorem 4.1 and:

$$\mathbf{K}_{LARC} \equiv \eta\rho\mathbf{B}^T\mathbf{P} \tag{4.21}$$

In addition, it is immediate from the proof of Lemma 2.3 that the linearized model (4.2)

is stable under (4.20) $\forall \rho \in \mathfrak{R}^+$ and $\eta \geq 1$. In this section, we fix $\eta = 1$ for simplicity and

thus we need only to select ρ. To select an appropriate value for ρ, we construct the

eigenvalue-ratio plot using the definition of eigenvalue ratio for MIMO systems given in

Section 4.4. Generally, We select from this plot a value of ρ that yields a small

eigenvalue ratio because this forces $S_{F_L=0}$ away from $S_{G_L=0}$. However, such a value of

ρ may correspond to a large $\mathbf{K}_{LARC}$. If the control energy is limited, we may be forced to

select a larger eigenvalue ratio to obtain a smaller $\mathbf{K}_{LARC}$. The tuning procedure

proposed in section 2.5 for SIMO systems is applicable to MIMO systems immediately.

Now, we point out the relationship between LQR and LARC for MIMO systems, which

turns out to be the same as that discovered in Chapter II. From linear optimal control

theory, we know by inspection that the Riccati equation (4.7) corresponds to the

quadratic performance index:

$$J = \int_0^\infty (\mathbf{x}^T \overline{\mathbf{Q}} \mathbf{x} + \mathbf{u}^T \overline{\mathbf{R}} \mathbf{u})\, dt$$
$$= \int_0^\infty (2c\mathbf{x}^T \mathbf{I} \mathbf{x} + \frac{1}{2\rho} \mathbf{u}^T \mathbf{I} \mathbf{u})\, dt \qquad (4.22)$$

where ρ, $c \in \mathfrak{R}^+$, $\overline{\mathbf{Q}} = 2c\mathbf{I}$ and $\overline{\mathbf{R}} = \dfrac{1}{2\rho} \mathbf{I}$. In addition, we recognize that the linear

optimal control that minimizes J is given by:

$$\mathbf{u}(\mathbf{x}) = \mathbf{u}_{LQR}(\mathbf{x}) = -\overline{\mathbf{R}}^{-1} \mathbf{B}^T \mathbf{P} \mathbf{x} = -2\rho \mathbf{B}^T \mathbf{P} \mathbf{x} \qquad (4.23)$$

We observe the same relationship between $\mathbf{u}_{LQR}(\mathbf{x})$ and $\mathbf{u}_{LARC}(\mathbf{x})$ pointed out in

Chapter II:

$$\mathbf{u}_{LQR}(\mathbf{x}) = \frac{2}{\eta} \mathbf{u}_{LARC}(\mathbf{x}) = \mathbf{u}_{LARC}(\mathbf{x})\big|_{\eta=2} \qquad (4.24)$$

Because of the relationship between LQR and LARC in (4.24), we note that for MIMO

linear systems:

1)   It can be inferred that <u>if the response characteristics resulting from LQR are</u>

<u>acceptable then so are those resulting from LARC with</u> $\eta = 2$.

2)   <u>Robustness properties of LARC can be drawn directly from those of LQR.</u>

However, we emphasize that LARC is primarily formulated for nonlinear systems.

Although it is possible to apply a LARC to a linear system, this may not offer advantages

over existing techniques because the available solutions of linear differential equations

have not been incorporated into the formulation of LARC.

4.2   Nominal Model Case

In the remainder of this chapter, we obtain a MIMO version of the robust LARC

developed in Chapter III. The system of interest is described by:

$$\dot{\mathbf{x}} = \mathbf{f}(\mathbf{x}, t) + \mathbf{g}(\mathbf{x}, t)\mathbf{u}(\mathbf{x}) \tag{4.25}$$

where the vectors $\mathbf{f}(\mathbf{x}, t) \in \mathfrak{R}^n$ and $\mathbf{g}(\mathbf{x}, t) \in \mathfrak{R}^{n \times m}$ are uncertain, and $\mathbf{u}(\mathbf{x}) = -\mathbf{Kx} \in \mathfrak{R}^m$.

These are such that $\dot{\mathbf{x}}$ is piecewise continuous in t, and is locally Lipschitz in the

operating region of interest in $\mathfrak{R}^n$ $\forall t \geq 0$. Recall from Chapter I that the above state

equations can be rewritten as:

$$\begin{aligned} \dot{\mathbf{x}} &= \mathbf{A}_n\mathbf{x} + \mathbf{B}_n\,\mathbf{u}(\mathbf{x}) + [\mathbf{f}(\mathbf{x}, t) - \mathbf{A}_n\mathbf{x} + \mathbf{g}(\mathbf{x}, t)\mathbf{u}(\mathbf{x}) - \mathbf{B}_n\mathbf{u}(\mathbf{x})] \\ &\equiv \mathbf{A}_n\mathbf{x} + \mathbf{B}_n\,\mathbf{u}(\mathbf{x}) + \mathbf{f}_\Sigma(\mathbf{x}, t, \mathbf{u}(\mathbf{x})) \\ &\equiv \overline{\mathbf{A}}_n\mathbf{x} + \mathbf{f}_\Omega(\mathbf{x}, t) \end{aligned} \tag{4.26}$$

where the elements of (4.26) are immediate from Section 3.1. The corresponding nominal

model is:

$$\dot{\mathbf{x}} = \mathbf{A}_n\mathbf{x} + \mathbf{B}_n\,\mathbf{u}(\mathbf{x}) \tag{4.27}$$

Uncertainty Specifications

Uncertainty specifications of MIMO systems are classified in the same fashion as those

for SIMO systems:

1) Structured uncertainty specifications for stability analysis

2) Unstructured uncertainty specifications for stability analysis

3) Structured uncertainty specifications for controller generation

4) Unstructured uncertainty specifications for controller generation

For stability analysis of MIMO systems, we say that the uncertain vector $\mathbf{f}_\Omega(\mathbf{x}, t)$ are

"structured" if it can be written as:

$$\mathbf{f}_\Omega(\mathbf{x}, t) \equiv [\mathbf{f}(\mathbf{x}, t) - \mathbf{A}_n \mathbf{x}] + [\mathbf{g}(\mathbf{x}, t) - \mathbf{B}_n]\mathbf{u}(\mathbf{x})\big|_{\mathbf{u} = -\mathbf{K}\mathbf{x}}$$
$$= \sum_{j=1}^{r} [h_j(\mathbf{x}, t)\mathbf{E}_j \mathbf{x}] \tag{4.28}$$

where $h_j(\mathbf{x}, t) \in [h_{lj}, h_{uj}] \in \mathfrak{R}$, $h_{lj} < h_{uj}$, and $\mathbf{E}_j \in \mathfrak{R}^{n \times n}$ $j = 1, 2, \ldots, r$. The availability of

the uncertainty specifications h_{lj} (a lower bound of $h_j(\mathbf{x}, t)$), h_{uj} (an upper bound of

$h_j(\mathbf{x}, t)$), and $\mathbf{E}_j$ $j = 1, \ldots, r$ is assumed. The uncertain vector $\mathbf{f}_\Omega(\mathbf{x}, t)$ are

"unstructured" if the only known information is a bound on $\dfrac{\|\mathbf{f}_\Omega(\mathbf{x}, t)\|}{\|\mathbf{x}\|}$. We see that the

MIMO "structured" and "unstructured" uncertainty specifications for stability analysis

are the same as those for SIMO systems. Indeed, all the uncertainty specifications for

MIMO systems are the same as those for SIMO systems given in Section 3.3.

Controller Selection and Generation

Using the MIMO uncertainty specifications, we notice that Theorem 3.2 and 3.3 apply to

MIMO systems as well as to SIMO systems because these theorems do not restrict the

dimension of **B**. Because of this result, it follows that:

1)   The reasoning for applying LARC to MIMO systems is the same as that for

     applying LARC to SIMO systems. This is given in section "Controller Selection"

     of Chapter III.

2)   The controller generation procedures for SIMO systems can be applied for MIMO

     systems immediately. These procedures are given in section "Controller

     Generation" of Chapter III.

It is straightforward from the remark given at the end of Section 3.5 that the procedure

for generating a LARC for the time-invariant system (4.1) can be applied to (4.25),

provided that the linearized model about the origin of (4.25) is given by (4.2) with known

A and **B**. Next, we give an example showing how to generate a robust LARC using the

controller generation procedure for structured uncertain systems.

Example 4.1   (A Helicopter)

In this example, we want to stabilize a helicopter in a vertical plane for a range of air

speed from 60 knots to 170 knots (Schmitendorf, 1988), (Chen, and Chen, 1991). The

dynamics of the helicopter is given by:

$$\dot{\mathbf{x}} = [\mathbf{A}_n + \Delta\mathbf{A}_n(\mathbf{x},t)]\mathbf{x} + [\mathbf{B}_n + \Delta\mathbf{B}_n(\mathbf{x},t)]\mathbf{u} \qquad (\text{E } 4.1.1)$$

$$\text{where } \mathbf{A}_n = \begin{bmatrix} -0.0366 & 0.0271 & 0.0188 & -0.4555 \\ 0.0482 & -1.01 & 0.0024 & -4.0208 \\ 0.1002 & 0.2855 & -0.707 & 1.3229 \\ 0 & 0 & 1 & 0 \end{bmatrix}, \ \mathbf{B}_n = \begin{bmatrix} 0.4422 & 0.1761 \\ 0.0447 & -7.5922 \\ -5.52 & 4.99 \\ 0 & 0 \end{bmatrix}, \ x_1 =$$

horizontal velocity, x_2 = vertical velocity, x_3 = pitch rate, x_4 = pitch angle, u_1 =

collective pitch control, and u_2 = longitudinal cyclic pitch control. The nominal model

$\dot{\mathbf{x}} = \mathbf{A}_n \mathbf{x} + \mathbf{B}_n \mathbf{u}$ is subjected to time-varying structured uncertainties. Significant

uncertainties are at the elements (3,2) and (3,4) of $\mathbf{A}_n$, and at the element (2,1) of $\mathbf{B}_n$.

The structured uncertainty specifications are given by:

$$\Delta \mathbf{A}_n(\mathbf{x}, t) = \sum_{\alpha=1}^{2} [h_{\alpha}^{A_n}(\mathbf{x}) \mathbf{E}_{\alpha}^{A_n}] \mathbf{x} \qquad \text{(E 4.1.2 a)}$$

$$\Delta \mathbf{B}_n(\mathbf{x}, t) = h_1^{B_n}(\mathbf{x}, t) \mathbf{E}_1^{\Delta B_n} \qquad \text{(E 4.1.2 b)}$$

$$\text{where } \mathbf{E}_1^{A_n} = \begin{bmatrix} 0 & 0 & 0 & 0 \\ 0 & 0 & 0 & 0 \\ 0 & 1 & 0 & 0 \\ 0 & 0 & 0 & 0 \end{bmatrix}, \ \mathbf{E}_2^{A_n} = \begin{bmatrix} 0 & 0 & 0 & 0 \\ 0 & 0 & 0 & 0 \\ 0 & 0 & 0 & 1 \\ 0 & 0 & 0 & 0 \end{bmatrix}, \ \mathbf{E}_1^{\Delta B_n} = \begin{bmatrix} 0 & 0 \\ 1 & 0 \\ 0 & 0 \\ 0 & 0 \end{bmatrix}, \ h_1^{A_n}(\mathbf{x}, t) \in [-0.2192$$

$, 0.2192]$, $h_2^{A_n}(\mathbf{x}, t) \in [-1.2031, 1.2031]$, and $h_1^{B_n}(\mathbf{x}, t) \in [-2.0673, 2.0673]$. To generate a

LARC for this uncertain system, we start Procedure 2 by generating a three-dimension

plot of $\lambda_{max}(\mathbf{Z})$ versus ρ and η. Using our computer, it takes approximately 5 seconds to

produce the plot shown in Fig. E4.1.1 and Fig. E4.1.2.

According to this plot, there are infinitely many pairs of (ρ, η) for which $\lambda_{max}(\mathbf{Z}) < 0$.

By Theorem 3.2, such a pair of (ρ, η) can be employed to generate a LARC to meet the

given uncertainty specifications. At this point, we assume that sufficient control energy is

available and we may choose (ρ, η) corresponding to the minimum of $\lambda_{max}(\mathbf{Z})$ in Fig.

E4.1.1 to gain the largest stability margin. In Fig. E4.1.1, the minimum value of

$\lambda_{max}(\mathbf{Z}) = -0.2672$ is at $(\rho^*, \eta^*) = (0.06, 1.6)$. This corresponds to:

$$\mathbf{K}_{LARC} = \begin{bmatrix} 0.3448 & -0.0113 & -0.3888 & -0.5856 \\ -0.0401 & -0.2724 & 0.1715 & 0.4940 \end{bmatrix} \qquad \text{(E 4.1.3 a)}$$
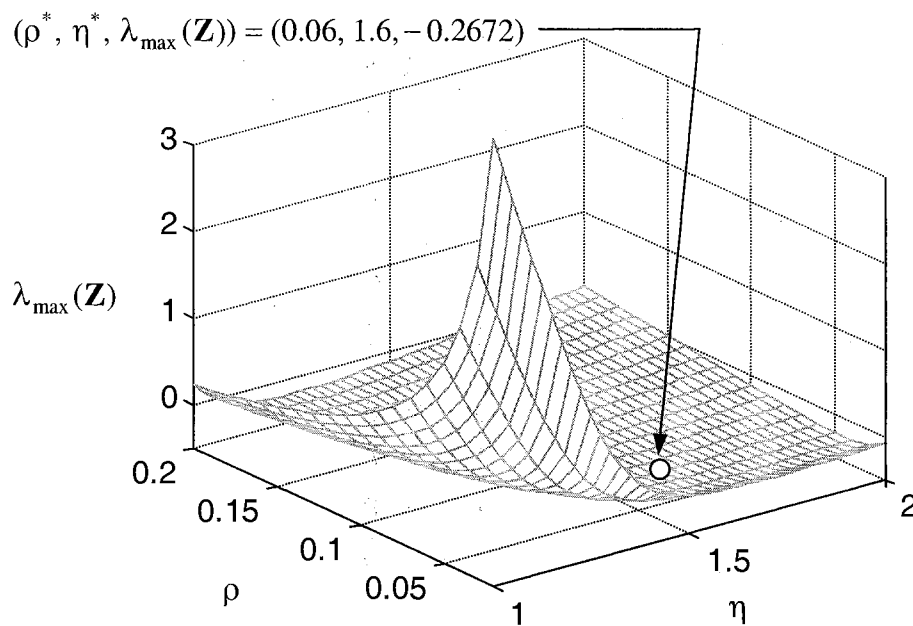
Fig. E4.1.1   A Plot of $\lambda_{max}(\mathbf{Z})$ versus $\rho \in [0.02, 0.2]$ and $\eta \in [1, 2]$
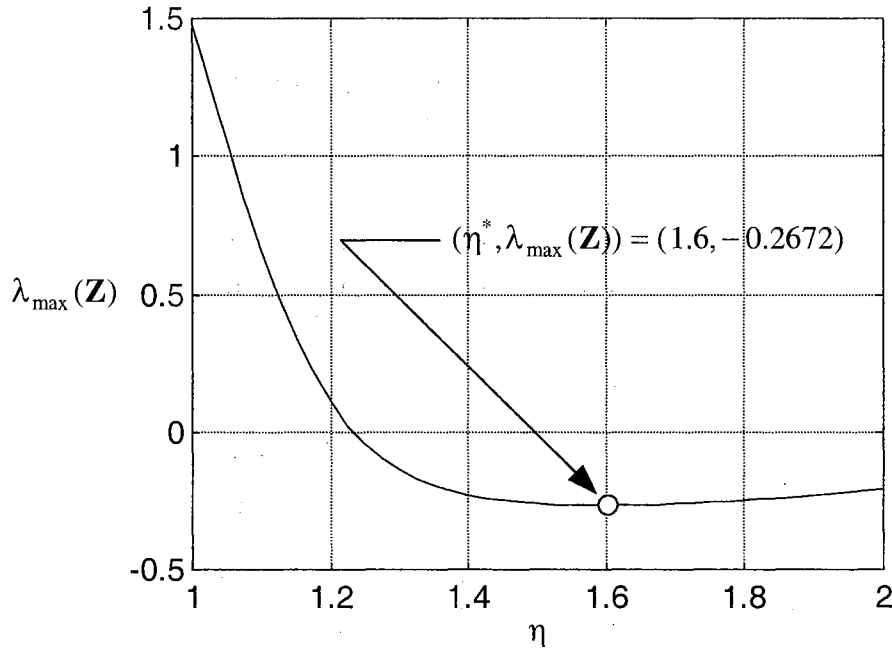
Fig. E4.1.2 A Plot of $\lambda_{max}(\mathbf{Z})$ versus $\eta \in [1, 2]$ when $\rho = \rho^* = 0.06$

$$\mathbf{Q} = \begin{bmatrix} 1.4706 & 0.0275 & -0.5504 & -0.8659 \\ 0.0275 & 1.2903 & -0.1654 & -0.4998 \\ -0.5504 & -0.1654 & 1.7054 & 1.2204 \\ -0.8659 & -0.4998 & 1.2204 & 3.2927 \end{bmatrix} \qquad \text{(E 4.1.3 b)}$$

where the eigenvalues of $\overline{\mathbf{A}}_n \equiv [\mathbf{A}_n - \mathbf{BK}_{LARC}]$ are given by $\lambda_1 = -0.3922$,

$\lambda_{2,3} = -0.8597 \pm j1.0525$, and $\lambda_4 = -4.8231$ in the LHP.

When the available control energy is limited, it is possible to find a pair of (ρ, η) from

Fig. E4.1.1 that generates a LARC to meet the given uncertainty specifications with a

smaller gain matrix. Indeed, we may zoom in Fig. E4.1.1 and find a pair of (ρ, η) that is

smaller than $(0.06, 1.6)$ such that the corresponding $\lambda_{max}(\mathbf{Z}) < 0$. The plot of $\lambda_{max}(\mathbf{Z})$

versus $\eta \in [1.2, 2]$ when $\rho = 0.0150$ is given in Fig E4.1.3. From Fig. E4.1.3, it is

sufficient to choose $\eta = 1.6$ with $\rho = 0.0150$ because these correspond to

$\lambda_{max}(\mathbf{Z}) = -0.0055 < 0$. The gain matrix corresponding to $(\rho, \eta) = (0.0150, 1.6)$ is given

by:

$$\mathbf{K}_{LARC} = \begin{bmatrix} 0.1560 & -0.0030 & -0.2370 & -0.3895 \\ -0.0342 & -0.0994 & 0.1475 & 0.3598 \end{bmatrix} \qquad \text{(E 4.1.4 a)}$$

$$\mathbf{Q} = \begin{bmatrix} 1.3983 & 0.0456 & -0.6563 & -1.1411 \\ 0.0456 & 1.1546 & -0.2179 & -0.5403 \\ -0.6563 & -0.2179 & 2.2177 & 2.2716 \\ -1.1411 & -0.5403 & 2.2716 & 5.3928 \end{bmatrix} \qquad \text{(E 4.1.4 b)}$$

where the eigenvalues of $\overline{\mathbf{A}}_n \equiv [\mathbf{A}_n - \mathbf{B}_n \mathbf{K}_{LARC}]$ are given by $\lambda_1 = -0.2540$,

$\lambda_{2,3} = -0.6432 \pm j0.9739$, and $\lambda_4 = -3.0660$ in the LHP. Note that it may be possible to

select other values for ρ and η to generate a LARC such that the uncertainty

specifications are met, and every element in the resulting gain matrix is smaller than the

respective one in (E 4.1.4 a). However, we do not pursue this further because the present

steps are sufficient to demonstrate how to select an appropriate coordinate of (ρ, η) from

the plot of $\lambda_{max}(\mathbf{Z})$ versus ρ and η.
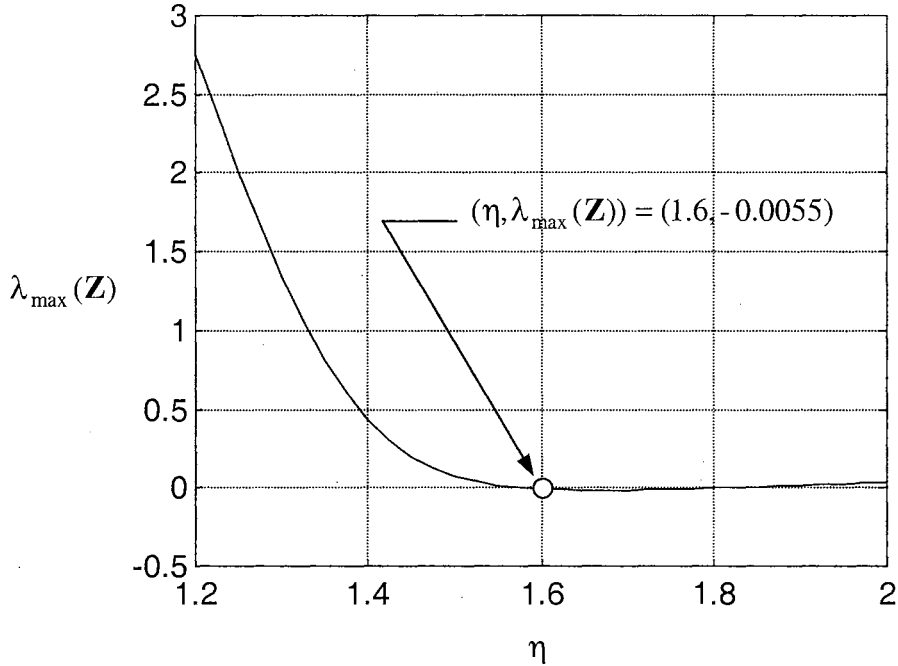
Fig. E4.1.3   A Plot of $\lambda_{max}(\mathbf{Z})$ versus $\eta \in [1.2, 2]$ when $\rho = 0.0150$

To compare our results with those in the literature, we now give the stabilizing gain

matrices from (Schmitendorf, 1988) and (Chen, and Chen, 1991) for the given

uncertainty specifications. The stabilizing gain matrix from (Schmitendorf, 1988) is:

$$\mathbf{K}_{[Sch]} = -\begin{bmatrix} -1.0181 & 0.2674 & 1.1123 & 1.7966 \\ 0.9531 & 0.8428 & -0.1412 & -0.7419 \end{bmatrix} \qquad \text{(E 4.1.5)}$$

The eigenvalues of $\overline{\mathbf{A}}_n \equiv [\mathbf{A}_n - \mathbf{B}_n \mathbf{K}_{[Sch]}]$ are given by $\lambda_{1,2} = -1.0202 \pm 0.1826$,

$\lambda_3 = -2.4804$, and $\lambda_4 = -9.9443$. The stabilizing gain matrix from (Chen, and Chen,

1991) is:

$$\mathbf{K}_{[CC]} = -\begin{bmatrix} -0.1640 & 0.2699 & 0.4511 & 0.4308 \\ 0.0364 & 0.1692 & -0.1066 & -0.4519 \end{bmatrix} \qquad \text{(E 4.1.6)}$$

The eigenvalues of $\overline{\mathbf{A}}_n \equiv [\mathbf{A}_n - \mathbf{B}_n \mathbf{K}_{[CC]}]$ are given by $\lambda_{1,2} = -0.4180 \pm j0.2700$, and

$\lambda_{3,4} = -2.2343 \pm j1.0195$. Notice that most of the elements in our stabilizing gain matrix

(E 4.1.4 a) are smaller than the respective ones in (E 4.1.5) (Schmitendorf, 1988) and (E

4.1.6) (Chen, and Chen, 1991). However, we know that the responses of the nominal

system corresponding to the linear state-feedback gain matrix (E 4.1.4 a) are slower than

those corresponding to (Schmitendorf, 1988) and (Chen, and Chen, 1991) because of the

nominal closed-looop pole at $\lambda_1 = -0.2540$. In practice, we may want to have a

reasonable stability margin to account for neglected uncertainties in other elements of

$\mathbf{A}_n$ and $\mathbf{B}_n$. Accordingly, the controller in (E 4.1.3 a) may be preferable to (E 4.1.4 a)

because $\lambda_{max}(\mathbf{Z})$ corresponding to (E 4.1.3 a) is less than that corresponding to (E 4.1.4

a). Note that optimization is not needed for these original "weak" uncertainty

specifications.

Now, we assume that the uncertainties in $h_1^{An}(\mathbf{x},t)$, $h_2^{An}(\mathbf{x},t)$, and $h_1^{Bn}(\mathbf{x},t)$ increases

by 72.5%, 72.5%, and 72% respectively. In other words, the variations of $h_1^{An}(\mathbf{x},t)$,

$h_2^{An}(\mathbf{x},t)$, and $h_1^{Bn}(\mathbf{x},t)$ are now given by:

$$\left.\begin{array}{l} h_1^{An}(\mathbf{x},t)\in 1.725[-0.2192,0.2192] \\ h_2^{An}(\mathbf{x},t)\in 1.725[-1.2031,1.2031] \\ h_1^{Bn}(\mathbf{x},t)\in 1.72[-2.0673,2.0673] \end{array}\right\} \qquad (E\ 4.1.7)$$

To generate a LARC for these "increased" uncertainty specifications, we reapply

Procedure 2. Fig. E4.1.4 shows the plot of $\lambda_{max}(\mathbf{Z})$ versus ρ and η. The minimum of

$\lambda_{max}(\mathbf{Z}) = 1.2680$ in Fig E4.1.4 is at $(\rho^*,\eta^*) = (0.54,1)$. Since the minimum of $\lambda_{max}(\mathbf{Z})$

is positive, optimization is now needed. Before we start our optimization, we examine

Fig. E4.1.4 and observe that a small value of $\lambda_{max}(\mathbf{Z}) = 1.3546$ occurs at $(\rho,\eta) =$

$(0.2, 1.275)$. Accordingly, we expect that this point corresponds to a reasonably good initial value in addition to that corresponding to the minimum of $\lambda_{max}(\mathbf{Z}(\rho^*, \eta^*)) = 1.2680$. Relatively, ρ is 63% smaller than ρ^* while η is 28% larger than η^*. This suggests that elements of $\mathbf{K}_{LARC}$ corresponding to (ρ, η) __may__ be smaller than the respective ones in that corresponding to (ρ^*, η^*). Indeed, $\{\mathbf{K}_{LARC}, \mathbf{Q}\}$ corresponding to $(\rho^*, \eta^*) = (0.54, 1)$ is given by:

$$\mathbf{K}_{LARC,1} = \begin{bmatrix} 0.6911 & -0.0490 & -0.6813 & -0.9745 \\ -0.0277 & -0.6418 & 0.1702 & 0.4887 \end{bmatrix} \qquad \text{(E 4.1.8 a)}$$

$$\mathbf{Q} = \mathbf{I}_{4 \times 4} \qquad \text{(E 4.1.8 b)}$$

The LARC gain matrix and $\mathbf{Q}$ corresponding to $(\rho, \eta) = (0.2, 1.275)$ is given by:

$$\mathbf{K}_{LARC,2} = \begin{bmatrix} 0.5250 & -0.0320 & -0.5383 & -0.7673 \\ -0.0371 & -0.4615 & 0.1684 & 0.5083 \end{bmatrix} \qquad \text{(E 4.1.9 a)}$$

$$\mathbf{Q} = \begin{bmatrix} 1.2343 & 0.0003 & -0.2444 & -0.3567 \\ 0.0003 & 1.1810 & -0.0512 & -0.1777 \\ -0.2444 & -0.0512 & 1.2691 & 0.4218 \\ -0.3567 & -0.1777 & 0.4218 & 1.7165 \end{bmatrix} \qquad \text{(E 4.1.9 b)}$$

Notice that most of the elements in $\mathbf{K}_{LARC,2}$ are smaller than the respective ones in $\mathbf{K}_{LARC,1}$. Starting from the initial value $\{\mathbf{K}_{LARC}, \mathbf{Q}\}$ in (E 4.1.8) corresponding to $(\rho^*, \eta^*) = (0.54, 1)$, the simple univariate optimization technique runs approximately 1 minute on our PC to find a LARC that meets the increased uncertainty specifications:

$$\mathbf{K}_{OLARC,1} = \begin{bmatrix} 0.1119 & -0.0814 & -1.0233 & -0.9239 \\ -0.0513 & -1.4803 & 0.1504 & 0.8280 \end{bmatrix} \qquad \text{(E 4.1.10 a)}$$

$$\mathbf{Q} = \begin{bmatrix} 7.3811 & 0.8808 & 6.0303 & 0.0009 \\ 0.8808 & 10.4920 & 2.3856 & -0.1883 \\ 6.0303 & 2.3856 & 15.2885 & 8.0140 \\ 0.0009 & -0.1883 & 8.0140 & 13.0632 \end{bmatrix}$$

(E 4.1.10 b)
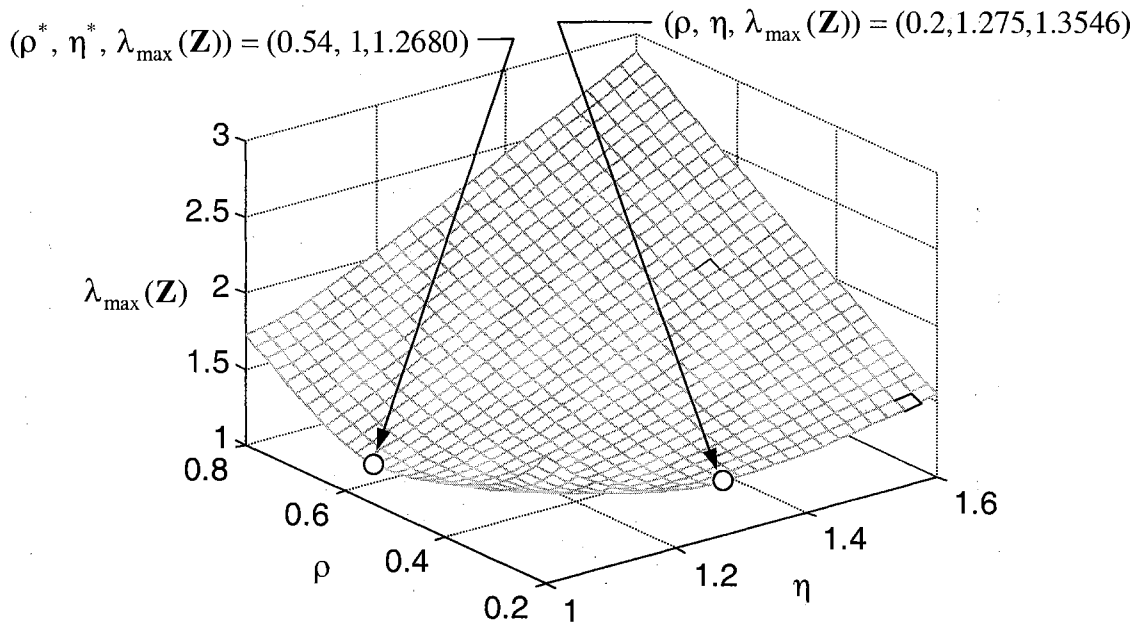
Fig. E4.1.4   A Plot of $\lambda_{max}(\mathbf{Z})$ versus $\rho \in [0.2,\ 0.8]$ and $\eta \in [1,\ 1.6]$

The solution in (E 4.1.10) corresponds to $\lambda_{max}(\mathbf{Z}) = -8.8989*10^{-3}$. The eigenvalues of

$\overline{\mathbf{A}}_n \equiv [\mathbf{A}_n - \mathbf{B}_n\mathbf{K}_{OLARC,1}]$ are given by $\lambda_1 = -0.1107$, $\lambda_2 = -1.5828$, $\lambda_3 = -2.2188$, and

$\lambda_4 = -15.2718$. When starting from the initial value in (E 4.1.9) corresponding to

$(\rho, \eta) = (0.2, 1.275)$, it takes approximately 1 minute to find the solution:

$$\mathbf{K}_{OLARC,2} = \begin{bmatrix} 0.4604 & -0.0310 & -0.9121 & -1.1086 \\ -0.0378 & -0.5740 & 0.1841 & 0.8699 \end{bmatrix}$$

(E 4.1.11 a)

$$\mathbf{Q} = \begin{bmatrix} 0.9627 & 0.0066 & -0.0247 & -0.4258 \\ 0.0066 & 0.1734 & -0.1309 & -0.1777 \\ -0.0247 & -0.1309 & 0.4298 & 0.4303 \\ -0.4258 & -0.1777 & 0.4303 & 0.7415 \end{bmatrix} \qquad \text{(E 4.1.11 b)}$$

This solution corresponds to $\lambda_{\max}(\mathbf{Z}) = -1.6585 * 10^{-3}$. The eigenvalues of

$\overline{\mathbf{A}}_n \equiv [\mathbf{A}_n - \mathbf{B}_n \mathbf{K}_{OLARC,2}]$ are given by $\lambda_1 = -0.3304$, $\lambda_{2,3} = -1.5465 \pm j0.6234$, and

$\lambda_4 = -8.7442$. For this particular problem and the particular two initial values in (E-

4.1.8) and (E 4.1.9), we notice that:

1)   A solution can be obtained to meet a given set of uncertainty specifications,

       although the initial value does not correspond to the minimum value of $\lambda_{\max}(\mathbf{Z})$

       in the three dimensional plot of $\lambda_{\max}(\mathbf{Z})$ versus ρ and η.

2)   When starting the optimization, most of the elements in the initial gain matrix

       corresponding to $(\rho^*, \eta^*) = (0.54, 1)$ are larger than the respective elements in that

       corresponding to $(\rho, \eta) = (0.2, 1.275)$. However, most of the elements in the

       solution gain matrix corresponding to $(\rho^*, \eta^*) = (0.54, 1)$ are smaller than the

       respective elements in that corresponding to $(\rho, \eta) = (0.2, 1.275)$.

3)   We find no controller in the literature that meets the increased uncertainty

       specifications in (E 4.1.7).

When a set of strong uncertainty specifications are given, we emphasize that a reasonably

good initial value is needed for the optimization algorithm to converge to a solution.

Indeed, the same optimization algorithm cannot find a solution when the initial value

$\{\mathbf{Q}, \mathbf{K}_{LARC}\}$ is generated from $(\rho, \eta) = (1, 2)$. Starting from this initial value, the

algorithm cannot find $\{\mathbf{Q}, \mathbf{K}_{LARC}\}$ such that $\lambda_{\max}(\mathbf{Z}) < 4.2407 * 10^{-2}$.

4.7   Summary

We have obtained a MIMO version of LARC by extending results we obtained for SIMO systems. It turns out that the equations, theorems, and procedures employed to generate LARC for SIMO systems can be extended to generate LARC for MIMO systems in a straightforward fashion.

Chapter V

Preliminary Investigations of Nonlinear LAR Controllers

5.1   Introduction

In this chapter, we give suggestions and recommendations for enhancing the ability of

LARC developed in the previous chapters. Using the concept of LAR, our primarily

objective in this chapter is to enlarge the LAR resulting from linear LAR controllers

when stabilizing the time-invariant nonlinear systems (4.1) about the equilibrium point at

the origin. Preliminary studies show that extending LARC according to our suggestions

and recommendations can yield promising results when the availability of a perfect

model is assumed. However, it is emphasized that the results in this chapter are

preliminary and thus further investigations are required. These include parameter

selections and robustness issues.

5.2   The Basic Idea of Nonlinear LAR Control

We propose the use of nonlinear controls to enhance the ability of LARC developed in

the previous chapters. Indeed, in the previous chapters LARC was restricted to be linear

because this simplifies analysis of stability and of key properties of the control systems.

Using this simplification, we obtained in the previous chapters some building blocks on

which our ongoing research is developed. When an exact model is available, it turns out

that these building blocks allow us to obtain satisfactory results in a straightforward

fashion. We investigate now how a nonlinear auxiliary control could for MIMO systems be used to augment the linear control $\mathbf{u}_{LARC}(\mathbf{x})$ in previous chapter, to enlarge the LAR resulting from $\mathbf{u}_{LARC}(\mathbf{x})$, which is called "the original LAR". We denote by $\mathbf{u}_a(\mathbf{x}) \in \mathfrak{R}^m$ a smooth auxiliary control for enlarging the original LAR. The auxiliary control $\mathbf{u}_a(\mathbf{x})$ is an augmentation of the linear control $\mathbf{u}_{LARC}(\mathbf{x})$, such that our "total" LARC $\mathbf{u}_{TLARC}(\mathbf{x})$ can be written as:

$$\mathbf{u}_{TLARC}(\mathbf{x}) = \mathbf{u}_{LARC}(\mathbf{x}) + \mathbf{u}_a(\mathbf{x}) \tag{5.1}$$

where the subscript "T" stands for "total" and $\mathbf{u}_a(\mathbf{0}) = \mathbf{0}$. In our preliminary studies, the system is described by (4.1):

$$\dot{\mathbf{x}} = \mathbf{f}(\mathbf{x}) + \mathbf{g}(\mathbf{x})\mathbf{u}(\mathbf{x}) \tag{4.1}$$

where the vectors $\mathbf{f}(\mathbf{x}) \in \mathfrak{R}^n$, $\mathbf{g}(\mathbf{x}) \in \mathfrak{R}^{n \times m}$ and we set $\mathbf{u}(\mathbf{x}) = \mathbf{u}_{TLARC}(\mathbf{x})$. These are such that $\dot{\mathbf{x}}$ is locally Lipschitz in the operating region of interest. We assume that (4.1) is a perfect description of the MIMO system of interest. The objective remains to stabilize (4.1) such that the equilibrium point at the origin is at least locally asymptotically stable with a reasonably large attractive region. When $\mathbf{u}(\mathbf{x})$ is set to $\mathbf{u}_{TLARC}(\mathbf{x})$, the time derivative of the quadratic Lyapunov function (1.5) along trajectories of the nonlinear system (4.1) is given by:

$$\begin{aligned}
\dot{V}_T(\mathbf{x}) &= \mathbf{x}^T \mathbf{Pf}(\mathbf{x}) + \mathbf{x}^T \mathbf{Pg}(\mathbf{x})\mathbf{u}_{TLARC}(\mathbf{x}) \\
&= F(\mathbf{x}) + G(\mathbf{x})\mathbf{u}_{LARC}(\mathbf{x}) + G(\mathbf{x})\mathbf{u}_a(\mathbf{x}) \\
&\equiv \dot{V}(\mathbf{x}) + \Omega(\mathbf{x})
\end{aligned} \tag{5.2}$$

where $\dot{V}(\mathbf{x}) = F(\mathbf{x}) + G(\mathbf{x})\mathbf{u}_{LARC}(\mathbf{x})$, and $\Omega(\mathbf{x}) \equiv G(\mathbf{x})\mathbf{u}_a(\mathbf{x})$ are smooth because of the smoothness and continuity of the equation of motion and of $\mathbf{u}_{TLARC}(\mathbf{x})$. These functions

vanish at the origin because $F(\mathbf{0}) = 0$ and $\mathbf{G(0)} = \mathbf{0}$. Because of these, $\dot{V}_T(\mathbf{x})$ is smooth,

is continuous and is vanishing at the origin. We now define the following regions:

$$B_T \equiv \{\mathbf{x} \mid \dot{V}_T(\mathbf{x}) < 0\} \cup \{\mathbf{0}\} \tag{5.3}$$

$$\beta_{C_T} \equiv \{\beta_C \mid \beta_{C, C=C_T} \subseteq B_T, \beta_{C, C>C_T} \not\subset B_T, C_T \in \mathfrak{R}^+\} \tag{5.4}$$

In addition, we recall from Chapter I that:

$$\beta_C \equiv \{\mathbf{x} \mid 0 \leq V(\mathbf{x}) < C, \ C \in \mathfrak{R}^+\} \tag{1.8}$$

$$B_L \equiv \{\mathbf{x} \mid \dot{V}(\mathbf{x}) < 0\} \cup \{\mathbf{0}\} \tag{1.9}$$

$$\beta_{C_L} \equiv \{\beta_C \mid \beta_{C, C=C_L} \subseteq B_L, \ \beta_{C, C>C_L} \not\subset B_L, \ C_L \in \mathfrak{R}^+\} \tag{1.10}$$

It is emphasized that:

1) β_{C_T} shrinks in all its dimensions as C_T decreases because $V(\mathbf{x})$ is a quadratic

      positive definite function.

2)   The definitions (5.3) and (5.4) guarantee that β_{C_T} and B_T have at least one

      common boundary point.

We now state the main theorem of this chapter:

Theorem 5.1   (Expansion of a LAR)

If the intersections of the boundaries of B_L and β_{C_L} or the "common boundary points" of

B_L and β_{C_L}, denoted by $\mathbf{p}_i$, $i = 1, 2, \ldots$ are contained in Π_0 then the smooth auxiliary

control $\mathbf{u}_a(\mathbf{x})$ enlarges the original LAR with an additional region contained in

$\overline{\Pi} \equiv (\Pi_0 \cup \Pi_1)$ provided that $\mathbf{u}_a(\mathbf{x})$ satisfies:

$$\Omega(\mathbf{p}_i) = \mathbf{G}(\mathbf{p}_i)\mathbf{u}_a(\mathbf{p}_i) < 0 \quad \forall i$$
$$\dot{V}_T(\mathbf{x}) = \dot{V}(\mathbf{x}) + \Omega(\mathbf{x}) < 0 \quad \forall \mathbf{x} \in \{B_L - \mathbf{0}\} \qquad (5.5)$$
$$\dot{V}_T(\mathbf{0}) = 0$$

where

$$\Pi_0 \equiv \{\mathbf{x} \mid \mathbf{G}(\mathbf{x}) \neq \mathbf{0} \text{ and } F(\mathbf{x}) \text{ is arbitrary } \} \qquad (5.6\,\text{a})$$

$$\Pi_1 \equiv \{\mathbf{x} \mid \mathbf{G}(\mathbf{x}) = \mathbf{0},\ F(\mathbf{x}) < 0\} \cup \{\mathbf{0}\} \qquad (5.6\,\text{b})$$

Proof

Since $\Omega(\mathbf{x}) \equiv \mathbf{G}(\mathbf{x})\mathbf{u}_a(\mathbf{x})$, the smooth auxiliary control $\mathbf{u}_a(\mathbf{x})$ can satisfy (5.5) if and only if $\mathbf{G}(\mathbf{p}_i) \neq \mathbf{0}$. By definition (1.18), we are guaranteed that β_{C_L} is contained in B_L such that the set of common boundary points of β_{C_L} and B_L contains at least one point. This can be illustrated graphically in Fig. 5.1. Fig. 5.1 (a) shows an artificial surface of $\dot{V}(\mathbf{x})$ for a two dimensional system and Fig. 5.1 (b) shows level curves of $\dot{V}(\mathbf{x})$ and the corresponding $V(\mathbf{x})$. In Fig. 5.1 (b), the boundary of B_L is shown as O_{B_L} while the boundaries of β_C at $C = C_L^-$, C_L, and C_L^+ are shown as $O_{\beta_{C,C=C_L^-}}$, $O_{\beta_{C,C=C_L}}$, and $O_{\beta_{C,C=C_L^+}}$ respectively. The number of common boundary points of β_C and B_L is assumed to be four in this illustration.

If $\mathbf{p}_i \in \Pi_0 \ \forall i$, we have that $\mathbf{G}(\mathbf{p}_i) \neq \mathbf{0}$ by the definition of Π_0 in (5.6 a). This allows us to choose $\mathbf{u}_a(\mathbf{x})$ such that $\Omega(\mathbf{p}_i) = \mathbf{G}(\mathbf{p}_i)\mathbf{u}_a(\mathbf{p}_i) < 0 \ \forall i$. We see from (5.2) that when (5.5) is satisfied:

1) $\dot{V}_T(\mathbf{x}) < 0$ in the B_L except at the origin where $\dot{V}_T(\mathbf{0}) = \dot{V}(\mathbf{0}) = 0$.

(Proof of Theorem 5.1 (Cont.))

2) $\dot{V}_T(\mathbf{p}_i) < \dot{V}(\mathbf{p}_i) = 0$ $\forall i$. This can be drawn from (5.2), knowing that $\dot{V}(\mathbf{p}_i) = 0$ by

the definition of $\mathbf{p}_i$, $\mathbf{G}(\mathbf{p}_i) \neq 0$, and $\mathbf{G}(\mathbf{p}_i)\mathbf{u}_a(\mathbf{p}_i) < 0$ by the choice of $\mathbf{u}_a(\mathbf{x})$.
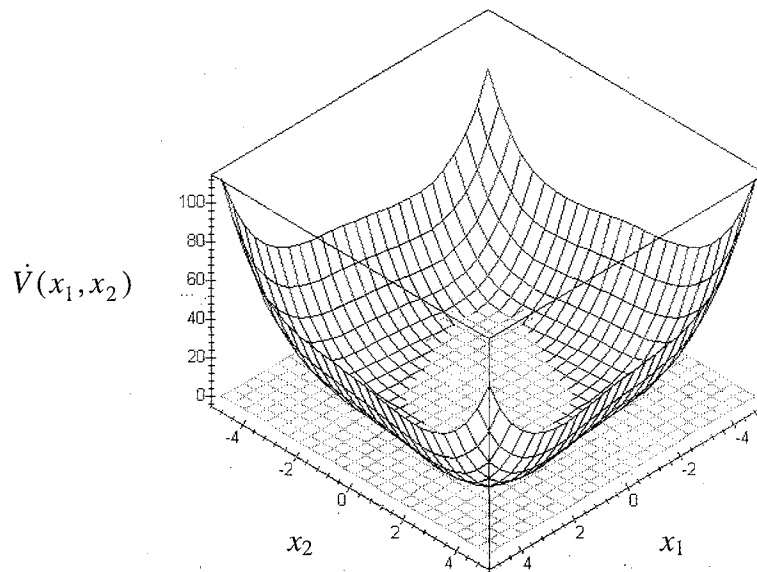
Fig. 5.1 (a)   Artificial Surface of $\dot{V}(x_1, x_2)$

Now, we consider $\dot{V}_T(\mathbf{x})$ in a neighborhood U_i about the common boundary point $\mathbf{p}_i$

$i = 1, 2, \ldots$. This neighborhood is defined as $U_i \equiv \{\mathbf{x} \mid \|\mathbf{x} - \mathbf{p}_i\| < \varepsilon_i\}$ where ε_i is a

sufficiently small positive number. Recall that when (5.5) is satisfied, we have for U_i

$i = 1, 2, \ldots$ that $\dot{V}_T(\mathbf{p}_i) < 0$. In this case, it follows from the continuity of $\dot{V}_T(\mathbf{x})$ that

$\dot{V}_T(\mathbf{x}) < 0$ $\forall \mathbf{x} \in U_i$. In other words, by the continuity of $\dot{V}_T(\mathbf{x})$, there exists a number

$\varepsilon_i > 0$, no matter how small, corresponding to a neighborhood U_i about $\mathbf{p}_i$ such that

$\dot{V}_T(\mathbf{x}) < 0$ for every point $\mathbf{x} \in U_i$ (Buck, 1987). A magnified view of Fig. 5.1 (b) in the

second quadrant provided in Fig. 5.2 is a graphical illustration for this argument.

(Proof of Theorem 5.1 (Cont.))
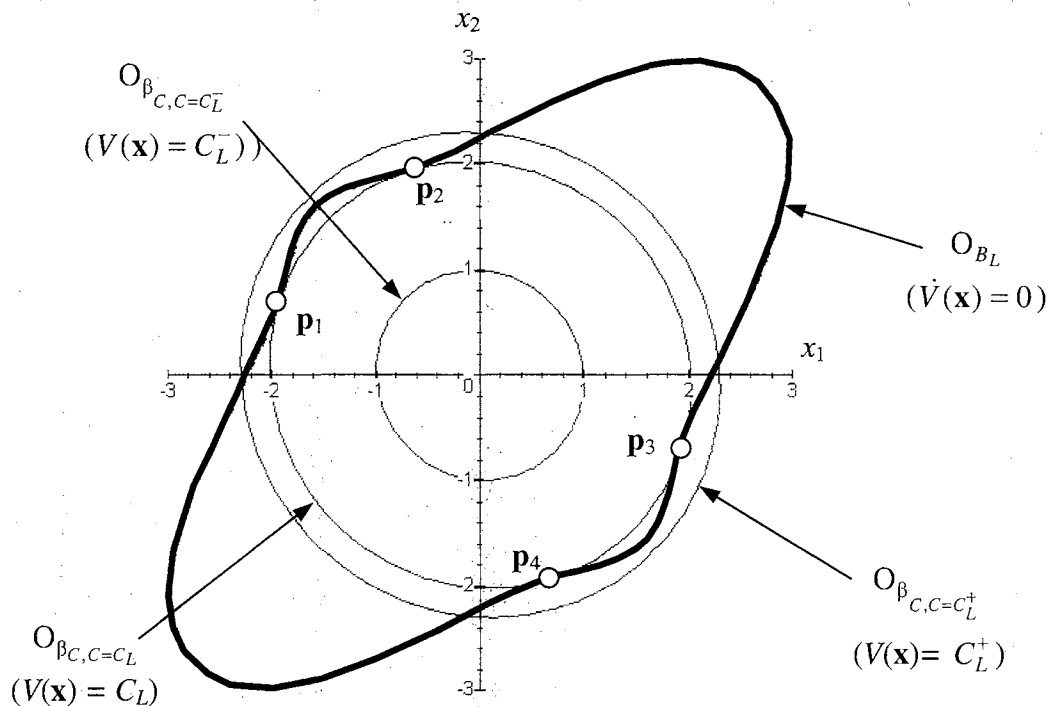
Fig. 5.1 (b) Conceptual Regions β_{C_L} and B_L Corresponding to Fig. 5.1 (a)

Symbol: $\circ \equiv$ common boundary points of β_{C_L} and B_L

Remark: $0 < C_L^- < C_L < C_L^+$

Because $\dot{V}_T(\mathbf{x}) < 0$ in B_L and in U_i including $\mathbf{p}_i$ $i = 1, 2, \ldots$, we see that B_T contains

B_L and $\mathbf{p}_i$, which are <u>not</u> on the boundary of B_T. Accordingly, β_{C_L} and B_T have no

common boundary point and B_T contains β_{C_L} because $\beta_{C_L} \subseteq B_L \subset B_T$. We then

expand $\beta_{C,C=C_L}$ in every direction by increasing C beyond C_L. The expansion occurs in

every direction because $V(\mathbf{x})$ is a quadratic positive definite function. We denote by C_T

the value of $C > C_L$ when the boundary of β_C <u>first</u> intersects the boundary of B_T, and by

β_{C_T} the region $\beta_{C,C=C_T}$. The existence of such $\beta_{C,C=C_T>C_L}$ is guaranteed because:

4

1

1

(Proof of Theorem 5.1 (Cont.))

1) $\beta_{C_L} \subset B_T$

2) β_{C_L} and B_T have no common boundary point.

Since $V(\mathbf{x})$ is a quadratic positive definite function and $C_T > C_L > 0$, we conclude that

$\beta_{C_L} \subset \beta_{C_T}$ and the boundaries of β_{C_L} and β_{C_T} do not intersect. Thus the original LAR

can be enlarged by the auxiliary control $\mathbf{u}_a(\mathbf{x})$ satisfying (5.5). This completes the proof.
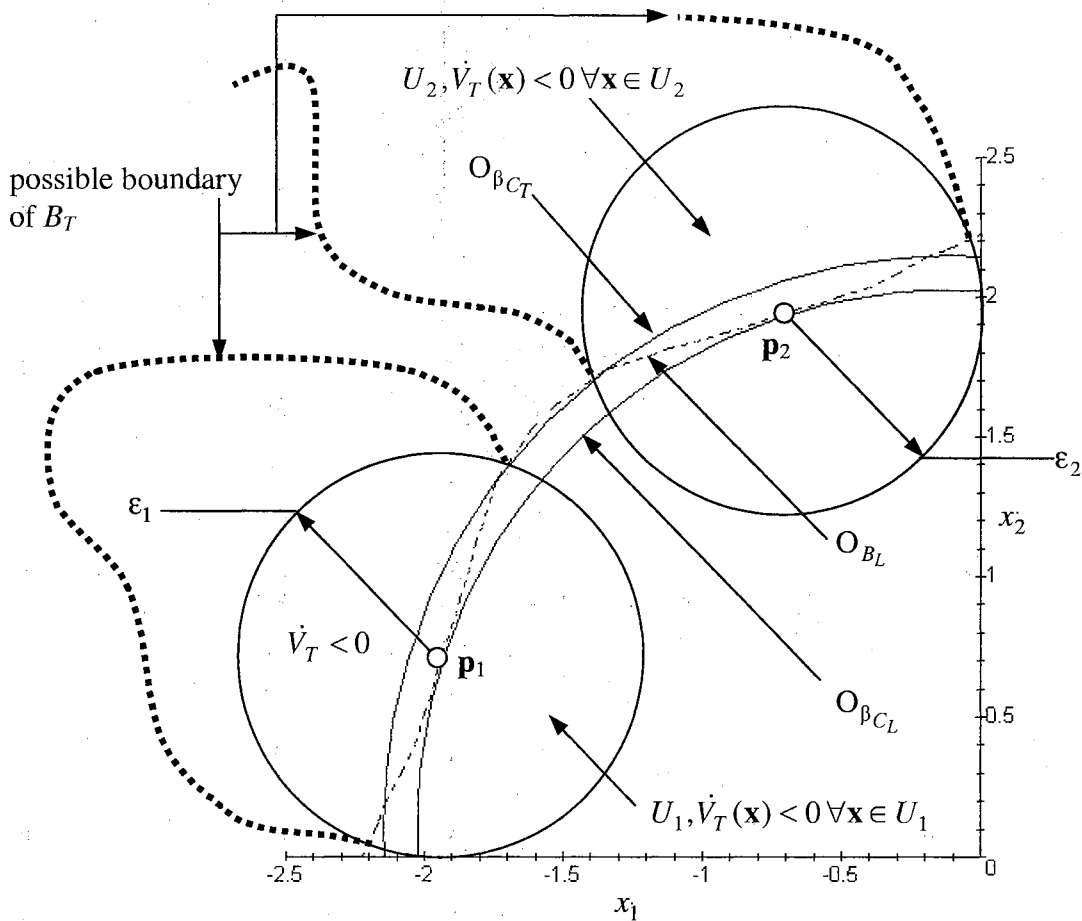
Fig. 5.2 Magnified View of Fig. 5.1 (b) Showing $\beta_{C_L}, \beta_{C_T}, B_L$, and B_T

Symbol: $O_\zeta \equiv$ boundaries of ζ, where $\zeta = \beta_{C_L}, \beta_{C_T}$, and B_L

It is clear that (5.5) suggests infinitely many possible choices for $\mathbf{u}_a(\mathbf{x})$. An obvious

possibility is given in Corollary 5.1:

Corollary 5.1 (A Choice of Auxiliary Control)

The conditions in (5.5) are satisfied if:

$$\mathbf{u}_a(\mathbf{x}) = -\gamma(\mathbf{x})\mathbf{G}^T(\mathbf{x}) = -\gamma(\mathbf{x})\mathbf{g}^T(\mathbf{x})\mathbf{P}\mathbf{x} \equiv -\mathbf{K}_a(\mathbf{x})\mathbf{x} \tag{5.7}$$

where $\gamma(\mathbf{x})\mathbf{g}^T(\mathbf{x})\mathbf{P}\mathbf{x} \equiv \mathbf{K}_a(\mathbf{x}) \in \mathfrak{R}^{m \times n}$, $\gamma(\mathbf{x}) > 0$, and $\mathbf{P}$ is obtained by using LARC

developed in the previous chapters because we desire that $\mathbf{p}_i$ are reasonably far from the

origin $\forall i$.

Under the choice of auxiliary control (5.7), the resultant nonlinear control is given by:

$$\mathbf{u}_{TLARC}(\mathbf{x}) = -\mathbf{K}_{LARCT}\mathbf{x} \tag{5.8}$$

where $\mathbf{K}_{TLARC} \equiv [\mathbf{K}_{LARC} + \mathbf{K}_a(\mathbf{x})]$ when no optimization is employed to find the linear

state-feedback gain matrix for LARC, and $\mathbf{K}_{TLARC} \equiv [\mathbf{K}_{OLARC} + \mathbf{K}_a(\mathbf{x})]$ otherwise.

Notice that:

1) $\mathbf{K}_{TLARC}$ is a nonlinear gain matrix obtained by weighting the linear gain matrix

$\mathbf{K}_{LARC}$ or $\mathbf{K}_{OLARC}$ against the nonlinear auxiliary gain matrix $\mathbf{K}_a(\mathbf{x})$.

2)   In this ongoing stage, we restrict that $\gamma(\mathbf{x})$ be a constant $\gamma_C \in \mathfrak{R}^+$ for simplicity.

Under this restriction, a technique for selecting an appropriate value for γ_C is

clearly required and is a subject of our current investigations. At the moment, we

choose a small γ_C to begin with, employ numerical simulations to estimate the resulting attractive region, and tune γ_C accordingly.

Example 5.1 (The Double-Inverted-Pendulum System with Lower-Joint Control)

In this example, we employ the double-inverted-pendulum system (Misawa, Arrington, and Ledgerwood, 1995) to determine if the auxiliary nonlinear control $u_a(\mathbf{x})$ can enlarge the attractive region resulting from the linear control $u_{LARC}(\mathbf{x})$. To do this, we invoke from (E 3.3.12) in Example 3.3 the linear gain matrix $\mathbf{K}_{OLARC}$ to produce:

$$u_{LARC}(\mathbf{x}) = [-0.0804 \quad -8.6189 \quad -0.5572 \quad -1.1748]\mathbf{x}$$
$$\equiv -\mathbf{K}_{OLARC}\mathbf{x}$$

(E 5.1.1)

where $\mathbf{K}_{OLARC} = [-0.0804 \quad -8.6189 \quad -0.5572 \quad -1.1748]$. This linear LARC corresponds to $\mathbf{P}$ in (E 3.3.14). For convenience, we reproduce:

$$\mathbf{P} = \begin{bmatrix} 4.6236 & 12.4067 & 1.4066 & 1.6109 \\ 12.4067 & 157.1118 & 17.1767 & 20.6637 \\ 1.4066 & 17.1767 & 2.0826 & 2.4550 \\ 1.6109 & 20.6637 & 2.4550 & 2.9956 \end{bmatrix}$$

(E 3.3.14)

We take from (5.7) in Corollary 5.1, the auxiliary nonlinear control:

$$\mathbf{u}_a(\mathbf{x}) = -\gamma(\mathbf{x})\mathbf{g}(\mathbf{x})^T \mathbf{P}\mathbf{x} \equiv -\mathbf{K}_a(\mathbf{x})\mathbf{x}$$

where $\gamma(\mathbf{x})\mathbf{g}(\mathbf{x})^T \mathbf{P} \equiv \mathbf{K}_a(\mathbf{x})$, and we set $\gamma(\mathbf{x}) = \gamma_C \in \mathfrak{R}^+$ for simplicity. We recall from Example 2.2 that:

$$\mathbf{g(x)} = \begin{bmatrix} 0 \\ 0 \\ \dfrac{-565.1008}{-5.9809 + \cos^2(x_1 - x_2)} \\ \dfrac{504.2688\cos(x_1 \text{-} x_2)}{-5.9809 + \cos^2(x_1 - x_2)} \end{bmatrix}$$

(E 2.2.2 d)

The total nonlinear control is then given by:

$$u_{TLARC}(\mathbf{x}) = -[\mathbf{K}_{OLARC} + \gamma_C \mathbf{g(x)}^T \mathbf{P}]\mathbf{x} = -\mathbf{K}_{TLARC}\mathbf{x}$$

(E 5.1.2)

where $\mathbf{K}_{TLARC} \equiv \mathbf{K}_{OLARC} + \gamma_C \mathbf{g(x)}^T \mathbf{P}$.

Now, we want to select an appropriate value for γ_C. Since we have not completed a

procedure for this, heuristics are employed to tune γ_C. Following the suggestion given

after Corollary 5.1, we start our tuning process from a small value of γ_C. Setting

$\gamma_C = 0.001$, numerical simulations show that the nonlinear auxiliary control can enlarge

the attractive region resulting from the linear LARC in (E 5.1.1). Increasing γ_C to 0.002

and to 0.003 produces increasingly better results. Next, we skip intermediate values and

set $\gamma_C = 0.01$. The attractive region corresponding to $\gamma_C = 0.01$ is smaller than that

corresponding to $\gamma_C = 0.003$. We do not pursue the optimal value for γ_C and accept

$\gamma_C = 0.003$ because the present results are sufficient to demonstrate the benefit of the

nonlinear auxiliary control $u_a(\mathbf{x})$. Fig. E5.1.1 (a) and (b) shows system responses under

$u_{LQR}(\mathbf{x})$ (Misawa, Arrington, and Ledgerwood, 1995) and $u_{TLARC}(\mathbf{x})$ when the system is

launched from two initial conditions. Notice that the responses under $u_{LQR}(\mathbf{x})$ are faster

than those under $u_{TLARC}(\mathbf{x})$, but $u_{LQR}(\mathbf{x})$ is not able to force the trajectory to converge to

the origin when the initial condition is large. Simulation results in Table E5.1.1 and Table

E5.1.2 compare the attractive region resulting from $u_{LQR}(\mathbf{x})$ (Misawa, Arrington, and

Ledgerwood, 1995) to that resulting from $u_{TLARC}(\mathbf{x})$ in (E 5.1.2) with $\gamma_C = 0.003$. Notice

that the latter is significantly larger than the former. In these tables, we define 1)

converge to the origin $\equiv \|\mathbf{x}(t)\| < 0.01$ for $40 \le t \le 50$, and 2) diverge from the origin $\equiv$

$\exists t$ such that $\|\mathbf{x}(t)\| > 2000$.
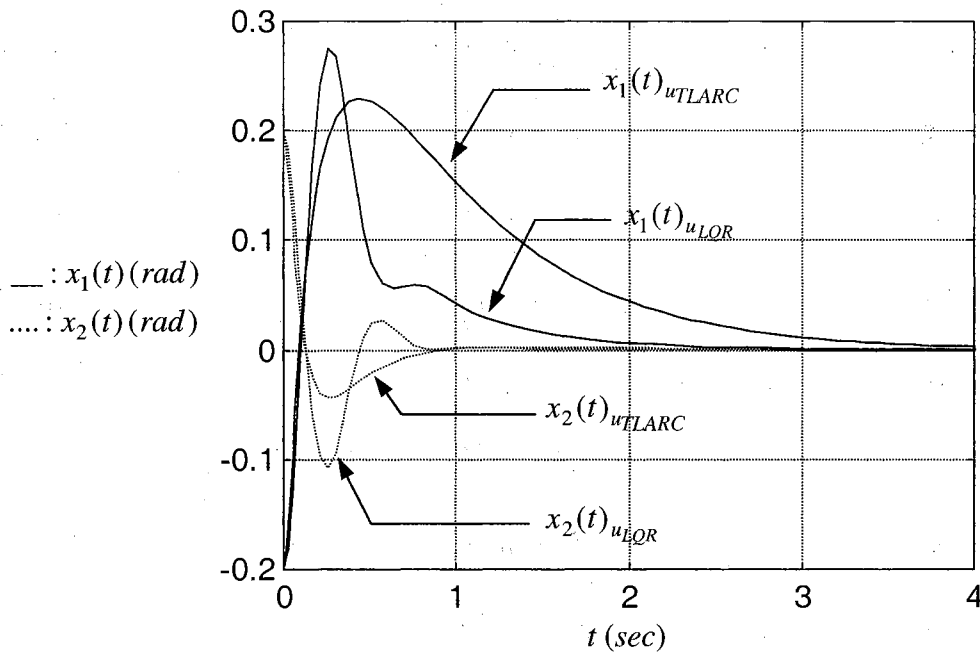
Fig. E5.1.1 (a) Responses of the Double-Inverted-Pendulum System under $u_{TLARC}(\mathbf{x})$

and $u_{LQR}(\mathbf{x})$ with $\mathbf{x}(0) = [-0.2 \quad 0.2 \quad -0.1 \quad -0.1]^T$
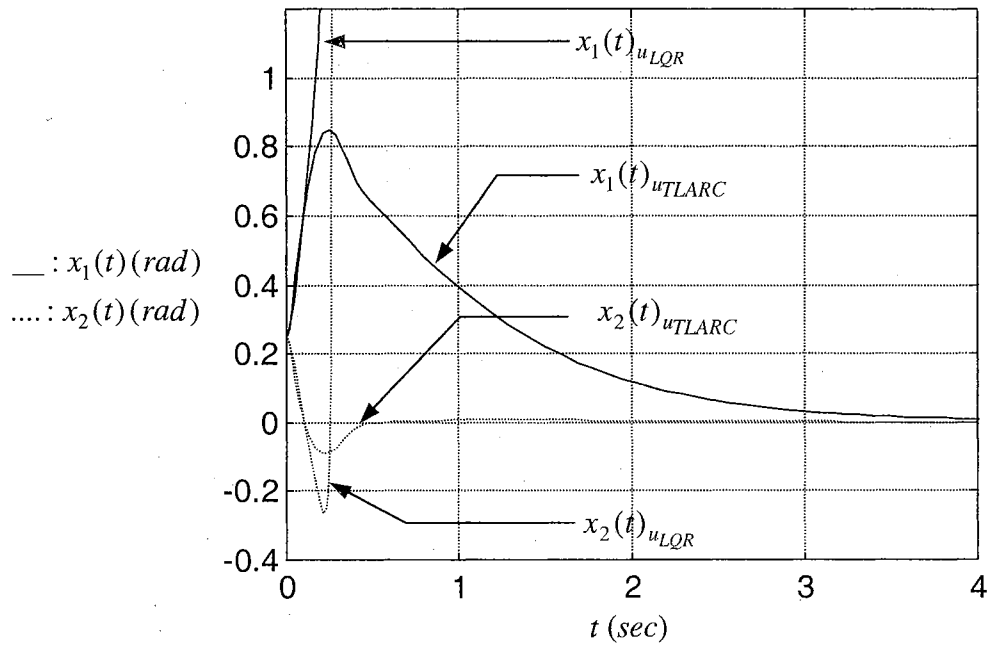
Fig. E5.1.1 (b) Responses of the Double-Inverted-Pendulum System under $u_{TLARC}(\mathbf{x})$

and $u_{LQR}(\mathbf{x})$ with $\mathbf{x}(0) = [0.25 \quad 0.25 \quad 0.1 \quad 0.1]^T$

Table E5.1.1   Simulation Results of the Double Inverted Pendulum System in Regions farther from the Origin ($x_1 > 0$, $x_2 > 0$)

Remark: Attractive regions do not differ significantly in small regions about the origin.

Legends: ▨ ≡ LQR, LARC, OLARC, and TLARC systems converge, ▨ ≡ LARC, OLARC, TLARC systems converge

▨ ≡ OLARC and TLARC systems converge, ▨ ≡ TLARC system converges, □ ≡ All system diverge

			x_2																						
			0.45					**.425**					**0.4**					**.375**					**0.35**				
			x_4																						
			-0.5	-.25	0	0.25	0.5	-0.5	-.25	0	0.25	0.5	-0.5	-.25	0	0.25	0.5	-0.5	-.25	0	0.25	0.5	-0.5	-.25	0	0.25	0.5
x_1	-0.45	x_3	-0.5 ... 0.5																								

Table E5.1.2 Simulation Results of the Double Inverted Pendulum System in Regions farther from the Origin ($x_1 < 0$, $x_2 > 0$)

Remark: Attractive regions do not differ significantly in small regions about the origin.

Legends: ▦ ≡ LQR, LARC, OLARC, and TLARC systems converge, ▨ ≡ LARC, OLARC, TLARC systems converge
▨ ≡ OLARC and TLARC systems converge, ▓ ≡ TLARC system converges, □ ≡ All system diverge

Example 5.2 (The Cart-and-Pole System with Force Control on Cart)

In this example, we employ the cart-and-pole system in Example 2.3 to determine if the auxiliary nonlinear control $u_a(\mathbf{x})$ can enlarge the attractive region resulting from the linear control $u_{LARC}(\mathbf{x})$. To do this, we invoke from (E 3.5.7) in Example 3.5 the linear gain matrix $\mathbf{K}_{LARC}$ to produce:

$$
\begin{aligned}
u_{LARC}(\mathbf{x}) &= [-2.5136 \quad -57.4749 \quad -5.1254 \quad -13.0073]\mathbf{x} \\
&\equiv -\mathbf{K}_{LARC}\mathbf{x}
\end{aligned}
\tag{E 5.2.1}
$$

where $\mathbf{K}_{LARC} = [-2.5136 \quad -57.4749 \quad -5.1254 \quad -13.0073]$. This linear LARC corresponds to $\mathbf{P}$ in (E 3.5.9). For convenience, we reproduce:

$$
\mathbf{P} = \begin{bmatrix}
4.0782 & 10.3497 & 3.1579 & 2.2951 \\
10.3497 & 119.5777 & 18.8090 & 25.7791 \\
3.1579 & 18.8090 & 5.3843 & 4.1524 \\
2.2951 & 25.7791 & 4.1524 & 5.7820
\end{bmatrix}
\tag{E 3.5.9}
$$

We take from (5.7) in Corollary 5.1, the auxiliary nonlinear control:

$$
\mathbf{u}_a(\mathbf{x}) = -\gamma(\mathbf{x})\mathbf{g}(\mathbf{x})^T\mathbf{P}\mathbf{x} \equiv -\mathbf{K}_a(\mathbf{x})\mathbf{x}
$$

where $\gamma(\mathbf{x})\mathbf{g}(\mathbf{x})^T\mathbf{P} \equiv \mathbf{K}_a(\mathbf{x})$, and we set $\gamma(\mathbf{x}) = \gamma_C \in \Re^+$ for simplicity. We recall from Example 2.3 that:

$$
\mathbf{g}(\mathbf{x}) = \begin{bmatrix}
0 \\
1 \\
\dfrac{1}{M+\sin^2(x_2)m} \\
-\dfrac{\cos(x_2)}{(M+\sin^2(x_2)m)l}
\end{bmatrix}
\tag{E 2.3.2 d}
$$

where $M = 2$ *kg*, $m = 0.1$ *kg*, $l = 0.5$ *m*, and $g = 9.81$ *kg.m.s^{-2}*. The total nonlinear control is then given by:

$$u_{TLARC}(\mathbf{x}) = -[\mathbf{K}_{LARC} + \gamma_C \mathbf{g}(\mathbf{x})^T \mathbf{P}]\mathbf{x} = -\mathbf{K}_{TLARC}\mathbf{x} \qquad \text{(E 5.2.2)}$$

where $\mathbf{K}_{TLARC} \equiv \mathbf{K}_{LARC} + \gamma_C \mathbf{g}(\mathbf{x})^T \mathbf{P}$.

Now, we want to select an appropriate value for γ_C. Since we have not completed a procedure for this, heuristics are employed to tune γ_C. Following the suggestion given after Corollary 5.1, we start our tuning process from a small value of γ_C. Setting with $\gamma_C = 0.001$, numerical simulations show that the attractive regions corresponding to $u_{LARC}(\mathbf{x})$ and $u_{TLARC}(\mathbf{x})$ are approximately the same, implying that effects of larger values of γ_C are to be examined. We increase γ_C gradually and observe some enlargement in attractive region. When $\gamma_C = 1.25$, numerical simulations show clearly that the attractive region corresponding to $u_{TLARC}(\mathbf{x})$ is larger than that corresponding to $u_{LARC}(\mathbf{x})$. We terminate the tuning procedure and accept $\gamma_C = 1.25$ because the present results are sufficient to demonstrate the benefit of the nonlinear auxiliary control $u_a(\mathbf{x})$. Simulation results in Table E5.2.1 and Table E5.2.2 compare the attractive regions resulting from $u_{PP}(\mathbf{x})$ (Ogata, 1997), from $u_{LARC}(\mathbf{x})$ (without uncertainty specifications), from $u_{LARC}(\mathbf{x})$ (with uncertainty specifications), and from $u_{TLARC}(\mathbf{x})$ (with $\gamma_C = 1.25$). Notice that the latter is the largest. In these tables, we define 1) converge to the origin $\equiv$ $\|\mathbf{x}(t)\| < 0.01$ for $40 \leq t \leq 50$, 2) diverge from the origin $\equiv \exists t$ such that $\|\mathbf{x}(t)\| > 2000$, and denote "uncertainty specifications" by "UCSPs".

				x_2																					
				1.25					1.00					0.75					0.50					0.25				
				x_4																					
				-1	-0.5	0	0.5	1	-1	-0.5	0	0.5	1	-1	-0.5	0	0.5	1	-1	-0.5	0	0.5	1	-1	-0.5	0	0.5	1
x_1	5	x_3	-1 / -0.5 / 0 / 0.5 / 1																								
	4		-1 / -0.5 / 0 / 0.5 / 1																								
	3		-1 / -0.5 / 0 / 0.5 / 1																								
	2		-1 / -0.5 / 0 / 0.5 / 1																								
	1		-1 / -0.5 / 0 / 0.5 / 1																								

Table E5.2.1   Simulation Results of the Cart and Pole System in Regions farther from the Origin ($x_1 > 0$, $x_2 > 0$)

Legends: ■ ≡ PP, LARC (with and without UCSPs) and TLARC systems converge,
▨ ≡ LARC (with and without UCSPs) and TLARC systems converge, ▨ ≡ LARC (<u>with</u> UCSPs) and TLARC systems converge
▥ ≡ LARC (<u>without</u> UCSPs) and TLARC systems converge, ▨ ≡ TLARC system converges

				x_2																						
				1.25					1.00					0.75					0.50					0.25				
				x_4																								
				-1	-0.5	0	0.5	1	-1	-0.5	0	0.5	1	-1	-0.5	0	0.5	1	-1	-0.5	0	0.5	1	-1	-0.5	0	0.5	1
x_1	-5	x_3	-1																									
			-0.5																									
			0																									
			0.5																									
			1																									
	-4		-1																									
			-0.5																									
			0																									
			0.5																									
			1																									
	-3		-1																									
			-0.5																									
			0																									
			0.5																									
			1																									
	-2		-1																									
			-0.5																									
			0																									
			0.5																									
			1																									
	-1		-1																									
			-0.5																									
			0																									
			0.5																									
			1																									

Table E5.2.2   Simulation Results of the Cart and Pole System in Regions farther from the Origin ($x_1 > 0$, $x_2 > 0$)

Legends: ■ ≡ PP, LARC (with and without UCSPs) and TLARC systems converge,

▨ ≡ LARC (with and without UCSPs) and TLARC systems converge, ▩ ≡ LARC (<u>with</u> UCSPs) and TLARC systems converge

▥ ≡ LARC (<u>without</u> UCSPs) and TLARC systems converge, ▨ ≡ TLARC system converges

5.3 Summary

1) In this section, we suggest that nonlinear controls be incorporated to the linear LARC developed in the previous chapters to enlarge the original LAR under the assumption that the available model is perfect. Indeed, we propose that a nonlinear auxiliary control be augmented to the linear LARC, and we denote this augmentation by TLARC.

2) Based on the idea in 1, we present our preliminary studies and Theorem 5.1, which leads to many forms of auxiliary controls that can be employed to enlarge the original LAR. We point out a simple auxiliary control for this purpose in Corollary 5.1. Using this auxiliary control, we require a technique for choosing an appropriate value for the parameter γ_C. This parameter weights the contribution of the linear LARC and that of the auxiliary control. A procedure for selecting an appropriate γ_C is a subject of our current studies. At the moment, we select γ_C heuristically. We initially choose a small γ_C, employ numerical simulations to estimate the corresponding attractive region, and tune γ_C accordingly.

3) Using the double-inverted-pendulum system (Misawa, Arrington, and Ledgerwood, 1995) with the optimized linear LARC obtained in Example 3.3 and the cart-and-pole system (Ogata, 1997) with the unoptimized linear LARC obtained in Example 3.5, we examine how the auxiliary control in Corollary 5.1 can enhance the ability of the linear LAR controllers. Numerical simulations show

that the attractive regions corresponding to TLARC are larger than those

corresponding to the linear LAR controllers, and are significantly larger than

those corresponding to LQR (Misawa, Arrington, and Ledgerwood, 1995) and

pole placement (Ogata, 1997). The tuning process for γ_C takes less than 5

minutes to complete in each of the two examples.

Chapter VI

Conclusions and Recommendations

6.1   Conclusions

There are numerous physical nonlinear systems whose mathematical descriptions present structural and algebraic difficulties when designing a globally stabilizing controller. For such systems, we often admit locally stabilizing controllers designed by applying linear system theory to suitable linearized models. Theoretically, we expect the linear controller to stabilize the nonlinear system in a region where the linear approximation is valid. However, it is traditional that we do not examine the extent of this region when designing a linear controller. After such design, simulations are employed to numerically estimate the resultant attractive region. A major drawback of a linear controller designed in this fashion is that the attractive region of the corresponding nonlinear system can be unsatisfactorily small. It is known that a linear controller can be designed either by relocating the eigenvalues of the linearized model, by optimizing a performance index subjected to the linearized model, or by shaping frequency-domain plots of the linearized model. However, their relationships to the attractive region of the corresponding nonlinear system are not obvious. Thus, it is not clear how several design parameters for the corresponding techniques should be chosen to obtain reasonably large attractive regions.

Using the concepts of eigenvector condition and eigenvalue ratio, systematic procedures for generating LAR controllers with and without uncertainty specifications are proposed.

In the formulations of these procedures, effects of nonlinearities and of uncertainties on LAR are handled implicitly using geometry. Given a linearized model about the origin, a LAR controller can be generated in a timely fashion using an eigenvalue-ratio plot. The resulting attractive region is reasonably large when compared to existing techniques such as pole placement and LQR. For uncertain systems with uncertainty specifications, our procedures typically call for an optimization routine. In this case, we provide a tool for determining reasonably good initial values for the optimization. Starting from these initial values, it appears that a simple optimization routine is sufficient to produce fast convergence to a stabilizing LAR controller, which cannot be reached from inappropriate initial values. When LARC is applied to common examples found in the literature for local stabilization, the attractive regions resulting from LARC are larger than those resulting from pole placement and LQR. For global stabilization, LARC produces the least conservative allowable uncertainty bounds when compared to those in the common examples. Because the available information and specific properties of the system of interest imposed in various chapters are different, several types of stability are discussed. The reader is cautioned about the applicability of LARC in these situations.

6.2   Recommendations for Future Work

1)   Because of the promising results in Chapter V, it is recommended that the nonlinear LARC be investigated further. Extending the results in Chapter V to handle time-varying cases is straightforward. However, it may not be obvious how such results can be extended to select systematically parameters for the

auxiliary control, and to handle robustness issues while maintaining applicability of the scheme for complex high-order nonlinear systems.

2)   The results obtained in various chapters suggest strongly the profound effects of a "reasonably good" Lyapunov function. Accordingly, it seems reasonable that LARC be improved by finding a new class of Lyapunov functions that can be of advantageous over the current quadratic Lyapunov function in the sense of LAR.

3)   When dealing with uncertain systems, we proposed a technique for selecting reasonably good initial values for optimizations. Starting from such initial values, it was found in all relevant examples that the simple univariate optimization technique could be employed to obtain stabilizing LAR controllers in a timely fashion. Note that the univariate optimization technique was primarily employed for simplicity, and thus we do not expect it to be the most efficient in general. It is encouraged that an optimization technique be developed to speed up convergence to the solution of LARC.

4)   In the formulation of LARC, it is desirable that $\mathbf{x}_{C_{Si}}$ be located far from the origin to obtain a reasonably large LAR. While this formulation is valid, we notice that it incorporates strongly effects of the location of $\mathbf{x}_{C_{Si}}$, but not effects of relative location of $\mathbf{x}_{C_{Si}}$ with respect to the resulting LAR. It is recommended that the latter be investigated in details, and be incorporated into the formulation.

5)   We suggest that a LAR observer be developed. Using results developed in the previous chapters, it may be possible to formulate such an observer in a straightforward fashion. Properties of a LAR output-feedback controller should then be investigated.

References

Barmish, B. R., 1985, "Necessary and sufficient conditions for quadratic stabilizability of an uncertain system," *Journal of Optimization Theory and Applications*, Vol. 46, No. 4.

Baumann, W. T., and Rugh, W. J., 1986, "Feedback control of nonlinear systems by extended linearization," *IEEE Transactions on Automatic Control*, Vol. Ac-31, No. 1.

Buck, R. C., 1987, *Advanced Calculus: Third Edition*, McGraw-Hill.

Burl, J. B., 1999, *Linear Optimal Control: H_2 and H_∞ Methods*, CA: Addison Wesley Longman.

Chen, H. -G., and Han, K. -W., 1994, "Improved quantitative measures of robustness for multivariable systems," *IEEE Transactions on Automatic Control*, Vol. 39, No. 4.

Chen, Y. H., and Chen, J. S., 1990, "Combined controller-observer design for uncertain systems using necessary and sufficient conditions," *Proceeding of the 29th Decision and Control*, IEEE.

Chen, Y. H., and Chen, J. S., 1991, "Robust control of uncertain systems with time-varying uncertainty: A computer-aided setting," *Lecture Notes in Control and Information Sciences*, Vol. 151, NY: Springer-Verlag.

Chen, Y. H., 1987, "On the robustness of mismatched uncertain dynamical systems," *Journal of Dynamic Systems, Measurement and Control*, Vol. 109.

Chen, Y. H., and Leitmann, G., 1987, "Robustness of uncertain systems in the absence of matching assumptions," *International Journal of Control*, Vol. 45.

Curtis, C. W., 1984, *Linear Algebra: An Introductory Approach*, Springer-Verlag.

DeCarlo, R. A., Zak, S. H., and Matthews, G. P., 1988, "Variable structure control of nonlinear multivariable systems: A Tutorial," in *Proc. IEEE Conf. Decision and Control*, Vol. 76, No. 3, 1988.

Doyle, J. C. et al., 1989, "State space solutions to standard H_2 and H_α control problems," *IEEE Transactions on Automatic Control*, Vol. 34, No. 8.

Fox, R. L., 1971, *Optimization Methods for Engineering Design*, Addison Wesley.

Gao, Z., and Antsaklis, P. J., 1993, "Explicit asymmetric bounds for robust stability of continuous and discrete-time systems," *IEEE Transactions on Automatic Control*, Vol. 38, No. 2.

Gu K. et al, 1990, "Necessary and sufficient conditions of quadratic stability of uncertain linear systems," *IEEE Transactions on Automatic Control*, Vol. 35, No. 5.

Hagan, M. T. et al, 1996, *Neural Network Design*, PWS Publishing Company,.

Hauser, J., Sastry S., and Kokotovic', P., 1992, "Nonlinear control via approximate input-output linearization: The ball and beam example," *IEEE Transactions on Automatic Control*, Vol. 37, No. 3.

Isidori, A., 1989, *Nonlinear Control Systems*, Berlin: Springer-Verlag.

Itkis, U. 1976, *Control Systems of Variable Structure*, NY: John Wiley & Sons.

Kailath, T., 1980, *Linear Systems*, Englewood Cliffs, NJ: Prentice-Hall, 1980.

Khalil, H. K., 1996, *Nonlinear Systems-Second Edition*, Upper Saddle River, NJ: Prentice-Hall

Khargonekar, P. P. et al, 1990, "Robust Stabilization of uncertain linear systems: Quadratic stabilizability and H^∞ control theory," *IEEE Transactions on Automatic Control*, Vol. 3.

Kim, J. -H., 1995, "Comments on improved quantitative measures of robustness for multivariable systems," *IEEE Transactions on Automatic Control*, Vol. 40, No. 9.

Krener, A. J., 1984 "Approximate linearization by state feedback and coordinate change," *Systems & Control Letters*, Vol. 5.

Kreyszig, E., and Norminton, E. J., 1994, *Advanced Engineering Mathematics: Maple Computer Manual*, John Wiley & Sons.

Kwakernaak, H., and Sivan, R., 1972, *Linear Optimal Control Systems*, NY: Wiley-Interscience.

Lancaster, P., 1969, *Theory of Matrices*, NY: Academic Press.

Lancaster, P., and Tismenetsky, M., 1985, *The Theory of Matrices: Second Edition with Applications*, CA: Academic Press.

Lee, J. –C. et al, 1996, "Expanded asymmetric stability bounds with first-order Lyapunov robustness method," *Proceeding of the ASME Dynamics Systems and Control Division*, ASME.

Li, H. X., Gatland, H. B., and Green, A. W., 1997, "Fuzzy variable structure control," *IEEE Transactions on Systems, Man, and Cybernetics*, Vol. 27, No. 2.

Misawa, E. A., Arrington, M. S., and Ledgerwood, T. D., 1995, "The benchmark problem: A rotational inverted pendulum," *Proc. IFAC 1995 World Congress*, SF.

Narendra, K. S., and Annaswamy, A. M., 1989, *Stable Adaptive Systems*, Englewood Cliffs, NJ: Prentice-Hall.

Nijmeijer, H., and Schaft, A. J. v. d., 1990, *Nonlinear Dynamical Control Systems*, NY: Springer-Verlag.

Nichols, R. A., Reichert, R. T., and Rugh, W. J., 1993, "Gain scheduling for H-infinity controllers: a flight control example," *IEEE Transactions on Control System Technology*, Vol. 1, No. 2.

Ogata, K., 1997, *Modern Control Engineering: 3rd Edition*, Upper Saddle River, NJ: Prentice Hall.

Olas, A., 1994, "Construction of optimal Lyapunov function for systems with structured uncertainties," *IEEE Transactions on Automatic Control*, Vol. 39, No. 1.

Olas, A., and Ahmadkhanlou, F., 1994, "Globally optimal quadratic Lyapunov functions for robust stability of systems with structured uncertainty," *Dynamics and Control*, Vol. 4.

Ortega, J. M., 1990, *Numerical Analysis: A Second Course*, SIAM.

Ortega, J. M., 1990b, *Matrix Theory: A Second Course*, Plenum Press, NY.

Patel, R.V., Toda, M., and Sridhar, B., 1977, "Robustness of linear quadratic state feedback designs in the presence of system uncertainty," *IEEE Transactions on Automatic Control*, Vol. AC-22, No. 6.

Petersen, I. R., 1987, "A stabilization algorithm for a class of uncertain linear systems," *System and Control Letters*, Vol. 8.

Petersen, I. R., 1988, "Stabilization of an uncertain linear system in which uncertain parameters enter into the input matrix," *SIAM Journal of Control and Optimization*, Vol. 26, No. 6.

Reboulet, C., and Champetier, C., 1984, "A new method for linearizing non-linear systems: the pseudolinearization," *International Journal of Control*, Vol. 40, No. 4.

Roman, S., 1992, *Advanced Linear Algebra*, Springer-Verlag.

Sastry, S., and Bodson, M., 1989, *Adaptive Control, Stability, Convergence, and Robustness*, Englewood Cliffs, NJ: Prentice-Hall.

Schaft, A. J. v. d., 1992, "L_2-gain analysis of nonlinear systems and nonlinear state feedback H_α control," *IEEE Transactions on Automatic Control*, Vol. 37, No. 6.

Schmitendorf, W. E., 1988, "Designing stabilizing controllers for uncertain systems using the Riccati equation approach," *IEEE Transactions on Automatic Control*, Vol. 33, No. 4.

Shamma, J. S., and Athans, M., 1990, "Analysis of gain scheduled control for nonlinear plant," *IEEE Transactions on Automatic Control*, Vol. 35, No. 8.

Skogestad, S., and Postlenthwaite, I., 1996, *Multivariable Feedback Control: Analysis and Design*, NY: John-Wiley & Sons.

Slotine, J.-J. E., and Li, W., 1991, *Applied Nonlinear Control*, Englewood Cliffs, NJ: Prentice-Hall.

Utkin, V. I., 1992, *Sliding Modes in Control and Optimization*, Springer-Verlag.

Vedavalli, R. K., 1985, "Improved measures of stability robustness for linear state space model", *IEEE Transactions on Automatic Control*, Vol. AC-30, No. 6.

Vedavalli, R. K., and Liang, Z., 1986, "Reduced conservatism in stability robustness bounds by state transformation," *IEEE Transactions on Automatic Control*, Vol. AC-31, No. 9.

Vidyasagar, M., 1993, *Nonlinear Systems Analysis: Second Edition*, Englewood Cliffs, NJ: Prentice-Hall.

Walker, G. et al., 1991, "Instabilities in the feedback linearization of a double inverted pendulum," *Proc. IEEE Conf. Decision and Control*, pp. 89-91.

Wang, L.-X., 1997, *A Course in Fuzzy Systems and Control*, NJ: Prentice-Hall.

Wang, L.-X., 1994, *Adaptive Fuzzy Systems and Control, Design and Stability Analysis*, Englewood Cliffs, NJ: Prentice-Hall.

Xu, Z., and Hauser, J., 1995, "Higher order approximation feedback linearization about a manifold for multi-input systems," *IEEE Transaction on Automatic Control*, Vol. 40, No. 5.

Yin, T.-K., and Lee, C. S. G., 1995, "Fuzzy model-reference adaptive control," *IEEE Transactions on Systems, Man, and Cybernetics*, Vol. 25, No. 12.

Zhou, K., and Khargonekar, P. P., 1987, "Stability robustness bounds for linear state-space models with structured uncertainty," *IEEE Transactions on Automatic Control*, Vol. AC-32, No. 7.

Zhou, K. et al, 1996, *Robust and Optimal Control*, NJ: Prentice-Hall.

Appendix I

Step-by-Step Procedure for Generating LARC

Using a Linearized Model about the Origin

The system of interest is given by:

$$\dot{\mathbf{x}} = \mathbf{f}(\mathbf{x}, t) + \mathbf{g}(\mathbf{x}, t)\mathbf{u} \qquad (\text{A } 1)$$

where $\mathbf{x}$, $\mathbf{f}(\mathbf{x}, t)$, $\mathbf{g}(\mathbf{x}, t) \in \mathfrak{R}^n$, and the control $\mathbf{u}$ is restricted to be a vector-valued

function of $\mathbf{x}$ for simplicity. The objective is to design $\mathbf{u}(\mathbf{x}) \in \mathfrak{R}^m$ such that the origin of

(A 1) is locally uniformly asymptotically stable with a reasonably large attractive region.

In this section, we assume the knowledge that the linearized model about the origin of (A

1) exists and is given by:

$$\dot{\mathbf{x}} = \mathbf{A}\mathbf{x} + \mathbf{B}\mathbf{u}(\mathbf{x}) \qquad (\text{A } 2)$$

where $\mathbf{A} \in \mathfrak{R}^{n \times n}$, $\mathbf{B} \in \mathfrak{R}^{n \times m}$. This is equivalent to knowing that:

$$\left.\begin{array}{l} \lim_{\|\mathbf{x}\| \to 0}\left(\sup_{t \geq 0}\left(\dfrac{\|\mathbf{f}(\mathbf{x}, t) - \mathbf{A}\mathbf{x}\|}{\|\mathbf{x}\|}\right)\right) = 0 \\[4mm] \lim_{\|\mathbf{x}\| \to 0}\left(\sup_{t \geq 0}\left(\dfrac{\|\mathbf{g}(\mathbf{x}, t) - \mathbf{B}\|}{\|\mathbf{x}\|}\right)\right) = 0 \end{array}\right\} \qquad (\text{A } 3)$$

In addition, $\mathbf{A}$ and $\mathbf{B}$ are known with $[\mathbf{A}, \mathbf{B}]$ being controllable or stabilizable. These are

all information required for generating LARC using the "first" procedure. The first

procedure is primarily formulated for the case in which $\mathbf{A}$ is unstable but it is also

applicable when $\mathbf{A}$ is stable. For the latter case, we rewrite (2) as suggested in Section

1.3. For simplicity, the control is restricted to be linear such that $\mathbf{u}(\mathbf{x}) = -\mathbf{Kx} \in \Re^m$,

$\mathbf{K} \in \Re^{m \times n}$ in the following procedure:

Step 1   Construct an array containing increasingly large numerical values of ρ.

Remark: Typically, our array of ρ is 0.0001, 0.001, 0.01, ..., 100, 1000,

10000. However, an appropriate range and step size depend of the

system at hands. The key is to capture a portion of the eigenvalue-

ratio plot (introduced in Step 2) where the slope changes

significantly. When such portion is captured, replot it using a linear

scale for ρ.

For each value of ρ, we execute the following substeps:

1) Solve the steady-state Riccati equation:

$$0 = -2\mathbf{Q} - [\mathbf{PA} + \mathbf{A}^T\mathbf{P}] + 2\rho\mathbf{PBB}^T\mathbf{P} = -\mathbf{I} - \mathbf{M} + \overline{\mathbf{N}} \qquad (A\,4)$$

where $\mathbf{Q} = \mathbf{I}$, $\mathbf{M} \equiv \dfrac{1}{2}[\mathbf{PA} + \mathbf{A}^T\mathbf{P}]$, $\overline{\mathbf{N}} \equiv \dfrac{1}{2}[[\mathbf{PB}]\mathbf{K} + \mathbf{K}^T[\mathbf{PB}]^T]\big|_{\mathbf{K}^T = \rho[\mathbf{PB}]}$.

2) Find the n eigenvalues of $\mathbf{M}$ and compute the eigenvalue ratio $r_{\lambda_\mathbf{M}}$. The

expression for $r_{\lambda_\mathbf{M}}$ given in (1.23) can be reduced to:

$$r_{\lambda_\mathbf{M}} = \left| \frac{\lambda_{\mathbf{M}1}}{\lambda_{\mathbf{M}(r+1)}} \right| = -\frac{\lambda_{\mathbf{M}1}}{\lambda_{\mathbf{M}(r+1)}} \qquad (A\,5)$$

where $\lambda_{\mathbf{M}1} \geq ... \geq \lambda_{\mathbf{M}r} > \lambda_{\mathbf{M}(r+1)} \geq ... \geq \lambda_{\mathbf{M}n}$ and $r = \text{rank}(\mathbf{PB})$. By

examining the proof of Theorem 4.1 and the statements thereafter, it

should appear that $\lambda_{M1} > 0 > \lambda_{M(r+1)} = \ldots = \lambda_{Mn} = -1$ and thus

$$r_{\lambda_M} = \lambda_{M1} .$$

Example Suppose we are given that:

$$A = \begin{bmatrix} -0.0366 & 0.0271 & 0.0188 & -0.4555 \\ 0.0482 & -1.0100 & 0.0024 & -4.0208 \\ 0.1002 & 0.2855 & -0.7070 & 1.3229 \\ 0 & 0 & 1 & 0 \end{bmatrix}, B = \begin{bmatrix} 0.4422 & 0.1761 \\ 3.0447 & -7.5922 \\ -5.5200 & 4.9900 \\ 0 & 0 \end{bmatrix}$$

and $\rho = 0.01$. We obtain:

$$P = \begin{bmatrix} 8.2875 & -0.0200 & -0.7288 & -3.3907 \\ -0.0200 & 0.9573 & 0.5717 & -0.4832 \\ -0.7288 & 0.5717 & 2.6766 & 3.4784 \\ -3.3907 & -0.4832 & 3.4784 & 10.5036 \end{bmatrix}$$

$$M = \begin{bmatrix} -0.3773 & 0.0704 & -1.1987 & -2.1047 \\ 0.0704 & -0.8042 & -0.3593 & -0.8472 \\ -1.1987 & -0.3593 & 1.5737 & 4.7768 \\ -2.1047 & -0.8472 & 4.7768 & 8.0889 \end{bmatrix}$$

$$\overline{N} = \begin{bmatrix} 0.6227 & 0.0704 & -1.1987 & -2.1047 \\ 0.0704 & 0.1958 & -0.3593 & -0.8472 \\ -1.1987 & -0.3593 & 2.5737 & 4.7768 \\ -2.1047 & -0.8472 & 4.7768 & 9.0889 \end{bmatrix}$$

$$\text{rank}(PB) = 2$$

$$T_M = \begin{bmatrix} -0.2047 & 0.6223 & -0.1645 & 0.7374 \\ -0.0758 & -0.6597 & -0.6355 & 0.3939 \\ 0.4567 & -0.3286 & 0.6233 & 0.5431 \\ 0.8625 & 0.2637 & -0.4249 & -0.0779 \end{bmatrix}$$

$$\Lambda_M = T_M^T M T_M = \text{diag}\,[11.1921 \quad -0.7109 \quad -1 \quad -1]$$

$$\Lambda_{\overline{N}} = T_M^T \overline{N} T_M = \text{diag}[12.1921 \ 0.2891 \ 0 \ 0]$$

$$r_{\lambda_M} = \left| \frac{11.1921}{-1} \right| = -\frac{11.1921}{-1} = 11.1921 = \lambda_{M1}$$

Step 2   Using the data obtained in Step 1, plot r_{λ_M} versus ρ. Then select a few

values of ρ from a "flat" portion of the plot at which the corresponding values

of r_{λ_M} are small. At such points, r_{λ_M} does not change significantly when ρ

changes. For each selected value of ρ, we find the corresponding LARC

using:

$$\mathbf{u}_{LARC}(\mathbf{x}) = -\eta\rho\mathbf{B}^T\mathbf{P}\mathbf{x}\big|_{\eta=1} \equiv -\mathbf{K}_{LARC}\mathbf{x} \qquad (A\ 6)$$

where $\mathbf{K}_{LARC} \equiv \eta\rho\mathbf{B}^T\mathbf{P}$. Selecting an appropriate value for ρ is best

illustrated by examples. See Example 2.2, 2.3, and 2.4.

Step 3   Verify that sufficient control energy is available to implement the controller

by considering the resulting linear gain matrix and the required operating

region. If not, reconsider the eigenvalue-ratio plot and choose a new value for

ρ. Normally, a larger value of ρ results in a larger $\mathbf{K}_{LARC}$ and a greater

demand of control energy. Now, examine the attractive regions corresponding

to the selected values of ρ in Step 2 using numerical simulations. Then select

a controller that best suit design objectives and constraints. In our examples,

selecting 2 values of ρ according to the guideline in Step 2 results in an LAR

controller that yields a satisfactorily large attractive region when compared to those resulting from conventional linear control techniques.

Step 4   This step is optional. The parameter η may now be tuned by means of numerical simulations. When this is completed, the direction of $\mathbf{K}_{LARC}$ may be tuned by writing:

$$
\begin{aligned}
u_{LARC}(\mathbf{x}) &= -\rho\|\mathbf{PB}\|\frac{\mathbf{B}^T\mathbf{P}}{\|\mathbf{PB}\|}\mathbf{x} \\
&= -\rho\|\mathbf{PB}\|\overline{\mathbf{K}}_{LARC}\mathbf{x} \\
&= -\rho\|\mathbf{PB}\|[\overline{k}_1 \quad \ldots \quad \overline{k}_n]\mathbf{x}
\end{aligned}
\tag{A 7}
$$

where $\dfrac{\mathbf{B}^T\mathbf{P}}{\|\mathbf{PB}\|} = [\overline{k}_1 \quad \ldots \quad \overline{k}_n] \equiv \overline{\mathbf{K}}_{LARC}^T$. Now, perturb the direction of $\overline{\mathbf{K}}_{LARC}^T$ by increasing a component $\overline{k}_j$, $j \in \{1,\ldots,n\}$ by a small value, normalize the perturbed $\overline{\mathbf{K}}_{LARC}^T$ using the 2-norm, and run simulations at initial conditions just outside the attractive region recorded in Step 3. If the simulations show convergence, restart Step 4. If the trajectories diverge, restore $\overline{k}_j$, change the index j, and restart Step 4. All components of $\overline{\mathbf{K}}_{LARC}^T$ are perturbed in the same fashion, and all perturbation must be "feasible" or

$$\lambda_i(\mathbf{A} - \rho\|\mathbf{PB}\|\overline{\mathbf{K}}_{LARC}) < 0 \quad \forall i \text{ for local stability.}$$

Appendix II

Step-by-Step Procedure for Generating LARC

Using a Nominal Model and Uncertainty Specifications

In this Appendix II, the system of interest is the same as that in Appendix I. The difference is that the availability of the linearized model about the origin of (A 1) is not required. We rewrite the nonlinear system (A 1)as:

$$\dot{\mathbf{x}} = \mathbf{A}_n \mathbf{x} + \mathbf{B}_n \, \mathbf{u}(\mathbf{x}) + [\mathbf{f}(\mathbf{x},t) - \mathbf{A}_n \mathbf{x} + \mathbf{g}(\mathbf{x},t)\mathbf{u}(\mathbf{x}) - \mathbf{B}_n \mathbf{u}(\mathbf{x})]$$
$$\equiv \mathbf{A}_n \mathbf{x} + \mathbf{B}_n \, \mathbf{u}(\mathbf{x}) + \mathbf{f}_\Sigma(\mathbf{x},t,\mathbf{u}(\mathbf{x}))$$

(A 8)

where the subscript "n" denotes the available "nominal" model, $\mathbf{A}_n \in \mathfrak{R}^{n \times n}$, $\mathbf{B}_n \in \mathfrak{R}^{n \times m}$,

$\mathbf{u}(\mathbf{x}) = -\mathbf{K}\mathbf{x} \in \mathfrak{R}^m$, $\mathbf{f}_\Sigma(\mathbf{x},t,\mathbf{u}(\mathbf{x})) \equiv [\mathbf{f}(\mathbf{x},t) - \mathbf{A}_n \mathbf{x} + \mathbf{g}(\mathbf{x},t)\mathbf{u}(\mathbf{x}) - \mathbf{B}_n u(\mathbf{x})] \in \mathfrak{R}^n$. It is

required that $\mathbf{A}_n$ be unstable, and $[\mathbf{A}_n, \mathbf{B}_n]$ be controllable or stabilizable. If $\mathbf{A}_n$ is

stable, we rewrite $\mathbf{A}_n$ as suggested in Section 1.3. The uncertain vector $\mathbf{f}_\Sigma(\mathbf{x},t,\mathbf{u}(\mathbf{x}))$

lumps together all the nonlinearities, uncertainties, and modeling errors entering the

nominal time-invariant linear system $\dot{\mathbf{x}} = \mathbf{A}_n \mathbf{x} + \mathbf{B}_n \, \mathbf{u}(\mathbf{x})$. It is desirable to choose $\mathbf{A}_n$

and $\mathbf{B}_n$ such that $\|\mathbf{f}_\Sigma(\mathbf{x},t,\mathbf{u}(\mathbf{x}))\|/\|\mathbf{x}\|$ is small. Provided we can write (A 8) such that

$\|\mathbf{f}_\Sigma(\mathbf{x},t,\mathbf{u}(\mathbf{x}))\|/\|\mathbf{x}\|$ is sufficiently small, the objective can be achieved using the

procedures in this section without knowing the linearized model of (A 2). Applications of

these procedures require that uncertainty specifications are available.

A 2.1   Systems with Structured Uncertainty Specifications

Consider the situation when it is known in the operating region of interest that:

$$\Delta \mathbf{A}_n(\mathbf{x}, t) = \mathbf{f}(\mathbf{x}, t) - \mathbf{A}_n \mathbf{x} = \sum_{\alpha=1}^{r_{A_n}} [h_\alpha^{A_n}(\mathbf{x}, t) \mathbf{E}_\alpha^{A_n}] \mathbf{x} \qquad (A\ 9)$$

$$\Delta \mathbf{B}_n(\mathbf{x}, t) = \mathbf{g}(\mathbf{x}, t) - \mathbf{B}_n = \sum_{\beta=1}^{r_{B_n}} [h_\beta^{B_n}(\mathbf{x}, t) \mathbf{E}_\beta^{\Delta B n}] \mathbf{x} \qquad (A\ 10)$$

where $h_\alpha^{A_n}(\mathbf{x}, t) \in [h_{l\alpha}^{A_n}, h_{u\alpha}^{A_n}] \in \Re$, $h_\beta^{B_n}(\mathbf{x}, t) \in [h_{l\beta}^{B_n}, h_{u\beta}^{B_n}] \in \Re$ are <u>uncertain</u> functions,

$h_{l\alpha}^{A_n} < h_{u\alpha}^{A_n}$, $h_{l\beta}^{B_n} < h_{u\beta}^{B_n}$, $\mathbf{E}_\alpha^{A_n} \in \Re^{n \times n}$, $\mathbf{E}_\beta^{B_n} \in \Re^{n \times m}$, $1 \le r_{A_n} \le n \times n$, and $1 \le r_{B_n} \le n \times m$.

The known uncertainty specifications are $h_{l\alpha}^{A_n}$ (a lower bound of $h_\alpha^{A_n}(\mathbf{x}, t)$), $h_{u\alpha}^{A_n}$ (an

upper bound of $h_\alpha^{A_n}(\mathbf{x}, t)$), $h_{l\beta}^{B_n}$ (a lower bound of $h_\beta^{B_n}(\mathbf{x}, t)$), $h_{u\beta}^{B_n}$ (an upper bound of

$h_\beta^{B_n}(\mathbf{x}, t)$), $\mathbf{E}_\alpha^{A_n}$, and $\mathbf{E}_\beta^{B_n}$. In this case, we suggest the following steps to generate an

LARC:

Step 1   Cast the uncertain vector in the standard form in the operating region of

interest. Using the notations defined previously, we write:

$$-[\Delta \mathbf{B}_n(\mathbf{x}, t)] \mathbf{K} \mathbf{x} = \sum_{\beta=1}^{r_{B_n}} [h_\beta^{B_n}(\mathbf{x}, t)[-\mathbf{E}_\beta^{\Delta B n} \mathbf{K}]] \mathbf{x} = \sum_{\beta=1}^{r_{B_n}} [h_\beta^{B_n}(\mathbf{x}, t) \mathbf{E}_\beta^{B_n}] \mathbf{x}$$

where $\mathbf{E}_\beta^{B_n} = [-\mathbf{E}_\beta^{\Delta B n} \mathbf{K}] \in \Re^{n \times n}$, and $1 \le r_{B_n} \le n \times m$. Thus, we can cast the

uncertain vector in the standard from in the operating region as:

$$\mathbf{f}_\Sigma(\mathbf{x}, t, \mathbf{u}(\mathbf{x}))|_{\mathbf{u} = -\mathbf{K}\mathbf{x}} = \sum_{\alpha=1}^{r_{A_n}} [h_\alpha^{A_n}(\mathbf{x}, t) \mathbf{E}_\alpha^{A_n}] \mathbf{x} + \sum_{\beta=1}^{r_{B_n}} [h_\beta^{B_n}(\mathbf{x}, t) \mathbf{E}_\beta^{B_n}] \mathbf{x} \equiv \sum_{j=1}^{r} [h_j(\mathbf{x}, t) \mathbf{E}_j] \mathbf{x}$$

where $\mathbf{E}_j \in \Re^{n \times n}$, and $r = r_{A_n} + r_{B_n}$.

Step 2   Construct the matrix $\mathbf{Z}$ in Theorem 3.2. To do this, we follow the following

substeps:

1) $-2\mathbf{Q} = \mathbf{P}\overline{\mathbf{A}}_n + \overline{\mathbf{A}}_n^T\mathbf{P}$, where $\mathbf{P}, \mathbf{Q} \in \Re^{n \times n}$ are symmetric positive definite,

and $\overline{\mathbf{A}}_n \equiv [\mathbf{A}_n - \mathbf{B}_n\mathbf{K}]$.

2) $\overline{\mathbf{A}}_l \equiv \overline{\mathbf{A}}_n + \sum_{j=1}^{r} h_{lj}\mathbf{E}_j$

3) $\mathbf{\Phi} \equiv \mathbf{P}\overline{\mathbf{A}}_l + \overline{\mathbf{A}}_l^T\mathbf{P}$, where $\mathbf{\Phi}$ is a symmetric matrix because

$[\mathbf{P}\overline{\mathbf{A}}_l]^T = \overline{\mathbf{A}}_l^T\mathbf{P}$ due to the symmetry of $\mathbf{P}$.

4) $\mathbf{\Psi}_j \equiv [\mathbf{P}\mathbf{E}_j + \mathbf{E}_j^T\mathbf{P}] = \mathbf{\Psi}_j^T$

5) $\mathbf{\Psi}_j^D = \mathbf{T}_{\mathbf{\Psi}_j}^T\mathbf{\Psi}_j\mathbf{T}_{\mathbf{\Psi}_j} = \mathrm{diag}[\lambda_{1j}(\mathbf{\Psi}_j) \quad \ldots \quad \lambda_{nj}(\mathbf{\Psi}_j)]$, where

$\mathbf{T}_{\mathbf{\Psi}_j} = [\mathbf{v}_{1j}(\mathbf{\Psi}_j) \mid \ldots \mid \mathbf{v}_{nj}(\mathbf{\Psi}_j)]$, $\mathbf{T}_{\mathbf{\Psi}_j}^T\mathbf{T}_{\mathbf{\Psi}_j} = \mathbf{I}$, $\{\mathbf{v}_{1j}(\mathbf{\Psi}_j) \quad \ldots \quad \mathbf{v}_{nj}(\mathbf{\Psi}_j)\}$

is the set of n orthonormal eigenvectors of $\mathbf{\Psi}_j$, and the superscript "D"

denotes "diagonal".

6) $\mathbf{\Psi}_j^{D,\,0+} = \mathbf{\Psi}_j^D \big|_{[\mathbf{\Psi}_j^D(i,i)<0] \to [\mathbf{\Psi}_j^D(i,i)=0]}$, where the subscript $[\mathbf{\Psi}_j^D(i,i) < 0] \to$

$[\mathbf{\Psi}_j^D(i,i) = 0]$ means that we obtain the diagonal matrix $\mathbf{\Psi}_j^{D,0+}$ from the

diagonal matrix $\mathbf{\Psi}_j^D$ by setting all negative diagonal elements of $\mathbf{\Psi}_j^D$ to

zero, and $\mathbf{\Psi}_j^D(i,i)$ denotes the (i, i) element of $\mathbf{\Psi}_j^D$. When the superscript

"0+" is employed with the superscript "D", we designate that the diagonal

matrix $\mathbf{\Psi}_j^{D,\,0+}$ has no negative element and is positive semidefinite or is

positive definite.

7) $\Psi_j^{0+} = [T_{\Psi_j}^{-1}]^T [\Psi_j^{D,0+}] T_{\Psi_j}^T = T_{\Psi_j} [\Psi_j^{D,0+}] T_{\Psi_j}^T$, where the superscript "0+"

designate that Ψ_j^{0+} is positive semidefinite or is positive definite but need

<u>not</u> be diagonal.

8) $Z \equiv \Phi + \sum_{j=1}^{r} [(h_{uj} - h_{lj}) \Psi_j^{0+}]$

Step 3   Solve for $\{K, Q, P\}$ such that in the operating region of interest:

$$\lambda_{max}(Z(K, Q, P)) < 0 \qquad\qquad (A\ 11)$$

For some simple systems, finding a solution analytically may be possible but

we do not expect this in general. A more practical approach is to solve for a

solution $\{K, Q, P\}$ for (A 11) using a numerical optimization technique. Since

$\{K, Q\}$ implies P, we usually abbreviate $\{K, Q, P\}$ by $\{K, Q\}$. The following

substeps are suggested to find a solution for (A 11):

1) Obtain reasonably good initial values $\{K, Q\}$ for the optimization such

that the corresponding $\lambda_{max}(Z(K, Q, P))$ is small by using LARC. To do

this, we choose a region $\{(\rho, \eta) \mid 0 < \rho_l \le \rho \le \rho_u, 1 \le \eta \le \eta_u\}$ and compute

$K = K_{LARC}$ and Q at points distributed evenly in this region. For each ρ,

we set $Q = I$ and obtain P by solving

$$0 = -2Q - [PA_n + A_n^T P] + 2\rho PB_n B_n^T P \qquad\qquad (A\ 12)$$

Using ρ and P, construct for each η:

$$K = K_{LARC} = \eta\rho B_n^T Px \qquad\qquad (A\ 13)$$

Using ρ, η and $\mathbf{P}$, obtain $\mathbf{Q}$ by solving:

$$0 = -2\mathbf{Q} - [\mathbf{PA}_n + \mathbf{A}_n^T\mathbf{P}] + 2\rho\eta\mathbf{PB}_n\mathbf{B}_n^T\mathbf{P} \qquad \text{(A 14)}$$

Using $\{\mathbf{K}_{LARC}, \mathbf{Q}\}$ determined for each (ρ, η), we plot $\lambda_{\max}(\mathbf{Z}(\rho, \eta))$

versus ρ and η in three dimensions, and find a region of (ρ, η) where

$\lambda_{\max}(\mathbf{Z}(\rho, \eta))$ is small or is negative from such plot. Depending on the

context, we alternately write $\lambda_{\max}(\mathbf{Z}(\rho, \eta))$ or $\lambda_{\max}(\mathbf{Z}(\mathbf{K}_{LARC}, \mathbf{Q}))$

because (ρ, η) implies $\{\mathbf{K}_{LARC}, \mathbf{Q}\}$ in our setup.

If we find from the plot that $\lambda_{\max}(\mathbf{Z}(\rho, \eta)) < 0$ at a particular (ρ, η), then

the matrix $\mathbf{K}_{LARC}$ corresponding to such (ρ, η) meets the uncertainty

specifications and we terminate the procedure. In this case, we usually

select $\{\mathbf{K}_{LARC}, \mathbf{Q}\}$ corresponding to the minimum of $\lambda_{\max}(\mathbf{Z}(\rho, \eta))$ in the

plots as our solution although we can accept any solutions such that

$\lambda_{\max}(\mathbf{Z}(\rho, \eta)) < 0$. If the minimum of $\lambda_{\max}(\mathbf{Z}(\rho, \eta))$ in the plot is positive,

we obtain from this plot an initial value $\{\mathbf{K}_{LARC}, \mathbf{Q}\}$ such that the

corresponding $\lambda_{\max}(\mathbf{Z}(\rho, \eta))$ is small for the optimization. When the

available control energy is limited, it is preferable to start the optimization

from an initial value in which $\mathbf{K}_{LARC}$ is small. This usually forces us to

admit an initial value $\{\mathbf{K}_{LARC}, \mathbf{Q}\}$ corresponding to a larger $\lambda_{\max}(\mathbf{Z}(\rho, \eta))$.

In this case, we select the initial value from a "flat" portion of the plot

where $\lambda_{\max}(\mathbf{Z}(\rho, \eta))$ is small. This is best illustrated by examples. See

Example 3.3, 3.4, 3.5, and 4.1.

2) Starting from the feasible initial value determined previously, we employ

an optimization technique to search for $\{\mathbf{K}_{LARC}, \mathbf{Q}\}$ such that

$\lambda_{\max}(\mathbf{Z}(\mathbf{K}_{LARC}, \mathbf{Q})) < 0$. <u>There are several applicable optimization</u>

<u>techniques</u> but we employ the straightforward "univariate" technique

(Fox, 1971) for simplicity although other techniques may produce better

results. We regard the elements of $\mathbf{K}_{LARC}$ and $\mathbf{Q}$ as our variables in the

objective function $\lambda_{\max}(\mathbf{Z}(\mathbf{K}_{LARC}, \mathbf{Q}))$. Then we perturb these variables

one at a time and examine the corresponding $\lambda_{\max}(\mathbf{Z}(\mathbf{K}_{LARC}, \mathbf{Q}))$. Our

perturbations must be such that $\{\mathbf{K}_{LARC}, \mathbf{Q}\}$ remains feasible. If the

objective function decreases, we continue to perturb this variable in the

same direction. Otherwise, we reverse the direction of the perturbation and

repeat the above sequences. When the decrement in $\lambda_{\max}(\mathbf{Z}(\mathbf{K}_{LARC}, \mathbf{Q}))$ is

less than a prescribed value, we perturb a new variable and repeat the

above sequences. These nested loops terminate when computation time is

expired or when the decrement in $\lambda_{\max}(\mathbf{Z}(\mathbf{K}_{LARC}, \mathbf{Q}))$ is less than a

prescribed value after all the variables are perturbed in this fashion. All the

"prescribed" values and the perturbations are determined by using

heuristics. In our codes, we set these to be between 0.5% - 1% of the

previous values. The procedure terminates successfully when (A15) is

satisfied and unsuccessfully otherwise. For the former case, the

corresponding gain matrix is denoted by $\mathbf{K}_{OLARC}$.

A 2.2   Systems with Unstructured Uncertainty Specifications

Now, the structure of the uncertain vector is unavailable or is inapplicable but bounds

on $\dfrac{\|\Delta f(x,t)\|}{\|x\|}$ and $\|\Delta g(x,t)\|$ are known in the operating of interest, where

$\Delta f(x,t) \equiv f(x,t) - A_n x$ and $\Delta g(x,t) \equiv g(x,t) - B_n$. We denote these bounds by

$\max\left(\dfrac{\|\Delta f(x,t)\|}{\|x\|}\right)$ and $\max(\|\Delta g(x,t)\|)$ respectively. In this case, we suggest the following

steps to generate an LARC:

Step 1   From Theorem 3.3, we construct:

$$\mu_{max} \equiv \max(\lambda_{min}^{1/2}(2\varepsilon Q - \varepsilon^2 PP)) \tag{A 15}$$

where P and Q are symmetric positive definite satisfying the Lyapunov

equation $-2Q = P\overline{A}_n + \overline{A}_n^T P$, $\overline{A}_n \equiv [A_n - B_n K]$ is stable, and

$$0 < \varepsilon < \frac{2}{\sigma_{max}^2(Q^{-1/2}P)} \equiv \varepsilon_{max} \tag{A 16}$$

where $\sigma_{max}(Q^{-1/2}P)$ is the maximum singular value of $[Q^{-1/2}P]$, and

$Q^{1/2}Q^{1/2} = Q$.

Step 2   Solve for $\{K, Q, P\}$ such that in the operating region of interest:

$$\max\left(\frac{\|\Delta f(x,t)\|}{\|x\|}\right) + \|K\|\max(\|\Delta g(x,t)\|) \leq \mu_{max} \tag{A 17}$$

For some simple systems, finding a solution analytically may be possible but

we do not expect this in general. A more practical approach is to solve for a

solution $\{K, Q, P\}$ for (A 17) using a numerical optimization technique. Now,

define:

$$\delta \equiv \max\left(\frac{\|\Delta \mathbf{f}(\mathbf{x},t)\|}{\|\mathbf{x}\|}\right) + \|\mathbf{K}_{LARC}\| \max(\|\Delta \mathbf{g}(\mathbf{x},t)\|) - \mu_{\max} \qquad (A\ 18)$$

Thus a set $\{\mathbf{K}, \mathbf{Q}, \mathbf{P}\}$ is a solution of (A 18) if $\delta(\mathbf{K},\mathbf{Q},\mathbf{P}) \le 0$. Since $\{\mathbf{K}, \mathbf{Q}\}$ implies $\mathbf{P}$, we usually abbreviate $\{\mathbf{K}, \mathbf{Q}, \mathbf{P}\}$ by $\{\mathbf{K}, \mathbf{Q}\}$. The following substeps are suggested to find a solution for (A 17):

1) Obtain reasonably good initial values $\{\mathbf{K}, \mathbf{Q}\}$ for the optimization such that the corresponding $\delta(\mathbf{K},\mathbf{Q})$ is small by using LARC. To do this, we choose a region $\{(\rho,\eta) \mid 0 < \rho_l \le \rho \le \rho_u, 1 \le \eta \le \eta_u\}$ and compute $\mathbf{K} = \mathbf{K}_{LARC}$ and $\mathbf{Q}$ at points distributed evenly in this region. For each ρ, we set $\mathbf{Q} = \mathbf{I}$ and obtain $\mathbf{P}$ by solving

$$0 = -2\mathbf{Q} - [\mathbf{PA}_n + \mathbf{A}_n^T\mathbf{P}] + 2\rho\mathbf{PB}_n\mathbf{B}_n^T\mathbf{P} \qquad (A\ 19)$$

Using ρ and $\mathbf{P}$, construct for each η:

$$\mathbf{K} = \mathbf{K}_{LARC} = \eta\rho\mathbf{B}_n^T\mathbf{Px} \qquad (A\ 20)$$

Using ρ, η and $\mathbf{P}$, obtain $\mathbf{Q}$ by solving:

$$0 = -2\mathbf{Q} - [\mathbf{PA}_n + \mathbf{A}_n^T\mathbf{P}] + 2\rho\eta\mathbf{PB}_n\mathbf{B}_n^T\mathbf{P} \qquad (A\ 21)$$

Using $\{\mathbf{K}_{LARC}, \mathbf{Q}\}$ determined for each (ρ,η), we plot $\delta(\rho,\eta)$ versus ρ and η in three dimensions, and find a region of (ρ,η) where $\delta(\rho,\eta)$ is small or is negative from such plot. Depending on the context, we alternately write $\delta(\rho,\eta)$ or $\delta(\mathbf{K}_{LARC},\mathbf{Q})$ because (ρ,η) implies $\{\mathbf{K}_{LARC}, \mathbf{Q}\}$ in our setup.

If we find from the plot that $\delta(\rho,\eta) \leq 0$ at a particular (ρ,η), then the matrix $\mathbf{K}_{LARC}$ corresponding to such (ρ,η) meets the uncertainty specifications and we terminate the procedure. In this case, we usually select $\{\mathbf{K}_{LARC},\mathbf{Q}\}$ corresponding to the minimum of $\delta(\rho,\eta)$ in the plots as our solution although we can accept any solutions such that $\delta(\rho,\eta) \leq 0$. If the minimum of $\delta(\rho,\eta)$ in the plot is positive, we obtain from this plot an initial value $\{\mathbf{K}_{LARC},\mathbf{Q}\}$ such that the corresponding $\delta(\rho,\eta)$ is small for the optimization. When the available control energy is limited, it is preferable to start the optimization from an initial value in which $\mathbf{K}_{LARC}$ is small. This usually forces us to admit an initial value $\{\mathbf{K}_{LARC},\mathbf{Q}\}$ corresponding to a larger $\delta(\rho,\eta)$. In this case, we select the initial value from a "flat" portion of the plot where $\delta(\rho,\eta)$ is small. This is the same as the selection of $\lambda_{\max}(\mathbf{Z}(\rho,\eta))$ illustrated in Example 3.3, 3.4, 3.5, and 4.1.

2) Starting from the feasible initial value determined previously, we employ an optimization technique to search for $\{\mathbf{K}_{LARC},\mathbf{Q}\}$ such that $\delta(\mathbf{K}_{LARC},\mathbf{Q}) < 0$. There are several applicable optimization techniques but we employ the straightforward "univariate" technique (Fox, 1971) for simplicity although other techniques may produce better results. We regard the elements of $\mathbf{K}_{LARC}$ and $\mathbf{Q}$ as our variables in the objective function $\delta(\mathbf{K}_{LARC},\mathbf{Q})$. Then we perturb these variables one at a time and

examine the corresponding $\delta(\mathbf{K}_{LARC}, \mathbf{Q})$. Our perturbations must be such

that $\{\mathbf{K}_{LARC}, \mathbf{Q}\}$ remains feasible. If the objective function decreases, we

continue to perturb this variable in the same direction. Otherwise, we

reverse the direction of the perturbation and repeat the above sequences.

When the decrement in $\delta(\mathbf{K}_{LARC}, \mathbf{Q})$ is less than a prescribed value, we

perturb a new variable and repeat the above sequences. These nested loops

terminate when computation time is expired or when the decrement in

$\delta(\mathbf{K}_{LARC}, \mathbf{Q})$ is less than a prescribed value after all the variables are

perturbed in this fashion. All the "prescribed" values and the perturbations

are determined by using heuristics. In our codes, we set these to be

between 0.5% - 1% of the previous values. The procedure terminates

successfully when (A 17) is satisfied and unsuccessfully otherwise. For

the former case, the corresponding gain matrix is denoted by $\mathbf{K}_{OLARC}$.

Appendix III

Step-by-Step Procedure for Generating LARC

Using an Exact Nonlinear Model

Now, the system of interest is given by:

$$\dot{\mathbf{x}} = \mathbf{f}(\mathbf{x}) + \mathbf{g}(\mathbf{x})\mathbf{u} \qquad \text{(A 22)}$$

where $\mathbf{x}$, $\mathbf{f}(\mathbf{x})$, $\mathbf{g}(\mathbf{x}) \in \mathfrak{R}^n$. We substitute for $\mathbf{u}$ the "total" LARC:

$$\mathbf{u}_{TLARC}(\mathbf{x}) = \mathbf{u}_{LARC}(\mathbf{x}) + \mathbf{u}_a(\mathbf{x}) \qquad \text{(A 23)}$$

where $\mathbf{u}_{LARC}(\mathbf{x})$ is generated by using a procedure in Appendix I or II. The objective is

to generate an auxiliary control $\mathbf{u}_a(\mathbf{x})$ to augment $\mathbf{u}_{LARC}(\mathbf{x})$ such that the corresponding

LAR is enlarged from that corresponding to $\mathbf{u}_{LARC}(\mathbf{x})$ when $\mathbf{f}(\mathbf{x})$ and $\mathbf{g}(\mathbf{x})$ are known

exactly. We suggest the following steps to generate $\mathbf{u}_a(\mathbf{x})$:

Step 1   Select a choice for $\mathbf{u}_a(\mathbf{x})$. It has been pointed out in Chapter V that there are

infinitely many choices of $\mathbf{u}_a(\mathbf{x})$ satisfying (5.5), and thus can be employed

to achieve the objective. A possibility is given by:

$$\mathbf{u}_a(\mathbf{x}) = -\gamma(\mathbf{x})\mathbf{g}^T(\mathbf{x})\mathbf{P}\mathbf{x} \equiv -\mathbf{K}_a(\mathbf{x})\mathbf{x} \qquad \text{(A 24)}$$

where $\gamma(\mathbf{x})\mathbf{g}^T(\mathbf{x})\mathbf{P}\mathbf{x} \equiv \mathbf{K}_a(\mathbf{x}) \in \mathfrak{R}^{m \times n}$, $\gamma(\mathbf{x}) > 0$, and $\mathbf{P}$ corresponds to

$\mathbf{u}_{LARC}(\mathbf{x})$. The choice of $\mathbf{u}_a(\mathbf{x})$ in (A 24) is selected for simplicity although

other choices may produce better results. Under the choice of auxiliary control

(5.7), the resultant nonlinear control is given by:

$$\mathbf{u}_{TLARC}(\mathbf{x}) = -\mathbf{K}_{LARCT}\mathbf{x} \qquad \text{(A 25)}$$

where $\mathbf{K}_{TLARC} \equiv [\mathbf{K}_{LARC} + \mathbf{K}_a(\mathbf{x})]$ when no optimization is employed to find the linear state-feedback gain matrix for $\mathbf{u}_{LARC}(\mathbf{x})$, and $\mathbf{K}_{TLARC} \equiv [\mathbf{K}_{OLARC} + \mathbf{K}_a(\mathbf{x})]$ otherwise.

Step 2   Tune parameters for $\mathbf{u}_a(\mathbf{x})$. When $\mathbf{u}_a(\mathbf{x})$ is given by (A 24), the only parameter is $\gamma(\mathbf{x})$. For simplicity, we restrict that $\gamma(\mathbf{x})$ be a positive constant denoted by γ_C. Because a tool for selecting an appropriate value for γ_C has not been established, we tune γ_C using heuristic. We begin by choosing a small positive value for $\gamma_C = \gamma_C[1]$. Typically, we set $\gamma_C[1] = 0.001$. Then employ numerical simulations to estimate the attractive region corresponding to $\mathbf{u}_{TLARC}(\mathbf{x})\big|_{\gamma_C = \gamma_C[1]}$ and compare this with that corresponding to $\mathbf{u}_{TLARC}(\mathbf{x})\big|_{\gamma=0} = \mathbf{u}_{TLARC}(\mathbf{x})$. We accept $\gamma_C = \gamma_C[1]$ if the attractive region corresponding to $\mathbf{u}_{TLARC}(\mathbf{x})\big|_{\gamma_C = \gamma_C[1]}$ is larger than or equal to that corresponding to $\mathbf{u}_{LARC}(\mathbf{x})$. The process is to be repeated until the computation time is expired or the attractive region corresponding to $\mathbf{u}_{TLARC}(\mathbf{x})\big|_{\gamma_C = \gamma_C[i]}$ is smaller than that corresponding to $\mathbf{u}_{TLARC}(\mathbf{x})\big|_{\gamma_C = \gamma_C[i-1]}$. In these case, we select $\gamma_C = \gamma_C[i-1]$ for generating $\mathbf{u}_a(\mathbf{x})$.

VITA

ℐ

Pinit Ngamsom

Candidate for the Degree of

Doctor of Philosophy

Thesis: ENLARGED LOCAL STABILIZATIONS OF A CLASS OF UNCERTAIN NONLINEAR SYSTEMS USING LYAPUNOV ATTRACTIVE REGION CONTROL

Major Field: Mechanical Engineering

Biographical:

Personal Data: Born in Bangkok, Thailand, on December 12, 1969, the son of Pipat and Saijai Ngamsom. Married to Bongkosh Rittichainuwat on December 8, 1997.

Education: Received a Bachelor of Engineering degree in Mechanical Engineering with Second-Class-Honors from King Mongkut's Institute of Technology-Ladkrabang, Thailand in April 1992, and a Master of Science degree in Mechanical Engineering from Texas A&M University-Kingsville, Texas in May 1996. Completed the requirements for the Doctor of Philosophy degree in Mechanical Engineering at Oklahoma State University in May 2001.

Experience: Worked as an Automotive Design Engineer for Isuzu Technical Center, Thailand, 1992-1994, and as a Plant Engineer for Goodyear, Thailand, 1994-1995. Appointed a Scholar by Rangsit University, Thailand, 1997-2000.